

Semi-classical simulation of spin-1 magnets

Kimberly Remund,^{1,*} Rico Pohle,^{2,3} Yutaka Akagi,⁴ Judit Romhányi,^{5,1} and Nic Shannon¹

¹Theory of Quantum Matter Unit, Okinawa Institute of Science and Technology Graduate University, Onna-son, Okinawa 904-0412, Japan

²Department of Applied Physics, University of Tokyo, Hongo, Bunkyo-ku, Tokyo, 113-8656, Japan

³Department of Applied Physics, Waseda University, Okubo, Shinjuku-ku, Tokyo 169-8555, Japan

⁴Department of Physics, Graduate School of Science, The University of Tokyo, Hongo, Tokyo 113-0033, Tokyo

⁵Department of Physics and Astronomy, University of California, Irvine, California 92697, USA

(Dated: June 24, 2022)

Theoretical studies of magnets have traditionally concentrated on either classical spins, or the extreme quantum limit of spin-1/2. However, magnets built of spin-1 moments are also intrinsically interesting, not least because they can support quadrupole, as well as dipole moments, on a single site. For this reason, spin-1 models have been extensively studied as prototypes for quadrupolar (spin-nematic) order in magnetic insulators, and Fe-based superconductors. At the same time, because of the presence of quadrupoles, the classical limit of a spin-1 moment is not an $O(3)$ vector, a fact which must be taken into account in describing their properties. In this Article we develop a method to simulate spin-1 magnets based on a $u(3)$ algebra which treats both dipole and quadrupole moments on equal footing. This approach is amenable to both classical and quantum calculations, and we develop the techniques needed to calculate thermodynamic properties through Monte Carlo simulations and classical low-temperature expansion, and dynamical properties, through “molecular dynamics” simulations and a multiple-boson expansion. As a case study, we present detailed analytic and numerical results for the thermodynamic properties of ferroquadrupolar order on the triangular lattice, and its associated dynamics. At low temperatures, we show that it is possible to “correct” for the effects of classical statistics in simulations, and extrapolate to the zero-temperature quantum results found in flavour-wave theory.

I. INTRODUCTION

Textbook discussions of magnetism usually begin either with classical spins, or with the spin-1/2 moment of an individual electron. However, magnetic ions exist in many different forms, each of which requires its own mathematical representation [1–4]. And this can have profound consequences, even for simple models. One celebrated example is the gap found in integer-spin quantum antiferromagnets in one dimension [5–7], while half-integer systems remain gapless [8]. The principles which underpin this gap are now well known [9, 10], but much remains to be understood about higher-spin moments in general. For example, it is not widely appreciated that an $O(3)$ vector only provides an appropriate (semi-)classical limit for a quantum spin in the case of spin-1/2 moments, a fact which has implications for both ground states and excitations. In particular, the usual classical mean-field approximations, and “large- S ” treatments of spin-wave excitations [11, 12], both break down for spins larger than 1/2, because they do not adequately describe multipole moments [13, 14].

Spin-1 magnets provide a natural focus for such questions. Spin-1 moments differ from both classical vectors and quantum spin-1/2 moments in that they can support a quadrupole on a single site [Fig. 1]. This leads to both new types of ground state, and new kinds of excitation [13, 14]. Spin-1 systems also support new forms of interaction, relative to a spin-1/2 moment, including single-ion anisotropies and bi-quadratic interactions, which can originate in exchange [3], or be generated by coupling to the lattice [15]. As a consequence, the range of phases predicted to occur in spin-1

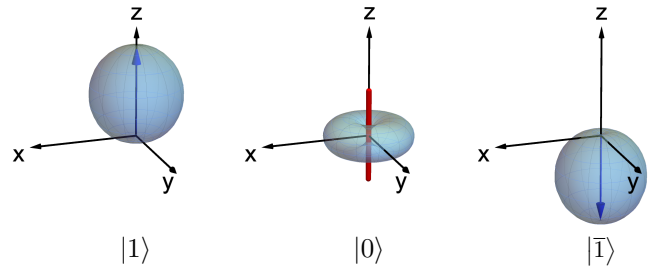


Figure 1. Usual, “magnetic” basis for a spin-1 moment, formed by eigenstates of S^z . States with $S^z = \pm 1$, labeled $|1\rangle$ and $|\bar{1}\rangle$, break time-reversal symmetry and have a finite spin-dipole moment (blue arrow). Meanwhile, the state with $S^z = 0$, labeled $|0\rangle$, has a quadrupolar magnetic moment, which can be represented through a director (red bar), perpendicular to the plane of the quadrupole. States are represented as probability surfaces in spin-space, as described in Appendix A.

magnets is very rich, including quadrupolar (spin-nematic) phases [13, 14, 16–20], and diverse forms of quantum spin liquid [21–26], as well conventional, dipolar, magnetic order.

Further strong motivation to study spin-1 magnets comes from experiment. A well-studied example is provided by NiGa_2S_4 , a triangular-lattice magnet which evades conventional magnetic order [27–29], and may realise a spin-nematic phase [18, 19, 30]. Spin-1 magnets on the pyrochlore lattice have also recently come into focus [31]. Among these, $\text{NaCaNi}_2\text{F}_7$ is particularly interesting, showing spin-liquid-like properties (above a spin-freezing temperature) [32], which cannot be explained within a framework based on $O(3)$ moments [33]. Other spin-1 materials discussed as candidate spin liquids include NiRh_2O_4 , whose moments inhabit a diamond lattice [34], and $\text{YCa}_3(\text{VO})_3(\text{BO}_3)_4$, which re-

* kimberly.remund@oist.jp

alises a Kagome lattice [35], and the triangular-lattice system $\text{Ba}_3\text{NiSb}_2\text{O}_9$ [36–38]. And in recent years, spin-1 models have also been intensively studied as a way of understanding nematic phases in both Fe-based superconductors [39–43], and systems of cold atoms [44–48].

Given this abundance of riches, there is clearly need for good theoretical tools to study spin-1 magnets. But the very things which make spin-1 moments interesting, also make them difficult to simulate numerically. Classical Monte Carlo (MC) simulations, based on $O(3)$ vector spins, fail to describe ground states or excitations built of local quadrupole moments. Exact diagonalisation does not suffer from this drawback, but the rapid growth of the Hilbert space typically restricts calculations to systems of 20 sites or less [19, 47]. Variational calculations, based on matrix- or tensor-product wave functions give a good account of dynamics in 1D [49], but cannot easily be extended beyond the calculation of ground-state properties in higher dimension [50, 51]. And while Quantum Monte Carlo (QMC) simulation has yielded insights into both quadrupolar order [17, 52], and the associated dynamics [53], its use is restricted to a relatively small number of cases which do not suffer from a sign problem. Moreover, within QMC, dynamics are only accessible for relatively small systems, through analytic continuation, which may be problematic for systems with complicated excitations. As a consequence, much of what we know about the exotic properties of spin-1 models is restricted to mean field theory (MFT), and the linear expansion of fluctuations about it, leaving many important questions out of reach.

In this Article, we develop a method of simulating spin-1 magnets, which treats both dipole and quadrupole moments on equal footing. Our approach is based on embedding the algebra $su(3)$ describing a spin-1 moment in the algebra $u(3)$, as discussed in earlier work of Papanicolaou [14]. This approach makes it possible to treat quantum aspects of the problem exactly, at the level of a single site. We arrive at a formulation in terms of the generators of $U(3)$, which is suitable for both analytic and numerical approaches to spin-1 magnets. In particular, the uncluttered structure of the algebra $u(3)$ makes it possible to derive very compact equations of motion (EoM), which can be integrated numerically to evaluate dynamics in cases with both conventional and unconventional forms of order.

We illustrate our method by applying it to a spin-1 model with the most general form of interactions allowed by $SU(2)$ symmetry, the bilinear-biquadratic (BBQ) Hamiltonian

$$\mathcal{H}_{\text{BBQ}} = \sum_{\langle i,j \rangle} \left[J_1 \hat{\mathbf{S}}_i \cdot \hat{\mathbf{S}}_j + J_2 (\hat{\mathbf{S}}_i \cdot \hat{\mathbf{S}}_j)^2 \right], \quad (1)$$

on a triangular lattice, reproducing, and in many cases extending, known results for its low-temperature phases [19, 20, 54]. We pay particular attention to the simplest phase to exhibit all the new features of a spin-1 moment, the ferroquadrupolar (FQ) order found for $J_2 < 0$ [Fig. 2]. In particular, we demonstrate that our approach reproduces known results for the dynamics of FQ order, where both QMC simulations [53] and analytic “flavour-wave” calculations [19] are available for comparison.

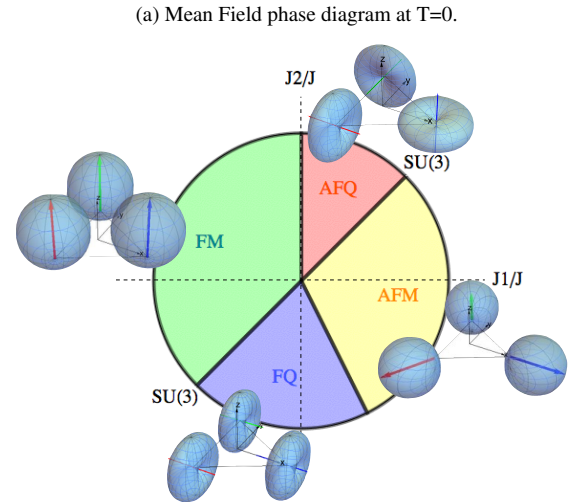


Figure 2. Mean-field phase diagram of the spin-1 bilinear-biquadratic (BBQ) model on the triangular lattice [Eq. (1)]. at $T = 0$, following [19, 20]. The model shows four distinct ordered ground states: ferromagnet (FM); three-sublattice antiferromagnet (AFM); ferroquadrupolar (FQ); and three-sublattice antiferroquadrupolar (AFQ). For $J_1 = J_2$ the model exhibits an enlarged, $SU(3)$ symmetry.

At the heart of this analysis is the need to introduce an extended set of operators to describe a single spin-1 moment. Any state of spin-1/2 moment can be represented as a point on a Bloch sphere, characterised by two polar angles [55]. By extension, any two states of a spin-1/2 moment can be connected by an $su(2)$ rotation, using two of the three generators of $su(2)$. This simple geometrical picture provides a natural classical limit of a spin-1/2 moment, as an $O(3)$ vector carrying a finite dipole moment

$$\hat{\mathbf{S}}_i = \begin{pmatrix} \hat{S}_i^x \\ \hat{S}_i^y \\ \hat{S}_i^z \end{pmatrix}. \quad (2)$$

In contrast, the usual magnetic basis for a spin-1 moment, Fig. 1, includes states with both dipole and quadrupole moments. There is no $su(2)$ rotation which connects dipoles with quadrupoles, and it follows that a general state of a spin-1 moment cannot be expressed in terms of two real angles. As a consequence, its classical limit cannot be an $O(3)$ vector.

To properly characterise a spin-1 moment, we therefore need to seek an algebra which encompasses quadrupole moments of spin

$$\mathbf{Q}_i = \begin{pmatrix} Q^{x^2-y^2} \\ Q^{3z^2-r^2} \\ Q^{xy} \\ Q^{yz} \\ Q^{xz} \end{pmatrix}_i = \begin{pmatrix} (S^x)^2 - (S^y)^2 \\ \frac{1}{\sqrt{3}}(3((S^z)^2 - S(S+1))) \\ S^x S^y + S^y S^x \\ S^y S^z + S^z S^y \\ S^x S^z + S^z S^x \end{pmatrix}_i. \quad (3)$$

The smallest algebra which can completely do so is $su(3)$, with a total of 8 generators [14, 20, 56]. In terms of these

operators, the BBQ Hamiltonian [Eq. (1)] can be expressed as

$$\mathcal{H}_{BBQ} = \sum_{(i,j)} \left(J_1 - \frac{J_2}{2} \right) \hat{\mathbf{S}}_i \cdot \hat{\mathbf{S}}_j + \frac{J_2}{2} \hat{\mathbf{Q}}_i \cdot \hat{\mathbf{Q}}_j + \frac{J_2}{3} s^2 (s+1)^2, \quad (4)$$

where it will prove convenient to write

$$J_1 = J \cos \theta, \quad J_2 = J \sin \theta. \quad (5)$$

Although the algebra $su(3)$ provides a complete portrait of

a spin-1 moment, its structure constants are very complicated [57]. This makes $su(3)$ a challenging starting point for descriptions of dynamics [58–60]. Happily, by adding just one more generator, the spin-length $\hat{\mathbf{S}}_i^2$, and subsequently imposing the constraint

$$\hat{\mathbf{S}}_i^2 = s(s+1) = 2, \quad (6)$$

it is possible to transition to a description of spin-1 moment in terms of the much simpler algebra $u(3)$ [14]. This approach is illustrated schematically in Eq. (7).

$$\begin{array}{c} su(3) \text{ algebra} \\ \left\{ \begin{array}{l} \text{Spin length} \\ 3 \text{ linearly} \\ \text{independent dipole} \\ \text{components} \\ \\ 5 \text{ linearly} \\ \text{independent} \\ \text{quadrupole} \\ \text{components} \end{array} \right. \end{array} \left\{ \begin{array}{l} \hat{\mathbf{S}}_i^2 \\ \hat{S}_i^x \\ \hat{S}_i^y \\ \hat{S}_i^z \\ \hat{Q}_i^{x^2-y^2} \\ \hat{Q}_i^{3z^2-s^2} \\ \hat{Q}_i^{xy} \\ \hat{Q}_i^{xz} \\ \hat{Q}_i^{yz} \end{array} \right\} \xrightarrow{\text{basis change}} \left\{ \begin{array}{l} \hat{A}_i^{xx} \\ \hat{A}_i^{xy} \\ \hat{A}_i^{xz} \\ \hat{A}_i^{yx} \\ \hat{A}_i^{yy} \\ \hat{A}_i^{yz} \\ \hat{A}_i^{zx} \\ \hat{A}_i^{zy} \\ \hat{A}_i^{zz} \end{array} \right\} u(3) \text{ algebra} \quad (7)$$

A convenient basis for $u(3)$ is provided by the tensors \hat{A}_i , a set of real, 3×3 matrices with only a single non-vanishing matrix element [14], and commutation relations

$$\begin{aligned} [\hat{A}_{i\beta}^\alpha, \hat{A}_{i\eta}^\gamma] &= \delta^{\gamma\beta} \hat{A}_{i\eta}^\alpha - \delta^{\alpha\eta} \hat{A}_{i\beta}^\gamma, \\ [\hat{A}_{i\beta}^\alpha, \hat{A}_{j\eta}^\gamma] &= 0. \end{aligned} \quad (8)$$

Written in terms of these matrices, the BBQ Hamiltonian [Eq. (1)] takes on the quadratic form

$$\mathcal{H}_{BBQ} = \sum_{(i,j)} [J_1 \hat{A}_{i\beta}^\alpha \hat{A}_{j\alpha}^\beta + (J_2 - J_1) \hat{A}_{i\beta}^\alpha \hat{A}_{j\beta}^\alpha + \frac{J_2}{4} s^2 (s+1)^2], \quad (9)$$

where we adopt the Einstein convention of summing over repeated indices. Projection into states with spin-1 can be accomplished by enforcing the constraint

$$\hat{A}_{i\alpha}^\alpha = \frac{1}{2} s(s+1) = 1, \quad (10)$$

on each site in the lattice.

From this starting point, we can carry out classical Monte Carlo (MC) simulations of the BBQ model in the basis of \hat{A}_i , treating dipole and quadrupole moments of a single site on an equal footing. We will refer to this approach as “u3MC”. Results for the finite-temperature phase diagram, obtained using u3MC, are shown in Fig. 3. At the level of thermodynamics, this approach is equivalent to the “semi-classical $SU(3)$ ”

simulations of Stoudenmire *et al.* [54], and yields identical results.

However the real advantages of working with a $u(3)$ representation become apparent when considering dynamics. Considering the Heisenberg equation of motion for \hat{A}_i , we find

$$\begin{aligned} \partial_t \hat{A}_{i\eta}^\gamma &= -i [\hat{A}_{i\eta}^\gamma, \mathcal{H}_{BBQ}] \\ &= -i \sum_{\delta} [J_1 (\hat{A}_{i\alpha}^\gamma \hat{A}_{i+\delta\eta}^\alpha - \hat{A}_{i\eta}^\alpha \hat{A}_{i+\delta\gamma}^\alpha) \\ &\quad + (J_2 - J_1) (\hat{A}_{i\alpha}^\gamma \hat{A}_{i+\delta\alpha}^\eta - \hat{A}_{i\eta}^\alpha \hat{A}_{i+\delta\gamma}^\alpha)], \end{aligned} \quad (11)$$

a simple form which automatically preserves the length of the spin [Eq. (10)], and is well-suited to numerical integration.

By combining classical MC simulation with numerical integration of the equation of motion, Eq. (11), we obtain an approach to dynamics analogous to “molecular dynamics” (MD) simulation, which can be used to calculate dynamical structure factors. We dub this “u3MD”. At low temperatures, we find it is possible to correct for the effect of classical statistics by multiplying structure factors by a temperature-dependent prefactor

$$S^{\text{QM}}(\mathbf{q}, \omega, T=0) = \lim_{T \rightarrow 0} \frac{\hbar \omega}{k_B T} S^{\text{MD}}(\mathbf{q}, \omega, T), \quad (12)$$

obtaining results in agreement with semi-classical quantum results at $T=0$. Results for u3MD simulations of the FQ phase are summarised in Fig. 4.

In remainder of this paper we describe these results in some detail, developing both analytic and numerical approaches

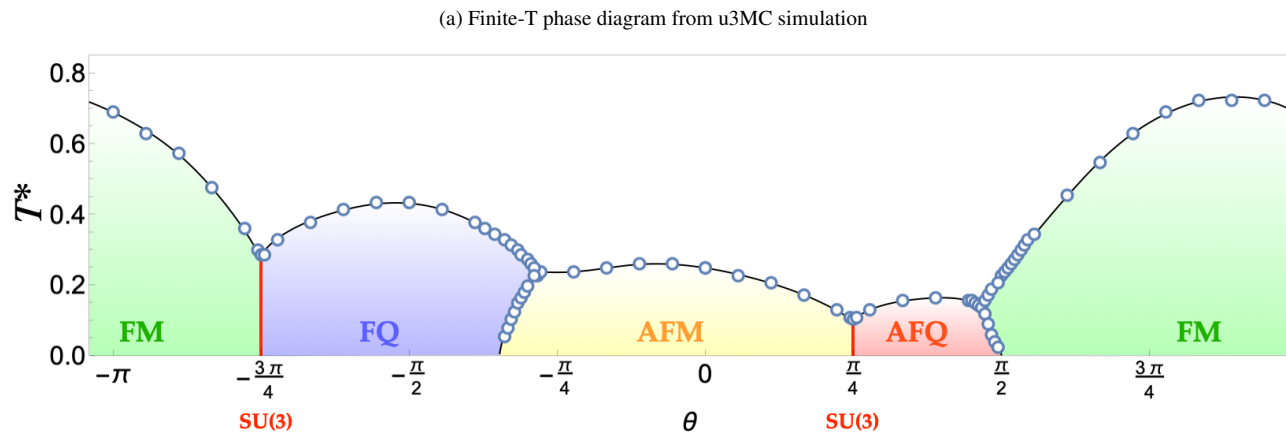


Figure 3. Finite-temperature phase diagram of the spin-1 bilinear-biquadratic (BBQ) model on the triangular lattice, obtained from Monte Carlo simulation of \mathcal{H}_{BBQ} [Eq. (9)] in the space of $u(3)$ matrices (u3MC). Points show the location of peaks in heat capacity; phases are labelled according to their dominant correlations (cf. Fig. 2 and Fig. 8). Details of simulation are provided in Section III A 2.

based on the $u(3)$ formalism. We benchmark simulations against these analytic results, and published numerical results from other approaches. We also explore some of the further ramifications of the $u(3)$ approach, particularly with respect to anisotropic exchange interactions, and the extent to which quantum results for dynamics can be inferred from (semi-)classical simulations.

In order to keep the paper self-contained, we provide a detailed account of derivations, and review all of the necessary mathematical formalism. However the paper is also constructed in such a way that readers uninterested in technical development of the method can skip directly to the results provided in Section VI, Section VII and Section VIII. Additional technical details are provided in a series of Appendices.

The paper is structured as follows:

Section II reviews the mathematical formalism needed to analyze spin-1 magnets in terms of a $u(3)$ algebra. A single spin-1 moment is analysed within a basis of time-reversal invariant states, where the most general possible spin configuration can be expressed in terms of a complex vector \mathbf{d} . The group $U(3)$ is shown to provide a convenient basis for all possible operations on spin-1 moments. Expressions are given for both the dipole and quadrupole associated with a spin-1 moment, in terms of the vector \mathbf{d} , and the 3×3 matrices \hat{A}_β^α , which provide a suitable representation of $u(3)$. The BBQ model [Section II C], and corresponding Heisenberg EoM [Section II D], are also developed in terms of \hat{A}_β^α , in a forms suitable for numerical simulation.

Section III introduces numerical simulation methods for spin-1 magnets. In Section III A, the $u(3)$ algebra described in Section II is shown to provide a convenient basis for (semi-)classical Monte Carlo simulations of spin-1 moments. A suitable MC update is developed in the basis of $u(3)$ matrices \hat{A}_β^α , and shown to be equivalent to earlier "sSU(3)" simulations of the spin-1 BBQ model in the basis of the complex vector \mathbf{d} . These calculations are extended to general J_1, J_2 , providing a finite-temperature phase diagram for the spin-1 BBQ model on a triangular lattice [Fig. 3]. In Section III B,

a MD simulation scheme is developed for spin-1 moments, based on the EoM for the matrices \hat{A}_β^α . The technical implementation of this MD update is described.

In Section IV we develop an analytic theory of classical fluctuations about a ferroquadrupolar (FQ) ground state of the spin-1 BBQ model on a triangular lattice, starting from the $u(3)$ representation introduced in Section II. In Section IV A, small fluctuations about FQ order are recast in terms of the matrices \hat{A}_β^α . In Section IV B these are shown to provide a natural basis for a classical, low-temperature expansion, within which it is possible to calculate thermodynamic properties. Finally, in Section IV C we use this theory to make explicit predictions for thermodynamic properties, including structure factors, for later comparison with MC simulation.

In Section V, we develop an equivalent, zero-temperature, quantum theory of fluctuations about a FQ ground state. First, in Section V A we quantize the fluctuations introduced in Section IV A, and show that the resulting multiple-Boson expansion is equivalent to earlier "flavor-wave" theory. Then, in Section V B, we use this quantum theory to make explicit predictions for dynamical structure factors, for later comparison with MD simulation.

In Section VI, the numerical methods developed in Section III are used to obtain a detailed portrait of FQ order in the spin-1 BBQ model on a triangular lattice. Monte Carlo simulation results for heat capacity [Section VI A], FQ order parameter [Section VI B], and equal-time structure factors [Section VI C], are compared explicitly with the analytic theory developed in Section IV C. The implications of the Mermin-Wagner Theorem are discussed, and the results of simulations at low temperatures are shown to conform exactly to the predictions of theory for a finite-size cluster. In Section VI D, numerical results are presented for the dynamics of the FQ state, based on MD simulations. The dynamical structure factors found in simulation are compared explicitly with the predictions of Section V B. Excitations are found to display the expected dispersion, but with intensities which, for $T \rightarrow 0$ differ from the analytic theory.

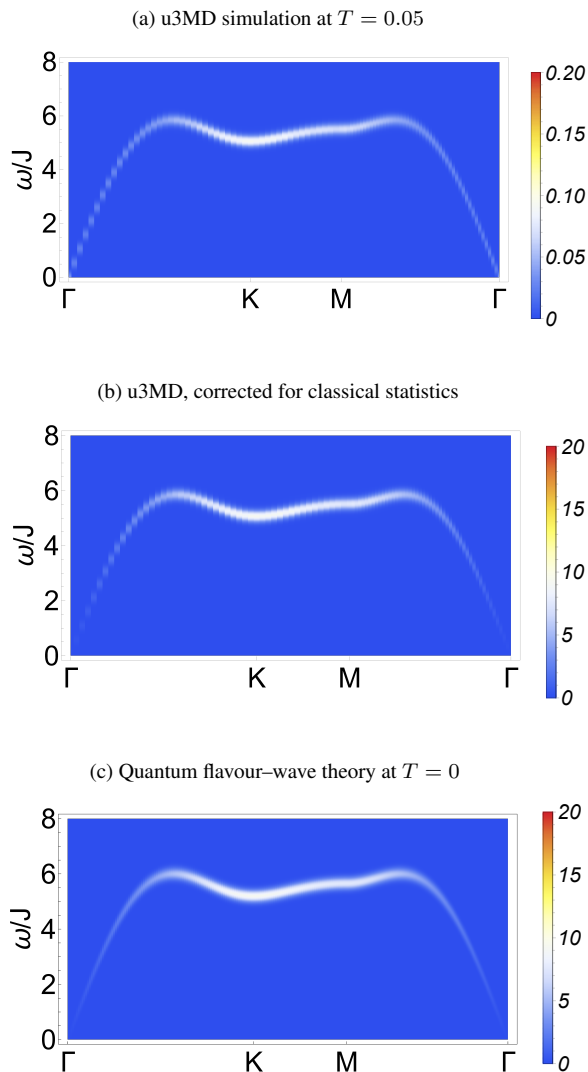


Figure 4. Dynamical structure factor $S_S(\mathbf{q}, \omega)$ for the ferro-quadrupolar (FQ) phase of the BBQ model on the triangular lattice. (a) Results of “molecular dynamics” (u3MD) simulation at finite T , showing a dispersive band of excitations which are the Goldstone modes of the FQ order. The spectral weight in these excitations is controlled by the classical statistics of the associated Monte Carlo (u3MC) simulations. (b) MD results corrected for the effects of classical statistics, for comparison with quantum results at $T = 0$. (c) Predictions of quantum flavour-wave theory at $T = 0$, showing agreement with the corrected results of MD simulation, as detailed in Fig. 19. Results are shown for Eq. (9) with $J_1 = 0.0$; $J_2 = -1.0$. Details of these calculations are provided in Section VII A.

Section VII resolves this paradox. By combining the low-temperature and multiple-Boson expansions developed in Section IV, we show that MD results can be understood in terms of a semi-classical dynamics, with spectral weight determined by a factor coming from classical statistics. Low-temperature MD results are corrected for this classical bias, and shown to agree exactly with the analytic theory of Section V, and equivalent “flavour-wave” calculations, in the limit $T \rightarrow 0$.

In Section VIII, we address the generalisation of simulation to which are anisotropic in spin-space. The EoM approach developed in Section IID and Section IIIB is shown to be robust against spin-anisotropy. Concrete results analytic and numerical results are provided for FQ order in the presence of single-ion anisotropy.

The paper concludes in Section IX with a brief summary of results, and discussion of potential future applications of the $u(3)$ approach.

A number of technical results are developed in Appendices.

Appendix A provides a framework for visualising the quantum states individual spin-1 moments starting from a coherent-state representation.

Appendix B details mathematical properties of the tensors \hat{A}_β^α , which act as generators of the group $U(3)$.

Appendix C sets out the conventions used in describing the triangular lattice.

Appendix D provides technical details of the calculation of equal-time structure factors within a classical low- T expansion.

Appendix E provides technical details of the Bogolibubov transformation used in the multiple-Boson expansion.

Appendix F provides technical details of calculations of dynamical structure factors within a multiple-Boson expansion.

Appendix G provides details of analytic calculations of the ordered moment for finite-size clusters.

Appendix H lists integrals used in developing the analytic theory of FQ order.

Appendix I develops an analytic theory of the excitations of a spin-1 easy-plane ferromagnet, based on generators of $U(3)$.

II. DESCRIPTION OF A SPIN-1 MOMENT USING A $u(3)$ ALGEBRA

In this Section, we develop the mathematical tools needed to describe a spin-1 moment, and explain how one naturally arrives at a general description in terms of operators satisfying a $u(3)$ algebra. These will form the basis for both the analytic calculations and the simulations described in the remaining parts of the Article. Our analysis builds on the earlier work by Papanicolou [14], and will also make connection with the notation of “ \mathbf{d} -vectors”, used in [19, 20, 56, 61].

We start in Section II A by reviewing the familiar description of a spin-1/2 moment in terms of eigenstates of S^z , and describe how its classical limit, an $O(3)$ vector, can be used as a basis for numerical simulations. In Section II B, we show how the usual magnetic basis for a single spin-1 moment (eigenstates of S^z), can be used to construct a new, non-magnetic, basis of states invariant under time-reversal. This motivates a general description of a spin-1 moment in terms of a complex vector \mathbf{d} , and of the introduction of the a set of 3×3 matrices A_β^α , which generate a representation of the algebra $u(3)$. Then, in Section II C, we show how the the BBQ model, Eq. (9), can be expressed in terms of the matrices A_β^α , providing a starting point for numerical simulation of thermodynamic properties. Finally, in Section IID, we use this

representation of the BBQ model to derive equations of motion for a spin-1 moment in terms of A_{β}^{α} , providing a starting point for numerical simulations of dynamics.

For compactness of notation, we set $\hbar = 1$.

A. Mathematical description of spin-1/2 moments

Before reviewing the mathematical description of a spin-1 moment, it is helpful to have in mind the usual picture of a spin-1/2 moment, and its (semi-)classical “large- S ” limit. Any quantum spin can be completely described by the eigenstates of \hat{S}^z

$$\hat{S}^z |m\rangle = m |m\rangle, \quad (13)$$

where the $2s+1$ states $|m\rangle$ form a closed orthogonal basis for $m = -j, -j+1, \dots, j-1, j$ [62]. In the case of spin-1/2, \hat{S}^z there are only two such eigenstates

$$\hat{S}^z |\pm \frac{1}{2}\rangle = \pm \frac{1}{2} |\pm \frac{1}{2}\rangle. \quad (14)$$

These states form a Kramers pair, related by time-reversal symmetry

$$\mathcal{T} |\pm \frac{1}{2}\rangle = \pm |\mp \frac{1}{2}\rangle. \quad (15)$$

As a consequence, individual spin-1/2 moments always break time-reversal symmetry, and always exhibit a finite spin-dipole moment.

From this starting point, it is possible to express any possible quantum state of a spin-1/2 moment in terms of two complex numbers

$$|\psi_{1/2}\rangle = c_1 |\frac{1}{2}\rangle + c_2 |-\frac{1}{2}\rangle \quad (16)$$

subject to the constraint

$$|c_1|^2 + |c_2|^2 = 1 \quad (17)$$

Resolving this constraint reduces the number of real parameters to three. And since the overall phase of $|\psi_{1/2}\rangle$ does not affect its physical properties, any state of a spin-1/2 moment can be specified using only two real numbers. Geometrically, this is equivalent to specifying the two angles needed to define a point on a Bloch sphere [55]. Formally, it is equivalent to working in the complex projective line $\mathbb{C}\mathbb{P}^1$.

Any two states within this space can be connected by an $SU(2)$ rotation, for which the Pauli Matrices

$$\sigma^x = \begin{pmatrix} 0 & 1 \\ 1 & 0 \end{pmatrix}, \quad \sigma^y = \begin{pmatrix} 0 & -i \\ i & 0 \end{pmatrix}, \quad \sigma^z = \begin{pmatrix} 1 & 0 \\ 0 & -1 \end{pmatrix}. \quad (18)$$

provide a convenient basis, with commutation relations

$$[\sigma_{\alpha}, \sigma_{\beta}] = 2i\epsilon_{\alpha\beta\gamma}\sigma_{\gamma}. \quad (19)$$

The classical, “large- S ” limit of a spin-1/2 can be taken through a coherent state representation [63], and is a $O(3)$ vector

$$\mathbf{S} = (S^x, S^y, S^z). \quad (20)$$

Since, for a single spin-1/2, all higher-order spin moments vanish, this vector describes all possible magnetic degrees of freedom, and can form the starting point for Monte Carlo (MC) simulation of thermodynamic properties [64].

The representation of spin-1/2 moments in terms of $O(3)$ vectors also provides the starting point for (semi-)classical descriptions of their dynamics, as determined by the Heisenberg equation of motion (EoM)

$$\frac{d\mathbf{S}_i}{dt} = -i[\mathbf{S}_i, \mathcal{H}] = \frac{d\mathcal{H}}{d\mathbf{S}_i} \times \mathbf{S}_i. \quad (21)$$

Numerical integration of these EoM, using spin configurations drawn from MC simulation, provides a (semi-)classical approach to spin dynamics which has been dubbed “Molecular Dynamics” (MD) simulation [33, 65, 66], and is closely analogous to simulations based on the (phenomenological) Landau-Lifshitz-Gilbert equations [67].

B. Description of a single quantum spin-1

1. Magnetic basis

Several new features arise in the case of a spin-1. Here, the eigenstates of \hat{S}^z comprise the 3 states

$$\mathcal{B}_1 = \{|1\rangle, |0\rangle, |\bar{1}\rangle\}. \quad (22)$$

forming the “magnetic” basis illustrated in Fig. 1. While the states $|1\rangle$ and $|\bar{1}\rangle$ are truly magnetic, in the sense of possessing a finite spin-dipole moment, the same is not true of $|0\rangle$, for which

$$\langle 0|\hat{S}^x|0\rangle = \langle 0|\hat{S}^y|0\rangle = \langle 0|\hat{S}^z|0\rangle = 0. \quad (23)$$

This result follows straightforwardly from the fact that

$$|z\rangle = -i|0\rangle, \quad (24)$$

is invariant under time-reversal symmetry [56]

$$\mathcal{T}|z\rangle = |z\rangle. \quad (25)$$

It follows that $|0\rangle \propto |z\rangle$ is incapable of supporting a dipole moment since, such a moment would, by definition, break time-reversal symmetry.

Instead, the state $|0\rangle$ possesses a finite spin-quadrupole moment. Spin quadrupoles are defined through the symmetric, traceless rank-2 tensor

$$\hat{Q}^{\alpha\beta} = \hat{S}^{\alpha}\hat{S}^{\beta} + \hat{S}^{\beta}\hat{S}^{\alpha} - \frac{2}{3}\delta^{\alpha\beta}s(s+1), \quad (26)$$

and so are invariant under time-reversal symmetry. The state $|0\rangle$, exhibits two non-zero matrix elements

$$\langle 0|\hat{S}^x\hat{S}^x|0\rangle = \langle 0|\hat{S}^y\hat{S}^y|0\rangle = 1, \quad (27)$$

implying that both Q^{xx} and Q^{yy} take on a finite value. Moreover the fact that

$$\langle 0|\hat{S}^z\hat{S}^z|0\rangle = 0 \quad (28)$$

implies that $|0\rangle$ breaks spin–rotation invariance, even though it does not possess a finite dipole moment.

The possibility of finding a finite quadrupole moment on a single site sharply distinguishes spin–1 moments from spin–1/2 moments. And spin–1 are special in the sense that they are the smallest spin able to support a quadrupole moment on a single site, making them a good candidate to illustrate both magnetism based on higher order–moments, and quantum effects.

More generally, any state of a spin–1 moment can be described through a linear superposition of the states \mathcal{B}_1

$$|\psi_1\rangle = c_1|1\rangle + c_2|0\rangle + c_3|\bar{1}\rangle, \quad (29)$$

where the complex numbers c_1, c_2, c_3 , are subject to the constraint

$$|c_1|^2 + |c_2|^2 + |c_3|^2 = 1. \quad (30)$$

Resolving this constraint immediately reduces the number of real parameters needed to specify $|\psi_1\rangle$ to five. Furthermore, no physical properties of the state depend on the overall phase of $|\psi_1\rangle$. It follows that any state of a spin–1 moment can be fully characterised using a total of four real numbers. Formally, this is equivalent to working in the complex projective plane $\mathbb{C}\mathbb{P}^2$.

The algebra which connects states within this Hilbert space is $su(3)$, with eight generators, for which the Gell–Mann matrices

$$\begin{aligned} \lambda_1 &= \begin{pmatrix} 0 & 1 & 0 \\ 1 & 0 & 0 \\ 0 & 0 & 0 \end{pmatrix}, \quad \lambda_2 = \begin{pmatrix} 0 & -i & 0 \\ i & 0 & 0 \\ 0 & 0 & 0 \end{pmatrix}, \quad \lambda_3 = \begin{pmatrix} 1 & 0 & 0 \\ 0 & -1 & 0 \\ 0 & 0 & 0 \end{pmatrix}, \\ \lambda_4 &= \begin{pmatrix} 0 & 0 & 1 \\ 0 & 0 & 0 \\ 1 & 0 & 0 \end{pmatrix}, \quad \lambda_5 = \begin{pmatrix} 0 & 0 & -i \\ 0 & 0 & 0 \\ i & 0 & 0 \end{pmatrix}, \quad \lambda_6 = \begin{pmatrix} 0 & 0 & 0 \\ 0 & 0 & 1 \\ 0 & 1 & 0 \end{pmatrix}, \\ \lambda_7 &= \begin{pmatrix} 0 & 0 & 0 \\ 0 & 0 & -i \\ 0 & i & 0 \end{pmatrix}, \quad \lambda_8 = \frac{1}{\sqrt{3}} \begin{pmatrix} 1 & 0 & 0 \\ 0 & 1 & 0 \\ 0 & 0 & -2 \end{pmatrix}, \end{aligned} \quad (31)$$

provide a convenient representation, albeit one with complex commutation relations [57].

It is immediately apparent that algebra describing a spin–1 moment is much richer than that describing a spin–1/2. In fact the three $SU(2)$ rotations needed to describe a spin–1/2 moment, Eq. (18), correspond to the generators of rotations

$$\hat{\mathbf{S}} = (\hat{S}^x, \hat{S}^y, \hat{S}^z)^t, \quad (32)$$

and form a closed sub–algebra of $su(3)$. Meanwhile the five additional generators found in $su(3)$ can be identified with the

quadrupole moments

$$\begin{aligned} \hat{\mathbf{Q}} &= \begin{pmatrix} \hat{Q}^{x^2-y^2} \\ \hat{Q}^{3z^2-s^2} \\ \hat{Q}^{xy} \\ \hat{Q}^{xz} \\ \hat{Q}^{yz} \end{pmatrix} = \begin{pmatrix} \frac{1}{2}(\hat{Q}^{xx} - \hat{Q}^{yy}) \\ \frac{1}{\sqrt{3}}(\hat{Q}^{zz} - \frac{1}{2}(\hat{Q}^{xx} + \hat{Q}^{yy})) \\ \hat{Q}^{xy} \\ \hat{Q}^{xz} \\ \hat{Q}^{yz} \end{pmatrix} \\ &= \begin{pmatrix} (\hat{S}^x)^2 - (\hat{S}^y)^2 \\ \frac{1}{\sqrt{3}}(2(\hat{S}^z)^2 - (\hat{S}^x)^2 - (\hat{S}^y)^2) \\ \hat{S}^x\hat{S}^y + \hat{S}^y\hat{S}^x \\ \hat{S}^x\hat{S}^z + \hat{S}^z\hat{S}^x \\ \hat{S}^y\hat{S}^z + \hat{S}^z\hat{S}^y \end{pmatrix}. \end{aligned} \quad (33)$$

as previously listed in Eq. (3). We note that the vector notation [Eq. (3)], and tensor notation [Eq. (26)], are linked by

$$\hat{\mathbf{Q}} \cdot \hat{\mathbf{Q}} = \sum_{\alpha} \hat{Q}^{\alpha} \hat{Q}^{\alpha} = \frac{1}{2} \sum_{\alpha\beta} \hat{Q}^{\alpha\beta} \hat{Q}^{\alpha\beta}, \quad (34)$$

and in what follows we shall follow the Einstein convention of assuming sums on repeated indices of tensors.

It is worth noting that, while the algebra $su(3)$ has eight generators, a general $SU(3)$ rotation can be constructed using a subset of four of these [68]. It follows that (as argued above), only four real parameters are needed to parameterise any spin–1 state.

2. Time–reversal invariant basis

The ‘‘magnetic’’ basis, Eq. (22), is the most commonly used description of a spin–1 moment. However this choice of basis is not unique, and any linear combination of Eq. (22) which forms 3 orthogonal states can serve equally well. For many purposes it is more convenient to describe spin–1 moments in a basis of time–reversal invariant states, satisfying

$$\mathcal{T}|\phi\rangle = |\phi\rangle. \quad (35)$$

A suitable time–reversal invariant basis is given by

$$\mathcal{B}_2 = \{|x\rangle, |y\rangle, |z\rangle\}, \quad (36)$$

where

$$|x\rangle = \frac{i}{\sqrt{2}}(|1\rangle - |\bar{1}\rangle), \quad |y\rangle = \frac{1}{\sqrt{2}}(|1\rangle + |\bar{1}\rangle), \quad |z\rangle = -i|0\rangle. \quad (37)$$

This basis is illustrated in Fig. 5. Within this basis, any state of a spin–1 can be decomposed in terms of complex coefficients d_{α}^*

$$|\mathbf{d}\rangle = \sum_{\alpha=x,y,z} d_{\alpha}^* |\alpha\rangle, \quad d_{\alpha}^* \in \mathbb{C}, \quad (38)$$

which we collect in a complex vector (director) \mathbf{d} , of unit length

$$\mathbf{d}^* \cdot \mathbf{d} = 1. \quad (39)$$

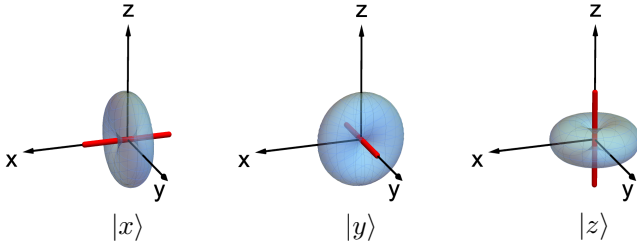


Figure 5. Time-reversal invariant basis for a spin-1 moment. The three states $|\alpha\rangle$, with $\alpha = x, y, z$, are invariant under time-reversal, and satisfy $\langle\alpha|S^\mu|\alpha\rangle = 0$, for $\mu = x, y, z$ referring to the usual spacial spin components. These states can be expressed in terms of the usual magnetic basis [Fig. 1] through Eq. (37), and exhibit a characteristic “doughnut-shaped” profile of spin fluctuations [Appendix A].

We can further separate this into a real and imaginary parts

$$\mathbf{d}^* = \mathbf{u} + i\mathbf{v}, \quad (40)$$

providing a represent of a spin-1 in terms of two real, three-dimensional vectors, subject to the constraint

$$\mathbf{u} \cdot \mathbf{u} + \mathbf{v} \cdot \mathbf{v} = 1. \quad (41)$$

All of the operators needed to characterise a spin-1 moment can also be written in terms of matrix elements of the time-reversal invariant basis [Eq. (37)], with spin operators given by the antisymmetric contraction

$$\hat{S}^\alpha = -i\epsilon^{\alpha\beta\gamma}|\beta\rangle\langle\gamma|, \quad (42)$$

while quadrupoles by the symmetric contraction

$$\hat{Q}^{\alpha\beta} = -|\alpha\rangle\langle\beta| - |\beta\rangle\langle\alpha| + \frac{2}{3}\delta^{\alpha\beta}|\gamma\rangle\langle\gamma|. \quad (43)$$

We can use these results to express the expected dipole-moment

$$\langle\mathbf{d}|\hat{S}^\alpha|\mathbf{d}\rangle = 2\epsilon^{\alpha\beta\gamma}u^\beta v^\gamma, \quad (44)$$

and quadrupole-moment

$$\langle\mathbf{d}|\hat{Q}^{\alpha\beta}|\mathbf{d}\rangle = -2(u^\alpha u^\beta + v^\alpha v^\beta) + \frac{2}{3}\delta^{\alpha\beta}(u^\gamma u^\gamma + v^\gamma v^\gamma), \quad (45)$$

moments of a general state $|\mathbf{d}\rangle$ [Eq. (38)], in terms of \mathbf{u} and \mathbf{v} [Eq. (40)]. In vector form, the equation for the dipole moment [Eq. (44)] then becomes

$$\langle\mathbf{S}\rangle = 2\mathbf{u} \times \mathbf{v}, \quad (46)$$

and we see that if the director \mathbf{d} is either purely real, or purely imaginary, the associated dipole moments will be zero.

3. Description in terms of $u(3)$

The form of the expressions for spin- [Eq. (42)] and quadrupole-moments [Eq. (43)], motivates us to introduce an object with matrix elements

$$\hat{\mathcal{A}}_\gamma^\alpha = |\alpha\rangle\langle\gamma|, \quad (47)$$

i.e.

$$\hat{\mathbf{A}} = \begin{pmatrix} |x\rangle\langle x| & |x\rangle\langle y| & |x\rangle\langle z| \\ |y\rangle\langle x| & |y\rangle\langle y| & |y\rangle\langle z| \\ |z\rangle\langle x| & |z\rangle\langle y| & |z\rangle\langle z| \end{pmatrix}, \quad (48)$$

colloquially referred to as the “*A*-matrix” [14]. (More precisely formulated, $\hat{\mathbf{A}}$ is a tensor, as described in Section II B 5). The matrix $\hat{\mathbf{A}}$ acts on the basis of time-reversal invariant states, and is subject to the constraint

$$\text{Tr } \hat{\mathbf{A}} = 1, \quad (49)$$

following from the normalisation of the spin state, Eq. (30). It is now straightforward to transcribe both spin-

$$\hat{S}^\alpha = -i\epsilon^{\alpha\beta\gamma}\hat{\mathcal{A}}_\gamma^\beta, \quad (50)$$

and quadrupole-moments

$$\hat{Q}^{\alpha\beta} = -\hat{\mathcal{A}}_\beta^\alpha - \hat{\mathcal{A}}_\alpha^\beta + \frac{2}{3}\delta^{\alpha\beta}\hat{\mathcal{A}}_\gamma^\gamma, \quad (51)$$

in terms of matrix elements of $\hat{\mathbf{A}}$ [Eq. (47)].

A convenient basis for $\hat{\mathbf{A}}$ is provided by a set of matrices with a single non-zero element [14],

$$\begin{aligned} \hat{\mathcal{A}}_1^1 &= \begin{pmatrix} 1 & 0 & 0 \\ 0 & 0 & 0 \\ 0 & 0 & 0 \end{pmatrix}, \quad \hat{\mathcal{A}}_2^1 = \begin{pmatrix} 0 & 1 & 0 \\ 0 & 0 & 0 \\ 0 & 0 & 0 \end{pmatrix}, \quad \hat{\mathcal{A}}_3^1 = \begin{pmatrix} 0 & 0 & 1 \\ 0 & 0 & 0 \\ 0 & 0 & 0 \end{pmatrix}, \\ \hat{\mathcal{A}}_1^2 &= \begin{pmatrix} 0 & 0 & 0 \\ 1 & 0 & 0 \\ 0 & 0 & 0 \end{pmatrix}, \quad \hat{\mathcal{A}}_2^2 = \begin{pmatrix} 0 & 0 & 0 \\ 0 & 1 & 0 \\ 0 & 0 & 0 \end{pmatrix}, \quad \hat{\mathcal{A}}_3^2 = \begin{pmatrix} 0 & 0 & 0 \\ 0 & 0 & 1 \\ 0 & 0 & 0 \end{pmatrix}, \\ \hat{\mathcal{A}}_1^3 &= \begin{pmatrix} 0 & 0 & 0 \\ 0 & 0 & 0 \\ 1 & 0 & 0 \end{pmatrix}, \quad \hat{\mathcal{A}}_2^3 = \begin{pmatrix} 0 & 0 & 0 \\ 0 & 0 & 0 \\ 0 & 1 & 0 \end{pmatrix}, \quad \hat{\mathcal{A}}_3^3 = \begin{pmatrix} 0 & 0 & 0 \\ 0 & 0 & 0 \\ 0 & 0 & 1 \end{pmatrix}, \end{aligned} \quad (52)$$

These matrices satisfy the closed algebra $u(3)$, with commutation relations

$$\begin{aligned} [\hat{\mathcal{A}}_{i\beta}^\alpha, \hat{\mathcal{A}}_{i\eta}^\gamma] &= \delta^{\gamma\beta}\hat{\mathcal{A}}_{i\eta}^\alpha - \delta^{\alpha\eta}\hat{\mathcal{A}}_{i\beta}^\gamma, \\ [\hat{\mathcal{A}}_{i\beta}^\alpha, \hat{\mathcal{A}}_{j\eta}^\gamma] &= 0, \end{aligned} \quad (53)$$

previously introduced in Eq. (8).

Alternative representations of $U(3)$ are possible, and have their own merits [69]. The specific advantage of the basis given in Eq. (52) is its simplicity. And, in conjunction with complex coefficients, this basis can be used to describe all possible states of a spin-1 moment. Once again, after constraints coming from the Hermitian nature of $\hat{\mathcal{A}}_\beta^\alpha$ [Eq. (48)], its trace [Eq. (49)], and the fact that it is proportional to a projection operator have been taken into account, this requires a total of four real coefficients [70].

4. Relationship between $U(3)$ and $SU(3)$ representations

The representation of a spin-1 moment in terms of the nine matrices $\hat{\mathcal{A}}_\beta^\alpha$ [Eq. (52)], contains one additional operator, relative to the eight generators of $SU(3)$ [Eq. (31)]. The resolution of this seeming paradox rests in enforcing the constraint that each site is occupied by a single spin-1 moment.

Relative to $U(3)$, the operator “missing” from $SU(3)$ is the spin-length $\hat{\mathbf{S}}^2$. Once this is included, there exists a specific transformation relating the representation of $SU(3)$ in terms of dipole [Eq. (32)] and quadrupole [Eq. (33)] moments, and the representation of $U(3)$ in terms of the nine generators $\hat{\mathbf{A}}_\beta^\alpha$ [Eq. (52)]

$$\begin{pmatrix} \hat{\mathbf{S}}^2 \\ \hat{S}^x \\ \hat{S}^y \\ \hat{S}^z \\ \hat{Q}^{x^2-y^2} \\ \hat{Q}^{3r^2-s^2} \\ \hat{Q}^{xy} \\ \hat{Q}^{xz} \\ \hat{Q}^{yz} \end{pmatrix} = C \begin{pmatrix} \hat{\mathcal{A}}_1^1 \\ \hat{\mathcal{A}}_2^1 \\ \hat{\mathcal{A}}_3^1 \\ \hat{\mathcal{A}}_1^2 \\ \hat{\mathcal{A}}_2^2 \\ \hat{\mathcal{A}}_3^2 \\ \hat{\mathcal{A}}_1^3 \\ \hat{\mathcal{A}}_2^3 \\ \hat{\mathcal{A}}_3^3 \end{pmatrix}, \quad (54)$$

where C is the 9×9 matrix.

$$C = \begin{pmatrix} 2 & 0 & 0 & 0 & 2 & 0 & 0 & 0 & 2 \\ 0 & 0 & 0 & 0 & 0 & -i & 0 & i & 0 \\ 0 & 0 & i & 0 & 0 & 0 & -i & 0 & 0 \\ 0 & -i & 0 & i & 0 & 0 & 0 & 0 & 0 \\ -1 & 0 & 0 & 0 & 1 & 0 & 0 & 0 & 0 \\ \frac{1}{\sqrt{3}} & 0 & 0 & 0 & \frac{1}{\sqrt{3}} & 0 & 0 & 0 & -\frac{2}{\sqrt{3}} \\ 0 & -1 & 0 & -1 & 0 & 0 & 0 & 0 & 0 \\ 0 & 0 & -1 & 0 & 0 & 0 & -1 & 0 & 0 \\ 0 & 0 & 0 & 0 & 0 & -1 & 0 & -1 & 0 \end{pmatrix}, \quad (55)$$

previously shown schematically as Eq. (7).

We can fix the spin sector, and thereby restrict fluctuations to the smaller group $SU(3)$, by imposing the constraint

$$\text{Tr} \mathcal{A} = \sum_\alpha \hat{\mathcal{A}}_i^\alpha = \sum_\alpha \frac{1}{2} \hat{S}_i^\alpha \hat{S}_i^\alpha = \frac{1}{2} s(s+1) = 1, \quad (56)$$

where we have used the property

$$\sum_\alpha \hat{Q}_i^{\alpha\alpha} = 0. \quad (57)$$

It follows that, for purposes of simulation of spin-1 moments, we can work directly with the matrices $\hat{\mathbf{A}}$, as long as these satisfy the constraint Eq. (49). This constraint was previously introduced as Eq. (10).

5. Mathematical properties of $\hat{\mathbf{A}}$ -matrices

While it is convenient to refer to the operators $\hat{\mathcal{A}}_\beta^\alpha$ as matrices, they are in fact tensors. The tensor nature of these objects is explored in Appendix B. Here we single out a property

which will prove useful in subsequent derivations, namely the way in which $\hat{\mathcal{A}}_\beta^\alpha$ transforms under a linear map.

The operator $\hat{\mathcal{A}}_\beta^\alpha$ is defined through matrix elements of the time-reversal invariant basis [Eq. (36)]. In defining $\hat{\mathcal{A}}_\gamma^\alpha$ [Eq. (47)], we introduced both a contravariant index α , and a covariant index γ . This distinction follows from the fact that the index α relates to a bra vector, while the index γ related to a ket vector. Bra-vectors and ket-vectors (such as the states in the basis \mathcal{B}_2 [Eq. (36)]), inhabit mutually-dual vector spaces. And for this reason, contravariant and covariant indexes will transform differently under a linear transformation of basis vectors.

Let us consider a general linear transformation

$$\Lambda : V \rightarrow V, \quad (58)$$

with

$$\det \Lambda \neq 0, \quad (59)$$

such that Λ is invertible, and define

$$\tilde{\Lambda} = (\Lambda^{-1})^T. \quad (60)$$

Under this transformation, the components of $\hat{\mathcal{A}}_\beta^\alpha$ will transform as

$$(\hat{\mathcal{A}}_\beta^\alpha)^\mu_\nu = \Lambda^\mu_\gamma \tilde{\Lambda}^\kappa_\nu (\hat{\mathcal{A}}_\beta^\alpha)^\gamma_\kappa = \Lambda^\mu_\gamma (\Lambda^{-1})^\kappa_\nu (\hat{\mathcal{A}}_\beta^\alpha)^\gamma_\kappa, \quad (61)$$

where we once again assume the Einstein convention of summing on repeated indices.

This result can be interpreted as follows: $\hat{\mathcal{A}}_\beta^\alpha$ is properly considered to be a $(1, 1)$ -tensor, implying that the linear map takes one element in the vector space V , and a second one in the dual vector space V^* , and assigns then a number in the field F , for which the multiplication of the vector space is defined. And, crucially, the only non-zero component of $(\hat{\mathcal{A}}_\beta^\alpha)^\gamma_\kappa$ in the time-reversal invariant basis is

$$(\hat{\mathcal{A}}_\beta^\alpha)^\alpha_\beta. \quad (62)$$

This fact, and the mapping Eq. (61) will prove important where we use the generators $\hat{\mathcal{A}}_\beta^\alpha$ to derive a theory of small fluctuations about an ordered state, in Section IV A.

We will briefly comment on two other mathematical properties of the operators $\hat{\mathbf{A}}$ which will prove useful in later calculations. Firstly, it is possible to construct any state $|\alpha = x, y, z\rangle$ in the basis \mathcal{B}_2 [Eq. (36)] as

$$|\alpha\rangle = d^{\dagger\alpha} |\text{vac}\rangle, \quad (63)$$

where \hat{d}_α satisfies the Bosonic commutation relation

$$[\hat{d}_\alpha, d^{\dagger\alpha}] = \delta_{\alpha\beta}, \quad (64)$$

and $|\text{vac}\rangle$ is the vacuum. It follows that we can build the matrix $\hat{\mathbf{A}}$ as the exterior product of the operators \hat{d}_α ,

$$\hat{\mathcal{A}}_\beta^\alpha = d^{\dagger\alpha} \hat{d}_\beta. \quad (65)$$

This particular representation will prove useful when it comes to constructing a quantum theory of excitations in [Section V](#). And an interesting corollary of [Eq. \(65\)](#) is that the overall phase of the operator \hat{d}_α plays no part in determining \hat{A}_{β}^α .

Secondly, it is helpful to note that

$$\sum_{\alpha,\beta} \hat{A}_{i\beta}^\alpha \hat{A}_j^\beta = \sum_{\alpha,\beta} \frac{1}{4} \hat{Q}_i^{\alpha\beta} \hat{Q}_j^{\beta\alpha} + \sum_{\alpha} \frac{1}{2} \hat{S}_i^\alpha \hat{S}_j^\alpha + \frac{1}{12} s^2 (s+1)^2. \quad (66)$$

This result will prove useful when considering the sum rules on structure factors in [Section IV C 2](#) and [Section V B](#).

C. Representation of the BBQ model within a $u(3)$ formalism

The most general form of nearest-neighbour Hamiltonian permitted by $SU(2)$ symmetry for a spin-1 magnet is the bilinear-biquadratic (BBQ) model

$$\mathcal{H}_{\text{BBQ}} = \sum_{\langle i,j \rangle} \left[J_1 \hat{S}_i \cdot \hat{S}_j + J_2 (\hat{S}_i \cdot \hat{S}_j)^2 \right], \quad (67)$$

previously introduced in [Eq. \(1\)](#). This model has been studied extensively, in the context of spin-1 magnets [[13](#), [14](#), [16–20](#), [52](#), [53](#), [56](#)], systems of cold atoms [[44–46](#), [71–75](#)], and as a toy model for nematic order in Fe-based superconductors [[39–43](#)] and spin-1/2 magnets [[76](#)].

The physical nature of the interactions in the BBQ model is most obvious once it is recast in terms of generators of $SU(3)$, via [Eq. \(33\)](#),

$$\mathcal{H}_{\text{BBQ}} = \sum_{\langle i,j \rangle} \left(J_1 - \frac{J_2}{2} \right) \hat{S}_i \cdot \hat{S}_j + \frac{J_2}{2} \hat{Q}_i \cdot \hat{Q}_j + \frac{4J_2}{3}, \quad (68)$$

a form previously introduced in [Eq. \(4\)](#). Here biquadratic interactions are revealed as an interaction between on-site quadrupoles, which are explicitly forbidden for spin-1/2 moments.

Biquadratic interactions can have a number of different microscopic origins. In insulating magnets, high-spin moments involve electrons with more than one orbital, and biquadratic interactions follow from the exchange of electrons in different orbitals, on different sites [[3](#)]. Similarly, in systems of cold atoms, biquadratic interactions follow from the structure of the underlying Mott physics, which may be Bosonic [[44–48](#), [71](#), [73](#), [74](#), [77](#)] or Fermionic [[72](#), [75](#), [78](#), [79](#)] in character. More generally, biquadratic interactions can also arise as an effective interaction coming from spin-lattice coupling [[80](#)], or as a consequence of integrating out quantum or thermal fluctuations [[81](#)].

The $SU(2)$ -invariance of \mathcal{H}_{BBQ} can be read directly from [Eq. \(67\)](#) or [Eq. \(68\)](#). The scalar contractions $\hat{S}_i \cdot \hat{S}_j$ and $\hat{Q}_i \cdot \hat{Q}_j$ are both unchanged by rotations belong to the group $O(3)$, which provides 2-fold cover for the group $SU(2)$. However $SU(2)$ is not the highest symmetry which can be achieved, and for the specific choice of parameters $J_1 = J_2 = J$, the symmetry of the model is enlarged to $SU(3)$ [[14](#), [20](#), [56](#)]. In

this case, the BBQ model can be rewritten

$$\mathcal{H}_{\text{BBQ}} = \frac{J}{2} \sum_{\langle i,j \rangle} \mathbf{T}_i \cdot \mathbf{T}_j + \frac{4J}{3}, \quad (69)$$

where \mathbf{T}_i is the eight-dimensional vector

$$\mathbf{T}_i = (\hat{S}_i^x, \hat{S}_i^y, \hat{S}_i^z, \hat{Q}_i^{x^2-y^2}, \hat{Q}_i^{3x^2-s^2}, \hat{Q}_i^{xy}, \hat{Q}_i^{xz}, \hat{Q}_i^{yz}), \quad (70)$$

and it is possible to rotate dipole moments into quadrupoles (or vice versa) without any cost in energy [[20](#)]. Consistent with this, the high-symmetry $SU(3)$ points define the zero-temperature boundaries between phases with dipolar and quadrupolar character, as illustrated in [Fig. 2](#).

It is also possible to transcribe \mathcal{H}_{BBQ} in terms of generators of $U(3)$. Starting from [Eq. \(68\)](#), and using [Eq. \(50\)](#) and [Eq. \(51\)](#) — or, equivalently, [Eq. \(54\)](#) — we find

$$\mathcal{H}_{\text{BBQ}} = \sum_{\langle i,j \rangle} \left[J_1 \hat{A}_{i\beta}^\alpha \hat{A}_j^\beta + (J_2 - J_1) \hat{A}_{i\beta}^\alpha \hat{A}_j^\alpha + J_2 \hat{A}_{i\alpha}^\alpha \hat{A}_j^\beta \right] \quad (71)$$

Imposing the constraint on the trace of the A-matrix [[Eq. \(56\)](#)], this simplifies to

$$\mathcal{H}_{\text{BBQ}} = \sum_{\langle i,j \rangle} \left[J_1 \hat{A}_{i\beta}^\alpha \hat{A}_j^\beta + (J_2 - J_1) \hat{A}_{i\beta}^\alpha \hat{A}_j^\beta + J_2 \right], \quad (72)$$

where sums on repeated indices are assumed. This result was previously introduced in [Eq. \(9\)](#).

The $U(3)$ formulation of the BBQ model, [Eq. \(72\)](#), contains terms which transform in two different ways under spin rotations. Using results of [Section II B 5](#), we can show that the second term,

$$\hat{A}_{i\beta}^\alpha \hat{A}_j^\alpha$$

is invariant under $O(3) \simeq SU(2)$ rotations. Meanwhile the first term

$$\hat{A}_{i\beta}^\alpha \hat{A}_j^\beta$$

has indices α and β which transform contravariantly on one site, and covariantly on the other, and therefore possesses $U(3)$ symmetry. This is in turn broken down to $SU(3)$ by the constraint, [Eq. \(56\)](#). Thus, for general parameters, [Eq. \(72\)](#) possesses $SU(2)$ symmetry, but for $J_1 = J_2$, the second term vanishes, and the symmetry is enlarged to $SU(3)$. Further details of this analysis can be found in [Appendix B 1](#).

Crucially, once written in terms of generators of $U(3)$, [Eq. \(72\)](#), the BBQ model takes on a form quadratic in $\hat{A}_{i\beta}^\alpha$, which treats dipole and quadrupole moments on an equal footing. This quadratic form is well-suited to the development of analytic, mean-field approaches, since it facilitates a straightforward decoupling of interactions [[14](#)]. And in [Section III A](#) we show how it can also be used to develop classical Monte Carlo simulations of the thermodynamic properties of spin-1 magnets, which respect the fact that the (semi-)classical limit of a spin-1 moment is not an $O(3)$ vector.

D. Heisenberg equations of motion within a $u(3)$ formalism

The quadratic form of Eq. (72) also makes it well-suited for the derivation of a Heisenberg EoM for a spin-1 magnets, in analogy with the well-known result for $O(3)$ -vectors, Eq. (21). By explicit calculation of commutators, using Eq. (53), and setting $\hbar = 1$, we find

$$\begin{aligned} \partial_t \hat{\mathcal{A}}_{i\eta}^\gamma &= -i \left[\hat{\mathcal{A}}_{i\eta}^\gamma, \mathcal{H}_{\text{BBQ}} \right] \\ &= -i \sum_{\delta} \left[J_1 (\hat{\mathcal{A}}_{i\alpha}^\gamma \hat{\mathcal{A}}_{i+\delta\eta}^\alpha - \hat{\mathcal{A}}_{i\eta}^\alpha \hat{\mathcal{A}}_{i+\delta\alpha}^\gamma) \right. \\ &\quad \left. + (J_2 - J_1) (\hat{\mathcal{A}}_{i\alpha}^\gamma \hat{\mathcal{A}}_{i+\delta\alpha}^\eta - \hat{\mathcal{A}}_{i\eta}^\alpha \hat{\mathcal{A}}_{i+\delta\gamma}^\alpha) \right] \end{aligned} \quad (73)$$

a result previously introduced in Eq. (11).

Like the Hamiltonian it descends from, the EoM, Eq. (73), treats dipole and quadrupole moments on a equal footing, and is ideally-suited to numerical integration, a subject we return to in Section III B. But since this EoM is written in terms of a representation of the algebra $u(3)$, it also describes the dynamics of the operator for the total spin $\hat{\mathbf{S}}^2$. And to correctly describe the dynamics of a spin-1 magnet, we require that

$$s = 1 \Rightarrow \text{Tr } \hat{\mathcal{A}} = 1 \quad (74)$$

throughout [cf. Eq. (56)]. Happily, the EoM for \mathcal{A} -matrices conserves the trace of \mathcal{A} , a fact which follows straightforwardly from Eq. (73)

$$\begin{aligned} \partial_t \left(\text{Tr } \hat{\mathcal{A}}_i \right) &= -i \text{Tr} \sum_{\delta} \left[J_1 (\hat{\mathcal{A}}_{i\alpha}^\gamma \hat{\mathcal{A}}_{i+\delta\eta}^\alpha - \hat{\mathcal{A}}_{i\eta}^\alpha \hat{\mathcal{A}}_{i+\delta\alpha}^\gamma) \right. \\ &\quad \left. + (J_2 - J_1) (\hat{\mathcal{A}}_{i\alpha}^\gamma \hat{\mathcal{A}}_{i+\delta\alpha}^\eta - \hat{\mathcal{A}}_{i\eta}^\alpha \hat{\mathcal{A}}_{i+\delta\gamma}^\alpha) \right] \\ &\equiv 0, \end{aligned} \quad (75)$$

The implication is that, as long as the EoM Eq. (73) is applied to a valid \mathcal{A} -matrix configuration, with $\text{Tr } \mathcal{A}_i \equiv 1$, the time-evolution of the operators $\hat{\mathcal{A}}_{i\beta}^\alpha$ will respect the constraint on spin length. As we shall see in Section VIII, this remains true for systems with interactions which are anisotropic in spin-space, making these EoM a powerful tool for the exploration of the dynamics of spin-1 magnets.

III. NUMERICAL SIMULATION OF SPIN-1 MAGNETS

In Section II, we introduced the technical framework needed to describe a spin-1 magnet in terms of a suitable representation of $u(3)$, \mathcal{A}_β^α [Eq. (48)]. This allowed us to write both the BBQ model, \mathcal{H}_{BBQ} [Eq. (72)], and its associated equation of motion [Eq. (73)], in a simple form, bilinear in \mathcal{A}_β^α , without making any approximation as to its physical content.

In what follows we develop these results into a practical scheme for the numerical simulation of spin-1 magnets, providing technical details the updates needed for both classical Monte Carlo (MC) and (semi-)classical Molecular Dynamics (MD) simulations, carried out in the space of the “A-matrices”, \mathcal{A}_β^α . We will refer to these approaches as “u3MC” and “u3MD”, respectively.

We demonstrate the validity of this approach by reproducing known results for the thermodynamics of the spin-1 BBQ model on the triangular lattice, at the border of ferroquadrupolar (FQ) and antiferromagnetic (AFM) order [54]. We also obtain a complete finite-temperature phase diagram for this model, previously exhibited in Fig. 3.

The detailed application of the method to the thermodynamics and dynamics of the ferroquadrupolar (FQ) phase will be described in Section VI.

A. Monte Carlo simulations within $u(3)$ framework

1. Implementation of u3MC update

The starting point for both MC and MD simulations of spin-1 magnets, is a product wave function written in the space of \mathcal{A} -matrices,

$$|\Psi_{\mathcal{A}}\rangle = \prod_{i=1}^N |\mathcal{A}_i\rangle = \prod_{i=1}^N \sum_{\alpha\beta} \hat{\mathcal{A}}_{i,\beta}^\alpha |\beta\rangle \equiv \prod_{i=1}^N |\mathbf{d}_i\rangle, \quad (76)$$

where \mathcal{A}_i denotes the nine parameters $\mathcal{A}_{i,\beta}^\alpha$, $|\beta\rangle$ is the basis of time-reversal invariant states [Eq. (36)], and $|\mathbf{d}_i\rangle$ is defined through Eq. (38). From Eq. (72), this state has an associated (classical) energy

$$\begin{aligned} E[\mathcal{A}_i] &= \langle \Psi_{\mathcal{A}} | \mathcal{H}_{\text{BBQ}} | \Psi_{\mathcal{A}} \rangle \\ &= \sum_{\langle i,j \rangle} \sum_{\alpha\beta} \left[J_1 \mathcal{A}_{i,\beta}^\alpha \mathcal{A}_{j,\alpha}^\beta + (J_2 - J_1) \mathcal{A}_{i,\beta}^\alpha \mathcal{A}_{j,\beta}^\alpha + J_2 \right]. \end{aligned} \quad (77)$$

By its nature, such a product wave function is unentangled, and cannot describe quantum effects extending beyond a single site. However it remains a semi-classical approximation in the sense that the quantum mechanics of each spin-1 moment is treated exactly at the level of a single site.

As can be seen from Eq. (76), the product wave function written in terms of \mathcal{A} -matrices is exactly equivalent to one expressed in terms of \mathbf{d} -vectors. It follows that MC simulations can equally well be carried out in the space of \mathbf{d} -vectors, with energy [20, 56]

$$\begin{aligned} E[\mathbf{d}_i] &= \langle \Psi_{\mathbf{d}} | \mathcal{H}_{\text{BBQ}} | \Psi_{\mathbf{d}} \rangle \\ &= \sum_{\langle i,j \rangle} \left[J_1 |\mathbf{d}_i \cdot \bar{\mathbf{d}}_j|^2 + (J_2 - J_1) |\mathbf{d}_i \cdot \mathbf{d}_j|^2 + J_2 \right]. \end{aligned} \quad (78)$$

This approach has been pursued elsewhere, under the name of “semiclassical $SU(3)$ ” or “s $SU(3)$ ” simulation [54]. However for MD simulations, and many analytic calculations, \mathcal{A} -matrices offer a more convenient representation. It is this line we pursue here.

The ingredient needed to convert Eq. (76) and Eq. (77) into a practical MC scheme, is an update capable of generating a sequence of spin configurations $\{\mathcal{A}_i\}$ corresponding to states drawn from a thermal ensemble. We approach this by constructing a Metropolis-style [82] update for a single spin-1

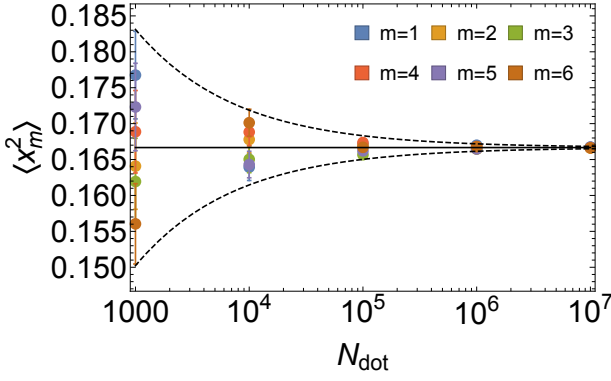


Figure 6. Statistical independence of points generated at random on a 5-dimensional sphere, using Eq. (81). The second moment $\langle x_m^2 \rangle$, of variables x_m , $m = 1, \dots, 6$ is plotted as function of the number of points, N_{dot} . In all cases $\langle x_m^2 \rangle \rightarrow 1/6$ (black line) as $N_{\text{dot}} \rightarrow \infty$. Statistical errors respect the central-limit theorem, and decrease as $1/\sqrt{N_{\text{dot}}}$ (dashed lines).

moment, as represented by a matrix \mathcal{A}_i . More general cluster- [64] or worm- [83] updates could be built along similar lines, but will not be considered here.

We start by revisiting the expression for an individual \mathcal{A} -matrix in terms of the director \mathbf{d} [Eq. (65)]

$$\mathcal{A}_\beta^\alpha = (\mathbf{d}^\alpha)^* \mathbf{d}_\beta, \quad (79)$$

where

$$\mathbf{d} = \begin{pmatrix} x_1 + i x_2 \\ x_3 + i x_4 \\ x_5 + i x_6 \end{pmatrix}; \quad \mathbf{d}^* \mathbf{d} = |\mathbf{d}|^2 = 1. \quad (80)$$

Written in this way, any matrix \mathcal{A}_β^α can be specified in terms of 5 linearly-independent variables, coming from the six coefficients of \mathbf{d} , x_1, x_2, \dots, x_6 , and the constraint on its length.

Constructing a general update for a single spin-1 moment therefore translates into sampling of statistically-independent, equally-distributed points on a 5-dimensional sphere, within a 6-dimensional space. By direct analogy with the Marsaglia construction [84], we write

$$x_1 = \theta_2^{1/4} \theta_1^{1/2} \sin \phi_1, \quad (81a)$$

$$x_2 = \theta_2^{1/4} \theta_1^{1/2} \cos \phi_1, \quad (81b)$$

$$x_3 = \theta_2^{1/4} \sqrt{1 - \theta_1} \sin \phi_2, \quad (81c)$$

$$x_4 = \theta_2^{1/4} \sqrt{1 - \theta_1} \cos \phi_2, \quad (81d)$$

$$x_5 = \sqrt{1 - \theta_2^{1/2}} \sin \phi_3, \quad (81e)$$

$$x_6 = \sqrt{1 - \theta_2^{1/2}} \cos \phi_3, \quad (81f)$$

where $0 \leq \theta_1, \theta_2 \leq 1$ and $0 \leq \phi_1, \phi_2, \phi_3 < 2\pi$ are parameters chosen at random from a uniform distribution. By construction, $|\mathbf{d}|^2 = 1$, and it follows from Eq. (79) that $\text{Tr } \mathcal{A} = 1$. This ensures that all states generated remain within the Hilbert space for a spin-1 moment [cf. Eq. (49)].

Evidence for the statistical validity of this generalised Marsaglia approach is shown in Fig. 6. The second moment $\langle x_m^2 \rangle$ of each variable x_1, \dots, x_6 [Eq. (81)] converges to $1/6$ (black line) as the number of points $N_{\text{dot}} \rightarrow \infty$, implying that x_m are uncorrelated. Statistical errors respect the central-limit theorem and decrease as $1/\sqrt{N_{\text{dot}}}$, indicated with a dashed line.

Eq. (81) provides a valid generalisation of Marsaglia construction from an $O(3)$ vector to a $U(3)$ matrix, and will form the basis for the majority of simulation results shown in this Article. None the less, it is worth noting that this approach is redundant, in that the matrix \mathcal{A}_β^α can be fully characterised using only 4 parameters. This fact is linked to the structure of representations of $SU(3)$ [68], and can be understood directly from Eq. (79): By construction, \mathcal{A}_β^α is independent of the overall phase of \mathbf{d} , leading to a gauge-like redundancy in the 5-dimensional parameterisation, Eq. (81). It must therefore be possible to define a Monte Carlo update which acts within a 4-dimensional subspace of the parameters in Eq. (81), corresponding to the $\mathbb{C}\mathbb{P}^2$ space of the spin-1 moment.

There is no unique prescription for obtaining a 4-dimensional update in the space of $U(3)$ matrices. But one very simple approach [85] is to set $\phi_3 = \pi/2$ in Eq. (81), so that the z -component of \mathbf{d} is purely real, vis

$$x_1 = \theta_2^{1/4} \theta_1^{1/2} \sin \phi_1, \quad (82a)$$

$$x_2 = \theta_2^{1/4} \theta_1^{1/2} \cos \phi_1, \quad (82b)$$

$$x_3 = \theta_2^{1/4} \sqrt{1 - \theta_1} \sin \phi_2, \quad (82c)$$

$$x_4 = \theta_2^{1/4} \sqrt{1 - \theta_1} \cos \phi_2, \quad (82d)$$

$$x_5 = \sqrt{1 - \theta_2^{1/2}}, \quad (82e)$$

$$x_6 = 0, \quad (82f)$$

We have confirmed that this alternative parameterisation of \mathcal{A}_β^α produces identical results in simulations of the BBQ model, a point which we return to below.

Irrespective of whether the update is 4- or 5-dimensional, our Monte Carlo scheme is defined by selecting a site within the lattice at random, and using Eq. (81) to generate a new configuration of the \mathcal{A} -matrix at that site. Following the standard Metropolis argument [82], the new state μ is accepted if

$$r_0 \leq e^{-\beta(E_\mu - E_\nu)}, \quad (83)$$

where r_0 is number chosen at random on the interval $r_0 \in (0, 1)$, $\beta = \frac{1}{k_B T}$ (we set $k_B = 1$), and E_ν is the energy of the initial configuration. A single MC step consists of N such local updates, where N is the total number of sites in the system. In addition, we use the replica-exchange method (parallel tempering) to reduce auto-correlation within the resulting Markov chain [86, 87]. An exchange of replicas is carried out every 100 MC steps.

Simulations are initialized from a state with randomly chosen \mathcal{A} -matrices, mimicking a high-temperature paramagnet. Thermalisation is accomplished by cooling the system adiabatically to the target temperature over 10^6 MC steps (simu-

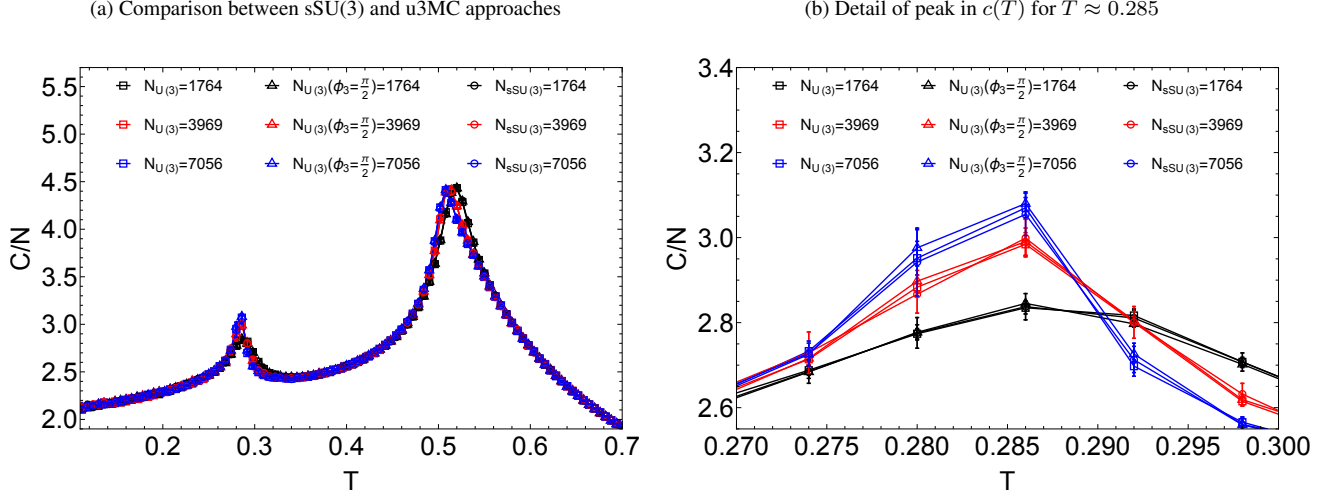


Figure 7. Benchmark of the $U(3)$ Monte Carlo (u3MC) method against published results for the spin-1 bilinear–biquadratic (BBQ) model on the triangular lattice. (a) Specific heat C/N , for parameters $J_1 = 1$, $J_2 = -1.5$, showing double-peak structure. Results are shown for u3MC simulations using both 5-dimensional updates [Eq. 81] — squares, and 4-dimensional double-peak with $\phi_3 = \pi/2$ [Eq. 82] — triangles, and for “sSU(3)” simulations in the space of the complex vector \mathbf{d} , following Stoudenmire *et al.* [54] — circles. Simulations were carried out for clusters of size $N = 1764$ spins (black symbols), 3969 spins (red symbols), and 7056 spins (blue symbols). The results of the three different approaches agree perfectly, within statistical errors. (b) Detail of peak in C/N for $T \approx 0.285$.

lated annealing), followed by a further 10^6 MC steps of thermalisation at that target temperature. Thermodynamic quantities were calculated using averages over 5×10^5 statistically-independent samples.

Further insight into correlations can be gained by calculating the equal-time structure factors

$$S_\lambda(\mathbf{q}) = \left\langle \sum_{\alpha\beta} |m_\lambda^\alpha(\mathbf{q})|^2 \right\rangle \quad (84)$$

where $\langle \dots \rangle$ represents an average over statistically-independent states, and we consider structure factors associated with dipole moments, $\lambda = \mathcal{S}$; quadrupole moments, $\lambda = \mathcal{Q}$; and A-matrices, $\lambda = \mathcal{A}$. Numerically, it is convenient to work with the lattice Fourier transform of $\mathcal{A}_{i\beta}^\alpha$,

$$m_{\mathcal{A}\beta}^\alpha(\mathbf{q}) = \frac{1}{\sqrt{N}} \sum_i e^{i\mathbf{r}_i \cdot \mathbf{q}} \mathcal{A}_{i\beta}^\alpha, \quad (85)$$

which can be found by fast Fourier transform (FFT). From this we can obtain structure factors for both dipole moments [Eq. (50)],

$$m_{\mathcal{S}\alpha}^\alpha(\mathbf{q}) = -i \sum_{\beta,\gamma} \epsilon_{\beta\gamma}^\alpha m_{\mathcal{A}\gamma}^\beta(\mathbf{q}), \quad (86)$$

and quadrupole moments [Eq. (51)],

$$m_{\mathcal{Q}\beta}^\alpha(\mathbf{q}) = -m_{\mathcal{A}\beta}^\alpha(\mathbf{q}) - m_{\mathcal{A}\alpha}^\beta(\mathbf{q}) + \frac{2}{3} \delta^{\alpha\beta} \sum_\gamma m_{\mathcal{A}\gamma}^\gamma(\mathbf{q}), \quad (87)$$

by direct substitution in Eq. (84).

2. Phase diagram and comparison with published results

As a first check on the method, we have carried out u3MC simulations of the thermodynamic properties of spin-1 BBQ model Eq. (67) on a triangular lattice for comparison with published results [19, 20, 54]. Typical results for the heat capacity are shown in Fig. 7, for parameters $J_1 = 1$, $J_2 = -1.5$, chosen to facilitate comparison with earlier work [54]. For these parameters, mean-field calculations find a ground state with 3-sublattice antiferromagnetic (AFM) order, close to a phase boundary with ferroquadrupolar (FQ) order [19, 20].

Simulating in the space of \mathcal{A} -matrices [cf. Section III A 1], we find two peaks in heat capacity, one at $T \approx 0.5 J_1$, corresponding to the onset of FQ fluctuations, and one at $T \approx 0.3 J_1$ corresponding to the onset of AFM fluctuations. In Fig. 7 we show results obtained using both 5-dimensional [Eq. (81)] and 4-dimensional [Eq. (82)] u3MC updates. For comparison, we have also carried out equivalent simulations in the space of \mathbf{d} -vectors, following the sSU(3) approach of Stoudenmire *et al.* [54]. Within statistical errors, we find quantitative agreement between the three different methods.

We have extended this analysis to obtain a complete finite-temperature phase diagram for the BBQ model, previously shown in Fig. 3. Results are shown for a cluster of linear dimension $L = 48$ [$N=2304$ spins]. Phase boundaries were obtained by tracking the evolution of peaks in heat capacity as a function of

$$J_1 = J \cos \theta, \quad J_2 = J \cos \theta \quad (88)$$

and using the equal-time structure factors $S_{\mathcal{S}}(\mathbf{q})$ and $S_{\mathcal{Q}}(\mathbf{q})$ [Eq. (84)] to determine the nature of each phase. Typical results for structure factors evaluated at known ordering vectors, for a temperature $T/J = 0.01$, are shown in Fig. 8.

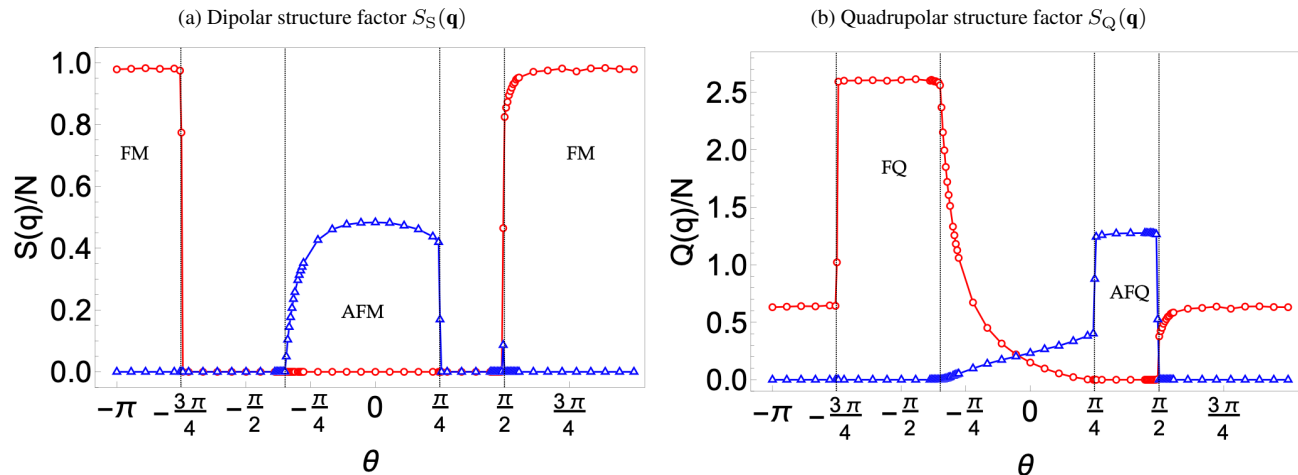


Figure 8. Phases occurring in the spin-1 BBQ model on a triangular lattice at finite temperature, as found in classical Monte Carlo simulation in the space of $u(3)$ matrices (u3MC). (a) Dipolar structure factor $S_S(\mathbf{q})$ [Eq. (84)], showing ferromagnetic (FM) correlations for $\mathbf{q} = \Gamma$ (red circles) and 3-sublattice antiferromagnetic (AFM) correlations for $\mathbf{q} = K$ (blue triangles). (b) Corresponding results for the quadrupolar structure factor $S_Q(\mathbf{q})$ [Eq. (84)], showing ferroquadrupolar (FQ) correlations for $\mathbf{q} = \Gamma$ (red circles) and 3-sublattice antiferroquadrupolar (AFQ) correlations for $\mathbf{q} = K$ (blue triangles). Simulations of Eq. (1) were carried out using the u3MC method described in Section III A 1, at a temperature $T = 0.01 J$, for cluster of linear dimension $L = 48$ ($N = 2304$ spins), with parameters given by Eq. (88). The phases found are in direct correspondence with known results for the mean-field ground state [19, 20, 56], summarised in Fig. 2. In each case the temperature associated with the onset of fluctuations corresponds to the peak found in specific heat, cf. Fig. 3.

The correlations found at low temperature exactly correspond to the four known mean-field ground states [19, 20], having ferromagnetic (FM), antiferromagnetic (AFM), ferroquadrupolar (FQ) and antiferroquadrupolar (AFQ) order, as illustrated in Fig. 2. As previously noted by Stoudenmire *et al.* [54], FQ order occurs as a secondary order parameter within the coplanar AFM ground state. Consistent with this, for $\theta \lesssim -\pi/4$ the onset of FQ fluctuations occurs at a higher temperature than the onset of AFM fluctuations (cf. results for $\theta \approx -0.313 \pi$ in Fig. 7).

We also find that there is a range of parameters $\theta \sim \pi/2$, near the border between FM and AFQ phases for which the onset of FM fluctuations occurs at a higher temperature than the onset of AFQ fluctuations. Here no interpretation in terms of a secondary order-parameter is possible, but once again it is the single-sublattice phase which dominates at higher temperatures. We infer that the entropy of fluctuations about the FM ground state is higher than the entropy of fluctuations about the AFQ ground state, presumably because of the k^2 dispersion of its excitations.

Perhaps the most striking feature of the phase diagram in Fig. 3 are the “vertical” phase boundaries between dipolar and quadrupolar phases at the two $SU(3)$ points, shown as solid red lines. These are consistent with the $SU(3)$ symmetry of the ground-state manifolds being preserved up to temperature associated with the onset of correlations, T^* . And this in turn raises the possibility of finding exotic topological phase transitions at T^* , mediated by topological defects specific to the $SU(3)$ points [61, 88]. We leave this interesting topic for future studies.

In conclusion, our survey of correlations at finite temperature, summarised in Fig. 3 and Fig. 8, provides strong

prima facie evidence that the u3MC approach introduced in Section III A 1 can describe the thermodynamic properties of spin-1 magnets. In Section VI we present a more rigorous test, in the form of a detailed study of the thermodynamic properties of the FQ phase at low temperatures, where we are able to make quantitative comparison with analytic predictions.

B. Molecular Dynamics simulations within $u(3)$ framework

Numerical integration of equations of motion provides a powerful approach to describing the (semi-)classical dynamics of quantum magnets, which can readily be combined with classical Monte Carlo simulation, an approach which has been referred to as “molecular dynamics” (MD) simulation [33, 65, 89–91]. Microscopic approaches typically start from the Heisenberg equation of motion for an $O(3)$ spin, Eq. (21), and have proved surprisingly effective in describing the dynamics of quantum magnets [33, 66, 92, 93].

The success of the MD approach in these cases rests on the fact that an $O(3)$ vector provides an appropriate (semi-)classical description of a spin-1/2 moment. However, in the case of spin-1 magnets, $O(3)$ vectors fail to provide an adequate description, since they do not properly account for quadrupole degrees of freedom [cf. Section II]. This problem has long been understood in the context of the analytic theory of nematic phases [13, 14]. And in general the band-like excitations of spin-1 magnets include both spin waves and quadrupole waves [94]. These can be addressed analytically through a multiple-Boson expansion, also known as “flavour-wave” theory [56].

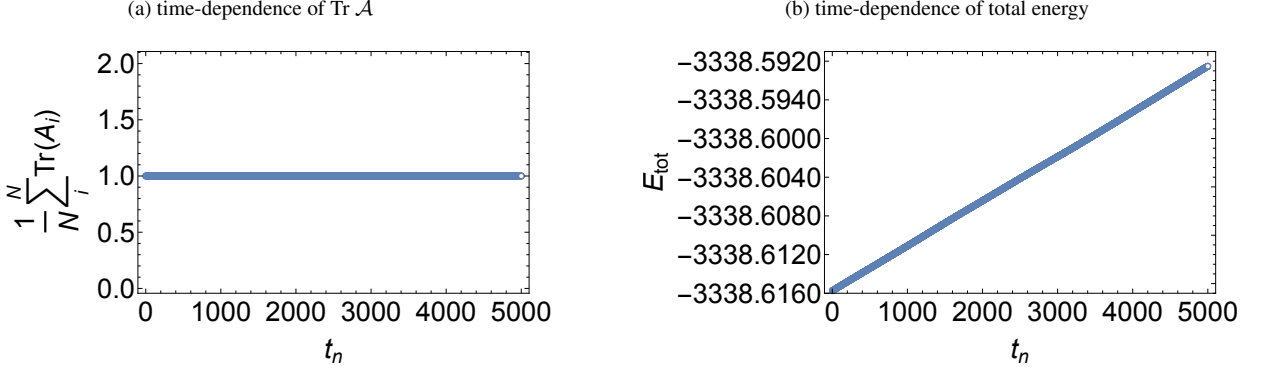


Figure 9. Evidence of stability of numerical integration of equations of motion. (a) Time-dependence of $\text{Tr} \mathcal{A}$ [Eq. (56)], showing conservation of spin to numerical precision. (b) Time-dependence of energy $E = \langle \mathcal{H}_{\text{BBQ}} \rangle$, showing conservation to the level expected for a 4th-order Runge-Kutta (RK-4) algorithm. Simulations were carried out for the spin-1 bilinear-biquadratic model [Eq. (72)], on a triangular-lattice cluster with linear dimension $L = 24$ ($N = 2304$ spins), for parameters $J_1 = 0$, $J_2 = -1$, at a temperature $T = 0.1 J$, using the equation of motion Eq. (73), with a time-step $\delta t = 0.4 J^{-1}$.

Equation of motion approaches to the dynamics of spin-1 magnets have also been developed in terms of spin- and quadrupole-operators [58–60]. However these approaches are complicated by the convoluted nature of the structure constants of the algebra $su(3)$. In contrast, the $u(3)$ framework established in Section II leads to a very compact EoM for \mathcal{A} -matrices, Eq. (73), ideally-suited to numerical integration. And the power of these EoM are greatly enhanced by the fact that they can be combined with the MC methods developed in Section III A, providing an “u3MD” approach to spin-1 magnets, on the same footing as the $O(3)$ methods applied to spin-1/2 magnets.

1. Implementation of u3MD update

Our MD simulations, like the MC simulations described in Section III A 1, are carried out in the basis of states defined by products of \mathcal{A} -matrices [Eq. (76)]. We implement simulations by using a 4th order Runge-Kutta (RK-4) algorithm [95, 96] to numerically integrate Eq. (73) for each component of $\mathcal{A}_{i,\beta}^\alpha$, using a fixed timestep δt_{RK} . Iterative application of RK-integration

$$\{\mathcal{A}_{i,\beta}^\alpha(t)\} \mapsto \{\mathcal{A}_{i,\beta}^\alpha(t + \delta t_{\text{RK}})\} + \mathcal{O}(\delta t_{\text{RK}}^5) \quad (89)$$

generates a time series for $\{\mathcal{A}_{i,\beta}^\alpha(t)\}$ with errors which are controlled by the size of δt_{RK} . A single RK update is defined through numerical integration of Eq. (73) for every spin in the lattice. In order to work with a manageable set of data, while retaining sufficient precision in numerical integration, we store only the result of every 20th global update.

The stored data defines a time series

$$\{\mathcal{A}_\beta^\alpha(i, t_n)\}, \quad t_n = n \delta t, \quad n = 1 \dots N_t, \quad (90)$$

where the size of the effective time step, δt , determines the highest frequency we are able to resolve

$$\delta t = \frac{2\pi}{\omega_{\text{max}}}. \quad (91)$$

Meanwhile the duration of the simulation

$$\Delta t = N_t \delta t, \quad (92)$$

determines the energy-resolution of results

$$\delta \omega = \frac{2\pi}{\Delta t}, \quad (93)$$

where we work in units such that $\hbar = 1$.

In practice, we typically work with a time-series of length

$$N_t = 1600, \quad (94)$$

with effective time-step

$$\delta t \approx 0.4 J^{-1}. \quad (95)$$

It follows that the time-interval used in RK integration for an individual spin is

$$\delta t_{\text{RK}} \equiv \delta t / 20 \approx 0.02 J^{-1}. \quad (96)$$

This choice of parameters is adequate to resolve excitations with energy up to

$$\omega_{\text{max}} \approx 16 J, \quad (97)$$

twice what is needed for individual excitations of the FQ state with parameters

$$(J = 1, \theta = -\frac{\pi}{2}) \Rightarrow (J_1 = 0.0, J_2 = -1.0), \quad (98)$$

cf. Fig. 4. The corresponding energy resolution

$$\delta \omega \approx 10^{-2} J, \quad (99)$$

is sufficient to resolve fine-structure in dynamical structure factors, described below.

The validity of this MD approach depends on the satisfaction of both the constraint on spin-length [Eq. (56)], and on the conservation of the total energy of the system, $E[\mathcal{A}_i]$ [Eq. (77)]. In Fig. 9 we show evidence that both are satisfied,

within controlled errors, for simulations of a triangular-lattice cluster of linear dimension $L = 24$ ($N = 2304$ spins), with model parameters Eq. (98), and time-step Eq. (95), at a temperature $T = 0.1 J$.

We consider first the constraint on spin-length. As discussed in Section II D, as long as the initial configuration $\{\hat{A}_i^\alpha(t=0)\}$ satisfies the spin-length constraint

$$\text{Tr } \hat{A}_i \equiv 1 \quad \forall i \in (1 \dots N), \quad (100)$$

[Eq. (56)], its continued satisfaction is guaranteed by the structure of the EoM, Eq. (73). From Fig. 9 (a), we see that the trace of \mathcal{A}_i is conserved, up to numerical precision, for simulations of duration $N_t = 5000$. This confirms that simulations of any feasible duration, continue to describe spin-1 moments.

We now turn to the conservation of energy. RK-integration is not a symplectic (energy-conserving) method. However the rate at which error accumulates depends on the size of the RK time step, δt_{RK} . And, by making δt_{RK} sufficiently small, errors in energy can be kept bounded. From Fig. 9 (b), we see that the error in energy which accumulates over simulations of duration $N_t = 5000$ is $\approx 0.03 J$. This implies that one ‘‘MD step’’, i.e. a single sweep of the entire lattice using an RK-4 algorithm, introduces an error in total energy of order $\sim 10^{-6} J$. This is sufficiently small to ensure adequate conservation of energy for simulations of practical duration, i.e. $N_t = 1600$, $\Delta t \approx 1600 \times \delta t = 640 J^{-1}$.

2. Calculation of dynamical structure factors

We can analyse the time series $\{\mathcal{A}_\beta^\alpha(i, t_n)\}$ by directly animating the evolution of spin configurations [97], or by calculating dynamical structure factors of the form

$$S_\lambda(\mathbf{q}, t_n) = \left\langle \sum_{\alpha\beta} (m_{\lambda\beta}^\alpha(\mathbf{q}, t_n))^* m_{\lambda\beta}^\alpha(\mathbf{q}, 0) \right\rangle, \quad (101)$$

with $\lambda = \mathcal{S}, \mathcal{Q}, \mathcal{A}$ [cf. Eq. (84)]. The dynamical structure factor for \mathcal{A} -matrices is defined through

$$m_{\mathcal{A}\beta}^\alpha(\mathbf{q}, t_n) = \frac{1}{\sqrt{N}} \sum_{i=1}^N e^{i\mathbf{r}_i \cdot \mathbf{q}} \mathcal{A}_{i\beta}^\alpha(t_n), \quad (102)$$

[cf. Eq. (85)], and equivalent structure factors for dipole- $m_{\mathcal{S}\alpha}^\alpha(\mathbf{q}, t)$ and quadrupole-moments $m_{\mathcal{Q}\beta}^\alpha(\mathbf{q}, t)$, can be defined by extension of Eq. (86) and Eq. (87).

For purposes of comparison with experiment, it is usually more convenient to work with the Fourier transform

$$S_\lambda(\mathbf{q}, \omega_m) = \frac{1}{\sqrt{N_t}} \sum_{n=1}^{N_t} e^{i\omega_n t_n} S_\lambda(\mathbf{q}, t_n), \quad (103)$$

where ω_m , like \mathbf{q} , takes on discrete values

$$\omega_m = m \delta\omega, \quad m = 0 \dots N_t - 1. \quad (104)$$

To avoid numerical artefacts (Gibbs phenomenon) coming from discontinuities at $t = 0$ and $t = \Delta t$ [98], we multiply the

time-series entering Eq. (103) by a Gaussian envelope centred on $t_n = \Delta t/2$. In practice, we evaluate the dynamical structure factor as

$$S_\lambda(\mathbf{q}, \omega_m) = \left\langle \sum_{\alpha\beta} |\bar{m}_{\lambda\beta}^\alpha(\mathbf{q}, \omega_m)|^2 \right\rangle, \quad (105)$$

where

$$\bar{m}_{\lambda\beta}^\alpha(\mathbf{q}, \omega_m) = \frac{1}{\sqrt{N_t}} \sum_{n=1}^{N_t} e^{i\omega_m t_n} \sqrt{\bar{g}(t_n)} m_{\lambda\beta}^\alpha(\mathbf{q}, t_n), \quad (106)$$

is found by Fast Fourier transform (FFT) [95]. The Gaussian envelope is implemented through the function

$$\bar{g}(t_n) = \frac{\delta t}{\delta\omega_n} \frac{\sigma}{\sqrt{2\pi}} e^{-\frac{\sigma^2}{2}(t_n - \Delta t/2)^2}, \quad (107)$$

and absorbs a dimensional factor $\delta t/\delta\omega$ associated with integrals. The value of σ is chosen such that the full-width half maximum (FWHM) of $\bar{g}(t_n)$ is $\approx \Delta t$. Introducing this envelope in time is equivalent to convoluting $S_\lambda(\mathbf{q}, \omega)$ with a Gaussian in frequency space, with

$$\text{FWHM} = 2\sqrt{2 \ln 2} \times \sigma, \quad (108)$$

approximately equal to $\delta\omega$. This determines the ultimate energy resolution of results. Structure factors calculated in this way are averaged over 500 independent time-series, each determined by a separate initial state drawn from classical MC simulation.

An example of a dynamical structure factor calculated using the u3MD approach has been presented in Fig. 4, where results are shown for the FQ phase of the BBQ model on the triangular lattice.

It is important to note that the EoM, Eq. (73), are invariant under time-reversal symmetry. Solutions to these equations therefore occur in pairs, with positive and negative eigenvalues

$$\omega = \pm \epsilon_{\mathbf{k}}. \quad (109)$$

Both positive and negative energy solutions play a role in experimental response functions, reflecting the absorption and emission of energy by the system. And numerical integration of EoM will generally recover both solutions with equal weight, leading to structure factors which are even functions of frequency

$$S_\lambda^{\text{MD}}(\mathbf{q}, \omega) = S_\lambda^{\text{MD}}(\mathbf{q}, -\omega) \quad (110)$$

None the less, in Fig. 4, and elsewhere in this Article, we concentrate on solutions at positive energy, $\omega > 0$, since these are the most relevant for the low-temperature properties of quantum magnets.

In Section VI and Section VII we delve deeper into u3MD results, and their connection with the analytic theory of the excitations about a FQ ground state. But before doing so, we first develop the analytic theory necessary to understand simulation.

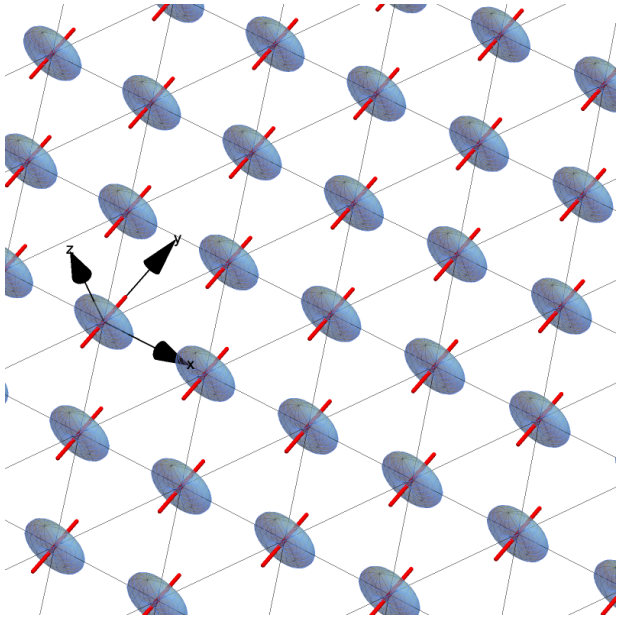


Figure 10. Ferroquadrupolar (FQ) ground state of a spin-1 magnet on a triangular lattice. Each magnetic moment has been plotted in the state $|y\rangle$, or equivalently in director representation $d^x = 0$, $d^y = 1$, $d^z = 0$, in Eq. (38). The corresponding spin probability distribution [Eq. (A3)] is shown in grayish blue, and the associated director in red.

IV. CLASSICAL THEORY OF FLUCTUATIONS ABOUT A FERROQUADRUPOLAR GROUND STATE

In this Section we use the $u(3)$ formalism introduced in Section II to develop a classical theory of fluctuations about a ferroquadrupolar (FQ) ground state. This will serve as a benchmark for the classical MC simulations presented in Section VI, and as the starting point for an analysis of quantum-classical correspondence in Section VII.

We chose to work with FQ order, since this is simplest of the non-trivial phases found in the BBQ model. Mean-field (MF) calculations for the spin-1 BBQ model on a triangular lattice [19, 20] predict a FQ ground state for a broad range of parameters [Fig. 2], and its existence has since been confirmed using exact-diagonalisation [19], QMC [52, 53] and tensor-network approaches [99]. The dynamics of this state have also been explored through both “flavour wave” theory [13, 19, 56, 100] and QMC simulation [53]. This makes FQ order a convenient point of reference, with many published results available for comparison. A classical theory of its low-temperature properties, however, is lacking.

We first show how small fluctuations about FQ order can be described using four of the nine generators of $U(3)$ [Section IV A]. This leads naturally to a low-temperature expansion scheme for the classical thermodynamic properties of FQ order [Section IV B]. This theory is used to make explicit predictions for the classical thermodynamic properties [Section IV B] of FQ order, for later comparison with simulation.

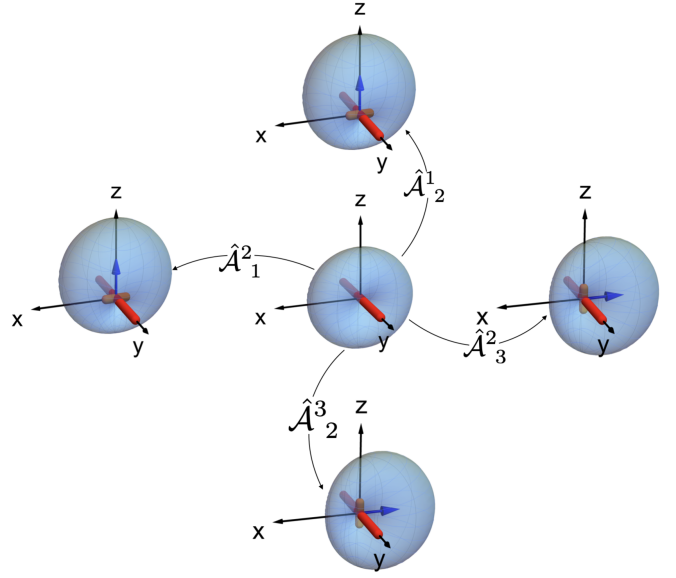


Figure 11. Effect of the four operators generating fluctuations about the ferroquadrupolar (FQ) ground state $|y\rangle$. The generators $\hat{\mathcal{A}}_2^1$ (acting on the right) and $\hat{\mathcal{A}}_1^2$ (acting on the left) introduce a complex component of the director \mathbf{d} , parallel to the x -axis. This has the effect of rotating the quadrupole moment about the z -axis, while simultaneously inducing a dipole moment along the z -axis [Eq. (46)]. Meanwhile the generators $\hat{\mathcal{A}}_3^2$ and $\hat{\mathcal{A}}_2^3$ rotate the quadrupole about the x -axis, and induce a dipole moment along the same axis. The effect of each generator is computed according to Eq. (115), for a rotation through an angle of $\phi = \frac{\pi}{8}$. The red bar represents the real part \mathbf{u} of the coefficients d^α [Eq. (40)] in Eq. (38), while the orange bar represents the imaginary part \mathbf{v} .

A. Expansion of small fluctuations

Our starting point is the FQ ground state found in mean-field calculations; a product wave function of on-site quadrupolar moments with a common orientation

$$|\Psi_0\rangle_{\text{FQ}}^{\text{MF}} = \prod_{i=1}^N |\mathbf{d}_i^{\text{FQ}}\rangle, \quad (111)$$

where $|\mathbf{d}_i\rangle$ is defined through Eq. (38). For concreteness, we assume the director to be along the y -axis for all lattice sites, i.e.

$$|\mathbf{d}_i^{\text{FQ}}\rangle = |y\rangle \text{ or equivalently } \mathbf{d}^{\text{FQ}} = \begin{pmatrix} 0 \\ 1 \\ 0 \end{pmatrix}. \quad (112)$$

This state is illustrated in Fig. 10. Once corrections to mean-field theory are taken into account, this product state will be dressed with thermal and/or quantum fluctuations, reducing the expectation value of the quadrupolar order parameter. We now derive a framework for describing these fluctuations in terms of generators belonging to the Lie algebra $u(3)$.

The first step of our analysis is to transcribe the MF ground state, Eq. (111), in terms of \mathcal{A} -matrices. Using Eq. (47), we

represent the ground state as

$$\langle \mathbf{d}_i^{\text{FQ}} | \mathcal{A} | \mathbf{d}_i^{\text{FQ}} \rangle = \mathbf{A}_0 = \begin{pmatrix} 0 & 0 & 0 \\ 0 & 1 & 0 \\ 0 & 0 & 0 \end{pmatrix}. \quad (113)$$

This in turn forms the basis for a product state

$$|\Psi_0\rangle_{\text{FQ}}^{\text{MF}} = \prod_{i=1}^N |\mathbf{A}_0\rangle, \quad (114)$$

in the space of \mathcal{A} -matrices.

Within a Lie algebra, local fluctuations about any state $|\psi_0\rangle$ can be written

$$|\psi\rangle = \hat{R}(\vec{\phi}) |\psi_0\rangle, \quad (115)$$

where the operator $\hat{R}(\vec{\phi})$ has the form

$$\hat{R}(\vec{\phi}) = e^{-i \sum_p \phi_p \hat{G}_p}, \quad (116)$$

and G_p are elements of the algebra, with $\phi_p \in \mathbb{R}$. In the case of $u(3)$, a suitable set of generators \hat{G}_p ($p = 1, 2, \dots, 9$) are the matrices \hat{A}_β^α [Eq. (52)], and we can write

$$\hat{R}(\vec{\phi}) = e^{-i \sum_{\alpha,\beta} \phi_{\alpha,\beta} \hat{A}_\beta^\alpha}, \quad (117)$$

where $\alpha, \beta = 1, 2, 3$. Under this operation, \mathcal{A} -matrices transform as

$$\mathbf{A}(\vec{\phi}) = \hat{R}(\vec{\phi}) \mathbf{A}_0 \hat{R}(\vec{\phi})^\dagger. \quad (118)$$

as determined by Eq. (61) [cf. Appendix B].

If we assume fluctuations to be small, i.e. $\phi_{\alpha,\beta} \ll 1$, we can expand the exponential in Eq. (117)

$$\hat{R}(\vec{\phi}) \simeq \mathbb{I} + i \sum_{\alpha,\beta} \phi_{\alpha,\beta} \hat{A}_\beta^\alpha + \dots \quad (119)$$

Considering the action of this operator on the FQ ground state, as characterised by the matrix \mathbf{A}_0 [Eq. (114)], the only \hat{A}_β^α that will give a non-zero result are \hat{A}_2^1, \hat{A}_3^2 on the left, \hat{A}_1^2, \hat{A}_3^1 on the right, and \hat{A}_2^2 , which preserves the ground state. Consequently, if we wish to describe fluctuations about the ground state, we need only keep four generators $\hat{A}_2^1, \hat{A}_3^2, \hat{A}_1^2, \hat{A}_3^1$. We can think of these operators as performing rotations in the space of \mathcal{A} -matrices or, equivalently, of \mathbf{d} -vectors [20]. Their effect is illustrated in Fig. 11.

Restricting Eq. (119) to the four relevant generators, and retaining all terms to order ϕ^2 , we arrive at a general expression for infinitesimal fluctuations about the FQ ground state

$$\hat{R}(\vec{\phi}) = \begin{pmatrix} 1 & & i\phi^{1,2} & 0 \\ 0 & 1 - \frac{1}{2}\phi^{1,2}\phi^{2,1} - \frac{1}{2}\phi^{2,3}\phi^{3,2} & 0 & 0 \\ 0 & & i\phi_{3,2} & 1 \end{pmatrix}, \quad (120)$$

where $\hat{R}(\vec{\phi})^\dagger$ is the transpose of Eq. (120), with the small subtlety that $\phi^{1,2\dagger} = \phi^{2,1}$.

Substituting Eq. (120) into Eq. (118), we find

$$\begin{aligned} \hat{\mathbf{A}}(\vec{\phi}) &= \hat{R}(\vec{\phi}) \mathbf{A}_0 \hat{R}(\vec{\phi})^\dagger \\ &= \begin{pmatrix} \phi^{1,2}\phi^{2,1} & i\phi^{1,2} & \phi^{1,2}\phi^{2,3} \\ -i\phi^{2,1} & 1 - \phi^{1,2}\phi^{2,1} - \phi^{2,3}\phi^{3,2} & -i\phi^{2,3} \\ \phi^{2,1}\phi^{3,2} & i\phi_{3,2} & \phi^{2,3}\phi^{3,2} \end{pmatrix}. \end{aligned} \quad (121)$$

Crucially, Eq. (121) satisfies the constraint $\text{Tr } \mathcal{A} = 1$ [Eq. (49)], implying that the spin length is conserved.

The effect of the four generators $\hat{A}_2^1, \hat{A}_3^2, \hat{A}_1^2, \hat{A}_3^1$ on the state $|y\rangle$ can now be quantified directly. Substituting Eq. (121) in Eq. (51), and keeping terms to $\mathcal{O}(\phi^2)$, we find

$$\hat{\mathbf{Q}}(\vec{\phi}) = \begin{pmatrix} \frac{2}{3} - 2\phi^{1,2}\phi^{2,1} & i(\phi^{2,1} - \phi^{1,2}) & -\phi^{1,2}\phi^{2,3} - \phi^{2,1}\phi^{3,2} \\ i(\phi^{2,1} - \phi^{1,2}) & -\frac{4}{3} + 2\phi^{1,2}\phi^{2,1} + 2\phi^{2,3}\phi^{3,2} & i(\phi^{2,3} - \phi^{3,2}) \\ -\phi^{1,2}\phi^{2,3} - \phi^{2,1}\phi^{3,2} & i(\phi^{2,3} - \phi^{3,2}) & \frac{2}{3} - 2\phi^{2,3}\phi^{3,2} \end{pmatrix}. \quad (122)$$

Similarly, from Eq. (50), to $\mathcal{O}(\phi^2)$ we find

$$\hat{\mathbf{S}}(\vec{\phi}) = \begin{pmatrix} -\phi^{2,3} - \phi^{3,2} \\ i(\phi^{1,2}\phi^{2,3} - \phi^{2,1}\phi^{3,2}) \\ \phi^{1,2} + \phi^{2,1} \end{pmatrix}. \quad (123)$$

From these results we understand that fluctuations introduce a small imaginary part to the director \mathbf{d} , parallel to either the x- or the z-axis. This leads to a rotation of the quadrupole moment about either the z- or the x-axis, and simultaneously introduces a dipole moment along that axis of

rotation. These changes are clearly visible in Fig. 11, where the orientation of the quadrupole moment is shown as a red bar. Meanwhile, the dipole moment induced by each fluctuation is indicated with a blue arrow, and is also visible as a (small) distortion of the spin-probability distribution.

We are now in a position to derive a Hamiltonian describing fluctuations about FQ order. Substituting Eq. (121) in

Eq. (72), we find

$$\mathcal{H}'_{\text{BBQ}} = E_0 + \frac{1}{2} \sum_{\mathbf{k}} \left[\vec{\phi}_{\mathbf{k}}^T M_{\mathbf{k}} \vec{\phi}_{-\mathbf{k}} \right] + \mathcal{O}(\phi^4), \quad (124)$$

where the energy of the MF ground state is

$$E_0 = NzJ_2, \quad (125)$$

and fluctuations are described by

$$\vec{\phi}_{\mathbf{k}} = \begin{pmatrix} \phi_{\mathbf{k}}^{2,1} \\ \phi_{\mathbf{k}}^{1,2} \\ \phi_{\mathbf{k}}^{3,2} \\ \phi_{\mathbf{k}}^{2,3} \end{pmatrix} = \frac{1}{\sqrt{N}} \sum_i \begin{pmatrix} e^{i\mathbf{k}\cdot\mathbf{r}_i} \phi_{\mathbf{r}_i}^{2,1} \\ e^{i\mathbf{k}\cdot\mathbf{r}_i} \phi_{\mathbf{r}_i}^{1,2} \\ e^{i\mathbf{k}\cdot\mathbf{r}_i} \phi_{\mathbf{r}_i}^{3,2} \\ e^{i\mathbf{k}\cdot\mathbf{r}_i} \phi_{\mathbf{r}_i}^{2,3} \end{pmatrix}, \quad (126)$$

with energy determined by a matrix

$$M_{\mathbf{k}} = \begin{pmatrix} A_{\mathbf{k}} & -B_{\mathbf{k}} & 0 & 0 \\ -B_{\mathbf{k}} & A_{\mathbf{k}} & 0 & 0 \\ 0 & 0 & A_{\mathbf{k}} & -B_{\mathbf{k}} \\ 0 & 0 & -B_{\mathbf{k}} & A_{\mathbf{k}} \end{pmatrix}, \quad (127)$$

for which

$$A_{\mathbf{k}} = z(J_1\gamma(\mathbf{k}) - J_2), \quad (128a)$$

$$B_{\mathbf{k}} = z\gamma(\mathbf{k})(J_2 - J_1), \quad (128b)$$

with lattice structure factor

$$\gamma(\mathbf{k}) = \frac{1}{z} \sum_{\delta} e^{-i\mathbf{k}\cdot\delta}. \quad (129)$$

For the triangular lattice, the lattice coordination number $z = 6$, and the vectors which connect neighbouring lattice sites, $\{\delta\}$, are listed in Appendix C. We note also that the transpose vector for the fluctuations has the property

$$\phi_{\mathbf{k}}^{T\mu,\nu} = \phi_{\mathbf{k}}^{\nu,\mu}. \quad (130)$$

This implies

$$\vec{\phi}_{\mathbf{k}}^T = (\phi_{\mathbf{k}}^{1,2}, \phi_{\mathbf{k}}^{2,1}, \phi_{\mathbf{k}}^{2,3}, \phi_{\mathbf{k}}^{3,2}). \quad (131)$$

The Hamiltonian $\mathcal{H}'_{\text{BBQ}}$ [Eq. (124)] describes all possible fluctuations about FQ order at a Gaussian (i.e. non-interacting) level, and can be used as a starting point for both classical and quantum theories of its excitations. The absence of terms linear in ϕ in Eq. (124) confirms that the MF ground state, Eq. (114), minimises energy, and is therefore a valid starting point for describing FQ order.

B. Classical low-temperature expansion

We now use the results of Section IV A to develop a classical theory of thermal fluctuations about FQ order at low temperature. From this we can calculate thermodynamic quantities in a form suitable for comparison with classical Monte Carlo simulation. Results will be quoted to linear order in T (i.e. quadratic in fluctuations).

1. Expression for free energy

Within the framework of Section IV A, fluctuations about FQ order can be described by the partition function

$$Z_0 = \int d\vec{\phi}_{\mathbf{k}} e^{-\beta\mathcal{H}'_{\text{BBQ}}[\vec{\phi}_{\mathbf{k}}]}, \quad (132)$$

where the measure of integration is

$$d\vec{\phi}_{\mathbf{k}} = d\phi_{\mathbf{k}}^{1,2} d\phi_{\mathbf{k}}^{2,1} d\phi_{\mathbf{k}}^{2,3} d\phi_{\mathbf{k}}^{3,2}, \quad (133)$$

the inverse temperature

$$\beta = \frac{1}{k_B T}, \quad (134)$$

and $\mathcal{H}'_{\text{BBQ}}[\vec{\phi}_{\mathbf{k}}]$ is defined through Eq. (124). Neglecting $\mathcal{O}(\phi^4)$ terms, we find

$$Z_0 = \prod_{\mathbf{k}} \int e^{-\beta \frac{1}{2} \vec{\phi}_{\mathbf{k}}^T M_{\mathbf{k}} \vec{\phi}_{-\mathbf{k}}} e^{-\beta \frac{E_0}{N}} d\vec{\phi}_{\mathbf{k}} \quad (135a)$$

$$= e^{-\beta E_0} \prod_{\mathbf{k}} \left[\sqrt{\frac{(2\pi)^n}{\beta^n \det M_{\mathbf{k}}}} \right], \quad (135b)$$

where E_0 is defined through Eq. (125), the 4×4 matrix $M_{\mathbf{k}}$ through Eq. (127), N is the number of lattice sites and n is the dimension of $M_{\mathbf{k}}$ (in this case, $n = 4$). It follows that the free energy per site is

$$\begin{aligned} f_0 &= -\frac{\log(Z_0)}{\beta N} \\ &= \frac{E_0}{N} + \frac{k_B T}{2N} \sum_{\mathbf{k}} \sum_{\lambda=1}^{N_{\lambda}} \log\left(\frac{\omega_{\mathbf{k},\lambda}}{2\pi k_B T}\right) + \mathcal{O}(T^2), \end{aligned} \quad (136)$$

where $\omega_{\mathbf{k},\lambda}$ are the eigenvalues of $M_{\mathbf{k}}$, and we have used the fact that

$$\log[\det M_{\mathbf{k}}] = \text{Tr} \log M_{\mathbf{k}} = \sum_{\lambda=1}^4 \log \omega_{\mathbf{k},\lambda}. \quad (137)$$

The free energy, Eq. (136), represents the first term in a classical low-temperature expansion of the thermodynamic properties of the BBQ model. To $\mathcal{O}(T)$, these are completely conditioned by the solutions of the eigensystem

$$M_{\mathbf{k}} \mathbf{v}_{\mathbf{k},\lambda} = \omega_{\mathbf{k},\lambda} \mathbf{v}_{\mathbf{k},\lambda}. \quad (138)$$

Working in the basis

$$\{\phi_{\mathbf{k}}^{2,1}, \phi_{\mathbf{k}}^{1,2}, \phi_{\mathbf{k}}^{3,2}, \phi_{\mathbf{k}}^{2,3}\}, \quad (139)$$

we find the eigenvalues

$$\omega_{\mathbf{k}}^+ = \omega_{\mathbf{k},1} = \omega_{\mathbf{k},3} = A_{\mathbf{k}} + B_{\mathbf{k}}, \quad (140a)$$

$$\omega_{\mathbf{k}}^- = \omega_{\mathbf{k},2} = \omega_{\mathbf{k},4} = A_{\mathbf{k}} - B_{\mathbf{k}}, \quad (140b)$$

with associated eigenvectors

$$\begin{aligned} v_1 &= \frac{1}{\sqrt{2}} \begin{pmatrix} -1 \\ 1 \\ 0 \\ 0 \end{pmatrix}, & v_2 &= \frac{1}{\sqrt{2}} \begin{pmatrix} 1 \\ 1 \\ 0 \\ 0 \end{pmatrix}, \\ v_3 &= \frac{1}{\sqrt{2}} \begin{pmatrix} 0 \\ 0 \\ -1 \\ 1 \end{pmatrix}, & v_4 &= \frac{1}{\sqrt{2}} \begin{pmatrix} 0 \\ 0 \\ 1 \\ 1 \end{pmatrix}. \end{aligned} \quad (141)$$

For quadrupolar order $\sim |y\rangle$, v_1 and v_2 are associated with rotations of quadrupole moments about the z -axis, while v_3 and v_4 are associated with rotations about the x -axis [cf. Fig. 11].

By construction, to $\mathcal{O}(\phi^2)$, the Hamiltonian $\mathcal{H}'_{\text{BBQ}}$ is diagonal in the basis

$$\vec{v}_{\mathbf{k}}^T = (v_{\mathbf{k},1}, v_{\mathbf{k},2}, v_{\mathbf{k},3}, v_{\mathbf{k},4}), \quad (142)$$

and can be written

$$\begin{aligned} \mathcal{H}'_{\text{BBQ}} &= E_0 + \frac{1}{2} \sum_{\mathbf{k}} \vec{v}_{\mathbf{k}}^T \tilde{M}_{\mathbf{k}} \vec{v}_{-\mathbf{k}} + \mathcal{O}(\vec{v}^4) \\ &= E_0 + \frac{1}{2} \sum_{\mathbf{k}} \sum_{\lambda=1}^4 \omega_{\mathbf{k},\lambda} v_{\mathbf{k},\lambda}^T v_{-\mathbf{k},\lambda} + \mathcal{O}(\vec{v}^4), \end{aligned} \quad (143)$$

where

$$\tilde{M}_{\mathbf{k}} = O^T M_{\mathbf{k}} O = \begin{pmatrix} \omega_{\mathbf{k},1} & 0 & 0 & 0 \\ 0 & \omega_{\mathbf{k},2} & 0 & 0 \\ 0 & 0 & \omega_{\mathbf{k},3} & 0 \\ 0 & 0 & 0 & \omega_{\mathbf{k},4} \end{pmatrix}. \quad (144)$$

and the orthogonal transformation O is defined by

$$\begin{pmatrix} \phi^{2,1} \\ \phi^{1,2} \\ \phi^{3,2} \\ \phi^{2,3} \end{pmatrix} = O \begin{pmatrix} v_1 \\ v_2 \\ v_3 \\ v_4 \end{pmatrix} \quad \text{where} \quad O = \frac{1}{\sqrt{2}} \begin{pmatrix} -1 & 1 & 0 & 0 \\ 1 & 1 & 0 & 0 \\ 0 & 0 & -1 & 1 \\ 0 & 0 & 1 & 1 \end{pmatrix}. \quad (145)$$

Of necessity, eigenmodes form an orthonormal set

$$v_{\mathbf{k},\lambda}^T v_{-\mathbf{k},\lambda'} = \delta_{\lambda\lambda'}. \quad (146)$$

This coordinate system will prove useful in the subsequent calculation of correlation functions and ordered moments, described below.

C. Calculation of thermodynamic quantities

Starting from the free energy f_0 [Eq. (136)], it is possible to calculate all thermodynamic properties of the FQ state as the leading term in a perturbative expansion about $T = 0$. This can be accomplished by taking appropriate (functional) derivatives of the free energy.

1. Heat capacity

The simplest thermodynamic property we can consider is the specific heat

$$c_v = \frac{C_v}{N} = -T \left(\frac{\partial^2 f_0}{\partial T^2} \right)_V. \quad (147)$$

In the limit $T \rightarrow 0$, this is controlled by the classical limit of the equipartition theorem, which implies that each quadratic mode contributes $k_B/2$ to $c_v(T \rightarrow 0)$ [89, 101, 102]. In the present case

$$c_v = -T \frac{-k_B N_\lambda}{2T} = k_B \frac{N_\lambda}{2}, \quad (148)$$

where

$$N_\lambda = 4, \quad (149)$$

counts the number of normal modes accessible per spin-1 moment [cf. Fig. 11]. It follows that, in the limit $T \rightarrow 0$,

$$c_v \rightarrow 2 \quad [u(3) \text{ matrix}], \quad (150)$$

where, for simplicity, we set

$$k_B = 1. \quad (151)$$

This should be contrasted with the usual result for classical fluctuations about an ordered state composed of $O(3)$ vectors: Here, at the level of a single spin, only two orthogonal fluctuations are possible, and so $N_\lambda = 2$ [89, 101, 102]:

$$c_v \rightarrow 1 \quad [O(3) \text{ vector}]. \quad (152)$$

The zero-temperature limit of specific heat will prove important in the interpretation of the results of Monte Carlo simulation, as discussed in Section VI.

2. Structure factors: general considerations

We now turn to the calculation of the structure factors associated with dipole moments, quadrupole moments, and A-matrices. To facilitate this, it will prove useful to introduce source terms

$$\mathcal{H} = \mathcal{H}_{\text{BBQ}} + \Delta\mathcal{H}[h_{i,\beta}^\alpha], \quad (153)$$

where

$$\Delta\mathcal{H}[h_{i,\beta}^\alpha] = - \sum_{i,\alpha} h_{i,\beta}^\alpha \hat{O}_{i,\beta}^\alpha, \quad (154)$$

describes the coupling of a fictitious field $h_{i,\beta}^\alpha$ to the observable

$$\hat{O}_{i,\beta}^\alpha \rightarrow \hat{S}_i^\alpha \delta_{\alpha\beta}, \hat{Q}_i^{\alpha\beta}, \hat{A}_{i,\beta}^\alpha. \quad (155)$$

Calculations proceed by expanding the observable $\hat{O}_{i,\beta}^\alpha$ in terms of the orthogonal eigenmodes $v_{\mathbf{k},\lambda}$ [Eq. (145)], and calculating thermodynamic averages through functional derivatives of the free energy [Eq. (136)] with respect to $h_{i,\beta}^\alpha$.

Details of these calculations, which involve contributions from both the ground state and thermal excitations, are given in [Appendix D](#). Where we come to compare with a quantum theory in [Section V](#), it will also prove useful to introduce a spectral decomposition of the structure factors, which resolves contributions from eigenmodes at different energies. These are defined in [Eq. \(D20\)](#).

In what follows, we list the results needed for subsequent comparison with numerics in [Section VI](#).

3. Structure factor for dipole moments

We first consider the structure factor for dipole moments of spin

$$S_S^{\text{CL}}(\mathbf{q}) = \sum_{\alpha} \langle \hat{S}_{\mathbf{q}}^{\alpha} \hat{S}_{-\mathbf{q}}^{\alpha} \rangle. \quad (156)$$

Within the classical low-temperature expansion, we find

$$S_S^{\text{CL}}(\mathbf{q}) = \frac{4}{\beta} \frac{1}{\omega_{\mathbf{q}}^{\pm}} + \mathcal{O}(T^2), \quad (157)$$

where $\omega_{\mathbf{q}}^{\pm}$ are defined through [Eq. \(140\)](#). Because the FQ phase does not break time-reversal symmetry, all ground-state averages of dipole moments vanish. None the less, fluctuations restore a finite value of $S_S^{\text{CL}}(\mathbf{q})$ at finite temperature. The absence of terms in $\omega_{\mathbf{q}}^+$ reflects the fact that only the ‘‘odd’’ modes $\lambda = 2, 4$ contribute to dipolar fluctuations.

The spectral decomposition of the structure factor, [Eq. \(157\)](#), is given by

$$S_S^{\text{CL}}(\mathbf{q}, \omega) = \frac{4}{\beta} \frac{1}{\omega_{\mathbf{q}}^{-}} \delta(\omega - \omega_{\mathbf{q}}^{-}) + \mathcal{O}(T^2). \quad (158)$$

This is plotted in [Fig. 12 \(a\)](#), for parameters

$$J_1 = 0.0, \quad J_2 = -1.0, \quad (159)$$

consistent with a FQ ground state, at a notional temperature $T/J = 1$. Within the classical theory, excitations with a dipolar character form a gapped, dispersing band, with spectral weight concentrated at $\mathbf{q} = \mathbf{K}$.

Further details of these calculations can be found in [Appendix D 2](#) [$\mathbf{q} \neq 0$] and [Appendix D 3](#) [$\mathbf{q} = 0$].

4. Structure factor for quadrupole moments

Next we consider the structure factor for quadrupole moments

$$S_Q^{\text{CL}}(\mathbf{q}) = \sum_{\alpha\beta} \langle \hat{Q}_{\mathbf{q}}^{\alpha\beta} \hat{Q}_{-\mathbf{q}}^{\beta\alpha} \rangle, \quad (160)$$

where the scalar contraction accomplished by the sum on α, β respects $SU(2)$ symmetry. We obtain

$$S_Q^{\text{CL}}(\mathbf{q}) = \frac{8}{\beta} \frac{1}{\omega_{\mathbf{q}}^{\pm}} (1 - \delta_{\mathbf{q},0}) + \frac{8}{3} \left[N - \frac{\Delta}{\beta} \right] \delta_{\mathbf{q},0} + \mathcal{O}(T^2), \quad (161)$$

where

$$\Delta = 3 \sum_{\mathbf{k} \neq 0} \left[\frac{1}{\omega_{\mathbf{k}}^+} + \frac{1}{\omega_{\mathbf{k}}^-} \right] + \frac{1}{\omega_{\mathbf{q}}^-}. \quad (162)$$

The structure factor for quadrupole moments is sensitive to the FQ ground state, and the term Δ/β describes corrections to ground-state averages for $T > 0$. The absence of terms in $\omega_{\mathbf{q}}^-$ for $\mathbf{q} \neq 0$ reflects the fact that only the ‘‘even’’ modes $\lambda = 1, 3$ contribute to quadrupolar fluctuations. However all four modes, $\lambda = 1, 2, 3, 4$, contribute to the reduction of the ordered moment, through [Eq. \(162\)](#).

The spectral decomposition of the structure factor, [Eq. \(161\)](#), is given by

$$S_Q^{\text{CL}}(\mathbf{q}, \omega) = \frac{8}{\beta} \frac{1}{\omega_{\mathbf{q}}^+} (1 - \delta_{\mathbf{q},0}) \delta(\omega - \omega_{\mathbf{q}}^+) + \frac{8}{3} \left[N - \frac{\Delta}{\beta} \right] \delta_{\mathbf{q},0} \delta(\omega) + \mathcal{O}(T^2). \quad (163)$$

This is illustrated in [Fig. 12 \(b\)](#), where the Bragg peak at $\mathbf{q} = \Gamma$ has been suppressed for simplicity. Within a classical theory, excitations with a quadrupolar character form a gapless dispersing band, with spectral weight concentrated at $\mathbf{q} = 0$.

Further details of these calculations are given in [Appendix D 4](#) [$\mathbf{q} \neq 0$] and [Appendix D 5](#) [$\mathbf{q} = 0$].

5. Structure factor for A-matrix

We now turn to the structure factor for the most fundamental object describing the spins, the matrix $\hat{\mathcal{A}}_{\beta}^{\alpha}$. This is defined by

$$S_A^{\text{CL}}(\mathbf{q}) = \sum_{\alpha\beta} \langle \hat{\mathcal{A}}_{\mathbf{q}}^{\alpha} \hat{\mathcal{A}}_{-\mathbf{q}}^{\beta} \rangle, \quad (164)$$

where the scalar contraction accomplished through the sum on α, β preserves the full $U(3)$ symmetry of the representation. To leading order in T , we find

$$S_A^{\text{CL}}(\mathbf{q}) = \frac{2}{\beta} \frac{1}{\omega_{\mathbf{q}}^-} + \frac{2}{\beta} \frac{1}{\omega_{\mathbf{q}}^+} (1 - \delta_{\mathbf{q},0}) + \left[N - \frac{2}{3} \frac{\Delta}{\beta} \right] \delta_{\mathbf{q},0} + \mathcal{O}(T^2). \quad (165)$$

This structure factor encompasses both dipoles and quadrupoles, and so is sensitive to FQ ground state order. All four modes, $\omega_{\mathbf{q}}^{\pm}$, contribute to fluctuation terms for $\mathbf{q} \neq 0$.

The spectral decomposition of the structure factor, [Eq. \(165\)](#), is given by

$$S_A^{\text{CL}}(\mathbf{q}, \omega) = \frac{2}{\beta} \frac{1}{\omega_{\mathbf{q}}^-} \delta(\omega - \omega_{\mathbf{q}}^-) + \frac{2}{\beta} \frac{1}{\omega_{\mathbf{q}}^+} (1 - \delta_{\mathbf{q},0}) \delta(\omega - \omega_{\mathbf{q}}^+) + \left[1 - \frac{2}{3} \frac{\Delta}{\beta} \right] \delta_{\mathbf{q},0} \delta(\omega) + \mathcal{O}(T^2). \quad (166)$$

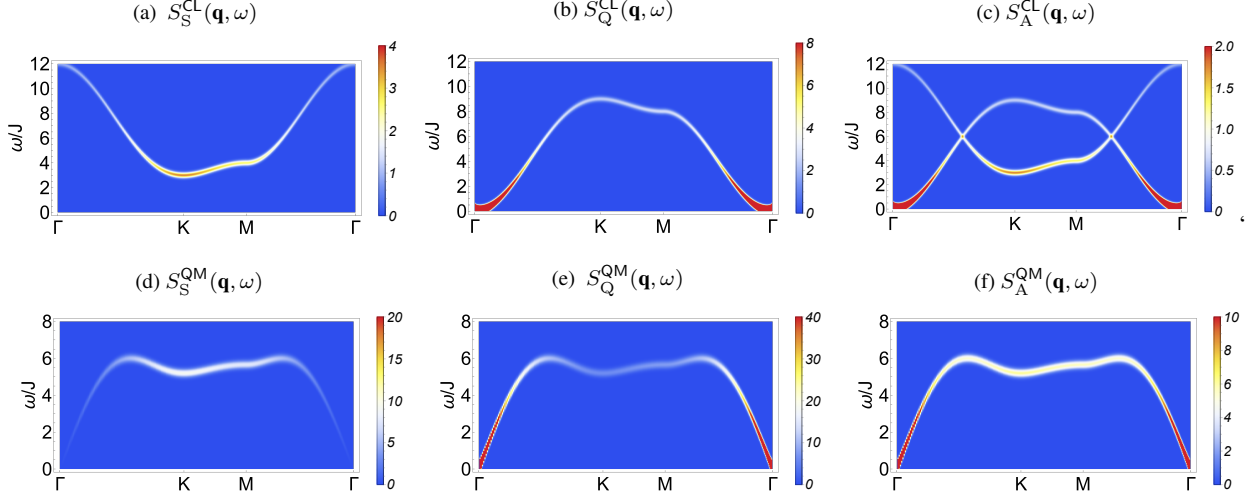


Figure 12. Comparison of band-like excitations found in classical and quantum theories of fluctuations about a Ferroquadrupolar (FQ) ground state. (a) Spectral representation of structure factor associated with dipole moments, $S_S^{\text{CL}}(\mathbf{q}, \omega)$ [Eq. (158)], within classical low-temperature expansion of Section IV, at a notional temperature $T = J$. (b) Equivalent results for quadrupole moments, $S_Q^{\text{CL}}(\mathbf{q}, \omega)$ [Eq. (163)]. (c) Equivalent results for A-matrices, $S_A^{\text{CL}}(\mathbf{q}, \omega)$ [Eq. (166)]. (d) Dynamical structure factor associated with dipole moments, $S_S^{\text{QM}}(\mathbf{q}, \omega)$ [Eq. (193)], within $T = 0$ quantum theory. (e) Equivalent results for quadrupole moments, $S_Q^{\text{QM}}(\mathbf{q}, \omega)$ [Eq. (201)]. (f) Equivalent results for A-matrices, $S_A^{\text{QM}}(\mathbf{q}, \omega)$ [Eq. (208)]. Comparing classical and quantum results, we see that the dispersion found in the quantum case is the geometric mean of the two different dispersions found for dipolar and quadrupolar excitations in the classical case. All results are shown for parameters Eq. (159), and have been convoluted with Gaussian of FWHM 0.35 J. Bragg peaks have been omitted for simplicity. Details of the quantum theory are given in Section V.

This is illustrated in Fig. 12 (c), where the Bragg peak at $\mathbf{q} = \Gamma$ has been suppressed for simplicity. Both dipolar and quadrupolar fluctuations are visible as independent, dispersing, bands in $S_A^{\text{CL}}(\mathbf{q}, \omega)$.

Further details of these calculations can be found in Appendix D 6 and [$\mathbf{q} \neq 0$] Appendix D 7 [$\mathbf{q} = 0$].

6. Sum rule for structure factors

The sum rule associated with A-matrices, Eq. (66), implies that the structure factors $S_S^{\text{CL}}(\mathbf{q})$, $S_Q^{\text{CL}}(\mathbf{q})$ and $S_A^{\text{CL}}(\mathbf{q})$, must also satisfy a sum rule. By Fourier transform of Eq. (66), we find

$$\begin{aligned} \hat{A}_{\mathbf{k}\beta}^{\alpha} \hat{A}_{-\mathbf{k}\alpha}^{\beta} &= \frac{1}{4} \hat{Q}_{\mathbf{k}}^{\alpha\beta} \hat{Q}_{-\mathbf{k}}^{\beta\alpha} + \sum_{\alpha} \frac{1}{2} \hat{S}_{\mathbf{k}}^{\alpha} \hat{S}_{-\mathbf{k}}^{\alpha} \\ &+ \frac{1}{12} s^2 (s+1)^2 N \delta_{\mathbf{k},0}. \end{aligned} \quad (167)$$

It follows that

$$S_A^{\text{CL}}(\mathbf{q}) = \frac{1}{4} S_Q^{\text{CL}}(\mathbf{q}) + \frac{1}{2} S_S^{\text{CL}}(\mathbf{q}) + \frac{1}{3} N \delta_{\mathbf{q},0}. \quad (168)$$

By direct substitution of Eq. (165), Eq. (157) and Eq. (161), it is easy to see that the results of the low-temperature expansion satisfy the sum rule Eq. (168).

7. Ordered Moments

Finally, we consider the quadrupole moment which characterises the FQ state, $\langle \mathbf{Q} \rangle$. This is most easily calculated through the associated equal-time structure factor

$$\langle \mathbf{Q} \rangle^2 = \frac{S_Q^{\text{CL}}(\mathbf{q} = \Gamma)}{N}, \quad (169)$$

where N denotes the number of lattice sites. From Eq. (161), we find

$$\langle \mathbf{Q} \rangle^2 \simeq \frac{8}{3} - \frac{8}{N\beta} \sum_{\mathbf{k} \neq 0} \left[\frac{1}{\omega_{\mathbf{k}}^+} + \frac{1}{\omega_{\mathbf{k}}^-} \right] + \mathcal{O}(T^2). \quad (170)$$

This is the result used for comparison with MC simulation in Section VI B.

V. QUANTUM THEORY OF FLUCTUATIONS ABOUT A FERROQUADRUPOLAR GROUND STATE

We now construct a quantum theory of fluctuations about FQ order, starting from the $u(3)$ formalism introduced in Section II. First we show how quantization of the fluctuations introduced in Section IV A leads to a multiple-Boson expansion exactly equivalent to published ‘‘flavour-wave’’ theory [19]. As with the classical theory of Section IV B, we treat fluctuations at a Gaussian level (i.e. one quadratic in bosons).

In [Section VB](#) we go on to provide explicit results for the dynamical structure factors associated with spin–dipole and quadrupole moments, and with the A –matrix describing fluctuations.

A. Quantization of fluctuations

In [Section IV A](#) we have shown that fluctuations about FQ order can be fully described using four generators $\hat{A}_2^1, \hat{A}_2^3, \hat{A}_3^1, \hat{A}_3^3$, which naturally form conjugate pairs [[Fig. 11](#)]. It follows that fluctuations can be parameterized through two pairs of real fields $(\phi^{1,2}, \phi^{2,1})$, and $(\phi^{2,3}, \phi^{3,2})$. Once quantum dynamics are taken into account, low–energy fluctuations must take the form of “quadrupole waves”, which are the Goldstone modes of FQ order. These carry integer spin, and will be Bosons. And since each Boson must be described by a complex field, we anticipate that the pairs of fields $(\phi^{1,2}, \phi^{2,1})$, and $(\phi^{2,3}, \phi^{3,2})$ will combine to give a total of two Bosonic degrees of freedom per site.

With these expectations in mind, we quantize fluctuations of each pair of fields through the Bosonic commutation relations

$$[\phi_i^{2,1}, \phi_j^{1,2}] = \delta_{ij}, \quad (171a)$$

$$[\phi_i^{2,3}, \phi_j^{3,2}] = \delta_{ij}. \quad (171b)$$

We can now associate each field $\phi^{\alpha,\beta}$ with a creation or annihilation operator

$$\phi_i^{1,2} = (\phi_i^{2,1})^\dagger = -i\hat{a}_i^\dagger, \quad (172a)$$

$$\phi_i^{2,3} = (\phi_i^{3,2})^\dagger = i\hat{b}_i. \quad (172b)$$

In this basis, a general fluctuation about a state $|y_i\rangle$ [[Eq. \(114\)](#)], can be written

$$\hat{\mathbf{A}}_i = \begin{pmatrix} \hat{a}_i^\dagger \hat{a}_i & \hat{a}_i^\dagger & \hat{a}_i^\dagger \hat{b}_i \\ \hat{a}_i & 1 - \hat{a}_i^\dagger \hat{a}_i - \hat{b}_i^\dagger \hat{b}_i & \hat{b}_i \\ \hat{b}_i^\dagger \hat{a}_i & \hat{b}_i^\dagger & \hat{b}_i^\dagger \hat{b}_i \end{pmatrix}, \quad (173)$$

cf. [Eq. \(121\)](#). To quadratic order in Bosons, the BBQ model, [Eq. \(72\)](#), then reads

$$\mathcal{H}'_{\text{BBQ}} = E_0 + \frac{1}{2} \sum_{\mathbf{k}} [\hat{\mathbf{w}}_{\mathbf{k}}^\dagger M_{\mathbf{k}} \hat{\mathbf{w}}_{\mathbf{k}}] + \mathcal{O}(\bar{w}^4), \quad (174)$$

where

$$\hat{\mathbf{w}}_{\mathbf{k}}^\dagger = (\hat{a}_{\mathbf{k}}^\dagger, \hat{a}_{-\mathbf{k}}, \hat{b}_{\mathbf{k}}^\dagger, \hat{b}_{-\mathbf{k}}), \quad \hat{\mathbf{w}}_{\mathbf{k}} = \begin{pmatrix} \hat{a}_{\mathbf{k}} \\ \hat{a}_{-\mathbf{k}}^\dagger \\ \hat{b}_{\mathbf{k}} \\ \hat{b}_{-\mathbf{k}}^\dagger \end{pmatrix}, \quad (175)$$

with ground–state energy E_0 [[Eq. \(125\)](#)], and fluctuations conditioned by the same matrix $M_{\mathbf{k}}$ [[Eq. \(127\)](#)] as appears in the classical theory [[Eq. \(124\)](#)].

From the Bosonic commutation relations [[Eq. \(172\)](#)], it follows that

$$[\hat{\mathbf{w}}_{\mathbf{k}\alpha}, \hat{\mathbf{w}}_{\mathbf{q}}^{\dagger\beta}] = \gamma_0 \alpha^\beta \delta_{\mathbf{k},\mathbf{q}}, \quad (176)$$

where

$$\gamma_0 = \begin{pmatrix} 1 & 0 & 0 & 0 \\ 0 & -1 & 0 & 0 \\ 0 & 0 & 1 & 0 \\ 0 & 0 & 0 & -1 \end{pmatrix}. \quad (177)$$

The excitations described by these operators form bands, whose dispersion can be found by solving the eigensystem

$$\gamma_0 M_{\mathbf{k}} u_{\mathbf{k},\lambda} = \epsilon_{\mathbf{k},\lambda} u_{\mathbf{k},\lambda} \quad \lambda = 1, 2, 3, 4, \quad (178)$$

with eigenvectors $u_{\lambda,\mathbf{k}}$, and associated eigenvalues $\epsilon_{\mathbf{k},\lambda}$. This is equivalent to diagonalising the matrix

$$\gamma_0 M_{\mathbf{k}} = \begin{pmatrix} A_{\mathbf{k}} & -B_{\mathbf{k}} & 0 & 0 \\ B_{\mathbf{k}} & -A_{\mathbf{k}} & 0 & 0 \\ 0 & 0 & A_{\mathbf{k}} & -B_{\mathbf{k}} \\ 0 & 0 & B_{\mathbf{k}} & -A_{\mathbf{k}} \end{pmatrix}, \quad (179)$$

where $A_{\mathbf{k}}, B_{\mathbf{k}}$ are defined through [Eq. \(128\)](#). This is a task which can, if necessary, be performed numerically. But in the present case, closed–form analytic solution is possible, and we find

$$\epsilon_{\mathbf{k},1} = -\epsilon_{\mathbf{k},2} = \epsilon_{\mathbf{k},3} = -\epsilon_{\mathbf{k},4} = +\sqrt{A_{\mathbf{k}}^2 - B_{\mathbf{k}}^2}. \quad (180)$$

Of these, only the two solutions with positive energy, $\epsilon_{\mathbf{k},1}$ and $\epsilon_{\mathbf{k},3}$, correspond to physical modes of the system, and so we have a total of two Bosonic modes per site, as anticipated. Further details of this calculation are given in [Appendix E](#).

The solution of the quantum eigensystem, [Eq. \(178\)](#), is equivalent to performing generalised Bogoliubov transformation between the original set of Bosons, [Eq. \(172\)](#), and a new set of Bosonic operators

$$[\hat{\alpha}_{\mathbf{k}}, \hat{\alpha}_{\mathbf{k}'}^\dagger] = [\hat{\beta}_{\mathbf{k}}, \hat{\beta}_{\mathbf{k}'}^\dagger] = \delta_{\mathbf{k}\mathbf{k}'}, \quad (181)$$

which diagonalize the Hamiltonian. These are defined through

$$\hat{\mathbf{w}}_{\mathbf{k}}^\dagger = \frac{1}{\sqrt{\Delta_{\mathbf{k}}^2 - B_{\mathbf{k}}^2}} \begin{pmatrix} \Delta_{\mathbf{k}} & -B_{\mathbf{k}} & 0 & 0 \\ -B_{\mathbf{k}} & \Delta_{\mathbf{k}} & 0 & 0 \\ 0 & 0 & \Delta_{\mathbf{k}} & -B_{\mathbf{k}} \\ 0 & 0 & -B_{\mathbf{k}} & \Delta_{\mathbf{k}} \end{pmatrix} \hat{\mathbf{u}}_{\mathbf{k}}^\dagger, \quad (182)$$

where

$$\hat{\mathbf{w}}_{\mathbf{k}}^\dagger = \begin{pmatrix} \hat{a}_{\mathbf{k}} \\ \hat{a}_{-\mathbf{k}}^\dagger \\ \hat{b}_{\mathbf{k}} \\ \hat{b}_{-\mathbf{k}}^\dagger \end{pmatrix}; \quad \hat{\mathbf{u}}_{\mathbf{k}}^\dagger = \begin{pmatrix} \hat{\alpha}_{\mathbf{k}} \\ \hat{\alpha}_{-\mathbf{k}}^\dagger \\ \hat{\beta}_{\mathbf{k}} \\ \hat{\beta}_{-\mathbf{k}}^\dagger \end{pmatrix}; \quad \Delta_{\mathbf{k}} = A_{\mathbf{k}} + \sqrt{A_{\mathbf{k}}^2 - B_{\mathbf{k}}^2}. \quad (183)$$

In this new basis, the Hamiltonian can be written

$$\mathcal{H}'_{\text{BBQ}} = E_0 + \Delta E_0 + \sum_{\mathbf{k}} \epsilon(\mathbf{k}) [\hat{\alpha}_{\mathbf{k}}^\dagger \hat{\alpha}_{\mathbf{k}} + \hat{\beta}_{\mathbf{k}}^\dagger \hat{\beta}_{\mathbf{k}}] + [\text{higher order terms}], \quad (184)$$

where

$$\epsilon(\mathbf{k}) = \sqrt{A_{\mathbf{k}}^2 - B_{\mathbf{k}}^2}, \quad (185)$$

and

$$\Delta E_0 = \sum_{\mathbf{k}} A_{\mathbf{k}} + \epsilon(\mathbf{k}), \quad (186)$$

represents the contribution to the ground state energy coming from the zero-point fluctuations, and E_0 is the ground state energy given in Eq. (125). Written in this form, the result is exactly equivalent to that found in an earlier, linear ‘‘flavour wave’’ treatment of FQ order [19], obtained through condensation of Schwinger Bosons [56].

B. Dynamical structure factors within zero-temperature quantum theory

From this starting point, it is a straightforward, if involved, exercise to calculate the dynamical structure factors which characterize the excitations of FQ order. These have the form

$$S_{\text{O}}^{\text{QM}}(\mathbf{q}, \omega) = \int_{-\infty}^{\infty} \frac{dt}{2\pi} e^{i\omega t} \sum_{\alpha, \beta} \langle \hat{O}_{\mathbf{q}, \beta}^{\alpha}(t) \hat{O}_{-\mathbf{q}, \alpha}^{\beta}(0) \rangle \quad (187)$$

where

$$\hat{O}_{\mathbf{q}, \beta}^{\alpha} = \frac{1}{\sqrt{N}} \hat{O}_{i, \beta}^{\alpha} e^{i\mathbf{q}\cdot\mathbf{r}_i}, \quad (188)$$

and the operator \hat{O}_{β}^{α} can reflect fluctuations of dipole moments, \hat{S}^{μ} ; quadrupole moments, $\hat{Q}^{\mu\nu}$; or the underlying representation of $u(3)$, \hat{A}_{ν}^{μ} .

We evaluate dynamical structure factors at finite energy ($\omega > 0$) through the explicit calculation of matrix elements within a multiple-Boson expansion. The structure of these calculations is described in Appendix F 1. Static structure factors ($\omega = 0$) can also be calculated through functional derivatives of the ground-state energy, in analogy with Section IV C. Details of this approach are given in Appendix F 5.

Below, we sketch key results at $T = 0$ which are needed for subsequent comparison with numerics [Section VI], and the exploration of the relationship between quantum and classical results [Section VII].

1. Dynamical spin structure factor

We consider first the dynamical spin structure factor

$$S_{\text{S}}^{\text{QM}}(\mathbf{q}, \omega) = \int_{-\infty}^{\infty} \frac{dt}{2\pi} e^{i\omega t} \sum_{\mu} \langle \hat{S}_{\mathbf{q}}^{\mu}(t) \hat{S}_{-\mathbf{q}}^{\mu}(0) \rangle. \quad (189)$$

Substituting Eq. (173) in the expression for spin operators, Eq. (50), and keeping terms to linear order, we find

$$\hat{S}_i^x \simeq i(\hat{b}_i^{\dagger} - \hat{b}_i), \quad (190a)$$

$$\hat{S}_i^y \simeq 0, \quad (190b)$$

$$\hat{S}_i^z \simeq -i(\hat{a}_i^{\dagger} - \hat{a}_i). \quad (190c)$$

Performing a Fourier transform and using the Bogoliubov transformation Eq. (182), we can express these as

$$\hat{S}_{\mathbf{q}}^x \simeq i\xi_{\text{S}}(\mathbf{q})(\hat{\beta}_{-\mathbf{q}}^{\dagger} - \hat{\beta}_{\mathbf{q}}), \quad (191a)$$

$$\hat{S}_{\mathbf{q}}^y \simeq 0, \quad (191b)$$

$$\hat{S}_{\mathbf{q}}^z \simeq -i\xi_{\text{S}}(\mathbf{q})(\hat{\alpha}_{-\mathbf{q}}^{\dagger} - \hat{\alpha}_{\mathbf{q}}), \quad (191c)$$

where $\xi_{\text{S}}(\mathbf{q})$ is the coherence factor

$$\xi_{\text{S}}(\mathbf{q}) = \frac{\Delta_{\mathbf{q}} + B_{\mathbf{q}}}{\sqrt{\Delta_{\mathbf{q}}^2 - B_{\mathbf{q}}^2}}. \quad (192)$$

From this starting point we can connect $S_{\text{S}}^{\text{QM}}(\mathbf{q}, \omega)$ directly with the multiple-Boson expansion of Section V A.

Since FQ order does not break time-reversal symmetry, static averages of dipole moments vanish, and all contributions to $S_{\text{S}}^{\text{QM}}(\mathbf{q}, \omega)$ come from excitations. Evaluating these, we find

$$S_{\text{S}}^{\text{QM}}(\mathbf{q}, \omega) = 2 \frac{\sqrt{A_{\mathbf{q}} + B_{\mathbf{q}}}}{\sqrt{A_{\mathbf{q}} - B_{\mathbf{q}}}} \delta(\omega - \omega_{\mathbf{q}}), \quad (193)$$

leading to an equal-time structure factor

$$S_{\text{S}}^{\text{QM}}(\mathbf{q}) = \int d\omega S_{\text{S}}^{\text{QM}}(\mathbf{q}, \omega) = 2 \frac{\sqrt{A_{\mathbf{q}} + B_{\mathbf{q}}}}{\sqrt{A_{\mathbf{q}} - B_{\mathbf{q}}}}. \quad (194)$$

Using Eq. (185), Eq. (183) and Eq. (192) we can show that

$$\xi_{\text{S}}^2(\mathbf{q}) = \frac{\sqrt{A_{\mathbf{q}} + B_{\mathbf{q}}}}{\sqrt{A_{\mathbf{q}} - B_{\mathbf{q}}}}, \quad (195)$$

and write Eq. (194) as

$$S_{\text{S}}^{\text{QM}}(\mathbf{q}) = 2\xi_{\text{S}}^2(\mathbf{q}). \quad (196)$$

This is a fact we will return to in Section VII A.

Further details of calculation of $S_{\text{S}}^{\text{QM}}(\mathbf{q}, \omega)$ are given in Appendix F 2 for $\mathbf{q} \neq 0$, and in Appendix F 6 for $\mathbf{q} = 0$.

2. Dynamical quadrupole structure factor

We now consider the dynamical structure factor associated with quadrupole moments

$$S_{\text{Q}}^{\text{QM}}(\mathbf{q}, \omega) = \int_{-\infty}^{\infty} \frac{dt}{2\pi} e^{i\omega t} \sum_{\mu\nu} \langle \hat{Q}_{\mathbf{q}}^{\mu\nu}(t) \hat{Q}_{-\mathbf{q}}^{\mu\nu}(0) \rangle. \quad (197)$$

Following the same steps as for the spin-structure factor, starting from Eq. (51), we find

$$\hat{Q}_i \cong \begin{pmatrix} \frac{2}{3} & -\hat{a}_i^{\dagger} - \hat{a}_i & 0 \\ -\hat{a}_i^{\dagger} - \hat{a}_i & -\frac{4}{3} & -\hat{b}_i^{\dagger} - \hat{b}_i \\ 0 & -\hat{b}_i^{\dagger} - \hat{b}_i & \frac{2}{3} \end{pmatrix}. \quad (198)$$

After Fourier transform, and transcription into the Bogoliubov basis, this yields

$$\hat{\mathbf{Q}}_{\mathbf{q}} \cong \begin{pmatrix} \frac{2}{3}\sqrt{N}\delta(\mathbf{q}) & \xi_{\mathbf{Q}}(\mathbf{q})(\hat{\alpha}_{-\mathbf{q}}^\dagger + \hat{\alpha}_{\mathbf{q}}) & 0 \\ \xi_{\mathbf{Q}}(\mathbf{q})(\hat{\alpha}_{-\mathbf{q}}^\dagger + \hat{\alpha}_{\mathbf{q}}) & -\frac{4}{3}\sqrt{N}\delta(\mathbf{q}) & \xi_{\mathbf{Q}}(\mathbf{q})(\hat{\beta}_{-\mathbf{q}}^\dagger + \hat{\beta}_{\mathbf{q}}) \\ 0 & \xi_{\mathbf{Q}}(\mathbf{q})(\hat{\beta}_{-\mathbf{q}}^\dagger + \hat{\beta}_{\mathbf{q}}) & \frac{2}{3}\sqrt{N}\delta(\mathbf{q}) \end{pmatrix}, \quad (199)$$

where N is the number of sites, and the relevant coherence factor is given by

$$\xi_{\mathbf{Q}}(\mathbf{q}) = \frac{B_{\mathbf{q}} - \Delta_{\mathbf{q}}}{\sqrt{\Delta_{\mathbf{q}}^2 - B_{\mathbf{q}}^2}}. \quad (200)$$

Quadrupole moments at $\mathbf{q} = 0$ take on a finite value in a FQ state, and both the ground state and excitations contribute to the structure factor $S_{\mathbf{Q}}^{\text{QM}}(\mathbf{q}, \omega)$. Evaluating both, we find

$$S_{\mathbf{Q}}^{\text{QM}}(\mathbf{q}, \omega) = \frac{8}{3}N(1 - \Delta^{\text{QM}})\delta(\mathbf{q})\delta(\omega) + 4\frac{\sqrt{A_{\mathbf{q}} - B_{\mathbf{q}}}}{\sqrt{A_{\mathbf{q}} + B_{\mathbf{q}}}}\delta(\omega - \omega_{\mathbf{q}}), \quad (201)$$

where Δ^{QM} is given by as

$$\Delta^{\text{QM}} = \frac{3}{N} \sum_{\mathbf{k}} \frac{A_{\mathbf{k}}}{\sqrt{A_{\mathbf{k}}^2 - B_{\mathbf{k}}^2}}. \quad (202)$$

The corresponding equal-time structure factor is given by

$$S_{\mathbf{Q}}^{\text{QM}}(\mathbf{q}) = \frac{8}{3}N(1 - \Delta^{\text{QM}})\delta(\mathbf{q}) + 4\frac{\sqrt{A_{\mathbf{q}} - B_{\mathbf{q}}}}{\sqrt{A_{\mathbf{q}} + B_{\mathbf{q}}}}. \quad (203)$$

Details of these calculations can be found in [Appendix F3](#) and in [Appendix F7](#) for $\mathbf{q} = 0$.

3. Structure factor for A matrices

The most fundamental objects in our theory are not dipoles or quadrupoles, but the A-matrices which describe the quantum state of the spin-1 moment. It is therefore useful to introduce a dynamical structure factor

$$S_{\mathbf{A}}^{\text{QM}}(\mathbf{q}, \omega) = \int_{-\infty}^{\infty} \frac{dt}{2\pi} e^{i\omega t} \sum_{\mu\nu} \langle \hat{A}_{\nu}^{\mu}(t) \hat{A}_{\mu}^{\nu}(0) \rangle. \quad (204)$$

This structure factors captures all dynamics that can be resolved at the level of a two-point correlation function, regardless of how that dynamics is expressed in spin correlations. Neglecting 2nd order and higher terms, [Eq. \(173\)](#) implies

$$\hat{\mathbf{A}}_i \cong \begin{pmatrix} 0 & \hat{a}_i^\dagger & 0 \\ \hat{a}_i & 1 & \hat{b}_i \\ 0 & \hat{b}_i^\dagger & 0 \end{pmatrix}. \quad (205)$$

Fourier transforming, and resolving non-zero matrix elements in terms of the Bogoliubov basis [Eq. \(204\)](#), we find

$$\hat{\mathbf{A}}_{\mathbf{q}} \cong \begin{pmatrix} 0 & \xi_{\mathbf{A}}^-(\mathbf{q})\hat{\alpha}_{-\mathbf{q}}^\dagger & 0 \\ -\xi_{\mathbf{A}}^+(\mathbf{q})\hat{\alpha}_{-\mathbf{q}}^\dagger & -\xi_{\mathbf{A}}^+(\mathbf{q})\hat{\alpha}_{\mathbf{q}} & -\xi_{\mathbf{A}}^+(\mathbf{q})\hat{\beta}_{-\mathbf{q}}^\dagger \\ +\xi_{\mathbf{A}}^-(\mathbf{q})\hat{\alpha}_{\mathbf{q}} & \sqrt{N}\delta_{\mathbf{q},0} & +\xi_{\mathbf{A}}^-(\mathbf{q})\hat{\beta}_{\mathbf{q}} \\ 0 & \xi_{\mathbf{A}}^-(\mathbf{q})\hat{\beta}_{-\mathbf{q}}^\dagger & 0 \\ & -\xi_{\mathbf{A}}^+(\mathbf{q})\hat{\beta}_{\mathbf{q}} & \end{pmatrix} \quad (206)$$

where N is the number of sites and $\xi_{\mathbf{A}}^+(\mathbf{q})$ and $\xi_{\mathbf{A}}^-(\mathbf{q})$ are the coherence factors for A-matrices defined as

$$\xi_{\mathbf{A}}^+(\mathbf{q}) = \frac{\xi_{\text{S}}(\mathbf{q}) + \xi_{\mathbf{Q}}(\mathbf{q})}{2}, \quad (207a)$$

$$\xi_{\mathbf{A}}^-(\mathbf{q}) = \frac{\xi_{\text{S}}(\mathbf{q}) - \xi_{\mathbf{Q}}(\mathbf{q})}{2}, \quad (207b)$$

where $\xi_{\text{S}}(\mathbf{q})$ and $\xi_{\mathbf{Q}}(\mathbf{q})$ are defined in [Eq. \(192\)](#) and [Eq. \(200\)](#) respectively.

From this starting point, we can calculate all of the quantum averages which enter into $S_{\mathbf{A}}^{\text{QM}}(\mathbf{q}, \omega)$. Like the structure factor for quadrupole moments, this entails contributions from both ground state and excitations. Evaluating these, we find

$$S_{\mathbf{A}}^{\text{QM}}(\mathbf{q}, \omega) = N(1 - \frac{2}{3}\Delta^{\text{QM}})\delta(\mathbf{q})\delta(\omega) + 2\frac{A_{\mathbf{q}}}{\sqrt{A_{\mathbf{q}}^2 - B_{\mathbf{q}}^2}}\delta(\omega - \omega_{\mathbf{q}}), \quad (208)$$

where Δ^{QM} is defined in [Eq. \(202\)](#). It follows that the equivalent equal-time structure factor given by

$$S_{\mathbf{A}}^{\text{QM}}(\mathbf{q}) = N(1 - \frac{2}{3}\Delta^{\text{QM}})\delta(\mathbf{q}) + 2\frac{A_{\mathbf{q}}}{\sqrt{A_{\mathbf{q}}^2 - B_{\mathbf{q}}^2}}. \quad (209)$$

Details of these calculations can be found in [Appendix F4](#) and in [Appendix F8](#) for $\mathbf{q} = 0$.

4. Sum rule on structure factors

The sum rule on moments, [Eq. \(66\)](#), implies that dynamical structure factors must satisfy a sum rule

$$S_{\mathbf{A}}(\mathbf{q}, \omega) = \frac{1}{4}S_{\mathbf{Q}}(\mathbf{q}, \omega) + \frac{1}{2}S_{\text{S}}(\mathbf{q}, \omega) + \frac{1}{3}N\delta(\omega), \quad (210)$$

of the same form as the sum rule for equal-time structure factors, [Eq. \(168\)](#).

It is easy to confirm, by direct substitution in [Eq. \(210\)](#), that the quantum results at $T = 0$ for $S_{\text{S}}^{\text{QM}}(\mathbf{q}, \omega)$ [[Eq. \(194\)](#)], $S_{\mathbf{Q}}^{\text{QM}}(\mathbf{q}, \omega)$ [[Eq. \(203\)](#)] and $S_{\mathbf{A}}^{\text{QM}}(\mathbf{q}, \omega)$ [[Eq. \(209\)](#)], satisfy this sum rule. It is also informative to verify the sum rule visually, by examining how the intensities in the dipole channel [[Fig. 12 \(d\)](#)] and quadrupole channel [[Fig. 12 \(e\)](#)] “add up” to give the intensity for A-matrices [[Fig. 12 \(f\)](#)].

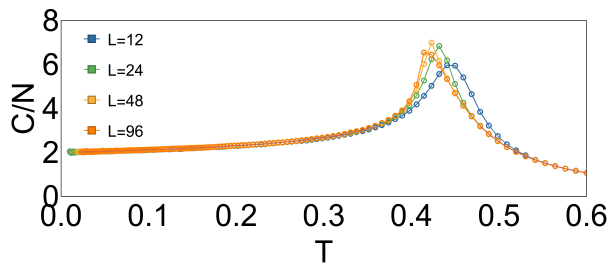


Figure 13. Temperature dependence of the specific heat per spin $c(T)$, found in $U(3)$ Monte Carlo (u3MC) simulations of \mathcal{H}_{BBQ} [Eq. (72)], for parameters consistent with a ferroquadrupolar (FQ) ground state. Results are shown for a series of clusters of increasing linear dimension L . The peak at $c(T)$ at $T^* \sim 0.43$ corresponds to the onset of fluctuations of FQ order, as shown in Fig. 14 (a). The low temperature asymptote $c(T \rightarrow 0) \rightarrow 2$ is consistent with the existence of four independent excitations about the the FQ ground state, as discussed in Section IV C. All simulations were carried out with parameters Eq. (212), using the MC scheme described in Section III A.

VI. LOW-TEMPERATURE PROPERTIES OF FERROQUADRUPOLAR ORDER FROM NUMERICAL SIMULATION

In this Section, we use the $U(3)$ Monte Carlo (u3MC) and Molecular Dynamics (u3MD) simulation schemes developed in Section III to explore thermodynamic and dynamic properties of ferroquadrupolar (FQ) order at low temperatures. Simulation results are compared directly with the analytic theory developed in Section IV. We start by analysing the heat capacity, which is shown to satisfy the correct classical limit $c(T \rightarrow 0) \rightarrow 2$ [Section VI A]. Next we consider the low-temperature properties of the ordered moment $\langle Q \rangle$. This takes on a finite value in simulation, but is shown to exhibit finite-size scaling consistent with the Mermin-Wagner theorem [Section VI B].

We then turn to the equal-time structure factors associated with dipole and quadrupole moments. At low-temperatures, these conform to the predictions of Section IV, confirming that simulations accurately describe correlations within the FQ state [Section VI C].

Finally, we present “raw” simulation results for dynamical structure factors [Section VI D]. These reproduce the dispersion predicted by the zero-temperature quantum theory [Section V], but with a mismatch in intensities. The way in which this mismatch can be corrected to achieve agreement with quantum theory in the limit $T \rightarrow 0$ will be analysed in Section VII.

A. Heat capacity

In Fig. 13 we present results for the heat capacity per spin

$$c(T) = C(T)/N = \frac{1}{N} \frac{1}{T^2} [\langle E(T)^2 \rangle - \langle E(T) \rangle^2], \quad (211)$$

obtained in simulations of \mathcal{H}_{BBQ} [Eq. (72)], for the same parameter set used in Fig. 12

$$J_1 = 0.0, \quad J_2 = -1.0. \quad (212)$$

Results were obtained using the $U(3)$ Monte Carlo (u3MC) formalism developed in Section III A, for clusters of linear dimension up to $L = 96$ ($N = 9216$ spins).

At low temperature, we find

$$c(T \rightarrow 0) \rightarrow 2. \quad (213)$$

This is the result anticipated from the classical theory developed in Section IV B [cf. Eq. (150)], and reflects the fact that the $u(3)$ formalism correctly describes the 4 orthogonal generators of fluctuations about the FQ ground state. Each of these contribute $1/2$ to $c(T)$ in the limit $T \rightarrow 0$, as discussed in Section IV C. This should be contrasted with classical MC simulations in an $O(3)$ basis, where at most two generators per spin are accessible and $c(T \rightarrow 0) \leq 1$ [Eq. (152)].

Meanwhile, the onset of fluctuations of FQ order is signaled by a pronounced peak at $T^* \sim 0.43$, which gradually sharpens and moves to lower temperatures with increasing system size. The scaling of this peak is not consistent with a conventional phase transition, and long range FQ order is not expected to occur in the two-dimensional BBQ model at finite temperature, because of the Mermin-Wagner theorem [103].

None the less, a BKT-like topological phase transition into a phase with algebraic correlations of FQ order is permitted, and would also give rise to a peak in heat capacity. Such a phase transition can be mediated by point-like,

$$\pi_1(RP_2) = \mathbb{Z}_2, \quad (214)$$

topological defects of FQ order, and has been observed in previous MC simulations of the $O(3)$ BBQ model on the triangular lattice [104]. A detailed analysis of topological phase transitions in the spin-1 BBQ model lies outside the scope of this paper, but contains many interesting features, which will be discussed elsewhere [97].

B. Ordered moment

We now consider the behaviour of the quadrupole-moment \mathbf{Q} , which acts as an order parameter for the FQ state. In Fig. 14 we show simulation results, obtained for the same parameter set, Eq. (212). The ordered moment was calculated through the equal-time structure factor

$$\mathbf{Q}^2 = \frac{S_{\mathbf{Q}}^{\text{CL}}(\mathbf{q} = \Gamma)}{N}. \quad (215)$$

and takes on a finite value in finite-size clusters, as shown in Fig. 14 (a). At low temperature, these results extrapolate to the expected ground-state value [Eq. (170)]

$$\mathbf{Q}^2|_{T \rightarrow 0} = Q_0^2 = \frac{8}{3}, \quad (216)$$

and are well-described by the function

$$\mathbf{Q}^2 = Q_0^2 + \alpha(L)T + \beta(L)T^2 + \dots, \quad (217)$$

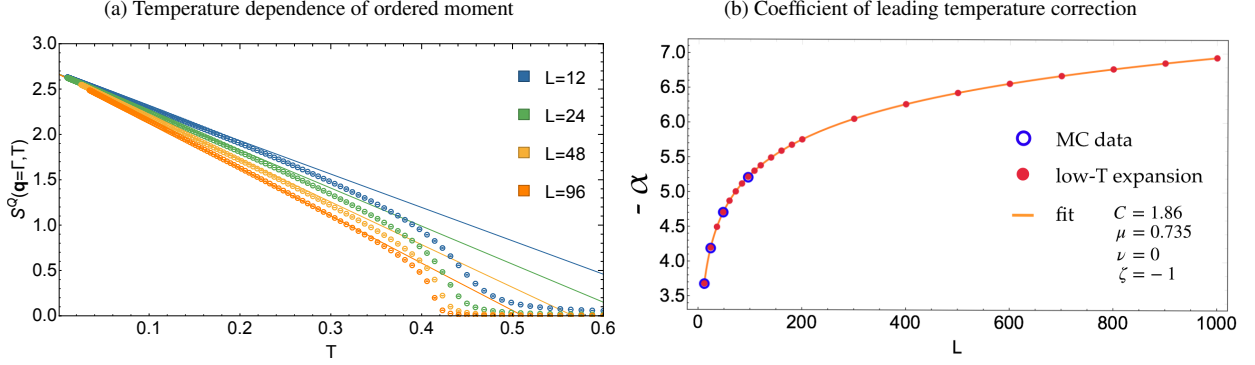


Figure 14. Temperature dependence of the quadrupole moment \mathbf{Q} found in $U(3)$ Monte Carlo (u3MC) simulations of \mathcal{H}_{BBQ} [Eq. (72)], for parameters consistent with a ferroquadrupolar (FQ) ground state. (a) Results for \mathbf{Q}^2 in a series of clusters of increasing linear dimension, L . The onset of fluctuations of FQ order at \mathbf{Q}^2 at $T^* \sim 0.43$, corresponds to the peak in heat capacity, shown in Fig. 13. At low temperatures, \mathbf{Q} tends to the ordered moment of the FQ ground state, Q_0 [Eq. (216)]. (b) Finite-size scaling of the coefficient $\alpha(L)$ [Eq. (217)], showing a logarithmic divergence in temperature-corrections to the ordered moment [Eq. (218)], consistent with the Mermin–Wagner Theorem. Results are shown for both u3MC simulations, and the analytic theory developed in Section IV B. All simulations were carried out with parameters Eq. (212), using the u3MC scheme described in Section III A.

where the coefficients $\alpha(L)$ and $\beta(L)$ are determined by fits to simulation results. At a temperature corresponding to the peak in heat capacity, $T \approx T^* \sim 0.43$ [Fig. 13], the value of \mathbf{Q}^2 collapses rapidly. Above this temperature, \mathbf{Q}^2 tends rapidly to zero with increasing system size.

For the Mermin–Wagner theorem to hold, we must find $\mathbf{Q}^2 \equiv 0$ in the thermodynamic limit, at any finite temperature [103]. It follows that the coefficient $\alpha(L)$ in Eq. (217) must diverge as $L \rightarrow \infty$. The trend in $\alpha(L)$ with increasing L is immediately apparent from Fig. 14 (a): the rate at which thermal fluctuations reduce the ordered moment is a monotonically increasing function of L . However, for all system sizes accessible to simulation, the ordered moment still takes on a substantial value at low temperatures.

This seeming-paradox can be resolved by turning to the analytic theory developed in Section IV B. In Fig. 14 (b) we plot the values of $\alpha(L)$ obtained in simulation, together with analytic results for systems of size up to $L = 1000$ ($N = 10^6$ spins). Analytic estimates of $\alpha(L)$ were found by evaluating the sum on \mathbf{k} in Eq. (170) numerically, for the specific set of wave vectors allowed by the geometry of the clusters. Evaluating the leading contribution to this sum as an integral, we can identify a logarithmic divergence in $\alpha(L)$ for large L . And consistent with this, both analytic and numerical results are well described by the function

$$-\alpha(L) = \alpha_0 + \mu \log L + \nu \frac{1}{L} + \xi \frac{1}{L^2}, \quad (218)$$

with fit parameters

$$\alpha_0 = 1.86, \quad \mu = 0.735, \quad \nu = 0, \quad \xi = -1. \quad (219)$$

It follows that $-\alpha(L \rightarrow \infty) \rightarrow \infty$, and the Mermin–Wagner Theorem is respected. Further details of this analysis can be found in Appendix G

C. Equal-time structure factor

We now turn to correlations between magnetic moments, as described by the equal-time structure factors $S_\lambda^{\text{CL}}(\mathbf{q})$ [Eq. (84)], found in u3MC simulations of \mathcal{H}_{BBQ} [Eq. (72)]. In Fig. 15, results are shown for the structure factors associated with dipole moments, $S_S(\mathbf{q})$, quadrupole moments $S_Q(\mathbf{q})$, and A-matrices, $S_A(\mathbf{q})$. Simulations were carried out for parameters consistent with a FQ ground state [Eq. (212)], at a temperature $T \approx 0.03$, in a cluster of linear dimension $L = 96$ ($N = 9216$ spins). All results are plotted on an irreducible wedge Γ –K–M– Γ [cf. Appendix C], and have been divided by temperature, T , to extract their leading temperature dependence.

Fluctuations of dipole moments vanish in the FQ ground state, but take on a finite value at finite temperature, as shown in Fig. 15 (a). Simulation results for $S_S(\mathbf{q})/T$ at low temperatures (points) are perfectly described by the low-temperature analytic prediction, Eq. (157), (solid line). A broad peak in $S_S(\mathbf{q})$ for $\mathbf{q} = \text{K}$ reflects the proximity of 3-sublattice antiferromagnetic order (AFM), as discussed in Section III A 2.

Meanwhile, the quadrupolar structure factor $S_Q(\mathbf{q})$ is sensitive to fluctuations of FQ order, and exhibits a \mathbf{q} -dependent contribution that diverges for $\mathbf{q} \rightarrow 0$, as shown in Fig. 15 (b). Once again, the agreement between simulation results for $S_Q(\mathbf{q})/T$ at low temperatures (points) and the low-temperature analytic prediction, Eq. (161), (line), is perfect.

Finally, the structure factor for A-matrices $S_A(\mathbf{q})$, shown in Fig. 15 (c), is sensitive to both quadrupolar and dipolar fluctuations. In keeping with this, it exhibits both a diverging contribution for $\mathbf{q} \rightarrow 0$, and a small peak at $\mathbf{q} = \text{K}$. Perfect agreement is found between simulation results for $S_A(\mathbf{q})/T$ at low temperatures (points) and the low-temperature analytic prediction, Eq. (165), (line).

Taken together, these results for $S_\lambda^{\text{CL}}(\mathbf{q})$ confirm the ability of the u3MC scheme developed in Section III A, to de-

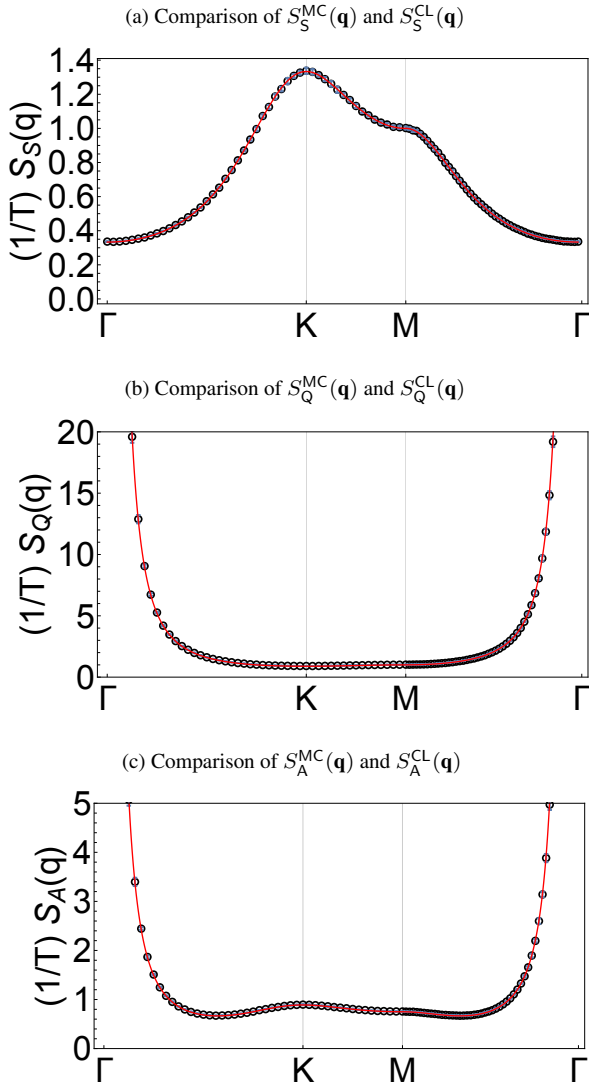


Figure 15. Results for equal-time structure factors $S_\lambda^{\text{CL}}(\mathbf{q})$ [Eq. (84)] found in $U(3)$ Monte Carlo (u3MC) simulations of \mathcal{H}_{BBQ} [Eq. (72)], for parameters consistent with a ferroquadrupolar (FQ) ground state. (a) Structure factor associated with dipole moments, $S_S^{\text{CL}}(\mathbf{q})$, showing correlations at the 3-sublattice ordering vector, \mathbf{K} . (b) Structure factor associated with quadrupole moments, $S_Q^{\text{CL}}(\mathbf{q})$, showing divergence associated with fluctuations of FQ order for $\mathbf{q} \rightarrow \Gamma$. (c) Structure factor associated with A-matrices, $S_A^{\text{CL}}(\mathbf{q})$, sensitive to both dipolar and quadrupolar fluctuations. In all cases, simulation results (points) have been divided by temperature T , and agree perfectly with the predictions of low-temperature analytic theory (line). All simulations were carried out with parameters Eq. (212), for a cluster with linear dimension $L = 96$ ($N = 9216$ spins), at $T \approx 0.03$, using the u3MC scheme described in Section III A.

scribe classical correlations of spin-1 magnets at low temperature. They will also play an important role in determining the quantum-classical correspondence discussed in Section VII.

D. Dynamics

We complete our survey of simulation results for the FQ phase of the spin-1 BBQ model by exploring the dynamics found in numerical integration of the equations of motion, Eq. (73), following the $U(3)$ Molecular Dynamics (u3MD) scheme introduced Section III B.

In Fig. 16 we present “raw” results for the dynamical structure factors $S_\lambda^{\text{MD}}(\mathbf{q}, \omega)$ [Eq. (103)] associated with dipole moments ($\lambda = S$), quadrupole moments ($\lambda = Q$), and A-matrices ($\lambda = A$). Results are plotted for the same path in reciprocal space as was used for $S_\lambda^{\text{MC}}(\mathbf{q})$ in Fig. 15, for positive frequency $\omega > 0$. MD solutions at negative energy will contribute with equal weight [Eq. (110)]. For convenience of visualization, all results have been convoluted with a Gaussian of FWHM = $0.35 J$.

Comparing with the predictions of the zero-temperature quantum theory, $S_\lambda^{\text{QM}}(\mathbf{q}, \omega)$ [Fig. 12], we see that u3MD correctly reproduces a dispersing band of excitations, with predominantly quadrupolar character for $\omega \rightarrow 0$, and predominantly dipolar character at the top of the band. Closer examination, however, reveals small differences in the energy of excitations, and dramatic differences in the distribution of spectral weight across the band. In particular, while analytic results for the dipolar fluctuations [Fig. 12 (d), Eq. (193)], exhibit a characteristic linear loss of spectral weight at low energies [20]

$$S_S^{\text{QM}}(\mathbf{q} \rightarrow \mathbf{0}, \omega) \propto \omega \delta(\omega - \mathbf{v}|\mathbf{q}|), \quad (220)$$

numerical results for $S_S^{\text{MD}}(\mathbf{q}, \omega)$ [Fig. 16 (a)] show a roughly constant spectral weight for $\omega \rightarrow 0$. The distribution of spectral weight in the quadrupolar channel $S_Q^{\text{MD}}(\mathbf{q}, \omega)$ [Fig. 16 (b)], is also visibly different from analytic predictions [Fig. 12 (e), Eq. (201)].

A more precise portrait of the “raw” u3MD results can be found by examining the temperature dependence of dynamical structure factors at fixed wavevector \mathbf{q} . In Fig. 17 we present results for $S_A^{\text{MD}}(\mathbf{q}, \omega > 0)$ (symbols), at wave vector $\mathbf{q} = \mathbf{K}$, with temperatures ranging from $T = 0.01 J$ to $T = 0.15 J$. The prediction of a zero-temperature quantum theory, $S_A^{\text{QM}}(\mathbf{q} = \mathbf{K}, \omega)$ [Eq. (208)], is shown for comparison (dashed line). Both analytic and simulation results (symbols) have been convoluted with a Gaussian of FWHM = $0.02 J$.

“Raw” simulation results show a single peak in $S_A^{\text{MD}}(\mathbf{q} = \mathbf{K}, \omega > 0)$, centered on an energy ω_0 which varies as a function of temperature. This peak is well described by Voigt profile

$$V(\omega, \sigma, \Gamma) = \frac{\text{Re}[w(z)]}{\sigma\sqrt{2\pi}}, \quad (221)$$

where the Faddeeva function

$$w(z) = e^{-z^2} \text{erfc}(-iz) \quad (222)$$

is evaluated for

$$z = \frac{(\omega - \omega_0) + i\Gamma}{\sigma\sqrt{2}}. \quad (223)$$

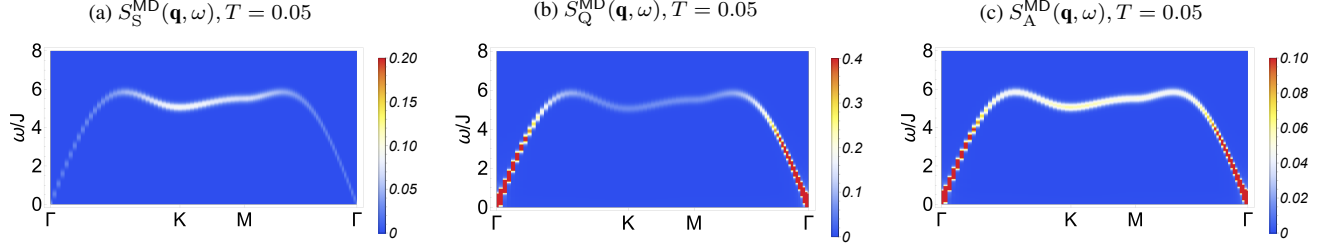


Figure 16. “Raw” results of $U(3)$ Molecular Dynamics (u3MD) simulations for parameters consistent with a ferroquadrupolar (FQ) ground state. (a) Dynamical structure factor associated with dipole moments, $S_S^{\text{MD}}(\mathbf{q}, \omega)$. (b) Dynamical structure factor associated with quadrupole moments, $S_Q^{\text{MD}}(\mathbf{q}, \omega)$. (c) Dynamical structure factor associated with A–matrices, $S_A^{\text{MD}}(\mathbf{q}, \omega)$. Comparison with the predictions of a quantum theory, Fig. 12 (d)–(f), suggests that “raw” simulation results accurately describe the dispersion of excitations, but with an incorrect distribution of intensity. Simulations were carried out using the u3MD simulation scheme described in Section III B, for \mathcal{H}_{BBQ} [Eq. (72)] with parameters Eq. (212), at a temperature $T = 0.05 J$, in a cluster of linear dimension $L = 96$ ($N = 9216$ spins). Results are shown only for positive energy, $\omega > 0$, and have been convoluted with a Gaussian envelope of FWHM = 0.35 J.

The Voigt profile reflects a Lorentzian lineshape

$$f(\omega) = \frac{\Gamma}{2\pi} \frac{1}{(\omega - \omega_0)^2 + \Gamma^2}, \quad (224)$$

appropriate to a single excitation of energy ω_0 and inverse lifetime Γ , convoluted with a Gaussian with full–width half–maximum (FWHM) determined by σ [Eq. (108)].

Empirical fits of Eq. (221) to simulation data are shown with solid lines in Fig. 17. The parameters used in MD simulation completely determine σ , leaving ω_0 , Γ , and the overall normalisation (total spectral weight) as a fit parameters. The fits found in the way are excellent, confirming that simulations recover a single excited mode for $\omega > 0$, with finite, temperature–dependent energy and lifetime.

As temperature is reduced, the peak in $S_A^{\text{MD}}(\mathbf{q} = \mathbf{K}, \omega)$ migrates to higher energies, and becomes sharper, while retaining its underlying Lorentzian structure. In both of these respects, for $T \rightarrow 0$, simulation results approach the $T = 0$ quantum result, where spectral weight is concentrated in a delta function, the $\Gamma \rightarrow 0$ limit of Eq. (224). However at low temperatures, the u3MD results also exhibit a dramatic loss of intensity, with integrated spectral weight tending to zero as $T \rightarrow 0$. And even at $T \sim 0.1$, the difference in intensity is at least a factor of $\times 100$, reflected in different scales on the axes for with $S_A^{\text{MD}}(\mathbf{q} = \mathbf{K}, \omega)$ and $S_A^{\text{QM}}(\mathbf{q} = \mathbf{K}, \omega)$. The reason for this discrepancy, and the way in which it can be corrected, will be discussed Section VII.

VII. QUANTUM–CLASSICAL CORRESPONDENCE

The reason why “raw” results of molecular dynamics simulations, presented in Section VID, capture the dispersion of quantum excitations, while failing to describe their spectral weight, is rooted in the classical statistics of the underlying classical Monte Carlo simulations.

The equation of motions (EoM) on which the u3MD is based, Eq. (73), correctly describe the dynamics of a spin–1

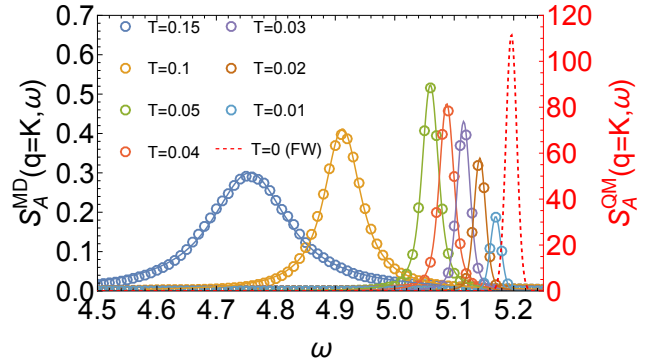


Figure 17. Temperature dependence of “raw” results of $U(3)$ Molecular Dynamics (u3MD) simulation, showing failure to converge to the predictions of a $T = 0$ quantum theory for $T \rightarrow 0$. Results are shown for the dynamical structure factor associated with A–matrices, $S_A^{\text{MD}}(\mathbf{q}, \omega)$ [Eq. (105)], for wave vector $\mathbf{q} = \mathbf{K}$, and temperatures ranging from $T = 0.01 J$ to $T = 0.15 J$. The $T = 0$ prediction of a quantum theory, $S_A^{\text{QM}}(\mathbf{q}, \omega)$ [Eq. (208)], is shown with a red dashed line. Solid lines represent fits to u3MD data using a Voigt profile [Eq. (221)]. “Raw” simulation results converge on energy predicted by the quantum theory for $T \rightarrow 0$, but suffer a dramatic loss of intensity. Simulations of \mathcal{H}_{BBQ} [Eq. (72)] were carried out using the MD simulation scheme described in Section III B, for parameters Eq. (212), in a cluster of linear dimension $L = 96$ ($N = 9216$ spins). Both simulation results and analytic prediction have been convoluted with a Gaussian of FWHM = 0.02 J.

moment, at a semi–classical level. And, solved analytically, with appropriate quantization, these EoM yield identical results to the linear multiple–Boson expansion developed in Section V [105]. However, the spectral weight found in u3MD simulation is not subject to any quantization condition. Instead this is determined by thermal fluctuations, subject to the classical statistics of Monte Carlo simulation. And for this reason, all spectral weight vanishes for $T \rightarrow 0$, as thermal fluctuations are eliminated, cf. Fig. 17.

None the less, the fact that spectral weight is concentrated

in a single peak, with Lorentzian lineshape, that becomes arbitrarily sharp for $T \rightarrow 0$, suggests that low-temperature simulation results can be understood within a single-mode approximation. And this encourages us to believe that it may be possible to “undo” the effect of classical statistics, in limit $T \rightarrow 0$. This line of reasoning, developed below, leads to a simple prescription for correcting MD simulation results

$$S^{\text{QM}}(\mathbf{q}, \omega, T = 0) = \lim_{T \rightarrow 0} \frac{\hbar\omega}{k_B T} S^{\text{MD}}(\mathbf{q}, \omega, T), \quad (225)$$

previously introduced in Eq. (12). This prescription is shown to restore to perfect agreement with zero-temperature quantum results, at a semi-classical level.

In what follows, we set out this analysis in more detail. In Section VII A, we “deconstruct” the dynamical structure factors found in u3MD simulations, analysing their intensities in terms of excitations with classical statistics, while retaining the quantum (more precisely, semi-classical) nature of their dynamics. Using what we have learned, in Section VII B, we show explicitly that u3MD simulation results can be corrected to yield dynamical structure factors in agreement with the predictions of Section V. We conclude, in Section VII C, with a comparison of u3MC and u3MD simulations with published results from Quantum Monte Carlo (QMC).

A. Molecular dynamics, deconstructed

We start by exploring the relationship between classical and quantum theories for fluctuations about FQ order, and their implication for the understanding of simulation. We concentrate on the experimentally-relevant structure factor for dipole moments $S_S(\mathbf{q})$, re-deriving the classical result quoted in Section IV in a framework which permits direct comparison with the quantum result given in Section V.

We take as starting point the quantum theory of excitations about the FQ state, Eq. (184), and include a term $\Delta\mathcal{H}[\mathbf{h}]$ describing coupling of dipole moments to a transverse field

$$\begin{aligned} \mathcal{H} &= \mathcal{H}'_{\text{BBQ}} + \Delta\mathcal{H}[\mathbf{h}] \\ &= E_0 + \Delta E_0 + \sum_{\mathbf{k}} \hbar\epsilon(\mathbf{k}) \left[\hat{\alpha}_{\mathbf{k}}^\dagger \hat{\alpha}_{\mathbf{k}} + \hat{\beta}_{\mathbf{k}}^\dagger \hat{\beta}_{\mathbf{k}} \right] \\ &\quad - \sum_{\mathbf{k}} \xi_S(\mathbf{k}) \left[i\hbar_{\mathbf{k}}^x (\hat{\beta}_{\mathbf{k}} - \hat{\beta}_{-\mathbf{k}}^\dagger) + i\hbar_{\mathbf{k}}^z (\hat{\alpha}_{-\mathbf{k}}^\dagger - \hat{\alpha}_{\mathbf{k}}) \right], \end{aligned} \quad (226)$$

where the excitation energy $\epsilon(\mathbf{k})$ is defined through Eq. (185), $\xi_S(\mathbf{k})$ is the coherence factor defined in Eq. (192), and all terms at cubic and higher order in Bosons have been neglected. Here and in what follows we restore dimensional constants \hbar and k_B , which have been set to unity elsewhere.

Recognising Eq. (226) as the Hamiltonian for a set of independent simple harmonic oscillators (SHO), we introduce a

new set of coordinates

$$\hat{\alpha}_{\mathbf{k}} = \sqrt{\frac{m\epsilon(\mathbf{k})}{2\hbar}} \hat{x}_{1,\mathbf{k}} + \frac{i}{\sqrt{2\hbar m\epsilon(\mathbf{k})}} \hat{p}_{1,\mathbf{k}}, \quad (227a)$$

$$\hat{\beta}_{\mathbf{k}} = \sqrt{\frac{m\epsilon(\mathbf{k})}{2\hbar}} \hat{x}_{2,\mathbf{k}} + \frac{i}{\sqrt{2\hbar m\epsilon(\mathbf{k})}} \hat{p}_{2,\mathbf{k}}, \quad (227b)$$

satisfying the canonical commutation relation

$$[\hat{x}_{\nu,\mathbf{k}}, \hat{p}_{\nu',\mathbf{k}'}] = i\hbar\delta_{\mathbf{k}\mathbf{k}'}\delta_{\nu\nu'}. \quad (228)$$

with $\nu = 1, 2$. Written in terms of these coordinates, the Hamiltonian [Eq. (226)] becomes

$$\begin{aligned} \mathcal{H} &= E_0 + \Delta E_0 \\ &\quad + \sum_{\nu,\mathbf{k}} \left[\frac{m\epsilon(\mathbf{k})^2}{2} \hat{x}_{\nu,\mathbf{k}}^2 + \frac{1}{2m} \hat{p}_{\nu,\mathbf{k}}^2 \right. \\ &\quad \left. - \sqrt{\frac{2\xi_S^2(\mathbf{k})}{m\hbar\epsilon(\mathbf{k})}} (\hbar_{\mathbf{k}}^z \delta_{1,\nu} + \hbar_{\mathbf{k}}^x \delta_{2,\nu}) \hat{p}_{\nu,\mathbf{k}} \right], \end{aligned} \quad (229)$$

As long as the commutation relation, Eq. (228), is respected, the excitations of Eq. (229) continue to have well-defined, Bosons statistics. Meanwhile, the neglect of higher-order terms means that the dynamics of these excitations are treated at the level of a semi-classical approximation. MD simulation, on the other hand, imposes quantum (semi-classical) dynamics on spin configurations drawn from classical MC simulation, and so not subject to any quantization condition. And, crucially, the thermal distribution of the states generated by MC simulation at low temperatures is conditioned by a classical, and not a quantum band dispersion [cf. Fig. 12].

We can model the classical statistics found in MD simulation by “turning off” the quantization of excitations in Eq. (229), and treating $x_{\nu,\mathbf{k}}$ and $p_{\nu,\mathbf{k}}$ as independent, classical, variables. This will inevitably lead us back to the classical theory developed in Section IV, but expressed in a form that makes it easier to draw conclusions about the relationship between classical and quantum results. Doing so, the partition function associated with Eq. (229) is given by

$$\begin{aligned} Z^{\text{CL}'} &= e^{-\beta(E_0 + \Delta E_0)} \prod_{\nu,\mathbf{k}} \left[\left(\int dx_{\nu,\mathbf{k}} e^{-\frac{1}{2}\beta m\epsilon(\mathbf{k})^2 x_{\nu,\mathbf{k}}^2} \right) \right. \\ &\quad \left. \times \left(\int dp_{\nu,\mathbf{k}} e^{-\frac{\beta}{2m} p_{\nu,\mathbf{k}}^2} e^{\beta \sqrt{\frac{2\xi_S^2(\mathbf{k})}{m\hbar\epsilon(\mathbf{k})}} (\hbar_{\mathbf{k}}^z \delta_{1,\nu} + \hbar_{\mathbf{k}}^x \delta_{2,\nu}) p_{\nu,\mathbf{k}}} \right) \right], \end{aligned} \quad (230)$$

where $\beta = 1/k_B T$. The integrals in Eq. (230) can be evaluated exactly [Eq. (H1a), Eq. (H1b)], to give

$$\begin{aligned} Z^{\text{CL}'} &= e^{-\beta(E_0 + \Delta E_0)} \prod_{\mathbf{k}} \left[\frac{2\pi}{\beta\epsilon(\mathbf{k})} e^{\frac{\beta\xi_S^2(\mathbf{k})(\hbar_{\mathbf{k}}^z)^2}{\hbar\epsilon(\mathbf{k})}} \right. \\ &\quad \left. \times \frac{2\pi}{\beta\epsilon(\mathbf{k})} e^{\frac{\beta\xi_S^2(\mathbf{k})(\hbar_{\mathbf{k}}^x)^2}{\hbar\epsilon(\mathbf{k})}} \right]. \end{aligned} \quad (231)$$

By construction, this theory now describes excitations subject to the classical (i.e. Boltzmann) statistics used in MC simulation. We are now in a position to calculate equal-time spin correlations using the same method as in [Section IV C 2](#), i.e. by constructing a free energy and differentiating this with respect to $h_{\mathbf{k}}^\alpha$. Doing so, we find

$$S_S^{\text{CL}'}(\mathbf{q}, T) = \sum_{\alpha} \langle \hat{S}_{\mathbf{q}}^{\alpha} \hat{S}_{\mathbf{q}}^{\alpha} \rangle = \frac{4\xi_S^2(\mathbf{q})}{\beta\hbar\epsilon(\mathbf{q})}, \quad (232)$$

where we have used the fact that $\langle \hat{S}_{\mathbf{q}}^{\alpha} \rangle \equiv 0$ in the FQ state.

The presence of the quantum dispersion $\epsilon(\mathbf{q})$ and coherence factor $\xi_S(\mathbf{q})$ in [Eq. \(232\)](#), is suggestive of the quantum theory developed in [Section V](#). And, by direct comparison with [Eq. \(194\)](#), we find

$$S_S^{\text{CL}'}(\mathbf{q}, T) = 2 \frac{S_S^{\text{QM}}(\mathbf{q}, T=0)}{\beta\hbar\epsilon(\mathbf{q})}, \quad (233)$$

a result which holds in the limit of low temperature. At the same time, $S_S^{\text{CL}'}(\mathbf{q})$ must ultimately be equivalent to the earlier classical result $S_S^{\text{CL}}(\mathbf{q})$ [[Eq. \(158\)](#)]. To this end, we can simplify [Eq. \(232\)](#) using [Eq. \(195\)](#), to recover

$$S_S^{\text{QM}}(\mathbf{q}) = 2\xi_S^2(\mathbf{q}), \quad (234)$$

previously introduced as [Eq. \(196\)](#). It follows that

$$S_S^{\text{CL}'}(\mathbf{q}, T) = \frac{4}{\beta(A_{\mathbf{q}} - B_{\mathbf{q}})} = S_S^{\text{CL}}(\mathbf{q}, T), \quad (235)$$

where this result also holds in the limit of low temperature. Combining this with [Eq. \(233\)](#), we arrive at a result which relates classical correlations at finite temperature, to those of a quantum system at $T = 0$:

$$S_S^{\text{QM}}(\mathbf{q}, T=0) = \lim_{T \rightarrow 0} \frac{\hbar\epsilon(\mathbf{q})}{2k_B T} S_S^{\text{CL}}(\mathbf{q}, T). \quad (236)$$

The approach developed above can be generalised from dipole moments $\lambda = S$, to quadrupole moments, $\lambda = Q$ and A -matrices, $\lambda = A$. This leads to the general result

$$S_{\lambda}^{\text{QM}}(\mathbf{q}, T=0) = \lim_{T \rightarrow 0} \frac{\hbar\epsilon(\mathbf{q})}{2k_B T} S_{\lambda}^{\text{CL}}(\mathbf{q}, T), \quad (237)$$

where we make explicit the role of temperature, and restore dimensional constants k_B and \hbar . We emphasize that the factor of $\epsilon(\mathbf{q})$ in [Eq. \(237\)](#) reflects the dispersion for a *quantized* excitation [[Eq. \(185\)](#)], and not the eigenvalue of a classical theory. It is also important to note that quantum mechanics have been treated at a semi-classical level, i.e. taking account of quantization, but considering only one path in the path integral. This approximation is, of course, exact for a SHO.

The principle problem encountered in “raw” MD results for dynamical structure factors, relative to quantum results at low temperatures, was the loss of spectral weight at low temperatures [cf. [Fig. 17](#)]. At low temperatures, we can equate $S_{\lambda}^{\text{CL}}(\mathbf{q}, T)$ with the structure factor found in MC simulation

$$\lim_{T \rightarrow 0} S_{\lambda}^{\text{MC}}(\mathbf{q}, T) = \lim_{T \rightarrow 0} S_{\lambda}^{\text{CL}}(\mathbf{q}, T), \quad (238)$$

permitting us to write

$$S_{\lambda}^{\text{QM}}(\mathbf{q}, T=0) = \lim_{T \rightarrow 0} \frac{\hbar\epsilon(\mathbf{q})}{2k_B T} S_{\lambda}^{\text{MC}}(\mathbf{q}, T). \quad (239)$$

We can therefore use MC simulation to estimate the total spectral weight in a zero-temperature quantum theory, at given \mathbf{q} , as long as we had prior knowledge of the characteristic energy scale $\epsilon(\mathbf{q})$. What remains is to understand the relationship between classical and quantum results in the absence of prior knowledge of the dispersion.

The effect of MD simulation is to redistribute the spectral weight at a given \mathbf{q} over a range of different ω , subject to the sum rule,

$$S_{\lambda}^{\text{MC}}(\mathbf{q}, T) = \int_{-\infty}^{\infty} d\omega S_{\lambda}^{\text{MD}}(\mathbf{q}, \omega, T). \quad (240)$$

To estimate the zero-temperature quantum result $S_{\lambda}^{\text{QM}}(\mathbf{q}, \omega, T=0)$, we therefore need to construct a model for this redistribution of spectral weight, subject to the condition that dynamics are treated at a semi-classical level.

Here it is instructive to return to the simulation results for fluctuations about FQ order, described in [Section VI D](#). From the “raw” results, [Fig. 16](#) and [Fig. 17](#), we learn that

- (i) for $T \rightarrow 0$, the characteristic energy scale of excitations converges on the exact quantum (semi-classical) result $\epsilon(\mathbf{q})$ [[Eq. \(185\)](#)], and
- (ii) excitations become sharp (resolution limited) for $T \rightarrow 0$.

FQ order, studied here, show a single, two-fold degenerate band of excitations. More generally, there may be many different excitations at a given \mathbf{q} . None the less, at a semi-classical level, (i.e. treated as a set of independent oscillators), in a finite-size system, each of these will have a well-defined energy. It is also important to remember that, while only results for positive frequency have been plotted in [Fig. 16](#), MD simulation will return solutions at both positive and negative energy, with equal weight [[Eq. \(110\)](#)].

With these assumptions in mind, we model MD simulation results in the limit $T \rightarrow 0$ in terms of delta-function peaks at energy $\omega = \pm\epsilon_{\nu}(\mathbf{k})$, with spectral weight shared equally between these two peaks, vis

$$\begin{aligned} & \lim_{T \rightarrow 0} S_{\lambda}^{\text{MD}}(\mathbf{q}, \omega, T) \\ &= \sum_{\nu} [A_{\lambda, \nu}(\mathbf{q}, T) \delta(\omega - \epsilon_{\nu}(\mathbf{k})) + A_{\lambda, \nu}(\mathbf{q}, T) \delta(\omega + \epsilon_{\nu}(\mathbf{k}))] \\ & \quad + \mathcal{O}(T^2). \end{aligned} \quad (241)$$

Here the sum on ν runs over all eigenmodes of the cluster with wavevector \mathbf{q} , and the corresponding spectral weight

$$A_{\lambda, \nu}(\mathbf{q}, T) = \frac{k_B T}{\hbar\epsilon_{\nu}(\mathbf{q})} \xi_{\lambda, \nu}^2(\mathbf{q}) \quad (242)$$

is defined through a generalized coherence factor

$$\xi_{\lambda, \nu}^2(\mathbf{q}) \geq 0, \quad (243)$$

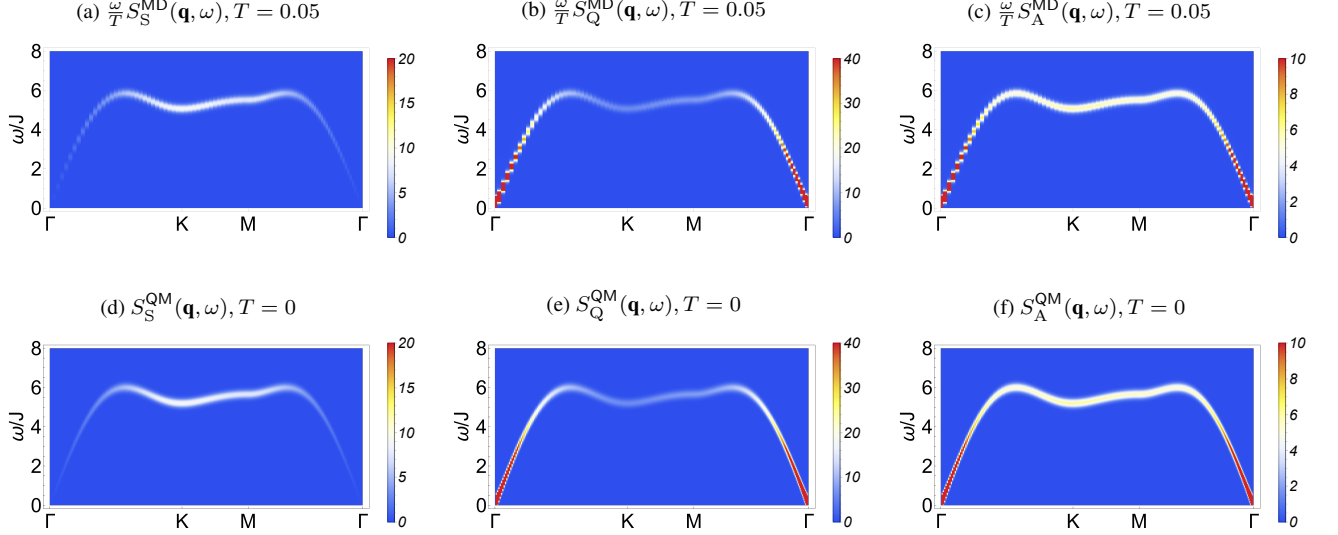


Figure 18. Comparison between dynamical structure factors found in molecular dynamics (u3MD) simulations of a ferroquadrupolar (FQ) state, and those found in a $T = 0$ quantum theory. (a) Simulation results for dynamical structure factor associated with dipole moments, $S_S^{\text{MD}}(\mathbf{q}, \omega)$, corrected for classical statistics, following Eq. (246). (b) Equivalent results for quadrupole moments, $S_Q^{\text{MD}}(\mathbf{q}, \omega)$. (c) Equivalent results for A-matrices, $S_A^{\text{MD}}(\mathbf{q}, \omega)$. (d) Prediction for $S_S^{\text{QM}}(\mathbf{q}, \omega)$ from $T = 0$ quantum theory [Eq. (193)]. (e) Equivalent prediction for $S_Q^{\text{QM}}(\mathbf{q}, \omega)$ [Eq. (201)]. (f) Equivalent prediction for $S_A^{\text{QM}}(\mathbf{q}, \omega)$ [Eq. (208)]. Simulations were carried out using the u3MD simulation scheme described in Section III B, for \mathcal{H}_{BBQ} [Eq. (72)] with parameters Eq. (212), at a temperature $T = 0.05 J$, in a cluster of linear dimension $L = 96$ ($N = 9216$ spins). All result have been convoluted with a Gaussian in frequency of FWHM = 0.35 J.

specific to the structure factor in question. The total spectral weight in these modes is constrained through Eq. (240), and satisfies

$$\begin{aligned} S_\lambda^{\text{QM}}(\mathbf{q}, T = 0) &= \int_{-\infty}^{\infty} d\omega S_\lambda^{\text{QM}}(\mathbf{q}, \omega, T = 0) \\ &= \sum_\nu \xi_{\lambda,\nu}^2(\mathbf{q}), \end{aligned} \quad (244)$$

where the sum on ν runs over the two degenerate branches of FQ excitations. For the dipolar structure factor, $\lambda = S$, this sum contributes a factor $\times 2$, and Eq. (244) can be compared directly with Eq. (196).

Where the model Eq. (241) holds, no prior knowledge of excitation energies $\epsilon_\nu(\mathbf{q})$ is needed to correct for the effect of classical statistics in MD simulation. And since only positive frequencies, corresponding to transfer of energy to the system, are relevant at $T = 0$, we can write

$$S_\lambda^{\text{QM}}(\mathbf{q}, \omega, T = 0) = \lim_{T \rightarrow 0} \frac{\hbar\omega}{k_B T} S_\lambda^{\text{MD}}(\mathbf{q}, \omega, T) \quad [\omega > 0]. \quad (245)$$

Here we understand that ‘‘QM’’ should be taken to imply ‘‘semi-classical’’, i.e. pertaining to excitations with quantum statistics, treated a Gaussian level of approximation. Empirical evidence for the validity of Eq. (245) is provided in Section VII B, below. Equivalent results for a system with many bands can be found in [66].

We conclude by noting that the approach of correcting for classical statistics by multiplying dynamical structure factors

by a prefactor ω/T has been anticipated several times in the literature of MD simulation, including in studies of the spin-1/2 magnet $\text{Ca}_{10}\text{Cr}_7\text{O}_{28}$ [66, 106], the spin-1 magnet $\text{NaCaNi}_7\text{O}_7$ [33], and dynamical scaling in $\text{Yb}_2\text{Ti}_2\text{O}_7$ [107]. The factor $\omega/2T$ used in [66] reflects a different normalisation of MD results.

B. Quantum results, reconstructed

Armed with Eq. (245), we are now in a position to revisit MD simulation results for excitations about a FQ ground state, previously discussed in Section VI D. In Fig. 18, we show a comparison between MD simulation results, and the predictions of the zero-temperature quantum theory developed in Section V. Following Eq. (245), simulation results have been corrected by multiplying them by prefactor ω/T , vis

$$\tilde{S}_\lambda^{\text{MD}}(\mathbf{q}, \omega, T) = \frac{\omega}{T} S_\lambda^{\text{MD}}(\mathbf{q}, \omega, T), \quad (246)$$

where the constants k_B and \hbar have again been set to unity. Results obtained at $T = 0.05 J$, corrected in this way, are shown in Fig. 18 (a)–(c). In this case, u3MD simulations were carried out at a resolution of $0.02 J$, corrected according to Eq. (246), and then further convoluted with with a Gaussian envelope of FWHM = $0.33 J$, so as to achieve a net energy resolution of $0.35 J$, directly comparable to results in Section VI D.

The results in Fig. 18 (a)–(c), should be contrasted with the ‘‘raw’’ results of MD simulation, shown Fig. 16 (a)–(c). Rela-

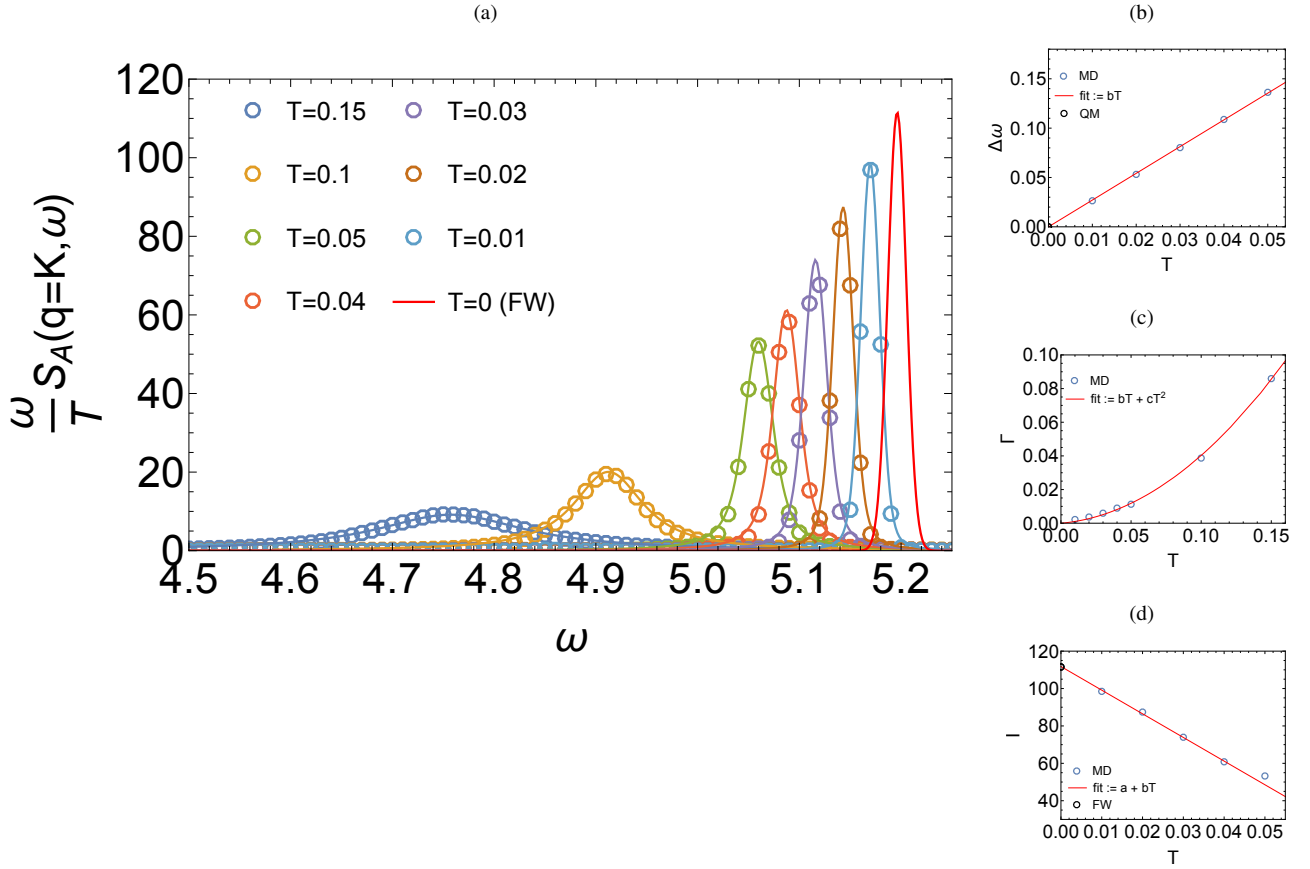


Figure 19. Temperature dependence of results of $U(3)$ Molecular Dynamics (u3MD) simulation after correction for classical statistics, showing convergence on the predictions of a $T \rightarrow 0$ quantum theory for $T \rightarrow 0$. (a) u3MD results for dynamical structure factor associated with A–matrices, $S_A^{\text{MD}}(\mathbf{q}, \omega)$, at wavevector $\mathbf{q} = \mathbf{K}$, for temperatures ranging from $T = 0.01$ J to $T = 0.15$ J. Simulation results (points), have energy resolution 0.02 J, and have been corrected for classical statistics through Eq. (246). Lines show fits to a Voigt profile, Eq. (221). The prediction of the $T = 0$ quantum theory, Eq. (208), convoluted with a Gaussian of FWHM = 0.02 J, is shown with a solid red line. (b) Shift in peak energy $\Delta\omega(T)$, found from fits to a Voigt profile, showing convergence of peak position on the prediction of $T = 0$ quantum theory. (c) Equivalent results for the inverse lifetime $\Gamma(T)$. (d) Equivalent results for the peak height, $I(T)$. Parameters for simulations are identical to those used in Fig. 18.

tive to these, corrected results show a far less spectral weight at low energies, an effect which is particularly evident for $S^{\text{MD}}(\mathbf{q}, \omega, T)$. Meanwhile, for comparison, in Fig. 18 (f)–(d), we reproduce equivalent results from the $T = 0$ analytic theory, previously shown in Fig. 12. Compared at the level of density plots, the agreement between corrected simulation results and the zero–temperature quantum prediction is essentially perfect, with no visible mismatches in dispersion or intensity.

A more precise comparison between simulation and zero–temperature quantum theory can be achieved by plotting $\tilde{S}_\lambda^{\text{MD}}(\mathbf{q}, \omega, T)$ at fixed wavevector \mathbf{q} , for a sequence of temperatures converging on $T = 0$. This is accomplished in Fig. 19 (a), where we plot results for $\tilde{S}_A^{\text{MD}}(\mathbf{q} = \mathbf{K}, \omega, T)$, for temperatures ranging from $T = 0.15$ J to $T = 0.01$ J. For comparison, we also show the result of the $T = 0$ analytic theory, Eq. (208). Both simulation and analytic prediction have been convoluted with a Gaussian of FWHM 0.02 J. Plotted in this way, the role of the limit in Eq. (245) becomes clear: MD

simulation results corrected using Eq. (246) form a sequence which converge on the $T = 0$ analytic prediction for $T \rightarrow 0$.

Having established the validity of Eq. (245), it is interesting to examine more precisely the way in which corrected simulation results converge on the zero–temperature quantum result. The dispersing peak in $\tilde{S}_\lambda^{\text{MD}}(\mathbf{q}, \omega, T)$ is still well–described by the Voigt lineshape, Eq. (221), with fits shown as solid lines in Fig. 18 (a)–(c). Within limits set by the energy resolution of simulations, these fits allow us to extract quantitative estimates for the shift in excitation energy $\Delta\omega(T)$ [Fig. 19 (b)], the inverse lifetime of the excitation, $\Gamma(T)$ [Fig. 19 (c)], and the intensity maximum $I(T)$ [Fig. 19 (d)], as a function of temperature.

We find that the peak position converges linearly on the zero–temperature quantum result from below, with

$$\Delta\omega(T) = bT + \mathcal{O}(T^3), \quad [b = 2.71], \quad (247)$$

Meanwhile, the inverse lifetime of the excitation vanishes (ap-

proximately) quadratically as $T \rightarrow 0$

$$\Gamma(T) = bT + cT^2 + \mathcal{O}(T^3), \quad [b = 0.07, c = 3.26] \quad (248)$$

while the maximum intensity of the peak also converges linearly on the expected value

$$I(T) = a + bT + \mathcal{O}(T^3), \quad [a = 111, b = -1230], \quad (249)$$

where the coefficient a matches the prediction of the $T = 0$ quantum theory.

It is possible to construct a diagrammatic expansion for the self energy of excitations within the mixed ensemble of MD simulation [108]. Such calculations lie beyond the scope of this paper but, on general grounds, it is possible to offer an interpretation of some of the trends observed in simulation.

At low temperatures, the shift in peak position, $\Delta\omega(T)$ will depend on the density of excitations (one-loop diagram). Because of the classical statistics of the MC simulation, this density is linear in T . Meanwhile, the inverse lifetime, $\Gamma(T)$, will be determined by interactions which are present in finite-temperature simulations, but absent from the Gaussian-level quantum theory developed in Section V. These processes correspond to Feynman diagrams with a finite imaginary part, and will generically have the form of “bubbles”. Empirically the dominant low-temperature contribution occurs at $\mathcal{O}(T^2)$, i.e. at second order in the density of fluctuations.

We leave a more quantitative analysis of these effects for future work.

C. Comparison with the results of QMC simulation

In Section VII B, we have explored the correspondence between u3MC simulation results at finite temperature, and analytic quantum (semi-classical) results at $T = 0$. It is also interesting to consider how they compare with published quantum Monte Carlo (QMC) simulation data.

1. Ground state

The spin-1 BBQ model on a triangular lattice [Eq. (1)] is accessible to QMC simulation for $J_1 \leq 0, J_2 \leq 0$. (Equivalently, from Eq. (5), the quadrant $-\pi \leq \theta \leq \pi/2$). Stochastic series expansion (SSE) methods have been used to obtain results for both thermodynamics and dynamics, at finite temperature, across this parameter range [53]. A more specialized loop-expansion method has also been used to study properties at the special point $J_1 = 0, J_2 = -1$ ($\theta = -\pi/2$) [52].

Both QMC results [53], and u3MC simulations [Section III A 2], are consistent with a FQ ground state extending from the special point $\theta = -\pi/2$, to the $SU(3)$ point, $\theta = -3\pi/4$. Meanwhile, for $-3\pi/4 < \theta - \pi$, both methods find a FM ground state. This distribution of FQ and FM ground states is consistent with mean-field predictions [Fig. 2], results from exact diagonalisation [19], and more recent calculations using tensor-network methods [99].

2. Dynamics

Comparison between semi-classical simulations based on $u(3)$, and QMC, is most straightforward for dynamics at low temperatures. Here, as shown above, the u3MD approach exactly reproduces published results from a (Gaussian-level) multiple-boson expansion [19]. The comparison between QMC and the predictions of this multiple-boson expansion is discussed in [53]. At a qualitative level, good agreement is found between the multiple-Boson expansion at $T = 0$, and QMC results for $T \ll J$. It follows that agreement between QMC and u3MD simulations is equally good, once the effect of classical statistics have been taken into account [Section VII B].

At a quantitative level, QMC results show some differences in values of hydrodynamic parameters governing long-wavelength excitations, such as the quadrupole-wave velocity [53]. At low temperatures, the renormalisation of these parameters is a consequence of quantum effects present in QMC, but not accessible within the semi-classical description provided by Gaussian-level flavor-wave theory, or u3MD. None the less, these quantum corrections are small, and become too small to measure approaching the $SU(3)$ point $\theta = -3\pi/4$.

Dynamics at temperatures $T \lesssim J$ have also been explored using QMC simulation [53]. As temperature is increased, excitations near the top of the band, which have predominantly spin-wave character, become heavily damped, and suffer a dramatic loss of intensity [cf. results for $S_Q(\mathbf{q}, \omega)$ in [53], Fig. 8]. Meanwhile quadrupolar fluctuations near the ordering vector show considerable spectral weight at low energy. The analysis of dynamics across the topological phase transition occurring for $T^* \approx 0.4 J$ lies outside the scope of this paper. However we note that similar trends in spectral weight are observed in u3MD results for $S_Q(\mathbf{q}, \omega)$, at temperatures $T \sim J$. These will be discussed elsewhere [97].

For completeness, we note that a phenomenological theory of the relaxational dynamics of spin-1 magnets has been introduced in [109]. This makes the prediction that long-wavelength quadrupolar waves have damping $\propto k^2$. To the best of our knowledge, this phenomenological approach has yet to be used to make quantitative predictions for FQ order in the BBQ model, or compared with QMC simulation results. We have made a preliminary analysis of damping as a function of \mathbf{k} , within u3MD simulation. Precise evaluations of the damping of long-lived excitations at low energy and temperature is challenging, but initial results are consistent with a damping

$$\Gamma(\mathbf{k}) \propto k^2 + \mathcal{O}(k^4), \quad (250)$$

at fixed temperature $T/J \ll 1$. We leave the further investigation of this point for future work.

3. Thermodynamics

Probably the most interesting thermodynamic quantity to compare between QMC and classical $U(3)$ simulations is the heat capacity. In Fig. 20 (b) we show results of simulations of

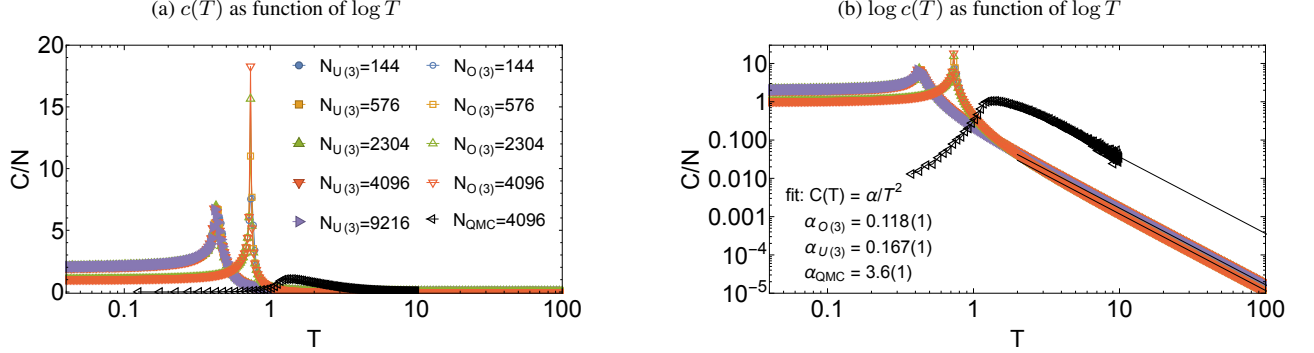


Figure 20. Temperature-dependence of heat capacity found in Monte Carlo simulations of the spin-1 bilinear-biquadratic model \mathcal{H}_{BBQ} [Eq. (1)]. (a) Heat capacity per spin, $c(T)$, plotted as a function of $\log T$. Results are shown for simulations using quantum Monte Carlo (QMC), classical Monte Carlo in space of $u(3)$ matrices (u3MC), and classical Monte Carlo in space of $O(3)$ vectors (o3MC). The peak in $c(T)$ at intermediate temperatures reflects the onset of fluctuations of ferroquadrupolar (FQ) order. (b) Equivalent results, plotted on a log-log scale. At low temperatures, classical results tend to a constant reflecting the number of generators of excitations about the ground state, while quantum results show a power-law onset $c(T) \propto T^2$. At high temperatures, all results scale as $c(T) = \alpha/T^2$. Simulations were carried out for parameters $J_1 = 0.0$ and $J_2 = -1.0$, with QMC data taken from [53].

the spin-1 BBQ model [Eq. (1)] carried out using QMC, classical MC in the space of A -matrices (u3MC), and classical MC carried out in the space of $O(3)$ vectors. QMC simulation results are taken from [53], while u3MC results have already been introduced in Section VI A. $O(3)$ MC simulations parallel earlier work [104]. Heat capacity per spin, $c(T)$, is shown plotted on both log-linear [Fig. 20 (a)] and log-log scales [Fig. 20 (b)], with temperature measured in units of J . We discuss the particulars of different temperature regimes below.

At low temperatures, $T/J \ll 1$, analytic theory for FQ order predicts

$$c(T \rightarrow 0) = 2 \times \frac{3\zeta(3)}{\pi v^2} T^2 + \dots \quad (251)$$

where $\zeta(3) \approx 1.2$, v is the velocity of the linearly-dispersing Goldstone modes, and the factor $\times 2$ comes from the fact these are two-fold degenerate [19]. This result follows from the Bosonic nature of low-lying excitations. Fits to QMC simulation, confirm the expected T^2 scaling [110], and return a value of v consistent with that found in simulations of dynamics [53].

In contrast, classical MC simulations carried out in the basis of $u(3)$ matrices find $c(T \rightarrow 0) = 2$ [Section IV C, Section VI A]. The profound difference between classical and quantum results for $c(T \rightarrow 0)$ is a consequence of the fact that, in the absence of quantum statistics, entropy is not well posed for $T \rightarrow 0$. And in this case, the effect of classical statistics cannot be corrected as easily as for the semiclassical dynamics discussed above.

At intermediate temperatures, $T/J \sim 1$ both classical and quantum simulation results for $c(T)$ are dominated by a large peak. In all three cases, this peak is associated with the onset of fluctuations of FQ order. The peak found in classical simulations, which are carried out for much larger systems, is sharp, and can be linked to the unbinding of \mathbb{Z}_2 vortices [97, 104]. Meanwhile, the peak found in QMC is much

broader, and occurs at a slightly higher temperature. These differences reflect both different statistics, and the large length scales needed to accurately describe a topological phase transition.

Finally, we turn to the limit of high temperature, $T/J \gg 1$. Here results must scale as

$$c(T \rightarrow \infty) = \lim_{T \rightarrow \infty} \frac{\langle E^2 \rangle - \langle E \rangle^2}{T^2} = \frac{\alpha}{T^2}, \quad (252)$$

where α is coefficient depending on model parameters and the ensemble of states sampled. In Fig. 20 (b) this behaviour is reflected in parallel lines with gradient

$$\frac{d \ln c(T)}{d \ln T} = -2, \quad (253)$$

for $T/J \gtrsim 10$. In this high-temperature limit, u3MC results ($\alpha_{\text{u3MC}} = 0.16$) are intermediate between conventional $O(3)$ MC simulations ($\alpha_{\text{o3MC}} = 0.11$), and QMC ($\alpha_{\text{QMC}} = 3$).

It has been argued elsewhere that simulation in the space of \mathbf{d} -vectors (vis A -matrices) should yield results equivalent to QMC at high temperature [54]. Empirically this is not the case. And since, at high temperatures, finite-size effects are small, we infer that the different values of α found in different simulations reflect different asymptotic values of the variance in energy, Eq. (252). This asymptote, and leading corrections to it, can be calculated within a high-temperature series expansion [111]. We find this expansion takes on a different form for quantum spin-1 moments and A -matrices, and so will generally lead to different results [112]. We leave further analysis of the high-temperature limit for future work.

VIII. GENERALIZATION TO SPIN-ANISOTROPIC INTERACTIONS

In the preceding sections of this paper, we have shown it is possible to calculate the thermodynamic and dynamical properties of spin-1 magnets through simulations carried out in

the basis of $u(3)$. So far, this analysis has been confined to the bilinear–biquadratic (BBQ) model, Eq. (1), which is invariant under $SU(2)$ spin rotations. Here we show that the same approach can be applied to models with interactions anisotropic in spin–space.

At first sight, this is not a trivial generalization, since the group $U(3)$ encompasses spins with length $\neq 1$. We therefore need to show that spin–anisotropic interactions do not mix different spin sectors, at the level of individual spin–1 moments. As we shall see, this condition is satisfied by both u3MC and u3MD simulations, as long as dynamical simulations are initiated from a valid spin–1 state.

A. Validity of u3MD approach

For simulations carried out in a $u(3)$ basis to be valid, it must remain true that each site in the lattice is host to a single spin–1 moment. Once spins are transcribed in terms of generators of $U(3)$, this imposes the condition that

$$\text{Tr } \hat{\mathcal{A}} \equiv 1, \quad (254)$$

[Eq. (10)]. This condition is true by construction in u3MC simulation [Section III A]. And, in Section II D, we showed that

$$\partial_t \text{Tr } \hat{\mathcal{A}}_i \equiv 0, \quad (255)$$

for u3MD simulations carried out for the spin–rotationally invariant BBQ model [Eq. (1)], implying that spin–length is conserved. We now extend this result to models which break spin–rotation invariance.

We consider most general form of spin–anisotropic Hamiltonian allowed for a spin–1 magnet

$$\mathcal{H}_\Delta = \sum_{\langle i,j \rangle} J_{\beta\nu}^{\alpha\mu} \hat{\mathcal{A}}_{i\beta}^\alpha \hat{\mathcal{A}}_{j\nu}^\mu + \sum_i L_\beta^\alpha \hat{\mathcal{A}}_{i\beta}^\alpha, \quad (256)$$

where the only restriction placed on the interactions $J_{\beta\nu}^{\alpha\mu}$, and single–ion anisotropy L_β^α , is the requirement that \mathcal{H}_Δ be Hermitian. It follows that

$$\begin{aligned} \partial_t \hat{\mathcal{A}}_{i\eta}^\gamma &= -i [\hat{\mathcal{A}}_{i\eta}^\gamma \mathcal{H}_\Delta] \\ &= -\frac{i}{2} \sum_\delta (J_{\mu\beta}^{\eta\alpha} \hat{\mathcal{A}}_{i\mu}^\gamma + J_{\beta\mu}^{\alpha\eta} \hat{\mathcal{A}}_{i\mu}^\gamma \\ &\quad - J_{\gamma\beta}^{\mu\alpha} \hat{\mathcal{A}}_{i\eta}^\mu - J_{\beta\gamma}^{\alpha\mu} \hat{\mathcal{A}}_{i\eta}^\mu) \hat{\mathcal{A}}_{i+\delta\beta}^\alpha \\ &\quad - \frac{i}{2} (L_\alpha^\eta \hat{\mathcal{A}}_{i\alpha}^\gamma - L_\gamma^\alpha \hat{\mathcal{A}}_{i\gamma}^\alpha). \end{aligned} \quad (257)$$

Setting $\eta = \gamma$ and taking the trace, we find

$$\begin{aligned} \partial_t \text{Tr } \mathcal{A}_i &= -\frac{i}{2} \sum_\delta (J_{\beta\mu}^{\alpha\gamma} \hat{\mathcal{A}}_{i\mu}^\gamma - J_{\beta\gamma}^{\alpha\mu} \hat{\mathcal{A}}_{i\gamma}^\mu) \hat{\mathcal{A}}_{i+\delta\beta}^\alpha \\ &\quad - \frac{i}{2} (L_\alpha^\gamma \hat{\mathcal{A}}_{i\alpha}^\gamma - L_\gamma^\alpha \hat{\mathcal{A}}_{i\gamma}^\alpha), \end{aligned} \quad (258)$$

where we have used the relationship

$$J_{\beta\nu}^{\alpha\mu} = J_{\nu\beta}^{\mu\alpha}, \quad (259)$$

which follows from the fact that components of \mathcal{A} on different lattice sites commute [Eq. (8)]. By rearranging indices on the right hand side of Eq. (258), we can easily show that

$$\partial_t \text{Tr } \hat{\mathcal{A}}_i = 0, \quad (260)$$

as required.

It follows that the trace of \mathcal{A} is conserved within u3MD simulations, and therefore that simulations carried out for arbitrary spin–anisotropic interactions respect the constraint on spin–length. The implication of this result is that solving the $u(3)$ equations of motion, Eq. (73), for a spin–1 state, is exactly equivalent to solving the much more complicated equations of motion for spin–1 moments found in the algebra $su(3)$ [58–60], regardless of spin–anisotropy.

B. Application to FQ state with easy–plane anisotropy: analytic theory

For illustration, we now consider the simplest extension of the results developed thus far to anisotropic interactions: the spin–1 BBQ model with single–ion, easy–plane anisotropy

$$\mathcal{H}_D = \mathcal{H}_{\text{BBQ}} + \mathcal{H}_{\text{SI}}, \quad (261)$$

where \mathcal{H}_{BBQ} is defined in Eq. (1), and

$$\mathcal{H}_{\text{SI}} = \sum_i D (\hat{S}_i^y)^2, \quad [D > 0]. \quad (262)$$

This model has previously been studied in [100].

Like the BBQ model it descends from, \mathcal{H}_D supports a FQ ground state for a wide range of $(J_1, J_2 < 0)$, and we can easily generalise the theory of excitations developed in Section V to take account of single–ion anisotropy. Transcribing \mathcal{H}_{SI} in terms of \mathcal{A} –matrices, by way of Eq. (50), we find

$$\mathcal{H}_{\text{SI}} = \sum_i D \left(-\frac{2}{3} \hat{\mathcal{A}}_{iy}^y + \frac{1}{3} \hat{\mathcal{A}}_{ix}^x + \frac{1}{3} \hat{\mathcal{A}}_{iz}^z + \frac{2}{3} \right). \quad (263)$$

Written in this form, it is immediately clear that \mathcal{H}_{SI} is a special case of the single–ion term in Eq. (256).

From here, we can use Eq. (173) to express \mathcal{H}_{SI} in terms of the Bosonic basis introduced in Section IV A. Its effect is to introduce new diagonal terms in the matrix controlling the dispersion of excitations [Eq. (175)], vis

$$M_{\mathbf{k}}^{\text{SI}} = \begin{pmatrix} A_{\mathbf{k}} + D & -B_{\mathbf{k}} & 0 & 0 \\ -B_{\mathbf{k}} & A_{\mathbf{k}} + D & 0 & 0 \\ 0 & 0 & A_{\mathbf{k}} + D & -B_{\mathbf{k}} \\ 0 & 0 & -B_{\mathbf{k}} & A_{\mathbf{k}} + D \end{pmatrix}, \quad (264)$$

where $A_{\mathbf{k}}$ and $B_{\mathbf{k}}$ are given in Eq. (128). Solving the appropriate eigensystem [Eq. (178)], we find two physical branches of excitation, with dispersion

$$\epsilon_{\mathbf{k}} = \sqrt{(A_{\mathbf{k}} + D)^2 - B_{\mathbf{k}}^2}. \quad (265)$$

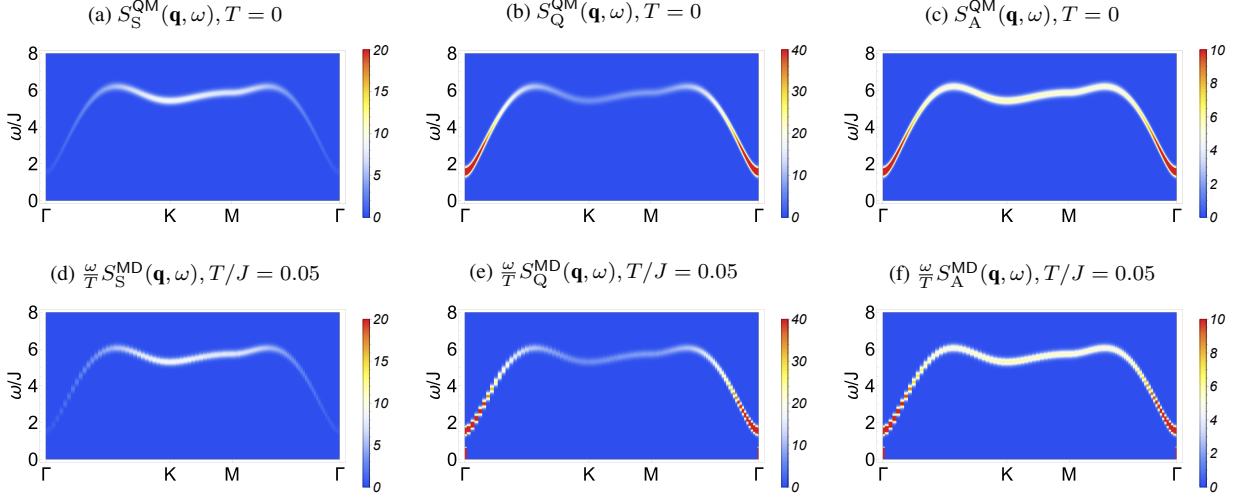


Figure 21. Dynamics of ferroquadrupolar (FQ) state in the spin-1 bilinear-biquadratic (BBQ) model with easy-plane anisotropy. (a) Dynamical structure factor for dipole moments, $S_S^{\text{QM}}(\mathbf{q}, \omega)$, as predicted by zero-temperature quantum theory of Section VIII B. (b) Equivalent results for quadrupole moments, $S_Q^{\text{QM}}(\mathbf{q}, \omega)$. (c) Equivalent results for A-matrices, $S_A^{\text{QM}}(\mathbf{q}, \omega)$. (d) Dynamical structure factor $S_S^{\text{MD}}(\mathbf{q}, \omega)$ found in molecular dynamics simulations within $u(3)$ representation (u3MD). (e) Equivalent results for $S_Q^{\text{MD}}(\mathbf{q}, \omega)$. (f) Equivalent results for $S_A^{\text{MD}}(\mathbf{q}, \omega)$. Simulations were carried out for \mathcal{H}_D [Eq. (261)], with parameters Eq. (268), at a temperature $T = 0.05 J$, for a cluster of linear dimension $L = 96$ ($N = 9216$ spins). Numerical results have been multiplied by a prefactor ω/T to correct for classical statistics, following Eq. (246). All results have been convoluted with a Gaussian in frequency of FWHM = 0.35 J.

It follows that the effect of easy-plane anisotropy is to open a gap

$$\Delta = \sqrt{2A_0 D + D^2}, \quad (266)$$

to the Goldstone modes of FQ order. This is to be expected since, in the presence of easy-plane anisotropy, the FQ ground state does not break spin-rotation symmetry.

It is also straightforward to generalise the calculations of structure factors described in Section V B. Results for $S_S^{\text{QM}}(\mathbf{q}, \omega)$ [Eq. (208)], $S_Q^{\text{QM}}(\mathbf{q}, \omega)$ [Eq. (201)] and $S_A^{\text{QM}}(\mathbf{q}, \omega)$ [Eq. (193)] can be adapted to easy-plane anisotropy through the simple substitution

$$A_{\mathbf{k}} \longrightarrow A_{\mathbf{k}} + D. \quad (267)$$

Doing so, and considering parameters

$$J_1 = 0, \quad J_2 = -1.0, \quad D = 0.2, \quad (268)$$

we obtain the predictions shown in Fig. 21 (a)–(c).

C. Application to FQ state with easy-plane anisotropy: numerical results

Building on Section VIII A, we can also apply the u3MD simulation approach to the easy-plane model \mathcal{H}_D [Eq. (261)]. In Fig. 21 (d)–(f), we show results obtained for the parameter set Eq. (268). Once corrected for the effect of classical statistics, through Eq. (246), simulations show good agreement with the predictions analytic theory developed in Section VIII B.

These results provide an explicit demonstration of the ability of u3MD simulations to describe the excitations of spin-1 models with spin-anisotropic interactions.

IX. SUMMARY, CONCLUSIONS AND OUTLOOK

In this Article, we have introduced a new method for simulating both the thermodynamics and dynamics of spin-1 magnets, established the validity of this method through detailed comparison with known limits, and used it to obtain a number of new results for the spin-1 bilinear-biquadratic (BBQ) model on a triangular lattice. Several other interesting findings entail. Foremost among these is an explicit connection between classical simulations at finite temperature, and zero-temperature quantum dynamics, treated at a semi-classical level. Also of interest are a low-temperature expansion for the thermodynamic properties of spin-1 magnets, and a novel derivation of a well-established multiple-Boson expansion.

The key to this method, introduced in Section II, is the representation of spin-1 moments through the algebra $u(3)$. Unlike mappings onto an $O(3)$ vector, this approach treats dipole and quadrupole moments on an equal footing. And for this reason, it provides a valid (semi-)classical limit of a spin-1 moment. From this starting point, we have developed a framework for classical Monte Carlo simulation in the space of “A-matrices”, \hat{A}_{β}^{α} , which act as generators belonging to $u(3)$ (u3MC). We also derived equations of motion (EoM) for \hat{A}_{β}^{α} in a form suitable for numerical integration [Eq. (73)]. These form the basis for a “molecular dynamics” scheme for

exploring the dynamics of spin-1 magnets (u3MD).

The numerical implementation of u3MC and u3MD simulations was described in [Section III](#). A Marasaglia-like update in the space of \hat{A}_β^α was introduced, and used to develop a MC scheme based on a local Metropolis update. The resulting u3MC approach was shown to reproduce known results for the thermodynamic properties of the spin-1 BBQ model on a triangular lattice, and used to derive a finite-temperature phase diagram [[Fig. 3](#)]. Meanwhile, numerical integration of EoM using an RK-4 update was shown to conserve the trace \hat{A}_β^α , establishing u3MD as valid approach for simulating the dynamics of spin-1 magnets.

In order to illustrate the u3MC and u3MD approaches, we then turned to the specific example of ferroquadrupolar (FQ) order, as found in the spin-1 BBQ model on a triangular lattice [[Fig. 10](#)]. To better understand simulations, we first developed an analytic theory of fluctuations about this state, described in [Section IV](#). Treated at a classical level, these fluctuations were shown to form bands with either dipolar or quadrupolar character [[Fig. 12 \(a\)–\(c\)](#)], which provide the framework for a classical low-temperature (low-T) expansion of the free energy [[Eq. \(136\)](#)]. This low-T expansion was used to make predictions for classical thermodynamic properties of the BBQ model, for subsequent comparison with u3MC simulation.

Next, in [Section V](#), we showed how these fluctuations could be quantized, leading to a multiple-Boson expansion of excitations about FQ order. This theory, which is exactly equivalent to a known “flavor-wave” expansion, was used to develop zero-temperature quantum predictions for dynamical structure factors within a FQ state, for subsequent comparison with u3MD simulation [[Fig. 12 \(d\)–\(f\)](#)].

With this ground work in place, in [Section VI](#) we explored both the predictions of u3MC for the low-temperature thermodynamic properties of the FQ phase, and the predictions of u3MD for its dynamics. u3MC results for heat capacity $c(T \rightarrow 0)$ [[Fig. 13](#)], ordered moment \mathbf{Q} [[Fig. 14](#)] and equal time structure factors $S_\lambda(\mathbf{q})$ [[Fig. 15](#)] were shown to be in perfect agreement with the predictions of the classical low-T expansion. Meanwhile “raw” u3MD results for dynamics were shown to give a good account of the dispersion of excitations, but fail to reproduce their spectral weight [[Fig. 16](#)].

The reason for the disagreement between u3MD and the $T = 0$ quantum theory was identified as coming from classical statistics, inherited from u3MC simulation. This observation formed the basis for a detailed exploration of quantum-classical correspondence within u3MD simulation, building on the analytic theories of classical and quantum excitations, and described in [Section VII](#). This analysis leads to a simple, and very general, prescription for correcting MD simulation for the effect of classical statistics, in the limit $T \rightarrow 0$ [[Eq. \(245\)](#)]. Corrected in this way, the predictions of u3MD were shown to perfectly reproduce the predictions of zero-temperature quantum theory, considered at a semi-classical level [[Fig. 18](#) and [Fig. 19](#)]. The comparison of u3MC and u3MD results with published QMC simulations of the FQ phase of the BBQ model was also discussed.

Up to this point, all results were derived under the assumption of $SU(2)$ symmetry, appropriate to the BBQ model.

However many spin-1 magnets display anisotropy in their exchange interactions, and at the level of individual ions. For this reason, in [Section VIII](#), we revisited the derivation of the u3MD method, establishing that it remains valid for the most general anisotropy permitted for a spin-1 magnet. To illustrate this result, we demonstrated that u3MD simulations correctly describe the dynamics of a FQ state in the presence of single-ion anisotropy, perfectly reproducing the predictions of a $T = 0$ quantum theory [[Fig. 21](#)].

We conclude that the u3MC and u3MD methods introduced in this Article provide a reliable guide to the classical thermodynamics, and semi-classical dynamics of spin-1 magnets. This opens many new perspectives for both theory, and the interpretation of experiment.

On the theoretical side, the lack of well-developed methods means that the thermodynamic properties of spin-1 magnets, and in particular their phase transitions, remain relatively unexplored. This is of particular interest for phases built of on-site quadrupole moments, which cannot occur in spin-1/2 magnets, and for orders which support interesting topological excitations. Moreover the possibility of combining u3MC with u3MD means that, where an interesting phase transition is identified, the associated dynamics can also be explored.

From this point of view, the phase diagram of the simple BBQ model shown in [Fig. 3](#) already poses many interesting questions. The ordered ground states of this model are already known to support a wide array of topological excitations [[23](#), [113–116](#)]. These take on particularly interesting form where the model has an enlarged, $SU(3)$ symmetry [[61](#), [88](#)], and the range of possibilities becomes still wider in the presence of spin-anisotropy [[117–120](#)]. In the context of a two-dimensional model, this presents the opportunity to study both the thermodynamics, and the dynamics, of a wide array of different topological phase transitions. We will return to this question elsewhere, in the context of FQ phase of the BBQ model [[97](#)].

It would also be interesting to use u3MD to look more deeply into the dynamics of spin-1 magnets at finite temperature. While MD simulation does not respect quantum statistics, it does allow for interactions between quasiparticles. Preliminary analysis of the damping of excitations, described in [Section VII](#) of this Article, suggest that u3MD results are consistent with the predictions of hydrodynamic theories, at least at a qualitative level. More work would be needed to put these results on a quantitative footing, but this remains a promising avenue for future exploration. To this end, it is worth noting that simulations based on $U(3)$ are still in their infancy, and there is considerable room for technical improvement, e.g., in Monte Carlo updates. And very recently, there have been encouraging developments in the application of $SU(3)$ approaches to spin-1 magnets, complementary to the results of this Article [[121](#), [122](#)].

It is also interesting to speculate about the possible extension of a $U(N)$ approach to higher-spin moments. Paradoxically, while increasing the size of the moment, S , will suppress quantum fluctuations, it also increases the complexity to the problem, through the number of parameters needed to describe a single site, and the number of bands of excitations

found on a lattice. For example, the passage from spin-1 to spin-3/2 increases the Hilbert space from to $\mathbb{C}\mathbb{P}^2$ to $\mathbb{C}\mathbb{P}^3$, and the number of parameters needed from 4 to 6. It also brings a new piece of physics, octupole moments at the level of a single site, and a new algebra, $su(4)$. This trend continues for larger S , with each moment possessing its own, unique, semi-classical limit. Taken appropriately, this limit should become an increasingly good approximation as $S \rightarrow \infty$.

For this reason, further development of semi-classical methods for high-spin moments makes very good sense. To this end, we note that coherent-state representation has already been used to derive general equations of motion for spin- S moments within the algebra $su(N)$, where $N = 2S + 1$ [60]. Quite generally, it is possible to embed such an $su(N)$ algebra within $u(N)$, and seek simplification of the algebra representing the original spin- S moment, of the type found for spin-1 in this paper. We leave this as a topic for future study.

On the experimental side, many interesting spin-1 magnets have come to light. Celebrated examples include the triangular-lattice spin-nematic candidate NiGa_2S_4 [18, 19, 27–30], and the pyrochlore spin-liquid candidate $\text{NaCaNi}_2\text{F}_7$ [32, 33]. However there are also steady stream of new arrivals, and interesting new results for older materials [123]. Spin-1 models also arise in the context of cold atoms [44–48], and as a proxy for describing various forms of quantum liquid crystal, including the nematic phases of Fe-based superconductors [39–43]. Many aspects of the physics of these systems remain ambiguous, and the ability to simulate the dynamics of realistic, microscopic, spin-1 models could prove decisive.

The second major conclusion of this work, is that it is possible to correct for the effect of classical statistics in finite-temperature “molecular dynamics” (MD) simulations of magnets, and thereby use them to study zero-temperature, quantum (semi-classical) dynamics. This is a result of broad relevance, applying equally to conventional MD simulations in the space of $O(3)$ vectors. And it goes some way to explaining why, despite its humble classical origins, MD simulation has been so successful in describing the dynamics of exotic quantum magnets [66, 92, 124]. The deeper exploration of this form of quantum-classical correspondence, for example by pairing u3MD with QMC simulations, is another promising avenue for future research. And the $u(3)$ basis which underpins this work could also be used as starting point for explicitly quantum calculations, e.g. through the use of variational wave functions based on tensor-networks.

Consider together, this is an absorbing set of problems, and it will be interesting to see how much more can be learned through the numerical simulation of spin-1 magnets.

ACKNOWLEDGMENTS

The authors are pleased to acknowledge helpful conversations with Yuki Amari, Owen Benton, Hoshio Katsura, Yuki-toshi Motome, Karlo Penc, and Mathieu Taillefumier, and are grateful to the authors of [53] for sharing numerical values of QMC data for heat capacity.

This work was supported by the Theory of Quantum Matter Unit, OIST, JSPS KAKENHI Grants No. JP17K14352 and No. JP20K14411, and JSPS Grants-in-Aid for Scientific Research on Innovative Areas Topological Materials Science (KAKENHI Grant No. JP18H04220), and Quantum Liquid Crystals (KAKENHI Grant No. JP20H05154 and JP22H04469).

Numerical calculations were carried out using HPC facilities provided by OIST, and the Supercomputer Center of the Institute of Solid State Physics, University of Tokyo.

Appendix A: Spin Fluctuation Probability

In this Appendix, we detail how the spin fluctuation probabilities drawn namely in Fig. 1, Fig. 5, Fig. 10, Fig. 11, Fig. 22, and Fig. 23 are calculated.

Fluctuations around a given state $|\alpha\rangle$ can be calculated by computing its spin fluctuation probability, defined as the spatial probability distribution of the overlapping between the state $|\alpha\rangle$ and the spin coherent state $|\Omega\rangle$. The spin coherent state $|\Omega\rangle$ is obtained by applying a rotation operator in 3 dimensions defined by the angles θ and ϕ on the $m=1$ state $|1\rangle$:

$$|\Omega\rangle = \mathcal{R}(\theta, \phi)|1\rangle. \quad (\text{A1})$$

The spin coherent state represents then a spin pointing in the direction defined by the angles θ and ϕ . In the case of a spin 1, the spin coherent state is expressed as:

$$|\Omega\rangle = \frac{1 + \cos\theta}{2} e^{-i\phi}|1\rangle + \frac{\sin\theta}{\sqrt{2}}|0\rangle + \frac{1 - \cos\theta}{2} e^{-i\phi}|\bar{1}\rangle. \quad (\text{A2})$$

The spin fluctuation probability of the state $|\alpha\rangle$ is defined as the norm of the scalar product with the spin coherent state:

$$P(\theta, \phi)_{|\alpha\rangle} = |\langle\alpha|\Omega\rangle|^2. \quad (\text{A3})$$

Appendix B: Properties of A matrices

Here, we present the fundamental properties of the "A-matrix". From its definition in Eq. (48), we note that the A-object is mathematically a (1,1)-tensor, but for simplicity, we might usually refer to it as a matrix. In this Appendix, we also give the detailed explanations accompanying the symmetry analysis of the BBQ Model [Eq. (9)] that we discuss at the end of Section II.

1. Properties of a single A matrix

First, we present how Eq. (61) is obtained. Eq. (61) tells us how an object like \hat{A}_β^α would transform under a general linear transformation Λ . To this end, as explained in Section II, we consider a general linear transformation $\Lambda : V \rightarrow V$, such that $\det\Lambda \neq 0$, so that Λ is invertible, and we define

$$\tilde{\Lambda} = \Lambda^{-1T}. \quad (\text{B1})$$

Under such a transformation, the basis vector \mathbf{e}_i of the vector space V will transform according to

$$\bar{\mathbf{e}}_i = \tilde{\Lambda}_i^j \mathbf{e}_j. \quad (\text{B2})$$

Since the vector $\mathbf{v} = v^i \mathbf{e}_i$ is a mathematical object which existence does not depend on the basis, the components v^i should transform according to

$$\bar{v}^i = \Lambda^i_j v^j, \quad (\text{B3})$$

such that the vector $\mathbf{v} = \bar{v}^i \bar{\mathbf{e}}_i = v^i \mathbf{e}_i$ stays invariant. It is then also possible to introduce the dual basis $\{\mathbf{e}^{*i}\}$ of the dual vector space V^* . The basis vectors can be defined by the relations

$$e^{*i}(e_j) = \delta_j^i. \quad (\text{B4})$$

Any element \mathbf{v}^* of V^* can be decomposed as

$$\mathbf{v}^* = v_i^* \mathbf{e}^{*i}, \quad (\text{B5})$$

where the components v_i^* are simply given by the value of the function \mathbf{v}^* on the basis vector \mathbf{e}_i of V

$$v_i^* = \mathbf{v}^*(\mathbf{e}_i). \quad (\text{B6})$$

Under a general transformation Λ on the basis vectors \mathbf{e}_i , the dual basis vectors \mathbf{e}^{*i} will transform according to

$$\bar{\mathbf{e}}^{*i} = \Lambda^i_j \mathbf{e}^{*j}, \quad (\text{B7})$$

in order to preserve Eq. (B4). And the component v_i^* will transform as

$$\bar{v}_i^* = \tilde{\Lambda}_i^j v_j^*. \quad (\text{B8})$$

Finally, under such a general transformation Λ , the component of an object like \hat{A}_{β}^{α} , which is actually a (1,1)-tensor, will transform as stated in Eq. (61).

2. Properties of quadratic terms of A matrices

We here show how the products of two objects like \hat{A}_{β}^{α} would transform under a linear transformation, in order to analyze the symmetry properties of the BBQ Hamiltonian rewritten in terms of \hat{A} -"matrices" [Eq. (9)]. Again, we emphasize that an object like \hat{A}_{β}^{α} is mathematically a tensor, but for simplicity, we might sometimes refer to them as matrices.

Going back to Eq. (9), it can easily be seen that the first term $\hat{A}_{i\beta}^{\alpha} \hat{A}_{j\alpha}^{\beta}$ is $U(3)$ symmetric because both indexes α and β are contravariant on one site and covariant on the other. The $\hat{A}_{i\beta}^{\alpha} \hat{A}_{j\alpha}^{\beta}$ will therefore stay invariant under a transformation $U \in U(3)$, for which we have

$$U \in U(3) : UU^{\dagger} = U^{\dagger}U = \mathbb{I} \Rightarrow U^{\dagger} = U^{-1}. \quad (\text{B9})$$

Indeed, under a $U(3)$ symmetry, the first term will transform as

$$\begin{aligned} (\hat{A}_{i\beta}^{\alpha})^{\mu} (\hat{A}_{j\alpha}^{\beta})^{\nu} &\rightarrow U_{\gamma}^{\mu} U^{\dagger \kappa}_{\nu} (\hat{A}_{i\beta}^{\alpha})^{\gamma} U_{\eta}^{\nu} U^{\dagger \lambda}_{\mu} (\hat{A}_{j\alpha}^{\beta})^{\eta} \\ &= U_{\gamma}^{\mu} U^{\dagger \lambda}_{\mu} U_{\eta}^{\nu} U^{\dagger \kappa}_{\nu} (\hat{A}_{i\beta}^{\alpha})^{\gamma} (\hat{A}_{j\alpha}^{\beta})^{\eta} \\ &= \delta_{\gamma}^{\lambda} \delta_{\eta}^{\kappa} (\hat{A}_{i\beta}^{\alpha})^{\gamma} (\hat{A}_{j\alpha}^{\beta})^{\eta} \\ &= (\hat{A}_{i\beta}^{\alpha})^{\gamma} (\hat{A}_{j\alpha}^{\beta})^{\kappa}. \end{aligned} \quad (\text{B10})$$

The second term in Eq. (9), on the other hand, is not $U(3)$ symmetric, but it is $O(3)$ symmetric. We can see that under a $U(3)$ transformation, it transforms as:

$$\begin{aligned} (\hat{A}_{i\beta}^{\alpha})^{\mu}_{\nu} (\hat{A}_{j\beta}^{\alpha})^{\mu}_{\nu} &\rightarrow U_{\gamma}^{\mu} U^{\dagger \kappa}_{\nu} (\hat{A}_{i\beta}^{\alpha})^{\gamma} U_{\eta}^{\mu} U^{\dagger \lambda}_{\nu} (\hat{A}_{j\beta}^{\alpha})^{\eta}_{\lambda} \\ &= U_{\gamma}^{\mu} U_{\eta}^{\mu} U^{\dagger \lambda}_{\nu} U^{\dagger \kappa}_{\nu} (\hat{A}_{i\beta}^{\alpha})^{\gamma} (\hat{A}_{j\beta}^{\alpha})^{\eta}_{\lambda}. \end{aligned} \quad (\text{B11})$$

Clearly, this is not invariant under a $U(3)$ transformation, but it is under a $O(3)$ transformation. If $U = O \in O(3)$, we have

$$O \in O(3) : OO^T = O^T O = \mathbb{I} \Rightarrow O^T = O^{-1}, \quad (\text{B12})$$

and under a $O(3)$ transformation, it transforms as:

$$\begin{aligned} (\hat{A}_{i\beta}^{\alpha})^{\mu}_{\nu} (\hat{A}_{j\beta}^{\alpha})^{\mu}_{\nu} &\rightarrow O_{\gamma}^{\mu} O_{\eta}^{\mu} O^T_{\nu} O^T_{\nu} (\hat{A}_{i\beta}^{\alpha})^{\gamma} (\hat{A}_{j\beta}^{\alpha})^{\eta}_{\lambda} \\ &= O^T_{\gamma} O_{\eta} O^T_{\nu} O_{\nu} (\hat{A}_{i\beta}^{\alpha})^{\gamma} (\hat{A}_{j\beta}^{\alpha})^{\eta}_{\lambda} \\ &= \delta_{\gamma\eta} \delta^{\kappa\lambda} (\hat{A}_{i\beta}^{\alpha})^{\gamma} (\hat{A}_{j\beta}^{\alpha})^{\eta}_{\lambda} \\ &= (\hat{A}_{i\beta}^{\alpha})^{\gamma} (\hat{A}_{j\beta}^{\alpha})^{\gamma}_{\kappa}. \end{aligned} \quad (\text{B13})$$

The Hamiltonian is therefore overall $O(3)$ symmetric, indeed both terms are invariant under an $O(3)$ symmetry. And in the case of $J_1 = J_2$, the second term in Eq. (9) vanishes, and the Hamiltonian is $U(3)$ symmetric. Therefore, working in $U(3)$ does not change the global symmetry of the Hamiltonian, since $o(3) \simeq su(2)$, and there is an homomorphism from $SU(2)$ into $O(3)$. However, the locally augmented $SU(3)$ symmetry of the Hamiltonian when $J_1 = J_2$ is enlarged from $SU(3)$ to $U(3)$.

The Hamiltonian can be rewritten in a more general form as

$$\mathcal{H}_{\text{BBQ}} = \sum_{\langle i,j \rangle} J_{\beta\nu}^{\alpha\mu} \hat{A}_{i\beta}^{\alpha} \hat{A}_{j\nu}^{\mu}, \quad (\text{B14})$$

with

$$J = \begin{pmatrix} \begin{pmatrix} J_2 & 0 & 0 \\ 0 & 0 & 0 \\ 0 & 0 & 0 \end{pmatrix} & \begin{pmatrix} 0 & J_2 - J_1 & 0 \\ 0 & 0 & 0 \\ 0 & 0 & 0 \end{pmatrix} & \begin{pmatrix} 0 & 0 & J_2 - J_1 \\ 0 & 0 & 0 \\ 0 & 0 & 0 \end{pmatrix} \\ \begin{pmatrix} J_2 & -J_1 & 0 & 0 \\ 0 & 0 & 0 & 0 \\ 0 & 0 & J_1 & 0 \\ 0 & 0 & 0 & 0 \end{pmatrix} & \begin{pmatrix} 0 & J_2 & 0 \\ 0 & 0 & 0 \\ 0 & 0 & 0 \\ 0 & 0 & 0 \end{pmatrix} & \begin{pmatrix} 0 & 0 & J_2 - J_1 \\ 0 & 0 & 0 \\ 0 & 0 & 0 \\ 0 & 0 & 0 \end{pmatrix} \\ \begin{pmatrix} 0 & 0 & 0 & 0 \\ 0 & 0 & 0 & 0 \\ 0 & 0 & 0 & 0 \\ J_2 - J_1 & 0 & 0 & 0 \end{pmatrix} & \begin{pmatrix} 0 & 0 & 0 & 0 \\ 0 & 0 & 0 & 0 \\ 0 & 0 & 0 & 0 \\ 0 & 0 & 0 & 0 \end{pmatrix} & \begin{pmatrix} 0 & 0 & 0 & 0 \\ 0 & 0 & 0 & 0 \\ 0 & 0 & 0 & 0 \\ 0 & 0 & 0 & 0 \end{pmatrix} \end{pmatrix}. \quad (\text{B15})$$

The indexes α and β correspond respectively to the line and the row of the table that assigns the designated matrix, whose components are then given by μ and ν . For example,

$$J_{2\nu}^{1\mu} = \begin{pmatrix} 0 & J_2 - J_1 & 0 \\ J_1 & 0 & 0 \\ 0 & 0 & 0 \end{pmatrix}, \quad J_{21}^{12} = J_1, \quad J_{22}^{11} = J_2 - J_1. \quad (\text{B16})$$

The symmetries of the Hamiltonian are now hidden in the symmetries of the tensor $J_{\beta\nu}^{\alpha\mu}$. Firstly, we see that the Hamiltonian is $O(3)$ symmetric, because the repeated summed indexes are always either covariant or contravariant. The tensor is also symmetric under the exchange $\alpha\beta \leftrightarrow \mu\nu$

$$J_{\beta\nu}^{\alpha\mu} = J_{\nu\beta}^{\mu\alpha}. \quad (\text{B17})$$

Eq. (B17) expresses the fact that there is actually a tensor product between the two operators $\hat{A}_{i,\beta}^\alpha$ and $\hat{A}_{j,\nu}^\mu$ acting on different sites. We also have $\alpha \leftrightarrow \nu$ with $\beta \leftrightarrow \mu$ together, which is just relabeling the indexes.

In the case of $J_1 = J_2$, the tensor is also symmetric under the exchanges $\alpha \leftrightarrow \mu$ and $\beta \leftrightarrow \nu$ or both

$$J_{\beta\nu}^{\alpha\mu} = J_{\beta\nu}^{\mu\alpha} = J_{\nu\beta}^{\alpha\mu}. \quad (\text{B18})$$

It is also symmetric under the exchanges $\beta \leftrightarrow \mu$ and $\alpha \leftrightarrow \nu$

$$J_{\beta\nu}^{\alpha\mu} = J_{\mu\nu}^{\alpha\beta} = J_{\beta\alpha}^{\nu\mu} = J_{\mu\alpha}^{\nu\beta}, \quad (\text{B19})$$

in which case, it can easily be seen that the Hamiltonian is $U(3)$ invariant, since every index is now summed covariantly.

Appendix C: Conventions for the triangular lattice

In this Appendix, we present the convention that we used to describe the triangular lattice and its reciprocal space. We choose the real space lattice vectors, linking a single site unit cell to another, to be

$$\mathbf{a} = \begin{pmatrix} 1 \\ 0 \end{pmatrix}; \quad \mathbf{b} = \frac{1}{2} \begin{pmatrix} 1 \\ \sqrt{3} \end{pmatrix}. \quad (\text{C1})$$

The associated vectors in reciprocal space are given by

$$\mathbf{k}_a = \frac{2\pi}{\sqrt{3}} \begin{pmatrix} \sqrt{3} \\ -1 \end{pmatrix}; \quad \mathbf{k}_b = \frac{2\pi}{\sqrt{3}} \begin{pmatrix} 0 \\ 2 \end{pmatrix}. \quad (\text{C2})$$

We define the points along the irreducible wedge in reciprocal space to be

$$\Gamma = \begin{pmatrix} 0 \\ 0 \end{pmatrix}; \quad \mathbf{K} = \frac{4\pi}{3} \begin{pmatrix} 1 \\ 0 \end{pmatrix}; \quad \mathbf{M} = \frac{\pi}{\sqrt{3}} \begin{pmatrix} \sqrt{3} \\ 1 \end{pmatrix}. \quad (\text{C3})$$

The vectors δ linking the 6 neighboring sites are given by

$$\delta = \begin{pmatrix} 1 \\ 0 \end{pmatrix}; \quad \frac{1}{2} \begin{pmatrix} 1 \\ \sqrt{3} \end{pmatrix}; \quad \frac{1}{2} \begin{pmatrix} -1 \\ \sqrt{3} \end{pmatrix}; \quad (\text{C4}) \\ \begin{pmatrix} -1 \\ 0 \end{pmatrix}; \quad \frac{1}{2} \begin{pmatrix} -1 \\ -\sqrt{3} \end{pmatrix}; \quad \frac{1}{2} \begin{pmatrix} 1 \\ -\sqrt{3} \end{pmatrix}.$$

For the triangular lattice, the coordination number and the geometrical factor given in Eq. (129) yield

$$z = 6; \quad \gamma_{\triangleleft}(\mathbf{k}) = \frac{1}{3} (\cos(k_x) + 2 \cos(\frac{k_x}{2}) \cos(\frac{\sqrt{3}k_y}{2})). \quad (\text{C5})$$

The numerical simulations that we present in this Article are all performed on a cluster of sites defined by the real space basis vectors given by Eq. (C1) and scaled by L , such that $N = L^2$ is the number of lattice sites, with periodic boundary conditions.

Appendix D: Structure factors classically

We present here in more detail the results obtained in Section IV C where we introduced a fictive field \mathbf{h} that couples

to the moments (dipoles, quadrupoles or A matrices) that we are considering [Eq. (154)]. This allows us to then take the appropriate derivatives of the free energy with respect to the fictive field components evaluated at zero-field, and calculate the desired thermodynamic quantities, such as the structures factors.

The calculation for the structure factors is divided into 2 parts. The first part is valid for $\mathbf{q} \neq 0$. It consists in taking into account up to linear order in the expansion of fluctuations and is presented below. We provide details of the calculation for $\mathbf{q} \neq 0$ for dipole moments in Appendix D 2, quadrupole moments in Appendix D 4, and A-matrices in Appendix D 6. The second part captures the ground state contribution at $\mathbf{q} = 0$ and consists in taking into account up to quadratic order in the expansion of fluctuations. The general steps of the calculation at $\mathbf{q} = 0$ are given in Appendix D 1. The details at $\mathbf{q} = 0$ are provided in Appendix D 3 for the dipole moments, in Appendix D 5 for the quadrupole moments, in Appendix D 7 for the A-matrices.

We assume that the field dependent part of the Hamiltonian is given by Eq. (154), and that the moment $\hat{O}_{i,\beta}^\alpha$ can be written down in terms of the fluctuations ϕ_i . Considering up to second order in fluctuations, the moments $\hat{O}_{i,\beta}^\alpha$ becomes

$$\hat{O}_{i,\beta}^\alpha = q_{\beta,\mu\nu}^\alpha \phi_i^\mu \phi_i^\nu + l_{\beta,\mu}^\alpha \phi_i^\mu + c_{\beta}^\alpha + \mathcal{O}(\phi^3), \quad (\text{D1})$$

where we implicitly sum over μ and ν , and where $q_{\beta,\mu\nu}^\alpha$, $l_{\beta,\mu}^\alpha$ and c_{β}^α , are respectively the quadratic, linear, and constant coefficients from the expansion of $\hat{O}_{i,\beta}^\alpha$ in terms of the fluctuations ϕ_i . The field depend part of the Hamiltonian then becomes

$$\Delta\mathcal{H}[\mathbf{h}_i] = - \sum_i h_{i,\beta}^\alpha q_{\beta,\mu\nu}^\alpha \phi_i^\mu \phi_i^\nu + h_{i,\beta}^\alpha l_{\beta,\mu}^\alpha \phi_i^\mu + h_{i,\beta}^\alpha c_{\beta}^\alpha, \quad (\text{D2})$$

where we also implicitly sum over α, β , and where we neglect terms in $\mathcal{O}(\phi^3)$, which will from now on be disregarded. We now perform a Fourier transform according to Eq. (126), and obtain

$$\Delta\mathcal{H}[\mathbf{h}_\mathbf{q}] = - \sum_{\mathbf{q}} \left[l_{\beta,\mu}^\alpha h_{\mathbf{q},\beta}^\alpha \phi_{-\mathbf{q}}^\mu + \sqrt{N} c_{\beta}^\alpha h_{\mathbf{q},\beta}^\alpha \delta_{\mathbf{q},0} \right] \\ - \sum_{\mathbf{q}} \sum_{\mathbf{k}} \frac{1}{\sqrt{N}} q_{\beta,\mu\nu}^\alpha h_{\mathbf{q},\beta}^\alpha \phi_{\mathbf{k}}^\mu \phi_{-\mathbf{q}-\mathbf{k}}^\nu, \quad (\text{D3})$$

where N is the number of lattice sites. We notice that if we were to include this in the total Hamiltonian Eq. (153) and write it down in the same form as Eq. (124), the interaction matrix $M_{\mathbf{k}}$ would take the same dimension as the number of lattice site, because of the form of quadratic term in Eq. (D3). We should then calculate if for a fixed \mathbf{q} . Namely for $\mathbf{q} = 0$, we get

$$\Delta\mathcal{H}[\mathbf{h}_{\mathbf{q}=0}] = - l_{\beta,\mu}^\alpha h_{\mathbf{q}=0,\beta}^\alpha \phi_{-\mathbf{q}=0}^\mu - \sqrt{N} c_{\beta}^\alpha h_{\mathbf{q}=0,\beta}^\alpha \\ - \sum_{\mathbf{k}} \frac{1}{\sqrt{N}} q_{\beta,\mu\nu}^\alpha h_{\mathbf{q}=0,\beta}^\alpha \phi_{\mathbf{k}}^\mu \phi_{-\mathbf{k}}^\nu. \quad (\text{D4})$$

We note that the form of Eq. (D4) is compatible with the form of Eq. (124). Indeed, for $\mathbf{q} = 0$, the contribution of the second order in fluctuations will enter the interaction matrix $M_{\mathbf{k}}$, modifying its eigenvalues, i.e., its relation dispersions, which will also depend on the field \mathbf{h} , and the interaction matrix $M_{\mathbf{k}}$ can be easily diagonalized. Therefore, we decide to only take into account up to second order in fluctuations for $\mathbf{q} = 0$, since it is exactly solvable and since we will need it when comparing the ordered moments at $\mathbf{q} = 0$, and to neglect them for $\mathbf{q} \neq 0$. To make the fact that we are taking the second order in fluctuations into account only at $\mathbf{q} = 0$ more obvious, we write

$$\begin{aligned} \Delta\mathcal{H}[\mathbf{h}_{\mathbf{q}}] &= - \sum_{\mathbf{q}} l_{\beta\mu}^{\alpha} h_{\mathbf{q},\beta}^{\alpha} \phi_{-\mathbf{q}}^{\mu} \\ &- \sum_{\mathbf{q}} \left(\sqrt{N} c_{\beta}^{\alpha} h_{\mathbf{q},\beta}^{\alpha} + \sum_{\mathbf{k}} \frac{1}{\sqrt{N}} q_{\beta\mu\nu}^{\alpha} h_{\mathbf{q},\beta}^{\alpha} \phi_{\mathbf{k}}^{\mu} \phi_{-\mathbf{k}}^{\nu} \right) \delta_{\mathbf{q},0}. \end{aligned} \quad (\text{D5})$$

We then rewrite the field depend part of the Hamiltonian such that the Hamiltonian is symmetric in $\vec{\phi}_{\mathbf{q}}$ and $\vec{\phi}_{\mathbf{q}}^T$ [Eq. (131)], which will be necessary when calculating the structure factors at $\mathbf{q} = 0$. We have

$$\Delta\mathcal{H}[\mathbf{h}_{\mathbf{q}}] = - \sum_{\mathbf{q}} \mathbf{N}_1[\mathbf{h}_{\mathbf{q}}]^T \vec{\phi}_{-\mathbf{q}} + \vec{\phi}_{\mathbf{q}}^T \mathbf{N}_2[\mathbf{h}_{-\mathbf{q}}] + \tilde{C}[\mathbf{h}_{\mathbf{q}}] \delta_{\mathbf{q},0}, \quad (\text{D6})$$

where we define

$$\mathbf{N}_1[\mathbf{h}_{\mathbf{q}}]^{\mu} = \frac{1}{2} l_{\beta\mu}^{\alpha} h_{\mathbf{q},\beta}^{\alpha}, \quad \mathbf{N}_2[\mathbf{h}_{-\mathbf{q}}]^{\mu} = \frac{1}{2} l_{\beta\mu}^{\alpha} h_{-\mathbf{q},\beta}^{\alpha}, \quad (\text{D7})$$

and

$$\tilde{C}[\mathbf{h}_{\mathbf{q}}] = \sqrt{N} c_{\beta}^{\alpha} h_{\mathbf{q},\beta}^{\alpha} + \sum_{\mathbf{k}} \frac{1}{\sqrt{N}} q_{\beta\mu\nu}^{\alpha} h_{\mathbf{q},\beta}^{\alpha} \phi_{\mathbf{k}}^{\mu} \phi_{-\mathbf{k}}^{\nu}. \quad (\text{D8})$$

$\mathbf{N}_{1,2}[\mathbf{h}_{\mathbf{q}}]$ are n -dimensional vectors whose components depend linearly on the fields $h_{\mathbf{q},\beta}^{\alpha}$ and represent the linear terms in $\phi_{\mathbf{q}}$ of the moments $\hat{O}_{\mathbf{q}}$. $\tilde{C}[\mathbf{h}_{\mathbf{q}}]$ represents the 0-order term and the 2nd-order contribution in $\phi_{\mathbf{q}}$ of the moments $\hat{O}_{\mathbf{q}}$ at $\mathbf{q} = 0$. $\tilde{C}[\mathbf{h}_{\mathbf{q}}]$ is also linear in the fields $h_{\mathbf{q},\beta}^{\alpha}$. Plugging Eq. (D6) in Eq. (153), using the definition of the partition function in Eq. (132), and using Eq. (H1e) to perform the integral, we get

$$\begin{aligned} Z[\mathbf{h}_{\mathbf{q}}] &= e^{-\beta E_0} \prod_{\mathbf{q}} \left[\sqrt{\frac{(2\pi)^n}{\beta^n \det(M_{\mathbf{q}})}} e^{2\beta \mathbf{N}_1[\mathbf{h}_{\mathbf{q}}]^T M_{\mathbf{q}}^{-1} \mathbf{N}_2[\mathbf{h}_{\mathbf{q}}]} \right. \\ &\quad \left. \times e^{\beta(\tilde{C}[\mathbf{h}_{\mathbf{q}}] \delta_{\mathbf{q},0})} \right], \end{aligned} \quad (\text{D9})$$

where E_0 is given in Eq. (125), and the $n \times n$ square matrix $M_{\mathbf{q}}$ is given by Eq. (127). n is the dimension of $M_{\mathbf{q}}$, i.e., the number of independent classical fluctuations. In our case, we have $n = 4$. N is the number of lattice sites.

The free energy then becomes

$$\begin{aligned} F[\mathbf{h}_{\mathbf{q}}] &= - \frac{\log(Z[\mathbf{h}_{\mathbf{q}}])}{\beta} \\ &= E_0 - \sum_{\mathbf{q}} \tilde{C}[\mathbf{h}_{\mathbf{q}}] \delta_{\mathbf{q},0} - 2 \sum_{\mathbf{q}} \mathbf{N}_1[\mathbf{h}_{\mathbf{q}}]^T M_{\mathbf{q}}^{-1} \mathbf{N}_2[\mathbf{h}_{-\mathbf{q}}] \\ &\quad + \frac{n}{2\beta} \sum_{\mathbf{q}} \log\left(\frac{\beta}{2\pi}\right) + \frac{1}{2\beta} \sum_{\mathbf{q}} \log(\det(M_{\mathbf{q}})) \\ &\quad + \mathcal{O}(T^2). \end{aligned} \quad (\text{D10})$$

The first derivatives of the free energy with respect to field components $\mathbf{h}_{\mathbf{q}}$ give

$$\langle \hat{O}_{\mathbf{q},\nu}^{\mu} \rangle = - \left. \frac{\partial F}{\partial h_{\mathbf{q},\nu}^{\mu}} \right|_{\mathbf{h}=0} = \left. \frac{\partial \tilde{C}[\mathbf{h}_{\mathbf{q}}]}{\partial h_{\mathbf{q},\nu}^{\mu}} \right|_{\mathbf{h}=0} \delta_{\mathbf{q},0}. \quad (\text{D11})$$

The second derivatives of the free energy with respect to field components $\mathbf{h}_{\mathbf{q}}$ correspond to

$$\langle \hat{O}_{\mathbf{q},\beta}^{\alpha} \hat{O}_{-\mathbf{q},\nu}^{\mu} \rangle - \langle \hat{O}_{\mathbf{q},\beta}^{\alpha} \rangle \langle \hat{O}_{-\mathbf{q},\nu}^{\mu} \rangle = - \left. \frac{1}{\beta} \frac{\partial^2 F}{\partial h_{\mathbf{q},\beta}^{\alpha} \partial h_{-\mathbf{q},\nu}^{\mu}} \right|_{\mathbf{h}=0} \quad (\text{D12a})$$

$$= \frac{2}{\beta} \frac{\partial^2}{\partial h_{\mathbf{q},\beta}^{\alpha} \partial h_{-\mathbf{q},\nu}^{\mu}} \sum_{\mathbf{q}} \left(\mathbf{N}_1[\mathbf{h}_{\mathbf{q}}]^T M_{\mathbf{q}}^{-1} \mathbf{N}_2[\mathbf{h}_{-\mathbf{q}}] \right) \Big|_{\mathbf{h}=0}, \quad (\text{D12b})$$

where we used the fact that $\tilde{C}[\mathbf{h}_{\mathbf{q}}]$ is linear in the field components $h_{\mathbf{q},\beta}^{\alpha}$. For $\mathbf{q} \neq 0$, it turns out to be more convenient to work with $\tilde{M}_{\mathbf{q}}$ [Eq. (144)] which is diagonal and which inverse then simply holds

$$(\tilde{M}_{\mathbf{q}}^{-1})^{\lambda\lambda} = \frac{1}{\tilde{M}_{\mathbf{q}}^{\lambda\lambda}} = \frac{1}{\omega_{\mathbf{q},\lambda}}. \quad (\text{D13})$$

We are allowed to do this because for $\mathbf{q} \neq 0$, the interaction matrix stays unchanged. However, we need to be more careful for $\mathbf{q} = 0$ as explained in Appendix D 1. Then, $\mathbf{N}_{1,2}[\mathbf{h}_{\mathbf{q}}]$ become $\tilde{\mathbf{N}}_{1,2}[\mathbf{h}_{\mathbf{q}}]$

$$\tilde{\mathbf{N}}_1[\mathbf{h}_{\mathbf{q}}]^T = \mathbf{N}_1[\mathbf{h}_{\mathbf{q}}]^T O, \quad (\text{D14a})$$

$$\tilde{\mathbf{N}}_2[\mathbf{h}_{-\mathbf{q}}] = O^T \mathbf{N}_2[\mathbf{h}_{-\mathbf{q}}], \quad (\text{D14b})$$

such that $\tilde{\mathbf{N}}_{1,2}[\mathbf{h}_{\mathbf{q}}]$ corresponds to the linear term when expressing the operators \hat{O}_i^{α} in terms of the fluctuations $\vec{v}_{\mathbf{q}}$ that diagonalize the BBQ Hamiltonian as shown in Eq. (142). Indeed, we then obtain

$$\Delta\mathcal{H}[\mathbf{h}_{\mathbf{q}}] = - \sum_{\mathbf{q}} \tilde{\mathbf{N}}_1[\mathbf{h}_{\mathbf{q}}]^T \vec{v}_{-\mathbf{q}} + \vec{v}_{\mathbf{q}}^T \tilde{\mathbf{N}}_2[\mathbf{h}_{-\mathbf{q}}] + \tilde{C}[\mathbf{h}_{\mathbf{q}}] \delta_{\mathbf{q},0}, \quad (\text{D15})$$

Therefore, we can simply write

$$F[\mathbf{h}_q] = E_0 + \sum_{\mathbf{q}} \tilde{C}[\mathbf{h}_q] \delta_{\mathbf{q},0} - 2 \sum_{\mathbf{q}} \sum_{\lambda=1}^{N_\lambda} \frac{(\tilde{\mathbf{N}}_1[\mathbf{h}_q]^T)^\lambda \tilde{\mathbf{N}}_2[\mathbf{h}_q]^\lambda}{\omega_{\mathbf{q},\lambda}} + \frac{N_\lambda}{2\beta} \sum_{\mathbf{q}} \log\left(\frac{\beta}{2\pi}\right) + \frac{1}{2\beta} \sum_{\mathbf{q}} \sum_{\lambda=1}^{N_\lambda} \log(\omega_{\mathbf{q},\lambda}) + \mathcal{O}(T^2), \quad (\text{D16})$$

where we have used Eq. (137) and where $N_\lambda = 4$ is the number of modes. Eq. (D11) stays unchanged, but Eq. (D12b) takes the simple form given by

$$\langle \hat{O}_{\mathbf{q},\beta}^\alpha \hat{O}_{-\mathbf{q},\nu}^\mu \rangle - \langle \hat{O}_{\mathbf{q},\beta}^\alpha \rangle \langle \hat{O}_{-\mathbf{q},\nu}^\mu \rangle = \quad (\text{D17})$$

$$\frac{2}{\beta} \frac{\partial}{\partial h_{\mathbf{q},\beta}^\alpha \partial h_{-\mathbf{q},\nu}^\mu} \left(\sum_{\lambda=1}^{N_\lambda} \frac{(\tilde{\mathbf{N}}_1[\mathbf{h}_q]^T)^\lambda \tilde{\mathbf{N}}_2[\mathbf{h}_q]^\lambda}{\omega_{\mathbf{q},\lambda}} \right) \Big|_{\mathbf{h}=0}. \quad (\text{D18})$$

The dynamical factor associated with the operator \hat{O} is defined by

$$S_{\text{O}}^{\text{CL}}(\mathbf{q}) = \sum_{\alpha,\beta} \langle \hat{O}_{\mathbf{q},\beta}^\alpha \hat{O}_{-\mathbf{q},\alpha}^\beta \rangle \quad (\text{D19})$$

We can generalize a spectral decomposition of the structure factors as

$$S_{\text{O}}^{\text{CL}}(\mathbf{q}, \omega) = \sum_{\alpha,\beta,\lambda} \langle \hat{O}_{\mathbf{q},\beta}^\alpha \hat{O}_{-\mathbf{q},\alpha}^\beta \rangle_\lambda \delta(\omega - \omega_{\mathbf{q},\lambda}), \quad (\text{D20})$$

and calculate the following quantity

$$S_{\text{O}}^{\text{CL}}(\mathbf{q}, \omega) = \sum_{\alpha,\beta,\lambda} \left[\langle \hat{O}_{\mathbf{q},\beta}^\alpha \rangle_\lambda \langle \hat{O}_{-\mathbf{q},\alpha}^\beta \rangle_\lambda + \chi_\lambda^{\alpha\beta\beta\alpha}(\mathbf{q}) \right] \times \delta(\omega - \omega_{\mathbf{q},\lambda}), \quad (\text{D21})$$

where generalized susceptibility

$$\chi_\lambda^{\alpha\beta\beta\alpha}(\mathbf{q}) = \langle \hat{O}_{\mathbf{q},\beta}^\alpha \hat{O}_{-\mathbf{q},\nu}^\mu \rangle_\lambda - \langle \hat{O}_{\mathbf{q},\beta}^\alpha \rangle_\lambda \langle \hat{O}_{-\mathbf{q},\nu}^\mu \rangle_\lambda = \frac{2}{\beta} \frac{\partial}{\partial h_{\mathbf{q},\beta}^\alpha \partial h_{-\mathbf{q},\nu}^\mu} \left(\frac{(\tilde{\mathbf{N}}_1[\mathbf{h}_q]^T)^\lambda \tilde{\mathbf{N}}_2[\mathbf{h}_q]^\lambda}{\omega_{\mathbf{q},\lambda}} \right) \Big|_{\mathbf{h}=0}. \quad (\text{D22})$$

is diagonal in λ . From Eq. (D11), we note that the first moments $\langle \hat{O}_{\mathbf{q},\beta}^\alpha \rangle$ will only contribute at $\mathbf{q} = 0$. Therefore, for $\mathbf{q} \neq 0$, we can neglect the $\langle \hat{O}_{\mathbf{q},\lambda}^\alpha \rangle \langle \hat{O}_{-\mathbf{q},\lambda}^\beta \rangle$ term and we obtain

$$S_{\text{O}}^{\text{CL}}(\mathbf{q} \neq 0) = \sum_{\alpha\beta\lambda} \chi_\lambda^{\alpha\beta\beta\alpha}(\mathbf{q}) + \mathcal{O}(T^2), \quad (\text{D23})$$

1. Structure factors classically at $\mathbf{q} = 0$

We here show how the calculation for the structure at $\mathbf{q} = 0$ is obtained. At $\mathbf{q} = 0$, the structure factor associated with the operator \hat{O} is defined by

$$S_{\text{O}}^{\text{CL}}(\mathbf{q} = 0) = \sum_{\alpha,\beta} \langle \hat{O}_{\mathbf{q}=0,\beta}^\alpha \hat{O}_{\mathbf{q}=0,\alpha}^\beta \rangle. \quad (\text{D24})$$

The relevant source term is given by Eq. (154). By expanding Eq. (154) in terms of the fluctuations, we obtained Eq. (D5). We see that the contribution of the second order in fluctuations has the same form as the Hamiltonian expressed as Eq. (124) and will enter the interaction matrix $M_{\mathbf{k}}$, modifying its eigenvalues, i.e., relation dispersion relations, which will all also depend on the field \mathbf{h} . We can therefore assume that, at $\mathbf{q} = 0$, the total Hamiltonian [Eq. (153)] has the following form

$$\mathcal{H} = E_0 + \frac{1}{2} \sum_{\mathbf{k}} \left[\vec{\phi}_{\mathbf{k}}^T M_{\mathbf{k}}[\mathbf{h}_{\mathbf{q}=0}] \vec{\phi}_{-\mathbf{k}} \right] + \sum_{\mathbf{k}} \left[N_1^T[\mathbf{h}_{\mathbf{k}}] \vec{\phi}_{-\mathbf{k}} + \vec{\phi}_{\mathbf{k}}^T N_2[\mathbf{h}_{-\mathbf{k}}] \right] \delta_{\mathbf{k},0} + \sum_{\mathbf{k}} C[\mathbf{h}_{\mathbf{q}=0}] \delta_{\mathbf{k},0} + \mathcal{O}(\phi^3), \quad (\text{D25})$$

where $C[\mathbf{h}_{\mathbf{q}=0}]$ represents the 0-order term in $\phi_{\mathbf{q}}$ of the moments $\hat{O}_{\mathbf{q}}$. The 2nd-order contribution at $\mathbf{q} = 0$ is now included in $M_{\mathbf{k}}[\mathbf{h}_{\mathbf{q}=0}]$. As before, $\mathbf{N}_{1,2}[\mathbf{h}_{\mathbf{k}}]$ are n -dimensional vectors whose components depend linearly on the fields $h_{\mathbf{k},\beta}^\alpha$ and represent the linear terms in $\phi_{\mathbf{k}}$ of the moments $\hat{O}_{\mathbf{k}}$. Neglecting terms in $\mathcal{O}(\phi^3)$, and using Eq. (H1e) to perform the integral, we find

$$Z = e^{-\beta E_0} \prod_{\mathbf{k}} \left[\int e^{-\beta \frac{1}{2} \vec{\phi}_{\mathbf{k}}^T M_{\mathbf{k}}[\mathbf{h}_{\mathbf{q}=0}] \vec{\phi}_{\mathbf{k}}} \times e^{-\beta [N_1^T[\mathbf{h}_{\mathbf{k}}] \vec{\phi}_{-\mathbf{k}} + \vec{\phi}_{\mathbf{k}}^T N_2[\mathbf{h}_{-\mathbf{k}}]] \delta_{\mathbf{k},0}} \times e^{-\beta C[\mathbf{h}_{\mathbf{q}=0}] \delta_{\mathbf{k},0}} \right] d\vec{\phi}_{\mathbf{k}} \quad (\text{D26a})$$

$$= e^{-\beta E_0} \prod_{\mathbf{k}} \left[\sqrt{\frac{(2\pi)^n}{\beta^n \det M_{\mathbf{k}}[\mathbf{h}_{\mathbf{q}=0}]}} \times e^{2\beta N_1^T[\mathbf{h}_{\mathbf{k}}] M_{\mathbf{k}}^{-1}[\mathbf{h}_{\mathbf{q}=0}] N_2[\mathbf{h}_{-\mathbf{k}}] \delta_{\mathbf{k},0}} e^{-\beta C[\mathbf{h}_{\mathbf{q}=0}] \delta_{\mathbf{k},0}} \right], \quad (\text{D26b})$$

where E_0 is defined through Eq. (125), and the $n \times n$ matrix $M_{\mathbf{k}}[h_{\mathbf{q}=0,\beta}^\alpha]$ through Eq. (D25) that includes up to second order in fluctuations. n is the dimension of $M_{\mathbf{k}}[h_{\mathbf{q}=0,\beta}^\alpha]$, i.e., the number of independent classical fluctuations. In our case, we have $n = 4$. N is the number of lattice sites. It follows that the free energy is

$$F = -\frac{\log(Z)}{\beta} = E_0 + \sum_{\mathbf{k}} C[\mathbf{h}_{\mathbf{q}=0}] \delta_{\mathbf{k},0} - \frac{n}{2\beta} \sum_{\mathbf{k}} \log\left(\frac{2\pi}{\beta}\right) + \frac{1}{2\beta} \sum_{\mathbf{k}} \sum_{\lambda=1}^{N_\lambda} \log(\omega_{\mathbf{k},\lambda}[\mathbf{h}_{\mathbf{q}=0}]) - 2 \sum_{\mathbf{k}} N_1^T[\mathbf{h}_{\mathbf{k}}] M_{\mathbf{k}}^{-1}[\mathbf{h}_{\mathbf{q}=0}] N_2[\mathbf{h}_{-\mathbf{k}}] \delta_{\mathbf{k},0} + \mathcal{O}(T^2), \quad (\text{D27})$$

where $\omega_{\mathbf{k},\lambda}[\mathbf{h}_{\mathbf{q}=0}]$ are the eigenvalues of $M_{\mathbf{k}}[\mathbf{h}_{\mathbf{q}=0}]$, and we have used Eq. (137). The moments are given by

$$\langle \hat{O}_{\mathbf{q}=0,\beta}^\alpha \rangle = - \left. \frac{\partial F}{\partial h_{\mathbf{q}=0,\beta}^\alpha} \right|_{\mathbf{h}=0}, \quad (\text{D28})$$

and

$$\begin{aligned} \langle \hat{O}_{\mathbf{q}=0,\beta}^\alpha \hat{O}_{\mathbf{q}=0,\nu}^\mu \rangle &= \langle \hat{O}_{\mathbf{q}=0,\beta}^\alpha \rangle \langle \hat{O}_{\mathbf{q}=0,\nu}^\mu \rangle \\ &\quad - \left. \frac{1}{\beta} \frac{\partial^2 F}{\partial h_{\mathbf{q}=0,\beta}^\alpha \partial h_{\mathbf{q}=0,\nu}^\mu} \right|_{\mathbf{h}=0}. \end{aligned} \quad (\text{D29})$$

Using Eq. (D27), Eq. (D28) yields

$$\begin{aligned} \langle \hat{O}_{\mathbf{q}=0,\beta}^\alpha \rangle &= - \left. \frac{\partial C[\mathbf{h}_{\mathbf{q}=0}]}{\partial h_{\mathbf{q}=0,\beta}^\alpha} \right|_{\mathbf{h}=0} \\ &\quad - \frac{1}{2\beta} \sum_{\mathbf{k}} \sum_{\lambda=1}^{N_\lambda} \frac{1}{\omega_{\mathbf{k},\lambda}[\mathbf{h}_{\mathbf{q}=0}]} \left. \frac{\partial \omega_{\mathbf{k},\lambda}[\mathbf{h}_{\mathbf{q}=0}]}{\partial h_{\mathbf{q}=0,\beta}^\alpha} \right|_{\mathbf{h}=0} \\ &\quad + 2 \left. \frac{\partial [N_1^T[\mathbf{h}_{\mathbf{q}=0}] M_{\mathbf{q}=0}^{-1}[\mathbf{h}_{\mathbf{q}=0}] N_2[\mathbf{h}_{\mathbf{q}=0}]]}{\partial h_{\mathbf{q}=0,\beta}^\alpha} \right|_{\mathbf{h}=0} \\ &\quad + \mathcal{O}(T^2), \end{aligned} \quad (\text{D30})$$

where the last derivative turns out to be null when evaluated at $\mathbf{h} = 0$, for dipoles, quadrupoles and A-matrices. Eq. (D29) becomes

$$\begin{aligned} \langle \hat{O}_{\mathbf{q}=0,\beta}^\alpha \hat{O}_{\mathbf{q}=0,\nu}^\mu \rangle &= \langle \hat{O}_{\mathbf{q}=0,\beta}^\alpha \rangle \langle \hat{O}_{\mathbf{q}=0,\nu}^\mu \rangle \\ &\quad - \left. \frac{1}{\beta} \frac{\partial^2 C[\mathbf{h}_{\mathbf{q}=0}]}{\partial h_{\mathbf{q}=0,\beta}^\alpha \partial h_{\mathbf{q}=0,\nu}^\mu} \right|_{\mathbf{h}=0} \\ &\quad + \frac{2}{\beta} \left. \frac{\partial^2 [N_1^T[\mathbf{h}_{\mathbf{q}=0}] M_{\mathbf{q}=0}^{-1}[\mathbf{h}_{\mathbf{q}=0}] N_2[\mathbf{h}_{\mathbf{q}=0}]]}{\partial h_{\mathbf{q}=0,\beta}^\alpha \partial h_{\mathbf{q}=0,\nu}^\mu} \right|_{\mathbf{h}=0} \\ &\quad + \mathcal{O}(T^2), \end{aligned} \quad (\text{D31})$$

where the terms including second derivatives of $C[\mathbf{h}_{\mathbf{q}=0}]$ are zero, since $C[\mathbf{h}_{\mathbf{q}=0}]$ is linear in $h_{\mathbf{q}=0,\beta}^\alpha$ by definition. Finally, Eq. (D24) can be calculated by using Eq. (D30) and Eq. (D31). For each type of moments, dipole, quadrupole or A-matrix, the interaction matrix $M_{\mathbf{k}}[\mathbf{h}_{\mathbf{q}=0}]$, the source terms $N_1^T[\mathbf{h}_{\mathbf{q}}]$ and $N_2[\mathbf{h}_{\mathbf{q}}]$ and the constant term will be different. They are given below.

2. Dipole moments: classical structure factor for $\mathbf{q} \neq 0$

First, we consider the structure factor for dipole moments of spin

$$S_S^{\text{CL}}(\mathbf{q}) = \sum_{\alpha} \langle \hat{S}_{\mathbf{q}}^\alpha \hat{S}_{-\mathbf{q}}^\alpha \rangle. \quad (\text{D32})$$

The relevant source term is

$$\Delta \mathcal{H}[h_{i,\beta}^\alpha] = - \sum_{i,\lambda} h_{i,\beta}^\alpha \delta_{\alpha\beta} \hat{S}_{i,\lambda}^\beta. \quad (\text{D33})$$

According to Eq. (50) and using Eq. (121), we can express the spin dipole components in function of the fluctuations. Considering fluctuation terms up to 1st order and using Eq. (145), the spin dipole moments in terms of the fluctuations diagonalizing the BBQ Hamiltonian are given by

$$\begin{aligned} \hat{S}_i^x &= -\sqrt{2}v_{4,i}, \\ \hat{S}_i^y &\simeq 0, \\ \hat{S}_i^z &= \sqrt{2}v_{2,i}. \end{aligned} \quad (\text{D34})$$

After performing a Fourier transform, the change in the Hamiltonian due to $\Delta \mathcal{H}[h_{i,\beta}^\alpha]$ [Eq. (D33)] yields

$$\begin{aligned} \Delta \mathcal{H}[\mathbf{h}_{\mathbf{q}}] &= - \sum_{\mathbf{q}} \left[\frac{\sqrt{2}}{2} h_{\mathbf{q}}^z v_{-\mathbf{q},2} + \frac{\sqrt{2}}{2} h_{-\mathbf{q}}^z v_{\mathbf{q},2} \right. \\ &\quad \left. - \frac{\sqrt{2}}{2} h_{\mathbf{q}}^x v_{-\mathbf{q},4} - \frac{\sqrt{2}}{2} h_{-\mathbf{q}}^x v_{\mathbf{q},4} \right], \end{aligned}$$

and according to Eq. (D15), we get

$$\tilde{C}[\mathbf{h}_{\mathbf{q}}] = 0, \quad (\text{D35})$$

where we neglected 2nd order terms in fluctuations, since they only contribute for $\mathbf{q} = 0$, and

$$\begin{aligned} \tilde{\mathbf{N}}_1[\mathbf{h}_{\mathbf{q}}]^T &= \left(0, \frac{\sqrt{2}}{2} h_{\mathbf{q}}^z, 0, -\frac{\sqrt{2}}{2} h_{\mathbf{q}}^x \right), \\ \tilde{\mathbf{N}}_2[\mathbf{h}_{-\mathbf{q}}] &= \begin{pmatrix} 0 \\ \frac{\sqrt{2}}{2} h_{-\mathbf{q}}^z \\ 0 \\ -\frac{\sqrt{2}}{2} h_{-\mathbf{q}}^x \end{pmatrix}. \end{aligned} \quad (\text{D36})$$

According to Eq. (D11), the first moments are given by the first derivative of $\tilde{C}[\mathbf{h}_{\mathbf{q}}]$ [Eq. (D35)] with respect to the fictive field \mathbf{h} . We get

$$\langle S_{\mathbf{q}}^x \rangle = \langle S_{\mathbf{q}}^z \rangle = 0. \quad (\text{D37})$$

The total structure factor for the dipole moment is given by Eq. (D32), and using Eq. (D22), Eq. (D23), and Eq. (D36), we obtain

$$S_S^{\text{CL}}(\mathbf{q} \neq 0) = \frac{2}{\beta\omega_{\mathbf{q},2}} + \frac{2}{\beta\omega_{\mathbf{q},4}} + \mathcal{O}(T^2) = \frac{4}{\beta\omega_{\mathbf{q}}} + \mathcal{O}(T^2), \quad (\text{D38})$$

where we used Eq. (140b). Its spectral decomposition [Eq. (D21)] becomes

$$S_S^{\text{CL}}(\mathbf{q} \neq 0, \omega) = \frac{4}{\beta\omega_{\mathbf{q}}} \delta(\omega - \omega_{\mathbf{q}}^-) + \mathcal{O}(T^2). \quad (\text{D39})$$

3. Dipole moments: classical structure factor at $\mathbf{q} = 0$

We now consider the dipole structure factor at the origin of the reciprocal space called the Γ -point. We consider the structure factor for the spin dipole moments

$$S_S^{\text{CL}}(\mathbf{q} = 0) = \sum_{\alpha} \langle \hat{S}_{\mathbf{q}=0}^\alpha \hat{S}_{\mathbf{q}=0}^\alpha \rangle. \quad (\text{D40})$$

We follow the procedure depicted in [Appendix D 1](#). The relevant source term for dipole moments is given by [Eq. \(D33\)](#) that we need to rewrite it in the same form as [Eq. \(D25\)](#). We use [Eq. \(124\)–Eq. \(127\)](#) for the BBQ Hamiltonian, as well as, [Eq. \(121\)](#) and [Eq. \(50\)](#) to express [Eq. \(D33\)](#) up to second order in terms of the fluctuations. For the total Hamiltonian given in [Eq. \(153\)](#), and written in the form of [Eq. \(D25\)](#), we obtain

$$M_{\mathbf{k}}[\mathbf{h}_{\mathbf{q}=0}] = \begin{pmatrix} A_{\mathbf{k}} & -B_{\mathbf{k}} & 0 & \frac{i}{\sqrt{N}}h_{\mathbf{q}=0,y}^y \\ -B_{\mathbf{k}} & A_{\mathbf{k}} & -\frac{i}{\sqrt{N}}h_{\mathbf{q}=0,y}^y & 0 \\ 0 & \frac{i}{\sqrt{N}}h_{\mathbf{q}=0,y}^y & A_{\mathbf{k}} & -B_{\mathbf{k}} \\ -\frac{i}{\sqrt{N}}h_{\mathbf{q}=0,y}^y & 0 & -B_{\mathbf{k}} & A_{\mathbf{k}} \end{pmatrix}, \quad (\text{D41})$$

$$\begin{aligned} \mathbf{N}_1[\mathbf{h}_{\mathbf{k}}]^T &= \frac{1}{2} (-h_{\mathbf{k},z}^z, -h_{\mathbf{k},z}^z, h_{\mathbf{k},x}^x, h_{\mathbf{k},x}^x), \\ \mathbf{N}_2[\mathbf{h}_{-\mathbf{k}}] &= \frac{1}{2} \begin{pmatrix} -h_{-\mathbf{k},z}^z \\ -h_{-\mathbf{k},z}^z \\ h_{-\mathbf{k},x}^x \\ h_{-\mathbf{k},x}^x \end{pmatrix}, \end{aligned} \quad (\text{D42})$$

$$C[\mathbf{h}_{\mathbf{k}}] = 0. \quad (\text{D43})$$

We diagonalize [Eq. \(D41\)](#) to obtain the eigenmodes. We find

$$\begin{aligned} \omega_{\mathbf{k}}^+[\mathbf{h}_{\mathbf{q}=0}] &= \omega_{\mathbf{k},1}[\mathbf{h}_{\mathbf{q}=0}] = \omega_{\mathbf{k},3}[\mathbf{h}_{\mathbf{q}=0}] \\ &= A_{\mathbf{k}} + \sqrt{\left(\frac{h_{0,y}^y}{\sqrt{N}}\right)^2 + B_{\mathbf{k}}^2}, \end{aligned} \quad (\text{D44a})$$

$$\begin{aligned} \omega_{\mathbf{k}}^-[\mathbf{h}_{\mathbf{q}=0}] &= \omega_{\mathbf{k},2}[\mathbf{h}_{\mathbf{q}=0}] = \omega_{\mathbf{k},4}[\mathbf{h}_{\mathbf{q}=0}] \\ &= A_{\mathbf{k}} - \sqrt{\left(\frac{h_{0,y}^y}{\sqrt{N}}\right)^2 + B_{\mathbf{k}}^2}. \end{aligned} \quad (\text{D44b})$$

We now can calculate the spin dipole moments through [Eq. \(D30\)](#), where we use [Eq. \(D43\)](#), and [Eq. \(D44\)](#), and where for the last term, we simply invert [Eq. \(D41\)](#) and multiply by the vectors in [Eq. \(D42\)](#). We obtain

$$\langle S_{\mathbf{q}=0}^x \rangle = \langle S_{\mathbf{q}=0}^y \rangle = \langle S_{\mathbf{q}=0}^z \rangle = 0. \quad (\text{D45})$$

For the square dipole moments, we use [Eq. \(D31\)](#). We find

$$\langle S_{\mathbf{q}=0}^x S_{\mathbf{q}=0}^x \rangle = \frac{2}{\beta} \frac{1}{A_{\mathbf{q}=0} - B_{\mathbf{q}=0}} = \frac{2}{\beta} \frac{1}{\omega_0^-}, \quad (\text{D46a})$$

$$\langle S_{\mathbf{q}=0}^y S_{\mathbf{q}=0}^y \rangle = 0, \quad (\text{D46b})$$

$$\langle S_{\mathbf{q}=0}^z S_{\mathbf{q}=0}^z \rangle = \frac{2}{\beta} \frac{1}{A_{\mathbf{q}=0} - B_{\mathbf{q}=0}} = \frac{2}{\beta} \frac{1}{\omega_0^-}, \quad (\text{D46c})$$

where we used [Eq. \(140\)](#).

Finally, we calculate the dipole structure factor at the Γ -point given by [Eq. \(D40\)](#). We get

$$S_S^{\text{CL}}(\mathbf{q} = 0) = \frac{4}{\beta} \frac{1}{\omega_0^-} + \mathcal{O}(T^2). \quad (\text{D47})$$

Because the $\mathbf{q} = 0$ contributions are coming from the ground state and happen for $\omega = 0$, the spectral representation of [Eq. \(D47\)](#) yields

$$S_S^{\text{CL}}(\mathbf{q} = 0, \omega) = \frac{4}{\beta} \frac{1}{\omega_0^-} \delta(\omega) + \mathcal{O}(T^2). \quad (\text{D48})$$

Combining [Eq. \(D38\)](#) and [Eq. \(D47\)](#), we get [Eq. \(157\)](#). And considering their respective spectral representation [Eq. \(D39\)](#) and [Eq. \(D48\)](#), we obtain [Eq. \(158\)](#).

4. Quadrupole moments: classical structure factor for $\mathbf{q} \neq 0$

Next, we consider the structure factor for quadrupole moments of spin

$$S_Q^{\text{CL}}(\mathbf{q}) = \sum_{\alpha\beta} \langle \hat{Q}_{\mathbf{q}}^{\alpha\beta} \hat{Q}_{-\mathbf{q}}^{\beta\alpha} \rangle, \quad (\text{D49})$$

where the scalar contraction implied by the sum on α, β respects $SU(2)$ symmetry. In this case the source term is

$$\Delta \mathcal{H}[\mathbf{h}_i] = - \sum_i h_{i,\beta}^\alpha \hat{Q}_i^{\alpha\beta}. \quad (\text{D50})$$

The quadrupole components $\hat{Q}_i^{\alpha\beta}$ in the function of the classical fluctuations can be found using [Eq. \(51\)](#) and [Eq. \(121\)](#). Using [Eq. \(145\)](#), we can express $\Delta \mathcal{H}[\mathbf{h}_i]$ in terms of the fluctuations that diagonalize the BBQ Hamiltonian. After performing a Fourier transform, and rewriting the Hamiltonian in the form of [Eq. \(D15\)](#), we get

$$\tilde{C}[\mathbf{h}_{\mathbf{q}}] = \sqrt{N} \left(-\frac{4}{3} h_{\mathbf{q}}^{yy} + \frac{2}{3} (h_{\mathbf{q}}^{xx} + h_{\mathbf{q}}^{zz}) \right), \quad (\text{D51})$$

where we neglected 2nd order terms in fluctuations, since they only contribute for $\mathbf{q} = 0$, and

$$\begin{aligned} \tilde{\mathbf{N}}_1[\mathbf{h}_{\mathbf{q}}]^T &= \left(0, \frac{i\sqrt{2}}{2} \xi_{\mathbf{q}}^1, 0, -\frac{i\sqrt{2}}{2} \xi_{\mathbf{q}}^1 \right), \\ \tilde{\mathbf{N}}_2[\mathbf{h}_{-\mathbf{q}}] &= \begin{pmatrix} 0 \\ \frac{i\sqrt{2}}{2} \xi_{-\mathbf{q}}^1 \\ 0 \\ -\frac{i\sqrt{2}}{2} \xi_{-\mathbf{q}}^1 \end{pmatrix}, \end{aligned} \quad (\text{D52})$$

where

$$\xi_{\mathbf{q}}^1 = (h_{\mathbf{q}}^{xy} + h_{\mathbf{q}}^{yx}), \quad \xi_{\mathbf{q}}^2 = (h_{\mathbf{q}}^{yz} + h_{\mathbf{q}}^{zy}). \quad (\text{D53})$$

The total quadrupole structure factor is given by [Eq. \(D49\)](#). According to [Eq. \(D22\)](#) and [Eq. \(D23\)](#), and using [Eq. \(D52\)](#), we obtain

$$S_Q^{\text{CL}}(\mathbf{q} \neq 0) = \frac{4}{\beta \omega_{\mathbf{q},1}} + \frac{4}{\beta \omega_{\mathbf{q},3}} + \mathcal{O}(T^2) = \frac{8}{\beta \omega_{\mathbf{q}}^+} + \mathcal{O}(T^2), \quad (\text{D54})$$

where we used [Eq. \(140a\)](#). and its spectral decomposition [[Eq. \(D21\)](#)] becomes

$$S_Q^{\text{CL}}(\mathbf{q} \neq 0, \omega) = \frac{8}{\beta \omega_{\mathbf{q}}^+} \delta(\omega - \omega_{\mathbf{q}}^+) + \mathcal{O}(T^2). \quad (\text{D55})$$

5. Quadrupole moments: classical structure factor at $\mathbf{q} = 0$

We now consider the quadrupole structure factor at the Γ -point, which is defined as

$$S_Q^{\text{CL}}(\mathbf{q} = 0) = \sum_{\alpha\beta} \langle \hat{Q}_{\mathbf{q}=0}^{\alpha\beta} \hat{Q}_{\mathbf{q}=0}^{\beta\alpha} \rangle. \quad (\text{D56})$$

We follow the same procedure as depicted in [Appendix D 1](#). The relevant source term for quadrupole moments is given by [Eq. \(D50\)](#). We use [Eq. \(127\)](#) for the BBQ Hamiltonian as well as [Eq. \(121\)](#) and [Eq. \(51\)](#) to express [Eq. \(D50\)](#) up to second order in terms of the fluctuations. For the total Hamiltonian given by [Eq. \(153\)](#), and written in the form of [Eq. \(D25\)](#), we obtain

$$M_{\mathbf{k}}[\mathbf{h}_{\mathbf{q}=0}] = \begin{pmatrix} A_{\mathbf{k}} + \alpha_1 & -B_{\mathbf{k}} & 0 & \beta_1 \\ -B_{\mathbf{k}} & A_{\mathbf{k}} + \alpha_1 & \beta_1 & 0 \\ 0 & \beta_1 & A_{\mathbf{k}} + \alpha_2 & -B_{\mathbf{k}} \\ \beta_1 & 0 & -B_{\mathbf{k}} & A_{\mathbf{k}} + \alpha_2 \end{pmatrix}, \quad (\text{D57})$$

$$\mathbf{N}_1[\mathbf{h}_{\mathbf{k}}]^T = \frac{-i}{2} (-\xi_{\mathbf{k}}^1, \xi_{\mathbf{k}}^1, \xi_{\mathbf{k}}^2, -\xi_{\mathbf{k}}^2),$$

$$\mathbf{N}_2[\mathbf{h}_{-\mathbf{k}}] = \frac{i}{2} \begin{pmatrix} -\xi_{-\mathbf{k}}^1 \\ \xi_{-\mathbf{k}}^1 \\ \xi_{-\mathbf{k}}^2 \\ -\xi_{-\mathbf{k}}^2 \end{pmatrix}, \quad (\text{D58})$$

$$C[\mathbf{h}_{\mathbf{q}=0}] = \sqrt{N} \left(\frac{4}{3} h_{\mathbf{q}=0,y}^y - \frac{2}{3} (h_{\mathbf{q}=0,x}^x + h_{\mathbf{q}=0,z}^z) \right), \quad (\text{D59})$$

where we define

$$\alpha_1 = \frac{2}{\sqrt{N}} (h_{\mathbf{q}=0,x}^x - h_{\mathbf{q}=0,y}^y), \quad \alpha_2 = \frac{2}{\sqrt{N}} (h_{\mathbf{q}=0,z}^z - h_{\mathbf{q}=0,y}^y),$$

$$\beta_1 = \frac{1}{\sqrt{N}} (h_{\mathbf{q}=0,z}^x + h_{\mathbf{q}=0,x}^z),$$

$$\xi_{\mathbf{k}}^1 = (h_{\mathbf{k},y}^x + h_{\mathbf{k},x}^y), \quad \xi_{\mathbf{k}}^2 = (h_{\mathbf{k},z}^y + h_{\mathbf{k},y}^z). \quad (\text{D60})$$

We diagonalize [Eq. \(D57\)](#) to obtain the eigenmodes. We find

$$\omega_{\mathbf{k},1}[\mathbf{h}_{\mathbf{q}=0}] = A_{\mathbf{k}} + B_{\mathbf{k}}^2 + \frac{1}{2}(\alpha_+ + \Delta), \quad (\text{D61a})$$

$$\omega_{\mathbf{k},2}[\mathbf{h}_{\mathbf{q}=0}] = A_{\mathbf{k}} - B_{\mathbf{k}}^2 + \frac{1}{2}(\alpha_+ + \Delta), \quad (\text{D61b})$$

$$\omega_{\mathbf{k},3}[\mathbf{h}_{\mathbf{q}=0}] = A_{\mathbf{k}} + B_{\mathbf{k}}^2 + \frac{1}{2}(\alpha_+ - \Delta), \quad (\text{D61c})$$

$$\omega_{\mathbf{k},4}[\mathbf{h}_{\mathbf{q}=0}] = A_{\mathbf{k}} - B_{\mathbf{k}}^2 + \frac{1}{2}(\alpha_+ - \Delta), \quad (\text{D61d})$$

where

$$\alpha_+ = \alpha_1 + \alpha_2, \quad \Delta = \sqrt{(\alpha_1 - \alpha_2)^2 + 4\beta_1^2}. \quad (\text{D62})$$

Finally, we use [Eq. \(D30\)](#) and [Eq. \(D31\)](#) to compute the quadrupole structure factor at the Γ -point given by [Eq. \(D56\)](#). When calculating [Eq. \(D30\)](#) and [Eq. \(D31\)](#), we use [Eq. \(D59\)](#) and [Eq. \(D61\)](#), and for the last term, we simply invert

[Eq. \(D57\)](#) and multiply by the vectors expressed in [Eq. \(D58\)](#). We obtain

$$S_Q^{\text{CL}}(\mathbf{q} = 0) = \frac{8}{\beta} \frac{1}{\omega_0^+} + \frac{8}{3} N - \frac{8}{\beta} \sum_{\mathbf{k}} \left[\frac{1}{\omega_{\mathbf{k}}^+} + \frac{1}{\omega_{\mathbf{k}}^-} \right] + \mathcal{O}(T^2). \quad (\text{D63})$$

However, we note that at the Γ -point, $\omega_0^+ = 0$. Therefore, in order to get rid of confounding divergent terms, we rewrite the quadrupole structure factor as

$$S_Q^{\text{CL}}(\mathbf{q} = 0) = -\frac{8}{\beta} \frac{1}{\omega_0^-} + \frac{8}{3} N - \frac{8}{\beta} \sum_{\mathbf{k} \neq 0} \left[\frac{1}{\omega_{\mathbf{k}}^+} + \frac{1}{\omega_{\mathbf{k}}^-} \right] + \mathcal{O}(T^2). \quad (\text{D64})$$

Because the $\mathbf{q} = 0$ contributions are coming from the ground state and happen for $\omega = 0$, the spectral representation of [Eq. \(D64\)](#) yields

$$S_Q^{\text{CL}}(\mathbf{q} = 0, \omega) = -\frac{8}{\beta} \frac{1}{\omega_0^-} \delta(\omega) + \frac{8}{3} N \delta(\omega) - \frac{8}{\beta} \sum_{\mathbf{k} \neq 0} \left[\frac{1}{\omega_{\mathbf{k}}^+} + \frac{1}{\omega_{\mathbf{k}}^-} \right] \delta(\omega) + \mathcal{O}(T^2). \quad (\text{D65})$$

Combining [Eq. \(D54\)](#) and [Eq. \(D64\)](#), we obtain [Eq. \(161\)](#). Considering their respective spectral representation given by [Eq. \(D55\)](#) and [Eq. \(D65\)](#), we obtain [Eq. \(163\)](#).

6. A-matrices: classical structure factor $\mathbf{q} \neq 0$

The matrix $\hat{\mathcal{A}}_{\beta}^{\alpha}$ is the most fundamental object describing the spins, and its structure factor is defined by

$$S_A^{\text{CL}}(\mathbf{q}) = \sum_{\alpha\beta} \langle \hat{\mathcal{A}}_{\mathbf{q}\beta}^{\alpha} \hat{\mathcal{A}}_{-\mathbf{q}\alpha}^{\beta} \rangle. \quad (\text{D66})$$

We note that the sum on the contracted indices α, β preserves the full $U(3)$ symmetry of the representation. The corresponding source term is

$$\Delta \mathcal{H}[\mathbf{h}_i] = - \sum_i h_{i,\beta}^{\alpha} \hat{\mathcal{A}}_{i\beta}^{\alpha}. \quad (\text{D67})$$

The components of the A matrix $\hat{\mathcal{A}}_{i\beta}^{\alpha}$ in the function of the classical fluctuations are given in [Eq. \(121\)](#). After expressing them in the function of the fluctuations that diagonalize the BBQ Hamiltonian [[Eq. \(145\)](#)], performing a Fourier transform, and rewriting the total Hamiltonian [[Eq. \(153\)](#)] according to [Eq. \(D15\)](#), we get

$$\tilde{C}[\mathbf{h}_{\mathbf{q}}] = \sqrt{N} h_{\mathbf{q}}^{yy}, \quad (\text{D68})$$

where we neglected 2nd order terms in fluctuations, since they only contribute for $\mathbf{q} = 0$,

$$\tilde{\mathbf{N}}_1[\mathbf{h}_{\mathbf{q}}]^T = \left(\frac{i\sqrt{2}}{2} \xi_{\mathbf{q}}^1, \frac{i\sqrt{2}}{2} \xi_{\mathbf{q}}^1, -\frac{i\sqrt{2}}{2} \xi_{\mathbf{q}}^2, -\frac{i\sqrt{2}}{2} \xi_{\mathbf{q}}^2 \right),$$

$$\tilde{\mathbf{N}}_2[\mathbf{h}_{-\mathbf{q}}] = \begin{pmatrix} \frac{i\sqrt{2}}{2} \xi_{-\mathbf{q}}^1 \\ \frac{i\sqrt{2}}{2} \xi_{-\mathbf{q}}^1 \\ -\frac{i\sqrt{2}}{2} \xi_{-\mathbf{q}}^2 \\ -\frac{i\sqrt{2}}{2} \xi_{-\mathbf{q}}^2 \end{pmatrix}, \quad (\text{D69})$$

where

$$\xi_{\mathbf{q}}^1 = (h_{\mathbf{q}}^{xy} + h_{\mathbf{q}}^{yx}) \quad , \quad \xi_{\mathbf{q}}^2 = (h_{\mathbf{q}}^{yz} + h_{\mathbf{q}}^{zy}) . \quad (\text{D70})$$

The total structure factor for A matrices is obtained by computing Eq. (D66). According to Eq. (D23), and Eq. (D22), and using Eq. (D69), we obtain

$$\begin{aligned} S_{\text{A}}^{\text{CL}}(\mathbf{q} \neq 0) &= \frac{1}{\beta\omega_{\mathbf{q},1}} + \frac{1}{\beta\omega_{\mathbf{q},2}} + \frac{1}{\beta\omega_{\mathbf{q},3}} + \frac{1}{\beta\omega_{\mathbf{q},4}} + \mathcal{O}(T^2) \\ &= \frac{2}{\beta\omega_{\mathbf{q}}^+} + \frac{2}{\beta\omega_{\mathbf{q}}^-} + \mathcal{O}(T^2) , \end{aligned} \quad (\text{D71})$$

where we used Eq. (140). It's spectral decomposition is given by

$$\begin{aligned} S_{\text{A}}^{\text{CL}}(\mathbf{q} \neq 0, \omega) &= \frac{2}{\beta\omega_{\mathbf{q}}^+} \delta(\omega - \omega_{\mathbf{q}}^+) + \frac{2}{\beta\omega_{\mathbf{q}}^-} \delta(\omega - \omega_{\mathbf{q}}^-) \\ &\quad + \mathcal{O}(T^2) . \end{aligned} \quad (\text{D72})$$

Again replacing the eigenvalues by their expressions given in Eq. (140), we have

$$\begin{aligned} S_{\text{A}}^{\text{CL}}(\mathbf{q} \neq 0, \omega) &= \frac{2}{\beta} \frac{1}{A_{\mathbf{q}} + B_{\mathbf{q}}} \delta(\omega - \omega_{\mathbf{q}}^+) \\ &\quad + \frac{2}{\beta} \frac{1}{A_{\mathbf{q}} - B_{\mathbf{q}}} \delta(\omega - \omega_{\mathbf{q}}^-) \\ &\quad + \mathcal{O}(T^2) . \end{aligned} \quad (\text{D73})$$

7. A-Matrices: classical structure factor at $\mathbf{q} = 0$

We now consider the structure factor for the A-matrix at the Γ -point, which is defined as

$$S_{\text{A}}^{\text{CL}}(\mathbf{q} = 0) = \sum_{\alpha\beta} \langle \hat{\mathcal{A}}_{\mathbf{q}=0}^{\alpha} \hat{\mathcal{A}}_{\mathbf{q}=0}^{\beta} \rangle . \quad (\text{D74})$$

Again, we follow the procedure depicted in Appendix D 1. The relevant source term for dipole moments is given by Eq. (D67). We use Eq. (127) for the BBQ Hamiltonian as well as Eq. (121) to express Eq. (D67) up to second order in terms of the fluctuations. For the total Hamiltonian given in Eq. (153), and written in the form of Eq. (D25), we obtain

$$M_{\mathbf{k}}[\mathbf{h}_{\mathbf{q}=0}] = \begin{pmatrix} A_{\mathbf{k}} - \alpha_1 & -B_{\mathbf{k}} & 0 & -\beta_1 \\ -B_{\mathbf{k}} & A_{\mathbf{k}} - \alpha_1 & -\beta_2 & 0 \\ 0 & -\beta_1 & A_{\mathbf{k}} - \alpha_2 & -B_{\mathbf{k}} \\ -\beta_2 & 0 & -B_{\mathbf{k}} & A_{\mathbf{k}} - \alpha_2 \end{pmatrix} , \quad (\text{D75})$$

$$\begin{aligned} \mathbf{N}_1[\mathbf{h}_{\mathbf{k}}]^T &= \frac{i}{2} (-h_{\mathbf{k},y}^x, h_{\mathbf{k},x}^y, h_{\mathbf{k},z}^y, -h_{\mathbf{k},y}^z) , \\ \mathbf{N}_2[\mathbf{h}_{-\mathbf{k}}] &= \frac{-i}{2} \begin{pmatrix} -h_{\mathbf{k},x}^y \\ h_{\mathbf{k},y}^x \\ h_{\mathbf{k},y}^z \\ -h_{\mathbf{k},z}^y \end{pmatrix} , \end{aligned} \quad (\text{D76})$$

$$C[\mathbf{h}_{\mathbf{q}=0}] = -\sqrt{N} h_{\mathbf{q}=0,y}^y , \quad (\text{D77})$$

where we defined

$$\begin{aligned} \alpha_1 &= \frac{1}{\sqrt{N}} (h_{\mathbf{q}=0,x}^x - h_{\mathbf{q}=0,y}^y) , \quad \alpha_2 = \frac{1}{\sqrt{N}} (h_{\mathbf{q}=0,z}^z - h_{\mathbf{q}=0,y}^y) , \\ \beta_1 &= \frac{1}{\sqrt{N}} h_{\mathbf{q}=0,x}^z , \quad \beta_2 = \frac{1}{\sqrt{N}} h_{\mathbf{q}=0,z}^x . \end{aligned} \quad (\text{D78})$$

We diagonalize Eq. (D57) to obtain the eigenmodes. We find

$$\omega_{\mathbf{k},1}[\mathbf{h}_{\mathbf{q}=0}] = A_{\mathbf{k}} - \frac{1}{2}(\alpha_+ - \Delta^-) , \quad (\text{D79a})$$

$$\omega_{\mathbf{k},2}[\mathbf{h}_{\mathbf{q}=0}] = A_{\mathbf{k}} - \frac{1}{2}(\alpha_+ + \Delta^-) , \quad (\text{D79b})$$

$$\omega_{\mathbf{k},3}[\mathbf{h}_{\mathbf{q}=0}] = A_{\mathbf{k}} - \frac{1}{2}(\alpha_+ - \Delta^+) , \quad (\text{D79c})$$

$$\omega_{\mathbf{k},4}[\mathbf{h}_{\mathbf{q}=0}] = A_{\mathbf{k}} - \frac{1}{2}(\alpha_+ + \Delta^+) , \quad (\text{D79d})$$

where

$$\begin{aligned} \alpha_+ &= \alpha_1 + \alpha_2 , \\ \Delta^- &= \sqrt{\alpha_-^2 + 4(B_{\mathbf{k}}^2 + \beta_1\beta_2 - \sqrt{B_{\mathbf{k}}^2(\alpha_-^2 + \beta_-^2)})} , \end{aligned} \quad (\text{D80})$$

$$\Delta^+ = \sqrt{\alpha_-^2 + 4(B_{\mathbf{k}}^2 + \beta_1\beta_2 + \sqrt{B_{\mathbf{k}}^2(\alpha_-^2 + \beta_-^2)})} ,$$

with

$$\begin{aligned} \alpha_- &= \alpha_1 - \alpha_2 , \\ \beta_- &= \beta_1 - \beta_2 . \end{aligned} \quad (\text{D81})$$

Finally, we use Eq. (D31) and Eq. (D30) to compute the structure factor for the A-matrix at the Γ -point given by Eq. (D74). When calculating Eq. (D31) and Eq. (D30), we use Eq. (D77) and Eq. (D79), and for the last term, we simply invert Eq. (D75) and multiply by the vectors in Eq. (D76).

$$\begin{aligned} S_{\text{A}}^{\text{CL}}(\mathbf{q} = 0) &= \frac{2}{\beta} \left[\frac{1}{\omega_0^+} + \frac{1}{\omega_0^-} \right] \\ &\quad + N - \frac{2}{\beta} \sum_{\mathbf{k}} \left[\frac{1}{\omega_{\mathbf{k}}^+} + \frac{1}{\omega_{\mathbf{k}}^-} \right] + \mathcal{O}(T^2) . \end{aligned} \quad (\text{D82})$$

Again, just as for the quadrupole structure factor, we note that at the Γ -point, $\omega_0^+ = 0$. Therefore, in order to get rid of confounding divergent terms, we rewrite the structure factor as

$$S_{\text{A}}^{\text{CL}}(\mathbf{q} = 0) = N - \frac{2}{\beta} \sum_{\mathbf{k} \neq 0} \left[\frac{1}{\omega_{\mathbf{k}}^+} + \frac{1}{\omega_{\mathbf{k}}^-} \right] + \mathcal{O}(T^2) . \quad (\text{D83})$$

Because the $\mathbf{q} = 0$ contributions are coming from the ground state and happen for $\omega = 0$, the spectral representation of Eq. (D83) yields

$$\begin{aligned} S_{\text{A}}^{\text{CL}}(\mathbf{q} = 0, \omega) &= N\delta(\omega) \\ &\quad - \frac{2}{\beta} \sum_{\mathbf{k} \neq 0} \left[\frac{1}{\omega_{\mathbf{k}}^+} + \frac{1}{\omega_{\mathbf{k}}^-} \right] \delta(\omega) + \mathcal{O}(T^2) . \end{aligned} \quad (\text{D84})$$

Combining Eq. (D71) and Eq. (D83), we obtain Eq. (165). Considering their respective spectral representation given by Eq. (D72) and Eq. (D84), we obtain Eq. (166).

Appendix E: Bogoliubov transformation

We here show how the Bogoliubov transformation that we present in [Section V](#) is performed.

A Bogoliubov transformation consists in finding new bosons $\hat{v}_{\mathbf{k}\alpha}^{\dagger}$ and $\hat{v}_{\mathbf{k}\alpha}$ expressed in terms of the bosons $\hat{w}_{\mathbf{k}}^{\dagger\alpha}$ and $\hat{w}_{\mathbf{k}\alpha}$ [[Eq. \(175\)](#)], such that they diagonalize the Hamiltonian

$$\mathcal{H}_{\text{BBQ}} \sim \sum_{\mathbf{k}} \epsilon_{\mathbf{k}} \hat{v}_{\mathbf{k}}^{\dagger} \hat{v}_{\mathbf{k}}. \quad (\text{E1})$$

Let us assume that the components are given by

$$\begin{aligned} \hat{v}_{\mathbf{k}\alpha} &= U_{\mathbf{k}\alpha}^{\beta} \hat{w}_{\mathbf{k}\beta}, \\ \hat{v}_{\mathbf{k}}^{\dagger\alpha} &= \hat{w}_{\mathbf{k}}^{\dagger\beta} U_{\mathbf{k}\beta}^{\alpha}, \end{aligned} \quad (\text{E2})$$

where $U_{\mathbf{k}}$ is the transformation from basis made out of bosons expressed by time-reversal basis states to the basis in which the Hamiltonian is diagonal. Requiring them to have bosonic commutation relations [[Eq. \(176\)](#)], leads to

$$\begin{aligned} [\hat{v}_{\mathbf{k}\alpha}, \hat{v}_{\mathbf{q}}^{\dagger\beta}] &= [U_{\mathbf{k}\alpha}^{\gamma} \hat{w}_{\mathbf{k}\gamma}, U_{\mathbf{q}}^{\dagger\beta} \hat{w}_{\mathbf{q}}^{\dagger\eta}] \\ &= U_{\mathbf{k}\alpha}^{\gamma} U_{\mathbf{q}}^{\dagger\beta} [\hat{w}_{\mathbf{k}\gamma}, \hat{w}_{\mathbf{q}}^{\dagger\eta}] \\ &= U_{\mathbf{k}\alpha}^{\gamma} U_{\mathbf{q}}^{\dagger\beta} \gamma_{0,\gamma}^{\eta} \delta_{\mathbf{k}\mathbf{q}} \stackrel{!}{=} \gamma_{0,\alpha}^{\beta} \delta_{\mathbf{k}\mathbf{q}} \\ \Rightarrow U_{\mathbf{k}\alpha}^{\gamma} \gamma_{0,\gamma}^{\eta} U_{\mathbf{k}\eta}^{\beta} &= \gamma_{0,\alpha}^{\beta} \\ \Rightarrow \gamma_{0,\gamma}^{\eta} U_{\mathbf{k}\eta}^{\dagger\beta} \gamma_{0,\beta}^{\alpha} &= U_{\mathbf{k}}^{-1}{}_{\gamma}^{\alpha}, \end{aligned} \quad (\text{E3})$$

where γ_0 is defined in [Eq. \(177\)](#), and where we used the fact that

$$\gamma_0 = \gamma_0^{-1}. \quad (\text{E4})$$

In the compact form, [Eq. \(E3\)](#) becomes

$$\gamma_0 U_{\mathbf{k}}^{\dagger} \gamma_0 = U_{\mathbf{k}}^{-1}. \quad (\text{E5})$$

We see that the transformation $U_{\mathbf{k}}$ is not unitary, $U_{\mathbf{k}}^{-1} \neq U_{\mathbf{k}}^{\dagger}$, and that we shall use [Eq. \(E5\)](#) to find the inverse transformation.

Inverting [Eq. \(E2\)](#) and plugging it into the Hamiltonian leads us to look for a transformation $U_{\mathbf{k}}$ such that $U_{\mathbf{k}} \gamma_0 M_{\mathbf{k}} U_{\mathbf{k}}^{-1}$ is diagonal. If we define $D_{\mathbf{k}}$ as being a diagonal matrix, we can write

$$\begin{aligned} U_{\mathbf{k}} \gamma_0 M_{\mathbf{k}} U_{\mathbf{k}}^{-1} &= D_{\mathbf{k}} \\ \Rightarrow \gamma_{0,\nu}^{\alpha} M_{\mathbf{k}\alpha}^{\beta} U_{\mathbf{k}}^{-1}{}_{\beta}^{\nu} &= U_{\mathbf{k}}^{-1}{}_{\nu}^i D_{\mathbf{k}i} \text{ for } i = 1, 2, 3, 4, \end{aligned} \quad (\text{E6})$$

where we see that $U_{\mathbf{k}}^{-1}{}_{\nu}^i$ is an eigenvector of $\gamma_0 M_{\mathbf{k}}$ with eigenvalue $D_{\mathbf{k}i}$. [Eq. \(E6\)](#) is rewritten as [Eq. \(178\)](#) in the main text. This means that we need to diagonalize $\gamma_0 M_{\mathbf{k}}$ and that the corresponding eigenvectors are the column of the matrix $U_{\mathbf{k}}^{-1}$.

Finding the Bogoliubov transformation reduces then to find the eigenvalues and eigenvectors of the system in [Eq. \(178\)](#). Since [Eq. \(178\)](#) consists of twice the same system, we only need to solve it once, and we only consider

$$\sigma_z m_{\mathbf{k}} e_i = \epsilon_{\mathbf{k},i} e_i \quad i = 1, 2, \quad (\text{E7})$$

where

$$\sigma_z = \begin{pmatrix} 1 & 0 \\ 0 & -1 \end{pmatrix}, \quad m_{\mathbf{k}} = \begin{pmatrix} A_{\mathbf{k}} & -B_{\mathbf{k}} \\ B_{\mathbf{k}} & -A_{\mathbf{k}} \end{pmatrix}, \quad (\text{E8})$$

and where σ_z plays the role of γ_0 but for the two independent subsystems for $(\hat{a}_{-\mathbf{k}}, \hat{a}_{\mathbf{k}}^{\dagger})$ and $(\hat{b}_{-\mathbf{k}}, \hat{b}_{\mathbf{k}}^{\dagger})$. The eigenvalues $\epsilon_{\mathbf{k},1/2}$ of $\sigma_z m_{\mathbf{k}}$ are given in [Eq. \(180\)](#). The eigenvectors are given by

$$e_1 = \begin{pmatrix} \alpha_1 \\ 1 \end{pmatrix}, \quad e_2 = \begin{pmatrix} \alpha_2 \\ 1 \end{pmatrix}, \quad (\text{E9})$$

in the basis $\{\hat{a}_{\mathbf{k}}, \hat{a}_{-\mathbf{k}}^{\dagger}\}$ and where we define

$$\alpha_i = -\frac{A_{\mathbf{k}} + \epsilon_{\mathbf{k},i}}{B_{\mathbf{k}}}. \quad (\text{E10})$$

The columns of the matrix $U_{\mathbf{k}}^{-1}$ are given by the eigenvectors

$$U_{\mathbf{k}}^{-1} = \begin{pmatrix} \alpha_1 & \alpha_2 \\ 1 & 1 \end{pmatrix}. \quad (\text{E11})$$

Using [Eq. \(E5\)](#), we can calculate $U_{\mathbf{k}}$ as follows:

$$U_{\mathbf{k}} = \sigma_z U_{\mathbf{k}}^{\dagger-1} \sigma_z = \begin{pmatrix} \alpha_1 & -1 \\ -\alpha_2 & 1 \end{pmatrix}. \quad (\text{E12})$$

Using [Eq. \(E2\)](#), the new bosons that diagonalize the Hamiltonian are given by

$$\hat{\alpha}_{\mathbf{k}} = \hat{v}_{\mathbf{k}1} = U_{\mathbf{k}1}^1 \hat{w}_{\mathbf{k}1} + U_{\mathbf{k}1}^2 \hat{w}_{\mathbf{k}2} = \alpha_1 \hat{a}_{\mathbf{k}} - \hat{a}_{-\mathbf{k}}^{\dagger}, \quad (\text{E13a})$$

$$\hat{\alpha}_{-\mathbf{k}}^{\dagger} = \hat{v}_{\mathbf{k}2} = U_{\mathbf{k}2}^1 \hat{w}_{\mathbf{k}1} + U_{\mathbf{k}2}^2 \hat{w}_{\mathbf{k}2} = -\alpha_2 \hat{a}_{\mathbf{k}} + \hat{a}_{-\mathbf{k}}^{\dagger}, \quad (\text{E13b})$$

$$\hat{\alpha}_{\mathbf{k}}^{\dagger} = \hat{v}_{\mathbf{k}}^{\dagger 1} = \hat{w}_{\mathbf{k}}^{\dagger 1} U_{\mathbf{k}1}^{\dagger 1} + \hat{w}_{\mathbf{k}}^{\dagger 2} U_{\mathbf{k}2}^{\dagger 1} = \alpha_1 \hat{a}_{\mathbf{k}}^{\dagger} - \hat{a}_{-\mathbf{k}}, \quad (\text{E13c})$$

$$\hat{\alpha}_{-\mathbf{k}} = \hat{v}_{\mathbf{k}}^{\dagger 2} = \hat{w}_{\mathbf{k}}^{\dagger 1} U_{\mathbf{k}1}^{\dagger 2} + \hat{w}_{\mathbf{k}}^{\dagger 2} U_{\mathbf{k}2}^{\dagger 2} = -\alpha_2 \hat{a}_{\mathbf{k}}^{\dagger} + \hat{a}_{-\mathbf{k}}. \quad (\text{E13d})$$

For instance, we note that we should have $\hat{v}_{\mathbf{k}1} = \hat{v}_{-\mathbf{k}}^{\dagger 2}$ i.e $\hat{\alpha}_{\mathbf{k}}(\mathbf{k}) = \hat{\alpha}_{-\mathbf{k}}(-\mathbf{k})$. However, we see that it is not the case

$$\hat{v}_{\mathbf{k}1} = \alpha_1 \hat{a}_{\mathbf{k}} - \hat{a}_{-\mathbf{k}}^{\dagger} \neq -\alpha_2 \hat{a}_{-\mathbf{k}}^{\dagger} + \hat{a}_{\mathbf{k}} = \hat{v}_{-\mathbf{k}}^{\dagger 2}. \quad (\text{E14})$$

For it to be the case, we see that we need the matrix element of the transformation to be

$$U_{\mathbf{k}1}^1 = U_{-\mathbf{k}2}^{\dagger 2}, \quad (\text{E15a})$$

$$U_{\mathbf{k}1}^2 = U_{-\mathbf{k}1}^{\dagger 2}. \quad (\text{E15b})$$

To solve this issue, we can assume that we can multiply the eigenvectors by some parameters, a and b for instance, such that [Eq. \(E15\)](#) is satisfied

$$e_1 = a \begin{pmatrix} \alpha_1 \\ 1 \end{pmatrix}, \quad e_2 = b \begin{pmatrix} \alpha_2 \\ 1 \end{pmatrix}. \quad (\text{E16})$$

And $U_{\mathbf{k}}^{-1}$ is given by

$$U_{\mathbf{k}}^{-1} = \begin{pmatrix} a\alpha_1 & b\alpha_2 \\ a & b \end{pmatrix}. \quad (\text{E17})$$

Using Eq. (E5), we can calculate $U_{\mathbf{k}}$ as follows:

$$U_{\mathbf{k}} = \sigma_z U_{\mathbf{k}}^{\dagger-1} \sigma_z = \begin{pmatrix} a\alpha_1 & -a \\ -b\alpha_2 & b \end{pmatrix}. \quad (\text{E18})$$

We also have

$$U_{\mathbf{k}}^{\dagger} = \begin{pmatrix} a\alpha_1 & -b\alpha_2 \\ -a & b \end{pmatrix}. \quad (\text{E19})$$

Note that the coefficients α_1 and α_2 depend on \mathbf{k} through $\epsilon_{\mathbf{k}}$. However we have $\epsilon_{\mathbf{k}} = \epsilon_{-\mathbf{k}}$ and the dependency in \mathbf{k} for α_1 and α_2 has been dropped. Eq. (E15) implies then

$$\begin{aligned} U_{\mathbf{k}_1}^1 &= U_{-\mathbf{k}_2}^{\dagger 2}, \\ a\alpha_1 &= b, \\ a \frac{-A_{\mathbf{k}} - \sqrt{A_{\mathbf{k}}^2 - B_{\mathbf{k}}^2}}{B_{\mathbf{k}}} &= b, \\ \frac{a}{-B_{\mathbf{k}}} &= \frac{b}{A_{\mathbf{k}} + \sqrt{A_{\mathbf{k}}^2 - B_{\mathbf{k}}^2}}, \end{aligned} \quad (\text{E20a})$$

and

$$\begin{aligned} U_{\mathbf{k}_1}^2 &= U_{-\mathbf{k}_1}^{\dagger 2}, \\ -b\alpha_2 &= -a, \\ -b \frac{-A_{\mathbf{k}} + \sqrt{A_{\mathbf{k}}^2 - B_{\mathbf{k}}^2}}{B_{\mathbf{k}}} &= -a, \\ \frac{b}{-B_{\mathbf{k}}} &= \frac{-a}{-A_{\mathbf{k}} + \sqrt{A_{\mathbf{k}}^2 - B_{\mathbf{k}}^2}}. \end{aligned} \quad (\text{E20b})$$

We see that if we multiply the last line of Eq. (E20b) by $\frac{-B_{\mathbf{k}}}{A_{\mathbf{k}} + \sqrt{A_{\mathbf{k}}^2 - B_{\mathbf{k}}^2}}$ we get

$$\begin{aligned} \frac{-B_{\mathbf{k}}}{A_{\mathbf{k}} + \sqrt{A_{\mathbf{k}}^2 - B_{\mathbf{k}}^2}} \frac{b}{-B_{\mathbf{k}}} &= \frac{-B_{\mathbf{k}}}{A_{\mathbf{k}} + \sqrt{A_{\mathbf{k}}^2 - B_{\mathbf{k}}^2}} \frac{-a}{-A_{\mathbf{k}} + \sqrt{A_{\mathbf{k}}^2 - B_{\mathbf{k}}^2}}, \end{aligned} \quad (\text{E21a})$$

$$\Rightarrow \frac{b}{A_{\mathbf{k}} + \sqrt{A_{\mathbf{k}}^2 - B_{\mathbf{k}}^2}} = \frac{a}{-B_{\mathbf{k}}}. \quad (\text{E21b})$$

We note that Eq. (E21b) is exactly the same condition as in the last line of Eq. (E20a). This makes sense, because the 1st condition, namely $U_{\mathbf{k}_1}^1 = U_{-\mathbf{k}_2}^{\dagger 2}$ is correlated the the second one $U_{\mathbf{k}_1}^2 = U_{-\mathbf{k}_1}^{\dagger 2}$, as the components $U_{\mathbf{k}_1}^1$, $U_{\mathbf{k}_1}^2$ are not independent, as they need to be eigenvectors, and nor are the components $U_{-\mathbf{k}_2}^{\dagger 2}$, $U_{-\mathbf{k}_1}^{\dagger 2}$. We could also choose the 2nd solution, as up to scalar multiplication, it gives the same eigenvectors. By normalizing the eigenvectors, we then get rid of this. This means, for instance, that we can choose

$$a = -B_{\mathbf{k}}, \quad (\text{E22})$$

$$b = A_{\mathbf{k}} + \sqrt{A_{\mathbf{k}}^2 - B_{\mathbf{k}}^2}. \quad (\text{E23})$$

In this case, the eigenvectors become

$$e_1 = \begin{pmatrix} \Delta_{\mathbf{k}} \\ -B_{\mathbf{k}} \end{pmatrix}, \quad e_2 = \begin{pmatrix} -B_{\mathbf{k}} \\ \Delta_{\mathbf{k}} \end{pmatrix}, \quad (\text{E24})$$

where $\Delta_{\mathbf{k}}$ is given Eq. (183). And the transformation matrix becomes

$$U_{\mathbf{k}}^{-1} = \begin{pmatrix} \Delta_{\mathbf{k}} & -B_{\mathbf{k}} \\ -B_{\mathbf{k}} & \Delta_{\mathbf{k}} \end{pmatrix}. \quad (\text{E25})$$

Using Eq. (E5), we can calculate $U_{\mathbf{k}}$ as follows:

$$U_{\mathbf{k}} = \sigma_z U_{\mathbf{k}}^{\dagger-1} \sigma_z = \begin{pmatrix} \Delta_{\mathbf{k}} & B_{\mathbf{k}} \\ B_{\mathbf{k}} & \Delta_{\mathbf{k}} \end{pmatrix}. \quad (\text{E26})$$

We also have

$$U_{\mathbf{k}}^{\dagger} = \begin{pmatrix} \Delta_{\mathbf{k}} & B_{\mathbf{k}} \\ B_{\mathbf{k}} & \Delta_{\mathbf{k}} \end{pmatrix}. \quad (\text{E27})$$

Using Eq. (E2), the new bosons that diagonalize the Hamiltonian are given by

$$\hat{\alpha}_{\mathbf{k}} = \hat{v}_{\mathbf{k}_1} = U_{\mathbf{k}_1}^{-1} \hat{w}_{\mathbf{k}_1} + U_{\mathbf{k}_1}^2 \hat{w}_{\mathbf{k}_2} = \Delta_{\mathbf{k}} \hat{a}_{\mathbf{k}} + B_{\mathbf{k}} \hat{a}_{-\mathbf{k}}^{\dagger}, \quad (\text{E28a})$$

$$\hat{\alpha}_{-\mathbf{k}}^{\dagger} = \hat{v}_{\mathbf{k}_2} = U_{\mathbf{k}_2}^{-1} \hat{w}_{\mathbf{k}_1} + U_{\mathbf{k}_2}^2 \hat{w}_{\mathbf{k}_2} = B_{\mathbf{k}} \hat{a}_{\mathbf{k}} + \Delta_{\mathbf{k}} \hat{a}_{-\mathbf{k}}^{\dagger}, \quad (\text{E28b})$$

$$\hat{\alpha}_{\mathbf{k}}^{\dagger} = \hat{v}_{\mathbf{k}}^{\dagger 1} = \hat{w}_{\mathbf{k}}^{\dagger 1} U_{\mathbf{k}_1}^{\dagger 1} + \hat{w}_{\mathbf{k}}^{\dagger 2} U_{\mathbf{k}_2}^{\dagger 1} = \Delta_{\mathbf{k}} \hat{a}_{\mathbf{k}}^{\dagger} + B_{\mathbf{k}} \hat{a}_{-\mathbf{k}}, \quad (\text{E28c})$$

$$\hat{\alpha}_{-\mathbf{k}} = \hat{v}_{\mathbf{k}}^{\dagger 2} = \hat{w}_{\mathbf{k}}^{\dagger 1} U_{\mathbf{k}_1}^{\dagger 2} + \hat{w}_{\mathbf{k}}^{\dagger 2} U_{\mathbf{k}_2}^{\dagger 2} = B_{\mathbf{k}} \hat{a}_{\mathbf{k}}^{\dagger} + \Delta_{\mathbf{k}} \hat{a}_{-\mathbf{k}}. \quad (\text{E28d})$$

We see that now we indeed have $\hat{v}_{\mathbf{k}_1} = \hat{v}_{-\mathbf{k}}^{\dagger 2}$, i.e., $\hat{\alpha}_{\mathbf{k}}(\mathbf{k}) = \hat{\alpha}_{-\mathbf{k}}(-\mathbf{k})$. However, we still need to normalize the new bosons. Indeed they should also satisfy bosonic commutation relations

$$\begin{aligned} [\hat{\alpha}_{\mathbf{k}}, \hat{\alpha}_{\mathbf{k}}^{\dagger}] &= \left[\frac{1}{\sqrt{N}} (\Delta_{\mathbf{k}} \hat{a}_{\mathbf{k}} + B_{\mathbf{k}} \hat{a}_{-\mathbf{k}}^{\dagger}), \frac{1}{\sqrt{N}} (\Delta_{\mathbf{k}} \hat{a}_{\mathbf{k}}^{\dagger} + B_{\mathbf{k}} \hat{a}_{-\mathbf{k}}) \right] \\ &= \frac{1}{N} (\Delta_{\mathbf{k}}^2 [\hat{a}_{\mathbf{k}}, \hat{a}_{\mathbf{k}}^{\dagger}] + B_{\mathbf{k}}^2 [\hat{a}_{-\mathbf{k}}^{\dagger}, \hat{a}_{-\mathbf{k}}]) \\ &= \frac{1}{N} (\Delta_{\mathbf{k}}^2 - B_{\mathbf{k}}^2) \stackrel{!}{=} 1 \end{aligned} \quad (\text{E29a})$$

$$\Rightarrow N = \Delta_{\mathbf{k}}^2 - B_{\mathbf{k}}^2. \quad (\text{E29b})$$

Finally, the transformation matrix becomes

$$U_{\mathbf{k}} = \frac{1}{\sqrt{\Delta_{\mathbf{k}}^2 - B_{\mathbf{k}}^2}} \begin{pmatrix} \Delta_{\mathbf{k}} & B_{\mathbf{k}} \\ B_{\mathbf{k}} & \Delta_{\mathbf{k}} \end{pmatrix}. \quad (\text{E30})$$

The inverse [Eq. (E5)] holds

$$U_{\mathbf{k}}^{-1} = \sigma_z U_{\mathbf{k}}^{\dagger} \sigma_z = \frac{1}{\sqrt{\Delta_{\mathbf{k}}^2 - B_{\mathbf{k}}^2}} \begin{pmatrix} \Delta_{\mathbf{k}} & -B_{\mathbf{k}} \\ -B_{\mathbf{k}} & \Delta_{\mathbf{k}} \end{pmatrix}. \quad (\text{E31})$$

By inverting the Bogolubov transformation [Eq. (E2)], we can express the old bosons in terms of the new Bogolubov bosons

using Eq. (E31),

$$\hat{a}_{\mathbf{k}} = \hat{w}_{\mathbf{k}1} = U_{\mathbf{k}}^{-1} \hat{v}_{\mathbf{k}\beta} = \frac{1}{\sqrt{\Delta_{\mathbf{k}}^2 - B_{\mathbf{k}}^2}} (\Delta_{\mathbf{k}} \hat{a}_{\mathbf{k}} - B_{\mathbf{k}} \hat{a}_{-\mathbf{k}}^\dagger), \quad (\text{E32a})$$

$$\hat{a}_{-\mathbf{k}}^\dagger = \hat{w}_{\mathbf{k}2} = U_{\mathbf{k}}^{-1} \hat{v}_{\mathbf{k}\beta} = \frac{1}{\sqrt{\Delta_{\mathbf{k}}^2 - B_{\mathbf{k}}^2}} (-B_{\mathbf{k}} \hat{a}_{\mathbf{k}} + \Delta_{\mathbf{k}} \hat{a}_{-\mathbf{k}}^\dagger), \quad (\text{E32b})$$

$$\hat{a}_{\mathbf{k}}^\dagger = \hat{w}_{\mathbf{k}}^{\dagger 1} = \hat{v}_{\mathbf{k}}^{\dagger\beta} U_{\mathbf{k}}^{\dagger-1} = \frac{1}{\sqrt{\Delta_{\mathbf{k}}^2 - B_{\mathbf{k}}^2}} (\Delta_{\mathbf{k}} \hat{a}_{\mathbf{k}}^\dagger - B_{\mathbf{k}} \hat{a}_{-\mathbf{k}}), \quad (\text{E32c})$$

$$\hat{a}_{-\mathbf{k}} = \hat{w}_{\mathbf{k}}^{\dagger 2} = \hat{v}_{\mathbf{k}}^{\dagger\beta} U_{\mathbf{k}}^{\dagger-1} = \frac{1}{\sqrt{\Delta_{\mathbf{k}}^2 - B_{\mathbf{k}}^2}} (-B_{\mathbf{k}} \hat{a}_{\mathbf{k}}^\dagger + \Delta_{\mathbf{k}} \hat{a}_{-\mathbf{k}}). \quad (\text{E32d})$$

For the other part of the Hamiltonian containing the \hat{b}^\dagger bosons, the problem is exactly the same, and therefore, we can just use the solutions we found above. The eigenvalues $\epsilon_{\mathbf{k},3}$ and $\epsilon_{\mathbf{k},4}$ associated to the Bogolubov bosons for the $(\hat{b}_{-\mathbf{k}}, \hat{b}_{\mathbf{k}}^\dagger)$ subsystem are given by Eq. (180). To express the old bosons in terms of the new Bogolubov bosons, we can just use Eq. (E32):

$$\hat{b}_{\mathbf{k}} = \frac{1}{\sqrt{\Delta_{\mathbf{k}}^2 - B_{\mathbf{k}}^2}} (\Delta_{\mathbf{k}} \hat{b}_{\mathbf{k}} - B_{\mathbf{k}} \hat{b}_{-\mathbf{k}}^\dagger), \quad (\text{E33a})$$

$$\hat{b}_{-\mathbf{k}}^\dagger = \frac{1}{\sqrt{\Delta_{\mathbf{k}}^2 - B_{\mathbf{k}}^2}} (-B_{\mathbf{k}} \hat{b}_{\mathbf{k}} + \Delta_{\mathbf{k}} \hat{b}_{-\mathbf{k}}^\dagger), \quad (\text{E33b})$$

$$\hat{b}_{\mathbf{k}}^\dagger = \frac{1}{\sqrt{\Delta_{\mathbf{k}}^2 - B_{\mathbf{k}}^2}} (\Delta_{\mathbf{k}} \hat{b}_{\mathbf{k}}^\dagger - B_{\mathbf{k}} \hat{b}_{-\mathbf{k}}), \quad (\text{E33c})$$

$$\hat{b}_{-\mathbf{k}} = \frac{1}{\sqrt{\Delta_{\mathbf{k}}^2 - B_{\mathbf{k}}^2}} (-B_{\mathbf{k}} \hat{b}_{\mathbf{k}}^\dagger + \Delta_{\mathbf{k}} \hat{b}_{-\mathbf{k}}). \quad (\text{E33d})$$

There is a constant term coming from the Bogolubov transformation [Eq. (E32) and Eq. (E33)]. For the bosons $\hat{a}_{\pm\mathbf{k}}^\dagger, \hat{a}_{\pm\mathbf{k}}$ it holds:

$$-A_{\mathbf{k}} + \sqrt{A_{\mathbf{k}}^2 - B_{\mathbf{k}}^2} = -A_{\mathbf{k}} + \epsilon_{\mathbf{k},1}, \quad (\text{E34a})$$

and for the bosons $\hat{b}_{\pm\mathbf{k}}^\dagger, \hat{b}_{\pm\mathbf{k}}$:

$$-A_{\mathbf{k}} + \sqrt{A_{\mathbf{k}}^2 - B_{\mathbf{k}}^2} = -A_{\mathbf{k}} + \epsilon_{\mathbf{k},3}, \quad (\text{E34b})$$

where we use Eq. (180).

After performing the Bogolubov transformation, the Hamiltonian becomes

$$\mathcal{H} = E_0 + \frac{1}{2} \left[\sum_{\mathbf{k}} \epsilon_{\mathbf{k},1} \hat{a}_{\mathbf{k}}^\dagger \hat{a}_{\mathbf{k}} + \epsilon_{\mathbf{k},1} \hat{a}_{-\mathbf{k}}^\dagger \hat{a}_{-\mathbf{k}} - A_{\mathbf{k}} + \epsilon_{\mathbf{k},1} \right] + \epsilon_{\mathbf{k},3} \hat{\beta}_{\mathbf{k}}^\dagger \hat{\beta}_{\mathbf{k}} + \epsilon_{\mathbf{k},3} \hat{\beta}_{-\mathbf{k}}^\dagger \hat{\beta}_{-\mathbf{k}} - A_{\mathbf{k}} + \epsilon_{\mathbf{k},3}, \quad (\text{E35})$$

that we can rewrite as

$$\mathcal{H} = E_0 + \left[\sum_{\mathbf{k}} \epsilon_{\mathbf{k},1} \left(\hat{a}_{\mathbf{k}}^\dagger \hat{a}_{\mathbf{k}} + \frac{1}{2} \right) + \epsilon_{\mathbf{k},3} \left(\hat{\beta}_{\mathbf{k}}^\dagger \hat{\beta}_{\mathbf{k}} + \frac{1}{2} \right) - A_{\mathbf{k}} \right], \quad (\text{E36})$$

where E_0 is given in Eq. (125). Eq. (E36) is given in the main text by Eq. (184), where we used the fact that $\epsilon_{\mathbf{k},1} = \epsilon_{\mathbf{k},3}$ [Eq. (180)], since they are the eigenvalues of an identical problem.

Appendix F: Dynamical structure factors within zero-temperature quantum theory

In this Appendix, we present the outline of the method used to calculate the zero-temperature quantum structure factors in Section V B.

In Appendix F 1, we first present how to calculate dynamical structure factors at finite energy through the explicit calculation of matrix elements within a multiple-Boson expansion, and its application to dipole [Appendix F 2], quadrupole [Appendix F 3], and A-matrix moments [Appendix F 4].

In Appendix F 5, we explain how the calculation for the static structure factors ($\omega = 0$) can also be computed through functional derivatives of the ground-state energy, in order to account for the ground-state and zero-point energy contribution at $\mathbf{q} = 0$. We show calculations for the dipole [Appendix F 6], quadrupole [Appendix F 7], and A-matrix moments [Appendix F 8].

1. Quantum structure factors at general values of \mathbf{q}

The definition of the structure factor is given by Eq. (187) and its components by

$$S_{\mathbf{O}}^{\text{QM}}(\mathbf{q}, \omega)_{\beta\nu}^{\alpha\mu} = \int_{-\infty}^{\infty} \frac{dt}{2\pi} e^{i\omega t} \langle \hat{O}_{\mathbf{q},\beta}^\alpha(t) \hat{O}_{-\mathbf{q},\nu}^\mu(0) \rangle. \quad (\text{F1})$$

where in our case, the averages $\langle \hat{O}_{\mathbf{q},\beta}^\alpha(t) \hat{O}_{-\mathbf{q},\nu}^\mu(0) \rangle$ are taken on the ground state. We can rewrite the time dependency of $\hat{O}_{\mathbf{q},\beta}^\alpha(t)$ in the Heisenberg picture using the time evolution operator, and we obtain

$$\hat{O}_{\mathbf{q},\beta}^\alpha(t) = e^{\frac{i\hat{H}t}{\hbar}} \hat{O}_{\mathbf{q},\beta}^\alpha(0) e^{-\frac{i\hat{H}t}{\hbar}}. \quad (\text{F2})$$

For a complete basis $\{|\nu\rangle\}$ of Hilbert space, the closure relation holds

$$\sum_{\nu} |\nu\rangle \langle \nu| = 1. \quad (\text{F3})$$

By using Eq. (F2) and inserting the closure relation, Eq. (F3) twice in Eq. (F1), we get

$$\begin{aligned} S_{\mathbf{O},\beta\mu}^{\alpha\mu}(\mathbf{q}, \omega) &= \int_{-\infty}^{\infty} \frac{dt}{2\pi} e^{i\omega t} \langle e^{\frac{i\hat{H}t}{\hbar}} \sum_{\nu} |\nu\rangle \langle \nu| \hat{O}_{\mathbf{q},\beta}^\alpha(0) \sum_{\mu} |\mu\rangle \\ &\times \langle \mu| e^{-\frac{i\hat{H}t}{\hbar}} \hat{O}_{-\mathbf{q},\nu}^\mu(0) \rangle + S_{\mathbf{O}}^{\text{GS}}(\mathbf{q} = 0, \omega) \\ &= \sum_{\mu} \langle 0| \hat{O}_{\mathbf{q},\beta}^\alpha(0) |\mu\rangle \langle \mu| \hat{O}_{-\mathbf{q},\nu}^\mu(0) |0\rangle \delta(\omega - \epsilon_{\mu}) \\ &+ S_{\mathbf{O}}^{\text{GS}}(\mathbf{q} = 0, \omega), \end{aligned} \quad (\text{F4})$$

where we assumed that $|\nu\rangle$ is an eigenstate of the Hamiltonian of energy $E_\nu = \hbar\epsilon_\nu$ and used

$$\begin{aligned} e^{\frac{i\hat{H}t}{\hbar}}|\nu\rangle &= \sum_{n=0}^{\infty} \frac{(i\hat{H}t)^n}{n} |\nu\rangle = \sum_{n=0}^{\infty} \frac{(iE_\nu t)^n}{n} |\nu\rangle \\ &= e^{\frac{iE_\nu t}{\hbar}} |\nu\rangle = e^{i\epsilon_\nu t} |\nu\rangle, \end{aligned} \quad (\text{F5})$$

and where $S_O^{\text{GS}}(\mathbf{q} = 0, \omega)$ represents the ground state and zero-point energy contribution to the structure factor, as explained below.

In order to compute Eq. (F4), we first note that, in our case, the excited states, for all values of \mathbf{k}

$$|\alpha_{\mathbf{k}}\rangle = \hat{\alpha}_{\mathbf{k}}^\dagger |0_\alpha\rangle, \quad (\text{F6})$$

$$|\beta_{\mathbf{k}}\rangle = \hat{\beta}_{\mathbf{k}}^\dagger |0_\beta\rangle, \quad (\text{F7})$$

form a complete basis, where $|0_\alpha\rangle$ is the Bogoliubov ground state for the $\hat{\alpha}$ bosons, i.e., $\hat{\alpha}_{\mathbf{k}}|0_\alpha\rangle = 0$, and similarly for the $\hat{\beta}$ bosons. Since the Hilbert space consists of the direct product $|\alpha\rangle \oplus |\beta\rangle$, we can replace

$$\sum_{\mu} |\mu\rangle\langle\mu| \rightarrow \sum_{\mathbf{k}} \hat{\alpha}_{\mathbf{k}}^\dagger |0_\alpha\rangle\langle 0_\alpha| \hat{\alpha}_{\mathbf{k}} + \sum_{\mathbf{k}} \hat{\beta}_{\mathbf{k}}^\dagger |0_\beta\rangle\langle 0_\beta| \hat{\beta}_{\mathbf{k}} = 1. \quad (\text{F8})$$

in Eq. (F4). However, by replacing Eq. (F3) by Eq. (F8) in Eq. (F4), we account for the 1st excited states and we therefore disregard the ground state and zero-point energy contribution to the structure factor, which is expressed by the term $S_O^{\text{GS}}(\mathbf{q} = 0, \omega)$ in Eq. (F4). The ground state and zero-point energy only contribute at $\mathbf{q} = 0$ and $\omega = 0$. We present how to calculate it below in Appendix F5.

2. Dipole moments: quantum structure factor at general values of \mathbf{q}

We consider first the dynamical spin structure factor

$$S_S^{\text{QM}}(\mathbf{q}, \omega) = \int_{-\infty}^{\infty} \frac{dt}{2\pi} e^{i\omega t} \sum_{\mu} \langle \hat{S}_{\mathbf{q}}^{\mu}(t) \hat{S}_{-\mathbf{q}}^{\mu}(0) \rangle. \quad (\text{F9})$$

Substituting Eq. (173) in the expression for spin operators, Eq. (50), and keeping terms to linear order, we find

$$\hat{S}_i^x \simeq i(\hat{b}_i^\dagger - \hat{b}_i), \quad (\text{F10a})$$

$$\hat{S}_i^y \simeq 0, \quad (\text{F10b})$$

$$\hat{S}_i^z \simeq -i(\hat{a}_i^\dagger - \hat{a}_i). \quad (\text{F10c})$$

Performing a Fourier transform and using the Bogoliubov transformation Eq. (182), we can express these as

$$\hat{S}_{\mathbf{q}}^x \simeq i\xi_S(\mathbf{q})(\hat{\beta}_{-\mathbf{q}}^\dagger - \hat{\beta}_{\mathbf{q}}), \quad (\text{F11a})$$

$$\hat{S}_{\mathbf{q}}^y \simeq 0, \quad (\text{F11b})$$

$$\hat{S}_{\mathbf{q}}^z \simeq -i\xi_S(\mathbf{q})(\hat{\alpha}_{-\mathbf{q}}^\dagger - \hat{\alpha}_{\mathbf{q}}), \quad (\text{F11c})$$

where $\xi(\mathbf{q})$ is the coherence factor

$$\xi_S(\mathbf{q}) = \frac{\Delta_{\mathbf{q}} + B_{\mathbf{q}}}{\sqrt{\Delta_{\mathbf{q}}^2 - B_{\mathbf{q}}^2}}. \quad (\text{F12})$$

Using Eq. (F4), we can then calculate the structure factor for dipole moments as

$$S_S^{\text{QM}}(\mathbf{q}, \omega) = \sum_{\mu, \mathbf{k}} \left| \langle n_{\mathbf{k}} | \hat{S}_{\mathbf{q}}^{\mu} | 0 \rangle \right|^2 \delta(\omega - \omega_{n_{\mathbf{k}}}) + S_S^{\text{GS}}(\mathbf{q} = 0, \omega), \quad (\text{F13})$$

where $|0\rangle$ is the FQ ground state [Eq. (114)], and

$$|n_{\mathbf{k}}\rangle = \hat{\alpha}_{\mathbf{k}}^\dagger |0\rangle \otimes \hat{\beta}_{\mathbf{k}}^\dagger |0\rangle. \quad (\text{F14})$$

represents the first excited states where \otimes implies a direct product, as the bosons $\hat{\alpha}_{\mathbf{q}}^\dagger$ and $\hat{\beta}_{\mathbf{q}}^\dagger$ are independent. By using Eq. (F14), we account for the 1st excited states and we therefore disregard the ground state and zero-point energy contribution to the structure factor which is expressed by the term $S_O^{\text{GS}}(\mathbf{q} = 0, \omega)$ in Eq. (F13).

Finally, we find

$$S_S^{\text{QM}}(\mathbf{q}, \omega) = 2 \frac{\sqrt{A_{\mathbf{q}} + B_{\mathbf{q}}}}{\sqrt{A_{\mathbf{q}} - B_{\mathbf{q}}}} \delta(\omega - \omega_{\mathbf{q}}) + S_S^{\text{GS}}(\mathbf{q} = 0, \omega), \quad (\text{F15})$$

where we used Eq. (183). Detailed calculations for $\mathbf{q} = 0$ contributions to the dipole moment structure factor can be found in Appendix F6. More precisely, $S_S^{\text{GS}}(\mathbf{q} = 0, \omega)$ is given by Eq. (F53), which combined with Eq. (F15) gives the total quantum structure factor for the dipole moments expressed in Eq. (193).

3. Quadrupole moments: quantum structure factor at general values of \mathbf{q}

We now consider the dynamical structure factor associated with quadrupole moments

$$S_Q^{\text{QM}}(\mathbf{q}, \omega) = \int_{-\infty}^{\infty} \frac{dt}{2\pi} e^{i\omega t} \sum_{\mu\nu} \langle \hat{Q}_{\mathbf{q}}^{\mu\nu}(t) \hat{Q}_{-\mathbf{q}}^{\mu\nu}(0) \rangle. \quad (\text{F16})$$

Following the same steps as for the spin-structure factor, we use Eq. (173) to express the quadrupole components up to linear order in Eq. (51). We find

$$\hat{Q}_i \simeq \begin{pmatrix} \frac{2}{3} & -\hat{a}_i^\dagger - \hat{a}_i & 0 \\ -\hat{a}_i^\dagger - \hat{a}_i & -\frac{4}{3} & -\hat{b}_i^\dagger - \hat{b}_i \\ 0 & -\hat{b}_i^\dagger - \hat{b}_i & \frac{2}{3} \end{pmatrix}, \quad (\text{F17})$$

An equivalent calculation of matrix elements in the Bogoliubov basis [Eq. (182)] yields

$$\hat{Q}_{\mathbf{q}} \simeq \begin{pmatrix} \frac{2}{3}\sqrt{N}\delta(\mathbf{q}) & \xi_{\mathbf{Q}}(\mathbf{q})(\hat{\alpha}_{-\mathbf{q}}^\dagger + \hat{\alpha}_{\mathbf{q}}) & 0 \\ \xi_{\mathbf{Q}}(\mathbf{q})(\hat{\alpha}_{-\mathbf{q}}^\dagger + \hat{\alpha}_{\mathbf{q}}) & -\frac{4}{3}\sqrt{N}\delta(\mathbf{q}) & \xi_{\mathbf{Q}}(\mathbf{q})(\hat{\beta}_{-\mathbf{q}}^\dagger + \hat{\beta}_{\mathbf{q}}) \\ 0 & \xi_{\mathbf{Q}}(\mathbf{q})(\hat{\beta}_{-\mathbf{q}}^\dagger + \hat{\beta}_{\mathbf{q}}) & \frac{2}{3}\sqrt{N}\delta(\mathbf{q}) \end{pmatrix}, \quad (\text{F18})$$

where N is the number of sites and where $\xi_Q(\mathbf{q})$ is the coherence factor for quadrupoles defined as

$$\xi_Q(\mathbf{q}) = \frac{B_{\mathbf{q}} - \Delta_{\mathbf{q}}}{\sqrt{\Delta_{\mathbf{q}}^2 - B_{\mathbf{q}}^2}}. \quad (\text{F19})$$

Using Eq. (F4), we can then calculate the structure factor for quadrupole moments as defined in Eq. (F16). We obtain

$$S_Q^{\text{QM}}(\mathbf{q}, \omega) = 4 \frac{\sqrt{A_{\mathbf{q}} - B_{\mathbf{q}}}}{\sqrt{A_{\mathbf{q}} + B_{\mathbf{q}}}} \delta(\omega - \omega_{\mathbf{q}}) + S_Q^{\text{GS}}(\mathbf{q} = 0, \omega), \quad (\text{F20})$$

where we used Eq. (183). Detailed calculations for $\mathbf{q} = 0$ contributions to the quadrupole moment structure factor can be found in Appendix F7. More precisely, $S_Q^{\text{GS}}(\mathbf{q} = 0, \omega)$ is given by Eq. (F64), which combined with Eq. (F20) gives the total quantum structure factor for the quadrupole moments expressed in Eq. (201).

4. A-matrices : quantum structure factors at general values of \mathbf{q}

The most fundamental objects in our theory are not dipoles or quadrupoles, but the A-matrices which describe the quantum state of the spin-1 moment. It is therefore useful to introduce a dynamical structure factor

$$S_A^{\text{QM}}(\mathbf{q}, \omega) = \int_{-\infty}^{\infty} \frac{dt}{2\pi} e^{i\omega t} \sum_{\mu\nu} \langle \hat{A}_{\nu}^{\mu}(t) \hat{A}_{\mu}^{\nu}(0) \rangle. \quad (\text{F21})$$

Neglecting 2nd order and higher terms, Eq. (173) becomes

$$\hat{\mathbf{A}}_i \simeq \begin{pmatrix} 0 & \hat{a}_i^{\dagger} & 0 \\ \hat{a}_i & 1 & \hat{b}_i \\ 0 & \hat{b}_i^{\dagger} & 0 \end{pmatrix}. \quad (\text{F22})$$

Once again we can use the Bogoliubov basis [Eq. (182)] to find

$$\hat{\mathbf{A}}_{\mathbf{q}} \simeq \begin{pmatrix} 0 & \xi_A^-(\mathbf{q}) \hat{\alpha}_{-\mathbf{q}}^{\dagger} & 0 \\ -\xi_A^+(\mathbf{q}) \hat{\alpha}_{-\mathbf{q}}^{\dagger} & \sqrt{N} \delta_{\mathbf{q},0} & -\xi_A^+(\mathbf{q}) \hat{\beta}_{-\mathbf{q}}^{\dagger} \\ +\xi_A^-(\mathbf{q}) \hat{\alpha}_{\mathbf{q}} & & +\xi_A^-(\mathbf{q}) \hat{\beta}_{\mathbf{q}} \\ 0 & \xi_A^-(\mathbf{q}) \hat{\beta}_{-\mathbf{q}}^{\dagger} & 0 \\ & -\xi_A^+(\mathbf{q}) \hat{\beta}_{\mathbf{q}} & \end{pmatrix} \quad (\text{F23})$$

where N is the number of sites and $\xi_A^+(\mathbf{q})$ and $\xi_A^-(\mathbf{q})$ are the coherence factors for A-matrices defined as

$$\xi_A^+(\mathbf{q}) = \frac{\xi_S(\mathbf{q}) + \xi_Q(\mathbf{q})}{2}, \quad (\text{F24a})$$

$$\xi_A^-(\mathbf{q}) = \frac{\xi_S(\mathbf{q}) - \xi_Q(\mathbf{q})}{2}, \quad (\text{F24b})$$

where $\xi_S(\mathbf{q})$ and $\xi_Q(\mathbf{q})$ are defined in Eq. (F12) and Eq. (F19) respectively.

Using Eq. (F4), we can then calculate the structure factor for quadrupole moments as defined in Eq. (F21). We obtain

$$S_A^{\text{QM}}(\mathbf{q}, \omega) = 2 \frac{A_{\mathbf{q}}}{\sqrt{A_{\mathbf{q}}^2 - B_{\mathbf{q}}^2}} \delta(\omega - \omega_{\mathbf{q}}) + S_A^{\text{GS}}(\mathbf{q} = 0, \omega), \quad (\text{F25})$$

where we used Eq. (183). Detailed calculations for $\mathbf{q} = 0$ contributions to the A-matrix structure factor can be found in Appendix F8. More precisely, $S_A^{\text{GS}}(\mathbf{q} = 0, \omega)$ is given by Eq. (F66), which combined with Eq. (F25) gives the total quantum structure factor for the A-matrices expressed in Eq. (208).

5. Quantum structure factors: contribution of the ground state at $\mathbf{q} = 0$

We here present how to describe the zero-temperature correction of the ground state and the zero-point energy fluctuations' contribution to the quantum structure factors, which is expected to happen at $\mathbf{q} = 0$ and $\omega = 0$.

We therefore consider the zero-temperature quantum structure factor at $\mathbf{q} = 0$ to be given by

$$S_O^{\text{GS}}(\mathbf{q} = 0) = \sum_{\alpha\beta} \langle \hat{O}_{\mathbf{q}=0,\beta}^{\alpha} \hat{O}_{\mathbf{q}=0,\alpha}^{\beta} \rangle_{T=0}. \quad (\text{F26})$$

Calculating the contribution of the ground state and the zero-point energy fluctuations to the zero-temperature quantum structure factor can be achieved by adding a source term to the BBQ Hamiltonian that includes a fictive field \mathbf{h} coupled to the spin moments, similarly to what we did for the classical case [see Section IV C 2 and Appendix D]. The structure factors can then be calculated by taking the appropriate derivative of the free energy with respect to the fictive field \mathbf{h} .

We consider the total Hamiltonian to be given by Eq. (153), and the source term to be of the form given in Eq. (154). We can then rewrite the operators $\hat{O}_{\mathbf{q}}^{\alpha}$ of Eq. (154) in function of the fluctuations orthogonal to the FQ ground state [Eq. (112)]. Refer to Section IV A for details on the creation of orthogonal fluctuations. Expanding the source term Hamiltonian [Eq. (154)] up to second order in bosons, Fourier transforming it and considering its contribution for $\mathbf{q} = 0$, we can assume that it takes the following form

$$\Delta \mathcal{H}[\mathbf{h}_{\mathbf{q}}] = C[\mathbf{h}_{\mathbf{q}=0}] + \frac{1}{2} \sum_{\mathbf{k}} \left[\hat{\mathbf{w}}_{\mathbf{k}}^{\dagger} m_{\mathbf{k}}[\mathbf{h}_{\mathbf{q}=0}] \hat{\mathbf{w}}_{\mathbf{k}} + \left[\mathbf{N}[\mathbf{h}_{\mathbf{k}}]^T \hat{\mathbf{w}}_{\mathbf{k}} + \hat{\mathbf{w}}_{\mathbf{k}}^{\dagger} \mathbf{N}[\mathbf{h}_{\mathbf{k}}] \right] \delta_{\mathbf{k},0} \right], \quad (\text{F27})$$

where $C[\mathbf{h}_{\mathbf{q}=0}]$ is the coefficient for the 0th order term of the source term expanded in terms of the fluctuations orthogonal to the FQ ground state, $\hat{\mathbf{w}}_{\mathbf{k}}$ represents these fluctuations orthogonal to the FQ ground state and is given Eq. (175), $m_{\mathbf{k}}[\mathbf{h}_{\mathbf{q}=0}]$ represents the interaction matrix for 2nd order terms in fluctuations and depends on $\mathbf{h}_{\mathbf{q}=0}$, and where $\mathbf{N}[\mathbf{h}_{\mathbf{k}}]^{\dagger}$ and $\mathbf{N}[\mathbf{h}_{\mathbf{k}}]$ are the coefficients for the linear terms in fluctuations.

By definition of the source term Hamiltonian [Eq. (154)], all the coefficients $C[\mathbf{h}_{\mathbf{q}=0}]$, $\mathbf{N}_1[\mathbf{h}_{\mathbf{k}}]^T$, $\mathbf{N}_2[\mathbf{h}_{\mathbf{k}}]$, and $m_{\mathbf{k}}[\mathbf{h}_{\mathbf{q}=0}]$ depend linearly on the fictive field \mathbf{h} and will be different whether we are considering dipole, quadrupole, or A-matrix moments for the source term [Eq. (154)].

Using Eq. (174) for the BBQ Hamiltonian, we can assume that the total Hamiltonian [Eq. (153)] in terms of the bosons then take the following form

$$\mathcal{H} = E_0 + C[\mathbf{h}_{\mathbf{q}=0}] + \frac{1}{2} \sum_{\mathbf{k}} \left[\hat{\mathbf{w}}_{\mathbf{k}}^\dagger M_{\mathbf{k}}[\mathbf{h}_{\mathbf{q}=0}] \hat{\mathbf{w}}_{\mathbf{k}} + \left[\mathbf{N}[\mathbf{h}_{\mathbf{k}}]^\dagger \hat{\mathbf{w}}_{\mathbf{k}} + \hat{\mathbf{w}}_{\mathbf{k}}^\dagger \mathbf{N}[\mathbf{h}_{\mathbf{k}}] \right] \delta_{\mathbf{k},0} \right], \quad (\text{F28})$$

where E_0 is the mean-field ground-state given in Eq. (125), and where $M_{\mathbf{k}}[\mathbf{h}_{\mathbf{q}=0}]$ is the interaction matrix for the total Hamiltonian. It includes contributions from the BBQ Hamiltonian and the source term $m_{\mathbf{k}}[\mathbf{h}_{\mathbf{q}=0}]$, and, therefore, depends on $\mathbf{h}_{\mathbf{q}=0}$.

Following the method described in Appendix E, we perform a Bogoliubov transformation in order to diagonalize the total Hamiltonian. We assume that the new Bogoliubov bosons $\hat{\mathbf{v}}_{\mathbf{k}}$

$$\hat{\mathbf{v}}_{\mathbf{k}} = \begin{pmatrix} \hat{\alpha}_{\mathbf{k}} \\ \hat{\alpha}_{-\mathbf{k}}^\dagger \\ \hat{\beta}_{\mathbf{k}} \\ \hat{\beta}_{-\mathbf{k}}^\dagger \end{pmatrix}, \quad (\text{F29})$$

are given in terms of the bosons orthogonal to the FQ ground state $\hat{\mathbf{w}}_{\mathbf{k}}$ by Eq. (E2). We can then assume that the total Hamiltonian in terms of the Bogoliubov bosons $\hat{\mathbf{v}}_{\mathbf{k}}$ becomes

$$\begin{aligned} \mathcal{H} = & E_0 + \Delta E_0[\mathbf{h}_{\mathbf{q}=0}] + C[\mathbf{h}_{\mathbf{q}=0}] \\ & + \frac{1}{2} \sum_{\mathbf{k}} \left[\epsilon_{\mathbf{k},\alpha}[\mathbf{h}_{\mathbf{q}=0}] \hat{\alpha}_{\mathbf{k}}^\dagger \hat{\alpha}_{\mathbf{k}} + \epsilon_{\mathbf{k},\beta}[\mathbf{h}_{\mathbf{q}=0}] \hat{\beta}_{\mathbf{k}}^\dagger \hat{\beta}_{\mathbf{k}} \right. \\ & \left. + \left[\tilde{\mathbf{N}}[\mathbf{h}_{\mathbf{k}}]^\dagger \hat{\mathbf{v}}_{\mathbf{k}} + \hat{\mathbf{v}}_{\mathbf{k}}^\dagger \tilde{\mathbf{N}}[\mathbf{h}_{\mathbf{k}}] \right] \delta_{\mathbf{k},0} \right], \end{aligned} \quad (\text{F30})$$

where $\epsilon_{\mathbf{k},\alpha}[\mathbf{h}_{\mathbf{q}=0}]$ and $\epsilon_{\mathbf{k},\beta}[\mathbf{h}_{\mathbf{q}=0}]$ are the two physical eigenvalues obtained by diagonalizing $M_{\mathbf{k}}[\mathbf{h}_{\mathbf{q}=0}]$ [see Eq. (E6)], where $\Delta E_0[\mathbf{h}_{\mathbf{q}=0}]$ is the ground state contribution of the Bogoliubov bosons and where

$$\begin{aligned} \tilde{\mathbf{N}}[\mathbf{h}_{\mathbf{k}}]^\dagger &= \mathbf{N}[\mathbf{h}_{\mathbf{k}}]^\dagger U^{-1}, \\ \tilde{\mathbf{N}}[\mathbf{h}_{\mathbf{k}}] &= U^{\dagger-1} \mathbf{N}[\mathbf{h}_{\mathbf{k}}]. \end{aligned} \quad (\text{F31})$$

Here, U is the Bogoliubov matrix change defined by Eq. (E2) and remains to be determined. We also note that U^{-1} (and $U^{\dagger-1}$) should be calculate from Eq. (E3).

The canonical partition function is defined by

$$Z = \text{Tr}(e^{-\beta \hat{\mathcal{H}}}), \quad (\text{F32})$$

where β is defined by Eq. (134), and $\hat{\mathcal{H}}$ is the operator Hamiltonian. However in order to compute the partition function and the free energy, we want to get rid of the linear terms $\tilde{\mathbf{N}}[\mathbf{h}_{\mathbf{k}}]^\dagger$ and $\tilde{\mathbf{N}}[\mathbf{h}_{\mathbf{k}}]$, which only contribute for $\mathbf{k} = 0$. The partition function is then the one of a set of independent harmonic

oscillators for the $\mathbf{k} \neq 0$ terms, but still contains linear terms with respect to the bosons for $\mathbf{k} = 0$:

$$\begin{aligned} Z = & \text{Tr} \left(e^{-\beta E_0 - \beta \Delta E_0[\mathbf{h}_{\mathbf{q}=0}] - \beta C[\mathbf{h}_{\mathbf{q}=0}]} \right. \\ & \times \prod_{\mathbf{k} \neq 0} \left(e^{-\beta \epsilon_{\mathbf{k},\alpha}[\mathbf{h}_{\mathbf{q}=0}] \hat{\alpha}_{\mathbf{k}}^\dagger \hat{\alpha}_{\mathbf{k}}} \right) \left(e^{\beta \epsilon_{\mathbf{k},\beta}[\mathbf{h}_{\mathbf{q}=0}] \hat{\beta}_{\mathbf{k}}^\dagger \hat{\beta}_{\mathbf{k}}} \right) \\ & \times \left(e^{-\frac{1}{2} \beta \epsilon_{\mathbf{k}=0,\alpha}[\mathbf{h}_{\mathbf{q}=0}] \hat{\alpha}_{\mathbf{k}=0}^\dagger \hat{\alpha}_{\mathbf{k}=0} - \frac{1}{2} \beta n_1[\mathbf{h}_{\mathbf{k}=0}] \hat{\alpha}_{\mathbf{k}=0}^\dagger - \frac{1}{2} \beta n_2[\mathbf{h}_{\mathbf{k}=0}] \hat{\alpha}_{\mathbf{k}=0}} \right. \\ & \left. \times \left(e^{-\frac{1}{2} \beta \epsilon_{\mathbf{k}=0,\beta}[\mathbf{h}_{\mathbf{q}=0}] \hat{\beta}_{\mathbf{k}=0}^\dagger \hat{\beta}_{\mathbf{k}=0} - \frac{1}{2} \beta n_3[\mathbf{h}_{\mathbf{k}=0}] \hat{\beta}_{\mathbf{k}=0}^\dagger - \frac{1}{2} \beta n_4[\mathbf{h}_{\mathbf{k}=0}] \hat{\beta}_{\mathbf{k}=0}} \right) \right). \end{aligned} \quad (\text{F33})$$

where

$$\begin{aligned} n_1[\mathbf{h}_{\mathbf{k}=0}] &= \tilde{N}[\mathbf{h}_{-\mathbf{k}=0}]^{\dagger,2} + \tilde{N}[\mathbf{h}_{\mathbf{k}=0}]^1, \\ n_2[\mathbf{h}_{\mathbf{k}=0}] &= \tilde{N}[\mathbf{h}_{\mathbf{k}=0}]^{\dagger,1} + \tilde{N}[\mathbf{h}_{-\mathbf{k}=0}]^2, \\ n_3[\mathbf{h}_{\mathbf{k}=0}] &= \tilde{N}[\mathbf{h}_{-\mathbf{k}=0}]^{\dagger,4} + \tilde{N}[\mathbf{h}_{\mathbf{k}=0}]^3, \\ n_4[\mathbf{h}_{\mathbf{k}=0}] &= \tilde{N}[\mathbf{h}_{\mathbf{k}=0}]^{\dagger,3} + \tilde{N}[\mathbf{h}_{-\mathbf{k}=0}]^4, \end{aligned} \quad (\text{F34})$$

with $\tilde{N}[\mathbf{h}_{\mathbf{k}}]^{\dagger,1}$ denoting the first component of $\tilde{\mathbf{N}}[\mathbf{h}_{\mathbf{k}}]^\dagger$. To do this, we note that we can perform a change a variables by completing the square. For the $\mathbf{k} = 0$ term, for the the $\hat{\alpha}_{\mathbf{k}}^\dagger, \hat{\alpha}_{\mathbf{k}}$ bosons for instance, we have

$$\begin{aligned} -\frac{1}{2} \beta \epsilon_{0,\alpha}[\mathbf{h}_{\mathbf{q}=0}] \hat{\alpha}_0^\dagger \hat{\alpha}_0 - \frac{1}{2} \beta n_1[\mathbf{h}_{\mathbf{k}=0}] \hat{\alpha}_0^\dagger - \frac{1}{2} \beta n_2[\mathbf{h}_{\mathbf{k}=0}] \hat{\alpha}_0 = \\ -\frac{1}{2} \beta \epsilon_{0,\alpha}[\mathbf{h}_{\mathbf{q}=0}] \left(\hat{\alpha}_0^\dagger + \frac{n_1[\mathbf{h}_{\mathbf{k}=0}]}{\epsilon_{0,\alpha}[\mathbf{h}_{\mathbf{q}=0}]} \right) \left(\hat{\alpha}_0 + \frac{n_2[\mathbf{h}_{\mathbf{k}=0}]}{\epsilon_{0,\alpha}[\mathbf{h}_{\mathbf{q}=0}]} \right) \\ + \beta \frac{n_1[\mathbf{h}_{\mathbf{k}=0}] n_2[\mathbf{h}_{\mathbf{k}=0}]}{\epsilon_{0,\alpha}[\mathbf{h}_{\mathbf{q}=0}]}, \end{aligned} \quad (\text{F35})$$

We note that we have

$$n_1[\mathbf{h}_{\mathbf{k}=0}] = n_2[\mathbf{h}_{\mathbf{k}=0}]^\dagger, \quad (\text{F36})$$

so that we can define the change of variable

$$\begin{aligned} \hat{\rho}_{\mathbf{k}=0}^\dagger &= \hat{\alpha}_{\mathbf{k}=0}^\dagger + \frac{n_1[\mathbf{h}_{\mathbf{k}=0}]}{\epsilon_{\mathbf{k}=0,\alpha}[\mathbf{h}_{\mathbf{q}=0}]}, \\ \hat{\rho}_{\mathbf{k}=0} &= \hat{\alpha}_{\mathbf{k}=0} + \frac{n_2[\mathbf{h}_{\mathbf{k}=0}]}{\epsilon_{\mathbf{k}=0,\alpha}[\mathbf{h}_{\mathbf{q}=0}]}, \end{aligned} \quad (\text{F37})$$

which ensures that $\hat{\rho}_{\mathbf{k}=0}^\dagger$ and $\hat{\rho}_{\mathbf{k}=0}$ have bosonic commutation relations and are associated with the eigenmode $\epsilon_{\mathbf{k}=0,\alpha}[\mathbf{h}_{\mathbf{q}=0}]$. We follow the same argument for the $\hat{\beta}_{\mathbf{k}=0}^\dagger, \hat{\beta}_{\mathbf{k}=0}$ bosons, and get new bosons $\hat{\sigma}_{\mathbf{k}=0}^\dagger$ and $\hat{\sigma}_{\mathbf{k}=0}$:

$$\begin{aligned} \hat{\sigma}_{\mathbf{k}=0}^\dagger &= \hat{\beta}_{\mathbf{k}=0}^\dagger + \frac{n_3[\mathbf{h}_{\mathbf{k}=0}]}{\epsilon_{\mathbf{k}=0,\beta}[\mathbf{h}_{\mathbf{q}=0}]}, \\ \hat{\sigma}_{\mathbf{k}=0} &= \hat{\beta}_{\mathbf{k}=0} + \frac{n_4[\mathbf{h}_{\mathbf{k}=0}]}{\epsilon_{\mathbf{k}=0,\beta}[\mathbf{h}_{\mathbf{q}=0}]}, \end{aligned} \quad (\text{F38})$$

associated with the eigenmode $\epsilon_{\mathbf{k}=0,\beta}[\mathbf{h}_{\mathbf{q}=0}]$. The partition function is then the one of a set of independent harmonic oscillators. We obtain

$$\begin{aligned} Z = & \text{Tr} \left(e^{-\beta E_0 - \beta \Delta E_0[\mathbf{h}_{\mathbf{q}=0}] - \beta C[\mathbf{h}_{\mathbf{q}=0}]} \right. \\ & \times \prod_{\mathbf{k} \neq 0} \left(e^{-\beta \epsilon_{\mathbf{k},\alpha}[\mathbf{h}_{\mathbf{q}=0}] \hat{\alpha}_{\mathbf{k}}^\dagger \hat{\alpha}_{\mathbf{k}}} \right) \left(e^{-\beta \epsilon_{\mathbf{k},\beta}[\mathbf{h}_{\mathbf{q}=0}] \hat{\beta}_{\mathbf{k}}^\dagger \hat{\beta}_{\mathbf{k}}} \right) \\ & \times \left(e^{-\beta \epsilon_{\mathbf{k}=0,\alpha}[\mathbf{h}_{\mathbf{q}=0}] \hat{\rho}_{\mathbf{k}=0}^\dagger \hat{\rho}_{\mathbf{k}=0}} \right) \left(e^{-\beta \epsilon_{\mathbf{k}=0,\beta}[\mathbf{h}_{\mathbf{q}=0}] \hat{\sigma}_{\mathbf{k}=0}^\dagger \hat{\sigma}_{\mathbf{k}=0}} \right) \\ & \times e^{\beta \frac{n_1[\mathbf{h}_{\mathbf{k}=0}] n_2[\mathbf{h}_{\mathbf{k}=0}]}{\epsilon_{\mathbf{k}=0,\alpha}[\mathbf{h}_{\mathbf{q}=0}]} - \beta \frac{n_3[\mathbf{h}_{\mathbf{k}=0}] n_4[\mathbf{h}_{\mathbf{k}=0}]}{\epsilon_{\mathbf{k}=0,\beta}[\mathbf{h}_{\mathbf{q}=0}]}} \right). \end{aligned} \quad (\text{F39})$$

We then perform the trace on the Fock space, and use the fact that the trace is independent of the choice of the basis. This means we can compute it separately for the $\hat{\alpha}_{\mathbf{k}}^\dagger$ bosons on their respective Fock basis $|n_{\mathbf{k}}^\alpha\rangle$ and for the $\hat{\rho}_{\mathbf{k}=0}^\dagger$ bosons on its respective Fock basis $|n_{\mathbf{k}=0}^\rho\rangle$, and similarly for $\hat{\beta}_{\mathbf{k}}^\dagger$ and $\hat{\sigma}_{\mathbf{k}=0}^\dagger$. Taking the trace over the Fock space as explained above, we obtain

$$Z = e^{-\beta E_0 - \beta \Delta E_0[\mathbf{h}_{\mathbf{q}=0}] - \beta C[\mathbf{h}_{\mathbf{q}=0}]} \times \prod_{\mathbf{k}} \frac{1}{1 - e^{-\beta \epsilon_{\mathbf{k},\alpha}[\mathbf{h}_{\mathbf{q}=0}]}} \frac{1}{1 - e^{-\beta \epsilon_{\mathbf{k},\alpha}[\mathbf{h}_{\mathbf{q}=0}]}} \times e^{\beta \frac{n_1[\mathbf{h}_{\mathbf{k}=0}]n_2[\mathbf{h}_{\mathbf{k}=0}]}{\epsilon_{\mathbf{k},\alpha}[\mathbf{h}_{\mathbf{q}=0}]}} e^{\beta \frac{n_3[\mathbf{h}_{\mathbf{k}=0}]n_4[\mathbf{h}_{\mathbf{k}=0}]}{\epsilon_{\mathbf{k},\alpha}[\mathbf{h}_{\mathbf{q}=0}]}}. \quad (\text{F40})$$

We note here that instead of doing the change of variable for $\mathbf{k} = 0$, we could also The free energy is given by

$$F = -\frac{\log(Z)}{\beta} = E_0 + \Delta E_0[\mathbf{h}_{\mathbf{q}=0}] + C[\mathbf{h}_{\mathbf{q}=0}] + \frac{1}{\beta} \sum_{\mathbf{k}} \log(1 - e^{-\beta \epsilon_{\mathbf{k},\alpha}[\mathbf{h}_{\mathbf{q}=0}]}) + \frac{1}{\beta} \sum_{\mathbf{k}} \log(1 - e^{-\beta \epsilon_{\mathbf{k},\beta}[\mathbf{h}_{\mathbf{q}=0}]}) - 2 \frac{n_1[\mathbf{h}_{\mathbf{k}=0}]n_2[\mathbf{h}_{\mathbf{k}=0}]}{\epsilon_{\mathbf{k},\alpha}[\mathbf{h}_{\mathbf{q}=0}]} - 2 \frac{n_3[\mathbf{h}_{\mathbf{k}=0}]n_4[\mathbf{h}_{\mathbf{k}=0}]}{\epsilon_{\mathbf{k},\alpha}[\mathbf{h}_{\mathbf{q}=0}]} + \mathcal{O}(T^2). \quad (\text{F41})$$

The moments are given by taking the appropriate derivative of the free energy. They are given by the same expression that we obtained for the classical case expressed in Eq. (D28) and Eq. (D29). We now note that we are interested in the zero temperature $T = 0$ structure factor, and we can disregard the terms with $\frac{1}{\beta}$ in the free energy. Eq. (D28) then becomes

$$\langle \hat{O}_{\mathbf{q}=0,\beta}^\alpha \rangle_{T=0} = - \left. \frac{\partial [\Delta E_0[\mathbf{h}_{\mathbf{q}=0}] + C[\mathbf{h}_{\mathbf{q}=0}]]}{\partial h_{\mathbf{q}=0,\beta}^\alpha} \right|_{\mathbf{h}=0} + 2 \left. \frac{\partial \left[\frac{n_1[\mathbf{h}_{\mathbf{k}=0}]n_2[\mathbf{h}_{\mathbf{k}=0}]}{\epsilon_{\mathbf{k},\alpha}[\mathbf{h}_{\mathbf{q}=0}]} + \frac{n_3[\mathbf{h}_{\mathbf{k}=0}]n_4[\mathbf{h}_{\mathbf{k}=0}]}{\epsilon_{\mathbf{k},\alpha}[\mathbf{h}_{\mathbf{q}=0}]} \right]}{\partial h_{\mathbf{q}=0,\beta}^\alpha} \right|_{\mathbf{h}=0}. \quad (\text{F42})$$

We also note that the terms with $n_1[\mathbf{h}_{\mathbf{k}=0}]n_2[\mathbf{h}_{\mathbf{k}=0}]$ and $n_3[\mathbf{h}_{\mathbf{k}=0}]n_4[\mathbf{h}_{\mathbf{k}=0}]$ are at least quadratic (if not of higher order, depending on $\epsilon_{\mathbf{k}}[\mathbf{h}_{\mathbf{q}=0}]$) in the field components $\mathbf{h}_{\mathbf{q}=0}$, as any of the $n_{i=1,2,3,4}$ is independently linear in $\mathbf{h}_{-\mathbf{k}=0}$ by definition. Therefore taking the first derivative of the terms with $n_1[\mathbf{h}_{\mathbf{k}=0}]n_2[\mathbf{h}_{\mathbf{k}=0}]$ and $n_3[\mathbf{h}_{\mathbf{k}=0}]n_4[\mathbf{h}_{\mathbf{k}=0}]$ and evaluating them at zero field will inevitably lead to a null contribution. We then are simply left with

$$\langle \hat{O}_{\mathbf{q}=0,\beta}^\alpha \rangle_{T=0} = - \left. \frac{\partial \Delta E_0[\mathbf{h}_{\mathbf{q}=0}] + C[\mathbf{h}_{\mathbf{q}=0}]}{\partial h_{\mathbf{q}=0,\beta}^\alpha} \right|_{\mathbf{h}=0}. \quad (\text{F43})$$

The second moments are given by Eq. (D28) and disregarding again the term with $\frac{1}{\beta}$, it simply becomes

$$\langle \hat{O}_{\mathbf{q}=0,\beta}^\alpha \hat{O}_{\mathbf{q}=0,\nu}^\mu \rangle_{T=0} = \langle \hat{O}_{\mathbf{q}=0,\beta}^\alpha \rangle_{T=0} \langle \hat{O}_{\mathbf{q}=0,\nu}^\mu \rangle_{T=0}. \quad (\text{F44})$$

We can insert Eq. (F44) into Eq. (F26) to calculate the ground state contribution to the quantum structure factor. Therefore all we need to do is find the 0th order contribution of the source term, i.e., find $C[\mathbf{h}_{\mathbf{q}=0}]$, and compute the zero-point energy of the Bogoliubov transformation $\Delta E_0[\mathbf{h}_{\mathbf{q}=0}]$.

6. Dipole moments: contribution of the ground state to the quantum structure factor at $\mathbf{q} = 0$

First, we consider the structure factor for dipole moments of spin

$$S_S^{\text{GS}}(\mathbf{q} = 0) = \sum_{\alpha} \langle \hat{S}_{\mathbf{q}=0}^\alpha \hat{S}_{-\mathbf{q}=0}^\alpha \rangle_{T=0}. \quad (\text{F45})$$

The relevant source term is given by Eq. (D33) According to Eq. (50) and using Eq. (173), we can express Eq. (D33) in function of fluctuations orthogonal to the FQ ground state [Eq. (112)]. Considering fluctuation terms up to 2nd order, we have

$$\begin{aligned} \hat{S}_i^x &= -i(\hat{b}_i - \hat{b}_i^\dagger), \\ \hat{S}_i^y &= i(\hat{a}_i^\dagger \hat{b}_i - \hat{a}_i \hat{b}_i^\dagger), \\ \hat{S}_i^z &= -i(\hat{a}_i^\dagger - \hat{a}_i). \end{aligned} \quad (\text{F46})$$

After performing a Fourier transform, and considering the source term Hamiltonian $\Delta \mathcal{H}[h_{i,\beta}^\alpha]$ [Eq. (D33)] at $\mathbf{q} = 0$, we have

$$\begin{aligned} \Delta \mathcal{H}[\mathbf{h}_{\mathbf{q}}] &= - \sum_{\mathbf{q}} \left[i h_{-\mathbf{q}}^x (\hat{b}_{\mathbf{q}}^\dagger - \hat{b}_{\mathbf{q}}) - i h_{-\mathbf{q}}^z (\hat{a}_{\mathbf{q}}^\dagger - \hat{a}_{\mathbf{q}}) \right] \delta_{\mathbf{q},0} \\ &\quad - \sum_{\mathbf{k}} \frac{i}{\sqrt{N}} h_{\mathbf{q}=0}^y (\hat{a}_{\mathbf{k}}^\dagger \hat{b}_{\mathbf{k}} - \hat{a}_{\mathbf{k}} \hat{b}_{\mathbf{k}}^\dagger). \end{aligned} \quad (\text{F47})$$

And using Eq. (174) for the BBQ Hamiltonian, the total Hamiltonian [Eq. (153)] in terms of the bosons takes the same form as in Eq. (F28), where $M_{\mathbf{k}}[\mathbf{h}_{\mathbf{q}=0}]$ is given by

$$M_{\mathbf{k}}[\mathbf{h}_{\mathbf{q}=0}] = \begin{pmatrix} A_{\mathbf{k}} & -B_{\mathbf{k}} & -\frac{i}{\sqrt{N}} h_{\mathbf{q}=0}^y & 0 \\ -B_{\mathbf{k}} & A_{\mathbf{k}} & 0 & \frac{i}{\sqrt{N}} h_{\mathbf{q}=0}^y \\ \frac{i}{\sqrt{N}} h_{\mathbf{q}=0}^y & 0 & A_{\mathbf{k}} & -B_{\mathbf{k}} \\ 0 & -\frac{i}{\sqrt{N}} h_{\mathbf{q}=0}^y & -B_{\mathbf{k}} & A_{\mathbf{k}} \end{pmatrix}, \quad (\text{F48a})$$

where $A_{\mathbf{k}}$ and $B_{\mathbf{k}}$ are given in Eq. (128) and where $\mathbf{N}[\mathbf{h}_{\mathbf{k}}]$ is given by

$$\mathbf{N}[\mathbf{h}_{\mathbf{k}}] = i \begin{pmatrix} h_{-\mathbf{k}}^z \\ -h_{\mathbf{k}}^z \\ -h_{-\mathbf{k}}^x \\ h_{\mathbf{k}}^x \end{pmatrix}, \quad (\text{F48b})$$

and where $C[\mathbf{h}_{\mathbf{q}=0}]$ holds

$$C[\mathbf{h}_{\mathbf{q}=0}] = 0. \quad (\text{F48c})$$

Following the procedure depicted in [Section V](#) and detailed in [Appendix E](#), we perform a Bogoliubov transformation and the eigenvalues $\epsilon_{\mathbf{k},\lambda}$ are given by

$$\epsilon_{\mathbf{k},1}[\mathbf{h}_{\mathbf{q}=0}] = -\epsilon_{\mathbf{k},2} = +\sqrt{A_{\mathbf{k}}^2 - B_{\mathbf{k}}^2} + \frac{1}{\sqrt{N}}h_{\mathbf{q}=0}^y, \quad (\text{F49a})$$

$$\epsilon_{\mathbf{k},3}[\mathbf{h}_{\mathbf{q}=0}] = -\epsilon_{\mathbf{k},4} = +\sqrt{A_{\mathbf{k}}^2 - B_{\mathbf{k}}^2} - \frac{1}{\sqrt{N}}h_{\mathbf{q}=0}^y. \quad (\text{F49b})$$

After performing the Bogoliubov transformation, the Hamiltonian can be rewritten as follows:

$$\begin{aligned} \mathcal{H} = & E_0 + \Delta E_0[\mathbf{h}_{\mathbf{q}=0}] \\ & + \left[\sum_{\mathbf{k}} \epsilon_{\mathbf{k},1}[\mathbf{h}_{\mathbf{q}=0}] \hat{\alpha}_{\mathbf{k}}^\dagger \hat{\alpha}_{\mathbf{k}} + \epsilon_{\mathbf{k},3}[\mathbf{h}_{\mathbf{q}=0}] \hat{\beta}_{\mathbf{k}}^\dagger \hat{\beta}_{\mathbf{k}} \right], \quad (\text{F50}) \end{aligned}$$

where $C[\mathbf{h}_{\mathbf{q}=0}]$ is disregarded since it is null [\[Eq. \(F48c\)\]](#), and where $\Delta E_0[\mathbf{h}_{\mathbf{q}=0}]$ is the zero-point energy

$$\Delta E_0[\mathbf{h}_{\mathbf{q}=0}] = \frac{1}{2} \sum_{\mathbf{k}} [\epsilon_{\mathbf{k},1}[\mathbf{h}_{\mathbf{q}=0}] + \epsilon_{\mathbf{k},3}[\mathbf{h}_{\mathbf{q}=0}]]. \quad (\text{F51})$$

According to [Eq. \(F43\)](#), the ground state contribution to the first moments yield

$$\langle S_{\mathbf{q}}^x \rangle_{T=0} = \langle S_{\mathbf{q}}^z \rangle_{T=0} = 0, \quad (\text{F52a})$$

$$\langle S_{\mathbf{q}}^y \rangle_{T=0} = \frac{1}{2} \sum_{\mathbf{k}} \left[\frac{1}{\sqrt{N}} - \frac{1}{\sqrt{N}} \right] = 0. \quad (\text{F52b})$$

And according to [Eq. \(F44\)](#) and [Eq. \(F45\)](#), the spin dipole structure factor at $\mathbf{q} = 0$ yields

$$S_{\mathbf{Q}}^{\text{GS}}(\mathbf{q} = 0) = 0. \quad (\text{F53})$$

Indeed, the ground state is quadrupolar and does not break time-reversal symmetry. Therefore, at zero temperature, the contribution of quantum fluctuations from the zero-point energy should average to zero for the spin dipole moments. The spectral representation of [Eq. \(F53\)](#) is then also trivially null. Combining [Eq. \(F15\)](#) and [Eq. \(F53\)](#), we obtain [Eq. \(193\)](#).

7. Quadrupole moments: contribution of the ground state to the quantum structure factor at $\mathbf{q} = 0$

We now consider the quadrupole structure factor at the Γ -point, which is defined as

$$S_{\mathbf{Q}}^{\text{GS}}(\mathbf{q} = 0) = \sum_{\alpha\beta} \langle \hat{Q}_{\mathbf{q}=0}^{\alpha\beta} \hat{Q}_{\mathbf{q}=0}^{\beta\alpha} \rangle_{T=0}. \quad (\text{F54})$$

We follow the same procedure as depicted in [Appendix F5](#). The relevant source term for quadrupole moments is given by [Eq. \(D50\)](#). We can express [Eq. \(D50\)](#) up to second order in terms of the bosons by using [Eq. \(173\)](#) and [Eq. \(51\)](#). We use

[Eq. \(174\)](#) for the BBQ Hamiltonian. We then obtain for the total Hamiltonian given by [Eq. \(153\)](#), written in the form of [Eq. \(F28\)](#), where $M_{\mathbf{k}}[\mathbf{h}_{\mathbf{q}=0}]$ is given by

$$M_{\mathbf{k}}[\mathbf{h}_{\mathbf{q}=0}] = \begin{pmatrix} A_{\mathbf{k}} + \alpha_1 & -B_{\mathbf{k}} & \beta_1 & 0 \\ -B_{\mathbf{k}} & A_{\mathbf{k}} + \alpha_1 & 0 & \beta_1 \\ \beta_1 & 0 & A_{\mathbf{k}} + \alpha_2 & -B_{\mathbf{k}} \\ \beta_1 & 0 & -B_{\mathbf{k}} & A_{\mathbf{k}} + \alpha_2 \end{pmatrix}, \quad (\text{F55a})$$

where $\mathbf{N}[\mathbf{h}_{\mathbf{k}}]$ is given by

$$\mathbf{N}[\mathbf{h}_{\mathbf{k}}] = \begin{pmatrix} \xi_{-\mathbf{k}}^1 \\ \xi_{\mathbf{k}}^1 \\ \xi_{-\mathbf{k}}^2 \\ \xi_{-\mathbf{k}}^2 \end{pmatrix}, \quad (\text{F55b})$$

and where $C[\mathbf{h}_{\mathbf{q}=0}]$ holds

$$C[\mathbf{h}_{\mathbf{q}=0}] = \sqrt{N} \left(\frac{4}{3} h_{\mathbf{q}=0,y}^y - \frac{2}{3} (h_{\mathbf{q}=0,x}^x + h_{\mathbf{q}=0,z}^z) \right), \quad (\text{F55c})$$

with $A_{\mathbf{k}}$ and $B_{\mathbf{k}}$ being given in [Eq. \(128\)](#) and with the following definitions

$$\alpha_1 = \frac{2}{\sqrt{N}} (h_{\mathbf{q}=0,x}^x - h_{\mathbf{q}=0,y}^y), \quad \alpha_2 = \frac{2}{\sqrt{N}} (h_{\mathbf{q}=0,z}^z - h_{\mathbf{q}=0,y}^y),$$

$$\beta_1 = \frac{1}{\sqrt{N}} (h_{\mathbf{q}=0,z}^x + h_{\mathbf{q}=0,x}^z),$$

$$\xi_{\mathbf{k}}^1 = (h_{\mathbf{k},y}^x + h_{\mathbf{k},x}^y), \quad \xi_{\mathbf{k}}^2 = (h_{\mathbf{k},z}^y + h_{\mathbf{k},y}^z). \quad (\text{F56})$$

Following the procedure depicted in [Section V](#) and detailed in [Appendix E](#), we perform a Bogoliubov transformation and the eigenvalues $\epsilon_{\mathbf{k},\lambda}$ are given by

$$\begin{aligned} \epsilon_{\mathbf{k},1}[\mathbf{h}_{\mathbf{q}=0}] = -\epsilon_{\mathbf{k},2}[\mathbf{h}_{\mathbf{q}=0}] = \\ \sqrt{A_{\mathbf{k}}^2 - B_{\mathbf{k}}^2 + \beta_1^2 + \frac{1}{2} (\alpha_1^2 + \alpha_2^2) + A_{\mathbf{k}} \alpha^+ - \Delta \left(A_{\mathbf{k}} + \frac{\alpha^+}{2} \right)}, \quad (\text{F57a}) \end{aligned}$$

$$\begin{aligned} \epsilon_{\mathbf{k},3}[\mathbf{h}_{\mathbf{q}=0}] = -\epsilon_{\mathbf{k},4}[\mathbf{h}_{\mathbf{q}=0}] = \\ \sqrt{A_{\mathbf{k}}^2 - B_{\mathbf{k}}^2 + \beta_1^2 + \frac{1}{2} (\alpha_1^2 + \alpha_2^2) + A_{\mathbf{k}} \alpha^+ + \Delta \left(A_{\mathbf{k}} + \frac{\alpha^+}{2} \right)}, \quad (\text{F57b}) \end{aligned}$$

where α^+ and Δ are defined in [Eq. \(D62\)](#). After performing the Bogoliubov transformation, the Hamiltonian can be rewritten as follows:

$$\begin{aligned} \mathcal{H} = & E_0 + \Delta E_0[\mathbf{h}_{\mathbf{q}=0}] + C[\mathbf{h}_{\mathbf{q}=0}] \\ & + \left[\sum_{\mathbf{k}} \epsilon_{\mathbf{k},1}[\mathbf{h}_{\mathbf{q}=0}] \hat{\alpha}_{\mathbf{k}}^\dagger \hat{\alpha}_{\mathbf{k}} + \epsilon_{\mathbf{k},3}[\mathbf{h}_{\mathbf{q}=0}] \hat{\beta}_{\mathbf{k}}^\dagger \hat{\beta}_{\mathbf{k}} \right], \quad (\text{F58}) \end{aligned}$$

where $C[\mathbf{h}_{\mathbf{q}=0}]$ is given in [Eq. \(F55c\)](#), and where $\Delta E_0[\mathbf{h}_{\mathbf{q}=0}]$ is the zero-point energy and yields

$$\Delta E_0[\mathbf{h}_{\mathbf{q}=0}] = \frac{1}{2} \sum_{\mathbf{k}} [\epsilon_{\mathbf{k},1}[\mathbf{h}_{\mathbf{q}=0}] + \epsilon_{\mathbf{k},3}[\mathbf{h}_{\mathbf{q}=0}]]. \quad (\text{F59})$$

According to Eq. (F43), the ground state contribution to the first moments yield

$$\langle Q_{\mathbf{q}=0}^{xx} \rangle_{T=0} = -\frac{2}{3}\sqrt{N} + \frac{1}{\sqrt{N}} \sum_{\mathbf{k}} \left[\frac{A_{\mathbf{k}}}{\sqrt{A_{\mathbf{k}}^2 - B_{\mathbf{k}}^2}} \right], \quad (\text{F60a})$$

$$\langle Q_{\mathbf{q}=0,y}^{xy} \rangle_{T=0} = \langle Q_{\mathbf{q}=0}^{yx} \rangle_{T=0} = 0, \quad (\text{F60b})$$

$$\langle Q_{\mathbf{q}=0,z}^{xz} \rangle_{T=0} = \langle Q_{\mathbf{q}=0}^{zx} \rangle_{T=0} = 0, \quad (\text{F60c})$$

$$\langle Q_{\mathbf{q}=0,y}^{yy} \rangle_{T=0} = \frac{4}{3}\sqrt{N} - \frac{1}{\sqrt{N}} \sum_{\mathbf{k}} \left[\frac{2A_{\mathbf{k}}}{\sqrt{A_{\mathbf{k}}^2 - B_{\mathbf{k}}^2}} \right], \quad (\text{F60d})$$

$$\langle Q_{\mathbf{q}=0,z}^{yz} \rangle_{T=0} = \langle Q_{\mathbf{q}=0}^{zy} \rangle_{T=0} = 0, \quad (\text{F60e})$$

$$\langle Q_{\mathbf{q}=0}^{zz} \rangle_{T=0} = -\frac{2}{3}\sqrt{N} + \frac{1}{\sqrt{N}} \sum_{\mathbf{k}} \left[\frac{A_{\mathbf{k}}}{\sqrt{A_{\mathbf{k}}^2 - B_{\mathbf{k}}^2}} \right]. \quad (\text{F60f})$$

Before calculating the structure factor, we note that, as given in Eq. (F60), the first quadrupole moments consist of two terms with different scaling behaviour with respect to the parameter we expand fluctuations about, which is the length of the spin s . Indeed, similarly to multi-boson expansion, or its linear spin-wave version with Holstein–Primakoff bosons or Schwinger bosons in the case of a $su(2)$ representation of the spin, we assume the fluctuation to be sufficiently small compared to the spin length s . In other words, $C[\mathbf{h}_{\mathbf{q}=0}]$ from Eq. (F55c) and the eigenvalues in Eq. (F57) scale with s as

$$C[\mathbf{h}_{\mathbf{q}=0}] \sim sh_{\mathbf{q}=0,\mu}^{\mu}, \quad (\text{F61a})$$

$$\epsilon_{\mathbf{k},\lambda}[\mathbf{h}_{\mathbf{q}=0}] \sim s\sqrt{\text{Const.} + \frac{h_{\mathbf{q}=0,\mu}^{\mu}}{s^2} + \frac{\mathcal{O}(\mathbf{h}_{\mathbf{q}=0}^2)}{s^2}}. \quad (\text{F61b})$$

Their derivatives with respect to $h_{\mathbf{q}=0,\mu}^{\mu}$ that enters the quadrupole moments [Eq. (F43)] yield

$$\left. \frac{C[\mathbf{h}_{\mathbf{q}=0}]}{\partial h_{\mathbf{q}=0,\mu}^{\mu}} \right|_{\mathbf{h}=0} \sim s, \quad (\text{F62a})$$

$$\left. \frac{\partial \epsilon_{\mathbf{k},\lambda}[\mathbf{h}_{\mathbf{q}=0}]}{\partial h_{\mathbf{q}=0,\mu}^{\mu}} \right|_{\mathbf{h}=0} \sim \frac{s}{\sqrt{\text{Const.}}} \frac{\partial \frac{h_{\mathbf{q}=0,\mu}^{\mu}}{s^2}}{\partial h_{\mathbf{q}=0,\mu}^{\mu}} \Big|_{\mathbf{h}=0} \sim \frac{1}{s}.$$

This implies that the scaling behaviour of the first quadrupole moments goes as

$$\langle Q_{\mathbf{q}=0}^{\mu\mu} \rangle_{T=0} \sim s + \frac{1}{s}, \quad (\text{F63})$$

where s is the length of the spin. We now argue that because our approximation is valid up to linear order in $\frac{1}{s}$, i.e., second order in fluctuations, we can disregard $\frac{1}{s^2}$ terms. $\frac{1}{s^2}$ terms are physical but should not enter into our level of approximation. Indeed, one would expect additional contribution to the $\frac{1}{s^2}$ term coming from higher orders in perturbation theory. However, we do not take these into account here and simply consider terms up to $\frac{1}{s}$. According to Eq. (F44) and Eq. (F54),

the spin quadrupole structure factor at $\mathbf{q} = 0$ yields

$$S_{\mathbf{Q}}^{\text{GS}}(\mathbf{q} = 0) = \frac{8}{3}N - 8 \sum_{\mathbf{k}} \left[\frac{A_{\mathbf{k}}}{\sqrt{A_{\mathbf{k}}^2 - B_{\mathbf{k}}^2}} \right] + \mathcal{O}\left(\frac{1}{s^2}\right). \quad (\text{F64})$$

Its spectral representation is given by

$$S_{\mathbf{Q}}^{\text{GS}}(\mathbf{q} = 0, \omega) = \left(\frac{8}{3}N - 8 \sum_{\mathbf{k}} \left[\frac{A_{\mathbf{k}}}{\sqrt{A_{\mathbf{k}}^2 - B_{\mathbf{k}}^2}} \right] \right) \delta(\omega) + \mathcal{O}\left(\frac{1}{s^2}\right). \quad (\text{F65})$$

Combining Eq. (F20) and Eq. (F65), we obtain Eq. (201).

8. A-matrices: contribution of the ground state to the quantum structure factor at $\mathbf{q} = 0$

For the quantum zero temperature structure factor for the A-matrices at $\mathbf{q} = 0$, we make use of the sum rule given in Eq. (66). This leads to

$$\begin{aligned} S_{\text{A}}^{\text{GS}}(\mathbf{q} = 0) &= \frac{1}{4}S_{\mathbf{Q}}^{\text{GS}}(\mathbf{q} = 0) + \frac{1}{2}S_{\text{S}}^{\text{GS}}(\mathbf{q} = 0) + \frac{1}{3}N\delta_{\mathbf{q},0} \\ &= N - 2 \sum_{\mathbf{k}} \left[\frac{A_{\mathbf{k}}}{\sqrt{A_{\mathbf{k}}^2 - B_{\mathbf{k}}^2}} \right] + \mathcal{O}\left(\frac{1}{s^2}\right), \end{aligned} \quad (\text{F66})$$

where we used Eq. (F53) and Eq. (F64). Its spectral representation yields

$$S_{\text{A}}^{\text{GS}}(\mathbf{q} = 0, \omega) = \left(N - 2 \sum_{\mathbf{k}} \left[\frac{A_{\mathbf{k}}}{\sqrt{A_{\mathbf{k}}^2 - B_{\mathbf{k}}^2}} \right] \right) \delta(\omega) + \mathcal{O}\left(\frac{1}{s^2}\right). \quad (\text{F67})$$

Combining Eq. (F25) with Eq. (F67) gives the total quantum structure factor for the A-matrices expressed in Eq. (208)

Appendix G: System size dependence of the ordered moments

We present in this Appendix, the details of the manufacturing of Section VI B. More precisely, we explain how we fitted the numerical data for the ordered moments and explain how we calculated the ordered moments from the analytical results.

In Table (I), we show the temperature intervals on which the corresponding ordered parameters values are used for the fits of the slope $\alpha(L)$ of the ordered parameters in Fig. 14 (a), for different system sizes.

We also present here how the ordered moments as expressed by Eq. (170) and presented in Fig. 14 (b) are calculated. In order to compute Eq. (170), we need to perform a sum in \mathbf{k} -space. We here also show that the sum scales

System size L	T_{min}	T_{max}
L=12	0.01	0.100177
L=24	0.01	0.100177
L=48	0.0252403	0.100177
L=96	0.0343658	0.100177

Table I. Temperature intervals used for fitting the parameter $\alpha(L)$ according to Eq. (218).

logarithmically with the system size L by explicitly calculating the coefficient μ correspond to the logarithmic behavior [Eq. (G5)]. To do this, we calculate the sum numerically for different system sizes L and fit it according to Eq. (G5) (as shown by the orange line in Fig. 14 (b)). Additionally, we also transform the sum into an integral and extract the logarithmic scaling behaviour.

The Brillouin zone is turned into a parallelogram of area $\frac{8\pi}{\sqrt{3}}$, as it is spanned by the reciprocal vectors \mathbf{K}_a and \mathbf{K}_b given in Eq. (C2). We then discretized it into $N = L^2$ tiles of dimension δA given by

$$\delta \mathbf{k}_a = \frac{1}{L} \mathbf{K}_a, \quad \delta \mathbf{k}_b = \frac{1}{L} \mathbf{K}_b, \quad (\text{G1})$$

such that

$$\delta A = \frac{8\pi}{\sqrt{3}L^2}. \quad (\text{G2})$$

In order to compare numerical with analytical results, we consider

$$\frac{1}{N} \sum_{\mathbf{k}} I_{\mathbf{k}} \Rightarrow N \delta A \sum_{k_x, k_y} I_{\mathbf{k}} = \int I_{\mathbf{k}} d\mathbf{k}, \quad (\text{G3})$$

We can now sum over the \mathbf{k} -space, numerically, or integrate, analytically.

In Eq. (G3), we take as integrand the term expressed as a sum in the result obtained in Eq. (170), as we wish to compute the temperature-dependent part of the ordered moment given in Eq. (170). Using Eq. (140), we obtain

$$I_{\mathbf{k}} = \frac{16A_{\mathbf{k}}}{\epsilon_{\mathbf{k},1}^2}, \quad (\text{G4})$$

where $\epsilon_{\mathbf{k},1}$ is given in Eq. (180). We then compute the discrete sum numerically according to Eq. (G3) for the different system sizes, including the ones given in Table (I). When performing the sum, we also avoid the origin $\mathbf{k} = (0, 0)$, where $\epsilon_{\mathbf{k},1}$ vanishes, (indeed, $\gamma(0) = 1$, and according to Eq. (128), $A_0 = B_0$) and which is not included in the sum of Eq. (170). For a specific system size, we then get a number as the results of the discrete sum obtained for that specific system size. These numbers are plotted as the red dots in Fig. 14 (b).

According to Eq. (218), we assume that the system size dependency should be of the form

$$-\left. \frac{dS_Q^{CL}(\mathbf{q} = \Gamma)}{dT} \right|_{T=0} = \frac{1}{N} \sum_{\mathbf{k}} I_{\mathbf{k}} \sim C + \mu \log(L) + \frac{\nu}{L} + \frac{\xi}{L^2}. \quad (\text{G5})$$

We use Eq. (G5) to fit the results obtained by computing the discrete sum in Eq. (G3), i.e., the red dots in Fig. 14 (b). The fit is shown in in Fig. 14 (b) by the orange line.

Additionally, we want to investigate how accurate the discrete sum is, compared to the integration, and how it depends on system size. If we consider the integral version in 2-dimensions for polar coordinates, we can cut off to some small $k_s = \frac{4\pi}{\sqrt{3}L}$ in order to avoid the origin $\mathbf{k} = (0, 0)$ as follows:

$$\int I_{\mathbf{k}} d\mathbf{k} = 2\pi \int_0^\Lambda I_{\mathbf{k}} k dk = 2\pi \int_0^{k_s} I_{\mathbf{k}} k dk + 2\pi \int_{k_s}^\Lambda I_{\mathbf{k}} k dk. \quad (\text{G6})$$

For the FQ state, where we chose, $J_1 = 0.0$ and $J_2 = -1.0$, the coefficients $A_{\mathbf{k}}$ and $B_{\mathbf{k}}$ [Eq. (128)] and the dispersion relation $\epsilon_{\mathbf{k},1}$ [Eq. (180)] become

$$\begin{aligned} A_{\mathbf{k}} &= z, \\ B_{\mathbf{k}} &= -z\gamma(\mathbf{k}), \\ \epsilon_{\mathbf{k}}^2 &= z^2(1 - \gamma(\mathbf{k})^2). \end{aligned} \quad (\text{G7})$$

For the triangular lattice, the geometrical factor is given by Eq. (C5), and for sufficiently small values of \mathbf{k} , we can use the Taylor expansion on it. We obtain

$$\gamma(\mathbf{k}) \simeq 1 - \frac{1}{4}(k_x^2 + k_y^2) = 1 - \frac{1}{4}k^2, \quad (\text{G8a})$$

$$\epsilon_{\mathbf{k}}^2 \simeq z^2 \frac{1}{2}k^2, \quad (\text{G8b})$$

$$I_{\mathbf{k}} = \frac{16A_{\mathbf{k}}}{\epsilon_{\mathbf{k},1}^2} \simeq \frac{16z}{z^2 \frac{1}{2}k^2} = \frac{32}{zk^2}, \quad (\text{G8c})$$

$$2\pi \int_{k_s}^{k_f} I_{\mathbf{k}} k dk \simeq 2\pi \int_{k_s}^{k_f} \frac{32}{zk^2} k dk. \quad (\text{G8d})$$

Since $z = 6$ for the triangular lattice, we have

$$\begin{aligned} \frac{2\pi 16}{3} \int_{k_s}^{k_f} \frac{1}{k} dk &= \frac{2\pi 16}{3} (\log(k_f) - \log(k_s)), \\ &= \frac{2\pi 16}{3} \log(L) + \frac{2\pi 16}{3} \log(k_f) - \frac{2\pi 16}{3} \log\left(\frac{4\pi}{\sqrt{3}}\right), \end{aligned} \quad (\text{G9})$$

where in the last line, we used the fact that we chose to cut off according to $k_s = \frac{4\pi}{\sqrt{3}L}$. Before we fit the sum with the expression given by Eq. (G5), we need to account for correction coming from the tiling of the \mathbf{k} -space as explained in Eq. (G3). Therefore, we need to divide by

$$\delta A * N = \frac{8\pi^2}{\sqrt{3}}. \quad (\text{G10})$$

From Eq. (G5), we can obtain the value for the coefficient μ for Eq. (G9), which we can compare with the fit from the values of the sum calculated numerically as shown in Fig. 14 (b):

$$\mu_{ana} = \frac{\frac{2\pi 16}{3}}{\frac{8\pi^2}{\sqrt{3}}} = \frac{4}{\sqrt{3}\pi} = 0.735, \quad \mu_{num} = 0.735. \quad (\text{G11})$$

Appendix H: Useful Gaussian integrals

We present here useful Gaussian integrals that we used to calculate partition functions for the analytic derivations. We namely used the following one-dimensional Gaussian integrals

$$\int e^{-\frac{1}{2}ax^2} dx = \sqrt{\frac{2\pi}{a}}, \quad (\text{H1a})$$

$$\int e^{-\frac{1}{2}ax^2} e^{\pm bx} dx = \sqrt{\frac{2\pi}{a}} e^{\frac{b^2}{2a}}, \quad (\text{H1b})$$

$$\int e^{-\frac{1}{2}ax^2} e^{\pm ibx} dx = \sqrt{\frac{2\pi}{a}} e^{-\frac{b^2}{2a}}, \quad (\text{H1c})$$

which we can also generalize to a multi-dimensions integral with a source term

$$\int e^{-\frac{1}{2}x_i A_{ij} x_j + B_i x_i} d\vec{x} = \sqrt{\frac{(2\pi)^n}{\det A}} e^{\frac{1}{2}\vec{B}^T A^{-1} \vec{B}}. \quad (\text{H1d})$$

or more generally,

$$\int e^{-\frac{1}{2}x_i A^i_j x^j + B^T_{1,i} x^i + x_i B^i_2} d\vec{x} = \sqrt{\frac{(2\pi)^n}{\det A}} e^{2\vec{B}^T_1 A^{-1} \vec{B}_2}. \quad (\text{H1e})$$

where n is the dimension of the matrix \mathbf{A} . Below, we give the proof for Eq. (H1e).

Proof: We assume \mathbf{A} to be a real symmetric $n \times n$ -matrix. This means that \mathbf{A} is orthogonally diagonalizable, i.e., it is similar to a diagonal matrix $\mathbf{D} = \text{diag}(d^1_1, \dots, d^n_n)$

$$\mathbf{A} = \mathbf{S} \mathbf{D} \mathbf{S}^{-1}, \quad (\text{H2})$$

and the $n \times n$ basis change matrix \mathbf{S} is orthogonal. The basis change matrix \mathbf{S} then satisfies

$$\mathbf{S}^T = \mathbf{S}^{-1}, \quad (\text{H3})$$

and the old coordinates are related to the new ones by

$$\vec{x} = \mathbf{S} \vec{y}, \quad (\text{H4a})$$

$$\vec{x}^T = \vec{y} \mathbf{S}^T, \quad (\text{H4b})$$

$$d\vec{x} = \det \mathbf{S} d\vec{y} = d\vec{y}, \quad (\text{H4c})$$

where in the last line we used the fact that the Jacobian matrix of the map $\vec{x}(\vec{y}) \rightarrow \mathbf{S} \vec{y}$ is the matrix \mathbf{S} itself, and that its determinant is 1, since it is an orthogonal matrix. The term in the exponential in Eq. (H1e) then becomes

$$E := -\frac{1}{2} \vec{x}^T \mathbf{A} \vec{x} + \vec{B}^T_1 \vec{x} + \vec{x}^T \vec{B}_2 \quad (\text{H5a})$$

$$= -\frac{1}{2} \vec{y}^T \mathbf{D} \vec{y} + \vec{B}^T_1 \mathbf{S} \vec{y} + \vec{y}^T \mathbf{S}^{-1} \vec{B}_2. \quad (\text{H5b})$$

If we expand, we obtain:

$$E = \sum_i \left[-\frac{1}{2} y_i d^i_i y^i + \sum_{\alpha} (B^T_{1,\alpha} S^{\alpha}_i y^i + y_i (S^{-1})^i_{\alpha} B^{\alpha}_2) \right], \quad (\text{H5c})$$

where we used the fact that \mathbf{D} is a diagonal matrix. For the i^{th} term, we can complete the square as

$$\begin{aligned} & -\frac{1}{2} y_i d^i_i y^i + \sum_{\alpha} (B^T_{1,\alpha} S^{\alpha}_i y^i + y_i (S^{-1})^i_{\alpha} B^{\alpha}_2) \\ &= -\frac{1}{2} d^i_i (y_i - \frac{2}{d^i_i} \sum_{\alpha} B^T_{1,\alpha} S^{\alpha}_i) (y^i - \frac{2}{d^i_i} \sum_{\beta} (S^{-1})^i_{\beta} B^{\beta}_2) \\ & \quad + 2 \sum_{\alpha} \sum_{\beta} B^T_{1,\alpha} S^{\alpha}_i \frac{1}{d^i_i} (S^{-1})^i_{\beta} B^{\beta}_2. \end{aligned} \quad (\text{H6})$$

Using again the fact that d^i_i is the i^{th} diagonal term of \mathbf{D} , and inverting Eq. (H2), we can rewrite $\frac{1}{d^i_i}$ as

$$\frac{1}{d^i_i} = (D^{-1})^i_i = \sum_{\mu,\nu} (S^{-1})^i_{\mu} (A^{-1})^{\mu}_{\nu} (S)^{\nu}_i. \quad (\text{H7})$$

Performing the variable change as

$$z_i = y_i - \frac{2}{d^i_i} \sum_{\alpha} B^T_{1,\alpha} S^{\alpha}_i, \quad (\text{H8a})$$

$$z^i = y^i - \frac{2}{d^i_i} \sum_{\beta} (S^{-1})^i_{\beta} B^{\beta}_2, \quad (\text{H8b})$$

$$d\vec{z} = d\vec{y}, \quad (\text{H8c})$$

and inserting Eq. (H7) into the last term of Eq. (H6), and summing over all the components, we obtain

$$E = -\frac{1}{2} \vec{z}^T \mathbf{D} \vec{z} + 2\vec{B}^T_1 (\mathbf{A}^{-1}) \vec{B}_2. \quad (\text{H9a})$$

We now have the product of n Gaussian integrals of the form of Eq. (H1a)

$$\begin{aligned} & \int e^{-\frac{1}{2}x_i A^i_j x^j + B^T_{1,i} x^i + x_i B^i_2} d\vec{x} = \\ &= \left[\prod_i \int e^{-\frac{1}{2}z_i d^i_i z^i} dz_i \right] e^{2\vec{B}^T_1 (\mathbf{A}^{-1}) \vec{B}_2} \\ &= \sqrt{\frac{(2\pi)^n}{\prod_i d^i_i}} e^{2\vec{B}^T_1 (\mathbf{A}^{-1}) \vec{B}_2}. \end{aligned} \quad (\text{H10})$$

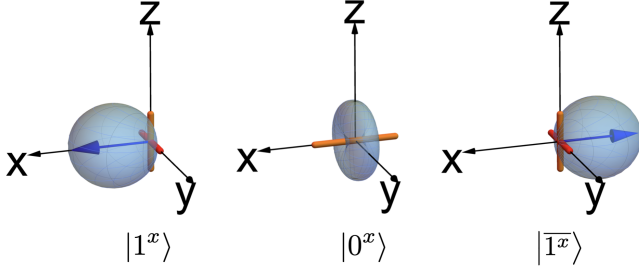
We then use the fact that

$$\det \mathbf{A} = \det \mathbf{S} \det \mathbf{D} \det \mathbf{S}^{-1} = \det \mathbf{D} = \prod_i d^i_i, \quad (\text{H11})$$

to obtain Eq. (H1e)

Appendix I: Application to an easy-plane ferromagnet

We here wish to apply the $u(3)$ formalism and its representation in terms of the A-matrices to the Heisenberg ferromagnetic easy-plane anisotropic model. The A-matrices are especially useful to work with on the TR-invariant basis, and relatively easy to use when the ground state is quadrupolar. However, some attention is demanded when working with systems

Figure 22. Eigenstates of \hat{S}_i^x and basis states of \mathcal{B}^x

where dipoles rather than quadrupoles order. We demonstrate here how one can carefully apply our method for dipolar ordering. Additionally, as explained in Section VIII, we make the interactions anisotropic. We show results for the zero-temperature quantum structure factors for dipole, quadrupole and A-matrix moments applied to the ferromagnetic (FM) state on the triangular lattice for the anisotropic Heisenberg Hamiltonian (BBQ Hamiltonian [Eq. (1)] with anisotropic J_1 and $J_2 = 0$), with single-ion anisotropy. such that

$$\langle 1^x | \hat{S}_i^x | 1^x \rangle = 1, \quad (\text{I1a})$$

$$\langle 0^x | \hat{S}_i^x | 0^x \rangle = 0, \quad (\text{I1b})$$

$$\langle \bar{1}^x | \hat{S}_i^x | \bar{1}^x \rangle = -1, \quad (\text{I1c})$$

$$\langle \alpha | \hat{S}_i^\mu | \alpha \rangle = 0 \quad \text{for } |\alpha\rangle \in \mathcal{B}^x \text{ and } \mu = y, z. \quad (\text{I1d})$$

We consider the following Hamiltonian

$$\mathcal{H} = \mathcal{H}^{\text{EP}} + \mathcal{H}^{\text{SI}}. \quad (\text{I2})$$

\mathcal{H}^{EP} represents the Heisenberg Hamiltonian for spin-1 with easy-plane Heisenberg anisotropic exchange couplings \mathbf{J}

$$\mathcal{H}^{\text{EP}} = \sum_{\langle i,j \rangle} [\hat{\mathbf{S}}_i \cdot \mathbf{J} \cdot \hat{\mathbf{S}}_j], \quad (\text{I3})$$

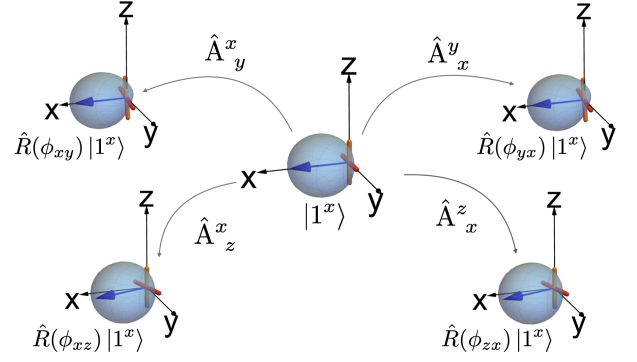
where the spin dipole operator $\hat{\mathbf{S}}_i$ is defined in Eq. (2), and where \mathbf{J} corresponds to the usual nearest neighbor spin-spin coupling tensor. \mathcal{H}^{SI} accounts for single-ion anisotropy and is given by

$$\mathcal{H}^{\text{SI}} = \sum_i \hat{\mathbf{S}}_i \mathbf{D} \hat{\mathbf{S}}_i, \quad (\text{I4})$$

where \mathbf{D} corresponds to the usual single site spin-spin coupling tensor. We assume the spin-spin coupling tensors \mathbf{J} and \mathbf{D} to only have diagonal components:

$$\mathcal{H}^{\text{EP}} = \sum_{\langle i,j \rangle} [J^{xx} \hat{S}_i^x \hat{S}_j^x + J^{yy} \hat{S}_i^y \hat{S}_j^y + J^{zz} \hat{S}_i^z \hat{S}_j^z], \quad (\text{I5})$$

$$\mathcal{H}^{\text{SI}} = \sum_i [D^{xx} \hat{S}_i^x \hat{S}_i^x + D^{yy} \hat{S}_i^y \hat{S}_i^y + D^{zz} \hat{S}_i^z \hat{S}_i^z]. \quad (\text{I6})$$

Figure 23. Fluctuations created by the generators $\hat{\mathcal{A}}_y^x$, $\hat{\mathcal{A}}_z^x$, $\hat{\mathcal{A}}_x^y$, and $\hat{\mathcal{A}}_x^z$, according to Eq. (117), for an angle $\phi_{\alpha\beta} = \frac{\pi}{8}$.

We also assume the coupling constants to be negative and the order to be ferromagnetic:

$$J^{\alpha\alpha} < 0, \quad (\text{I7})$$

$$D^{\alpha\alpha} < 0. \quad (\text{I8})$$

We can assume the ground state to be a state with the spin pointing somewhere in the xy-plane, and we can choose it to be pointing along the x-axis:

$$|GS\rangle = |1^x\rangle. \quad (\text{I9})$$

As a basis, we choose the eigenstates of \hat{S}_i^x :

$$\mathcal{B}^x = \{|1^x\rangle, |0^x\rangle, |\bar{1}^x\rangle\}, \quad (\text{I10})$$

as represented in Fig. 22,

Even though the A-matrices are deeply linked to the time-reversal (TR) invariant basis, we will here mostly focus on the basis \mathcal{B}^x [Eq. (I10)] and then transform the required quantities accordingly.

To do that, we remember that the spin dipole moments can be rewritten in terms of the A matrices [Eq. (50)], expressed in the time-reversal (TR) invariant basis [Eq. (36)] as shown in Fig. 5. Using Eq. (50), the terms of the easy-plane anisotropic Hamiltonian [Eq. (15)], in terms of the A-matrices, becomes

$$\hat{S}_i^x \hat{S}_j^x = -(\hat{\mathcal{A}}_{i,z}^y - \hat{\mathcal{A}}_{i,y}^z)(\hat{\mathcal{A}}_{j,z}^y - \hat{\mathcal{A}}_{j,y}^z), \quad (\text{I11a})$$

$$\hat{S}_i^y \hat{S}_j^y = -(\hat{\mathcal{A}}_{i,x}^z - \hat{\mathcal{A}}_{i,z}^x)(\hat{\mathcal{A}}_{j,x}^z - \hat{\mathcal{A}}_{j,z}^x), \quad (\text{I11b})$$

$$\hat{S}_i^z \hat{S}_j^z = (\hat{\mathcal{A}}_{i,y}^x - \hat{\mathcal{A}}_{i,x}^y)(\hat{\mathcal{A}}_{j,y}^x - \hat{\mathcal{A}}_{j,x}^y). \quad (\text{I11c})$$

For the single ion terms, we use Eq. (26) and Eq. (51) to rewrite the terms $\hat{S}_i^\alpha \hat{S}_i^\alpha$ of the single-ion anisotropic Hamiltonian [Eq. (16)] in the function of the A-matrices, as

$$\hat{S}_i^x \hat{S}_i^x = -\frac{2}{3} \hat{\mathcal{A}}_{i,x}^x + \frac{1}{3} \hat{\mathcal{A}}_{i,y}^y + \frac{1}{3} \hat{\mathcal{A}}_{i,z}^z + \frac{2}{3}, \quad (\text{I12a})$$

$$\hat{S}_i^y \hat{S}_i^y = -\frac{2}{3} \hat{\mathcal{A}}_{i,y}^y + \frac{1}{3} \hat{\mathcal{A}}_{i,x}^x + \frac{1}{3} \hat{\mathcal{A}}_{i,z}^z + \frac{2}{3}, \quad (\text{I12b})$$

$$\hat{S}_i^z \hat{S}_i^z = -\frac{2}{3} \hat{\mathcal{A}}_{i,z}^z + \frac{1}{3} \hat{\mathcal{A}}_{i,y}^y + \frac{1}{3} \hat{\mathcal{A}}_{i,x}^x + \frac{2}{3}. \quad (\text{I12c})$$

Using Eq. (I11) and Eq. (I12), the total Hamiltonian [Eq. (I2)] in terms of the A-matrices then becomes

$$\begin{aligned} \mathcal{H} = & \sum_{\langle i,j \rangle} \left[-J^{xx}(\hat{\mathcal{A}}_{i,z}^y - \hat{\mathcal{A}}_{i,y}^z)(\hat{\mathcal{A}}_{j,z}^y - \hat{\mathcal{A}}_{j,y}^z) \right. \\ & -J^{yy}(\hat{\mathcal{A}}_{i,x}^z - \hat{\mathcal{A}}_{i,z}^x)(\hat{\mathcal{A}}_{j,x}^z - \hat{\mathcal{A}}_{j,z}^x) \\ & \left. -J^{zz}(\hat{\mathcal{A}}_{i,y}^x - \hat{\mathcal{A}}_{i,x}^y)(\hat{\mathcal{A}}_{j,y}^x - \hat{\mathcal{A}}_{j,x}^y) \right] \\ & + \sum_i \left[D^{xx} \left(-\frac{2}{3}\hat{\mathcal{A}}_{i,x}^x + \frac{1}{3}\hat{\mathcal{A}}_{i,y}^y + \frac{1}{3}\hat{\mathcal{A}}_{i,z}^z + \frac{2}{3} \right) \right. \\ & + D^{yy} \left(-\frac{2}{3}\hat{\mathcal{A}}_{i,y}^y + \frac{1}{3}\hat{\mathcal{A}}_{i,x}^x + \frac{1}{3}\hat{\mathcal{A}}_{i,z}^z + \frac{2}{3} \right) \\ & \left. + D^{zz} \left(-\frac{2}{3}\hat{\mathcal{A}}_{i,z}^z + \frac{1}{3}\hat{\mathcal{A}}_{i,y}^y + \frac{1}{3}\hat{\mathcal{A}}_{i,x}^x + \frac{2}{3} \right) \right]. \quad (\text{I13}) \end{aligned}$$

If we define the basis change Λ_3 to be the basis change matrix between \mathcal{B}_2 and \mathcal{B}^x , such that if a state $|\phi\rangle_{\mathcal{B}_2}$ is given in the TR invariant basis \mathcal{B}_2 , in the basis \mathcal{B}^x , its components are given by

$$|\phi\rangle_{\mathcal{B}^x} = \Lambda_3 |\phi\rangle_{\mathcal{B}_2}. \quad (\text{I14})$$

We found that the basis change matrix Λ_3 yields

$$\Lambda_3 = \begin{pmatrix} 0 & \frac{1}{\sqrt{2}} & \frac{i}{\sqrt{2}} \\ -i & 0 & 0 \\ 0 & \frac{1}{\sqrt{2}} & -\frac{i}{\sqrt{2}} \end{pmatrix}. \quad (\text{I15})$$

An operator $\hat{\mathcal{O}}_{\mathcal{B}_2}$ given in the TR invariant basis \mathcal{B}_2 is expressed as

$$\hat{\mathcal{O}}_{\mathcal{B}^x} = \Lambda_3 \hat{\mathcal{O}}_{\mathcal{B}_2} \Lambda_3^\dagger, \quad (\text{I16})$$

in the basis \mathcal{B}^x .

We will start working the basis \mathcal{B}^x , where everything is simple, since the ground state is one of the basis states and the orthogonal fluctuations can be expressed in terms of the other orthogonal basis states. Indeed, the ground state matrix takes the simple form

$$\mathbf{A}_{\mathbf{0}\mathcal{B}^x} = \begin{pmatrix} 1 & 0 & 0 \\ 0 & 0 & 0 \\ 0 & 0 & 0 \end{pmatrix}, \quad (\text{I17})$$

since the ground state is simply the state $|1^x\rangle$ [Eq. (I9)] or expressed in terms of director components

$$\mathbf{d}_{\mathbf{0}\mathcal{B}^x}^\dagger = \begin{pmatrix} 1 \\ 0 \\ 0 \end{pmatrix}. \quad (\text{I18})$$

We can generate orthogonal fluctuations by application of the exponential map given in Eq. (I17). The new state describing the fluctuations around the ground state is given by

$$\mathbf{d}^\dagger(\phi) = \hat{R}(\phi) \mathbf{d}_{\mathbf{0}}^\dagger. \quad (\text{I19})$$

The A matrix transforms according to Eq. (I18). Only the generators $\hat{\mathcal{A}}_x^x$, $\hat{\mathcal{A}}_y^y$, $\hat{\mathcal{A}}_z^z$, $\hat{\mathcal{A}}_x^y$, and $\hat{\mathcal{A}}_x^z$ will have non zero contribution when applied to the ground state matrix [Eq. (I17)]. Fig. 23 represents the action of the generators on the ground state. We can see, for example, that the generator $\hat{\mathcal{A}}_y^x$, will create a fluctuation along $|0^x\rangle$, i.e. an \hat{a}^\dagger boson, and will induce the new state to exhibit some quadrupolar features.

Using the constraint on the trace of A-matrices [Eq. (49)], we express the contribution from $\hat{\mathcal{A}}_x^x$ in terms of the others components in order to ensure the length of the spin to be $S = 1$ (which is equivalent to constraining the trace of A to be equal to 1), so that we properly restrict to $su(3)$ and make sure that we are correctly representing a spin-1. We obtain

$$\mathbf{A}(\phi)_{\mathcal{B}^x} = \begin{pmatrix} 1 - \phi_{xy}\phi_{yx} - \phi_{xz}\phi_{zx} & i\phi_{xy} & i\phi_{xz} \\ -i\phi_{yx} & \phi_{xy}\phi_{yx} & \phi_{xz}\phi_{yx} \\ -i\phi_{zx} & \phi_{xy}\phi_{zx} & \phi_{xz}\phi_{zx} \end{pmatrix}. \quad (\text{I20})$$

We can then easily introduce bosonic fluctuations by

$$i\phi_{xy} = \hat{a}, \quad (\text{I21a})$$

$$-i\phi_{yx} = \hat{a}^\dagger, \quad (\text{I21b})$$

$$i\phi_{xz} = \hat{b}, \quad (\text{I21c})$$

$$-i\phi_{zx} = \hat{b}^\dagger, \quad (\text{I21d})$$

such that we get

$$\hat{\mathbf{A}}_{\mathcal{B}^x} = \begin{pmatrix} 1 - \hat{a}_i^\dagger \hat{a}_i - \hat{b}_i^\dagger \hat{b}_i & \hat{a}_i & \hat{b}_i \\ \hat{a}_i^\dagger & \hat{a}_i^\dagger \hat{a}_i & \hat{a}_i^\dagger \hat{b}_i \\ \hat{b}_i^\dagger & \hat{a}_i \hat{b}_i^\dagger & \hat{b}_i^\dagger \hat{b}_i \end{pmatrix}. \quad (\text{I22})$$

According to Eq. (I16), the A matrices expressed in the TR invariant basis \mathcal{B}_2 are given by

$$\begin{aligned} \hat{\mathbf{A}}_{\mathcal{B}_2} &= \Lambda_3^\dagger \hat{\mathbf{A}}_{\mathcal{B}^x} \Lambda_3 \\ &= \begin{pmatrix} \hat{a}_i^\dagger \hat{a}_i & & & & & \\ -\frac{i}{\sqrt{2}} \hat{a}_i - \frac{i}{\sqrt{2}} \hat{a}_i \hat{b}_i^\dagger & \frac{1}{2} + \frac{1}{2} \hat{b}_i^\dagger + \frac{1}{2} \hat{b}_i - \frac{1}{2} \hat{a}_i^\dagger \hat{a}_i & & & & \\ -\frac{1}{\sqrt{2}} \hat{a}_i + \frac{1}{\sqrt{2}} \hat{a}_i \hat{b}_i^\dagger & -\frac{i}{2} - \frac{i}{2} \hat{b}_i + \frac{i}{2} \hat{b}_i^\dagger + \frac{i}{2} \hat{a}_i^\dagger \hat{a}_i + i \hat{b}_i^\dagger \hat{b}_i & & & & \\ & & \frac{i}{2} + \frac{i}{2} \hat{b}_i^\dagger - \frac{i}{2} \hat{b}_i - \frac{i}{2} \hat{a}_i^\dagger \hat{a}_i - i \hat{b}_i^\dagger \hat{b}_i & & & \\ & & \frac{1}{2} - \frac{1}{2} \hat{b}_i^\dagger - \frac{1}{2} \hat{b}_i - \frac{1}{2} \hat{a}_i^\dagger \hat{a}_i & & & \end{pmatrix}. \quad (\text{I23}) \end{aligned}$$

Inserting Eq. (I23) into Eq. (I12), we get the single-ion terms in the function of the bosons

$$\begin{aligned}\hat{S}_i^x \hat{S}_i^x &= 1 - \hat{a}_i^\dagger \hat{a}_i, \\ \hat{S}_i^y \hat{S}_i^y &= \frac{1}{2}(1 + \hat{a}_i^\dagger \hat{a}_i - \hat{b}_i^\dagger - \hat{b}_i), \\ \hat{S}_i^z \hat{S}_i^z &= \frac{1}{2}(1 + \hat{a}_i^\dagger \hat{a}_i + \hat{b}_i^\dagger + \hat{b}_i).\end{aligned}\quad (\text{I24})$$

We notice that if D^{yy} is not equal to D^{zz} , then the Hamiltonian [Eq. (I13)] has single bosons terms, meaning that the state about which we expanded the fluctuations is not the ground state any more. Therefore, to be consistent with the easy-plane FM order and the ground state [Eq. (I9)], we choose

$$D^\perp = D^{yy} = D^{zz} \text{ with } |D^\perp| < |D^{xx}|. \quad (\text{I25})$$

After inserting Eq. (I23) into the total Hamiltonian [Eq. (I13)], only keeping fluctuations up to 2nd order, and performing a Fourier transform, the Hamiltonian [Eq. (I13)] becomes

$$\begin{aligned}\mathcal{H} &= \frac{1}{2} \sum_{\mathbf{k}} \left[\begin{pmatrix} \hat{a}_{\mathbf{k}}^\dagger & \hat{a}_{-\mathbf{k}} \end{pmatrix} \begin{pmatrix} A_{\mathbf{k}} & B_{\mathbf{k}} \\ B_{\mathbf{k}} & A_{\mathbf{k}} \end{pmatrix} \begin{pmatrix} \hat{a}_{\mathbf{k}} \\ \hat{a}_{-\mathbf{k}}^\dagger \end{pmatrix} \right. \\ &\quad \left. + \begin{pmatrix} \hat{b}_{\mathbf{k}}^\dagger & \hat{b}_{-\mathbf{k}} \end{pmatrix} \begin{pmatrix} C_{\mathbf{k}} & 0 \\ 0 & C_{\mathbf{k}} \end{pmatrix} \begin{pmatrix} \hat{b}_{\mathbf{k}} \\ \hat{b}_{-\mathbf{k}}^\dagger \end{pmatrix} \right] \\ &\quad + \frac{1}{2} N z J^{xx} + N(D^{xx} + D^\perp),\end{aligned}\quad (\text{I26})$$

where

$$\begin{aligned}A_{\mathbf{k}} &= -J^{xx} z + \frac{1}{2} z (J^{yy} + J^{zz}) \gamma(\mathbf{k}) + (D^\perp - D^{xx}), \\ B_{\mathbf{k}} &= \frac{1}{2} z (J^{zz} - J^{yy}) \gamma(\mathbf{k}), \\ C_{\mathbf{k}} &= -2z J^{xx}.\end{aligned}\quad (\text{I27})$$

Similarly to the FQ case, we need to solve an eigensystem analogous to Eq. (I78). The dispersion relations for $\hat{a}_{\mathbf{k}}^\dagger$ and $\hat{a}_{\mathbf{k}}$ can be found by imposing them to have bosonic commutation relations [Eq. (E3)], and diagonalizing

$$\sigma_z \begin{pmatrix} A_{\mathbf{k}} & B_{\mathbf{k}} \\ B_{\mathbf{k}} & A_{\mathbf{k}} \end{pmatrix} = \begin{pmatrix} 1 & 0 \\ 0 & -1 \end{pmatrix} \begin{pmatrix} A_{\mathbf{k}} & B_{\mathbf{k}} \\ B_{\mathbf{k}} & A_{\mathbf{k}} \end{pmatrix} = \begin{pmatrix} A_{\mathbf{k}} & B_{\mathbf{k}} \\ -B_{\mathbf{k}} & -A_{\mathbf{k}} \end{pmatrix}, \quad (\text{I28})$$

where the multiplication by σ_z imposes the bosonic commutation relations. The eigenvalues $\epsilon_{\mathbf{k}}$ are given by

$$\epsilon_{\mathbf{k},1} = +\sqrt{A_{\mathbf{k}}^2 - B_{\mathbf{k}}^2}, \quad \epsilon_{\mathbf{k},2} = -\sqrt{A_{\mathbf{k}}^2 - B_{\mathbf{k}}^2}. \quad (\text{I29})$$

The dispersion relations for the $\hat{b}_{\mathbf{k}}^\dagger$ and $\hat{b}_{\mathbf{k}}$ are obtained by diagonalizing

$$\sigma_z \begin{pmatrix} C_{\mathbf{k}} & 0 \\ 0 & C_{\mathbf{k}} \end{pmatrix} = \begin{pmatrix} C_{\mathbf{k}} & 0 \\ 0 & -C_{\mathbf{k}} \end{pmatrix}. \quad (\text{I30})$$

The eigenvalues $\epsilon_{\mathbf{k}}$ are given by

$$\epsilon_{\mathbf{k},3} = -C_{\mathbf{k}}, \quad \epsilon_{\mathbf{k},4} = +C_{\mathbf{k}}. \quad (\text{I31})$$

Because the coupling constants are negative, the physical results are

$$\epsilon_{\mathbf{k},1} = +\sqrt{A_{\mathbf{k}}^2 - B_{\mathbf{k}}^2}, \quad \epsilon_{\mathbf{k},3} = -C_{\mathbf{k}} = 2z|J^{xx}|, \quad (\text{I32})$$

where $A_{\mathbf{k}}$, $B_{\mathbf{k}}$, and $C_{\mathbf{k}}$ are given in Eq. (I27).

Following the same procedure as for the FQ state in Section V, we calculate dynamical structure factors for the anisotropic FM case. We start by finding the Bogoliubov transformation that diagonalizes Eq. (I26). Following the steps given in Appendix E, we get

$$\hat{a}_{\mathbf{k}} = \frac{1}{\sqrt{\Delta_{\mathbf{k}}^2 - B_{\mathbf{k}}^2}} (\Delta_{\mathbf{k}} \hat{\alpha}_{\mathbf{k}} - B_{\mathbf{k}} \hat{\alpha}_{-\mathbf{k}}^\dagger), \quad (\text{I33a})$$

$$\hat{a}_{-\mathbf{k}}^\dagger = \frac{1}{\sqrt{\Delta_{\mathbf{k}}^2 - B_{\mathbf{k}}^2}} (-B_{\mathbf{k}} \hat{\alpha}_{\mathbf{k}} + \Delta_{\mathbf{k}} \hat{\alpha}_{-\mathbf{k}}^\dagger), \quad (\text{I33b})$$

$$\hat{a}_{\mathbf{k}}^\dagger = \frac{1}{\sqrt{\Delta_{\mathbf{k}}^2 - B_{\mathbf{k}}^2}} (\Delta_{\mathbf{k}} \hat{\alpha}_{\mathbf{k}}^\dagger - B_{\mathbf{k}} \hat{\alpha}_{-\mathbf{k}}), \quad (\text{I33c})$$

$$\hat{a}_{-\mathbf{k}} = \frac{1}{\sqrt{\Delta_{\mathbf{k}}^2 - B_{\mathbf{k}}^2}} (-B_{\mathbf{k}} \hat{\alpha}_{\mathbf{k}}^\dagger + \Delta_{\mathbf{k}} \hat{\alpha}_{-\mathbf{k}}), \quad (\text{I33d})$$

and

$$\hat{b}_{\mathbf{k}} = \hat{\beta}_{\mathbf{k}}, \quad (\text{I34a})$$

$$\hat{b}_{-\mathbf{k}}^\dagger = \hat{\beta}_{-\mathbf{k}}^\dagger, \quad (\text{I34b})$$

$$\hat{b}_{\mathbf{k}}^\dagger = \hat{\beta}_{\mathbf{k}}^\dagger, \quad (\text{I34c})$$

$$\hat{b}_{-\mathbf{k}} = \hat{\beta}_{-\mathbf{k}}, \quad (\text{I34d})$$

where $\Delta_{\mathbf{k}}$ is given in Eq. (I83), and where $A_{\mathbf{k}}$ and $B_{\mathbf{k}}$ are given in Eq. (I27).

We follow now the calculations outlined in Section F1 in order to calculate the quantum structure factors. Since we are working in the Bogoliubov representation, the ground state |GS) is the vacuum state |vac) for the Bogoliubov bosons. The structure factors are given by Eq. (I87). We calculate $\langle \text{vac} | \hat{O}_{\mathbf{q}}^\alpha | \mu \rangle$ with $|\mu\rangle = \hat{\alpha}_{\mathbf{k}}^\dagger |\text{vac}\rangle \oplus \hat{\beta}_{\mathbf{k}}^\dagger |\text{vac}\rangle$ and $\hat{O}_{\mathbf{q}}^\alpha = \hat{S}_{\mathbf{k}}^\alpha$ with $\alpha = x, y, z$, for the dipole structure factor for instance. Using Eq. (50), Eq. (51) and Eq. (I23), we can rewrite the spin dipole, the spin quadrupole, and the A-matrix operators in terms of the bosons up to linear order, and after performing a Fourier transform, we can rewrite them in terms of the Bogoliubov bosons using Eq. (I33) and Eq. (I34). This allows to easily calculate the structure factors [Eq. (I87)].

Using Eq. (F4), the dynamical spin dipole structure factor, defined by Eq. (F9), is given by

$$S_S^{\text{FM}}(\mathbf{q}, \omega) = \frac{A_{\mathbf{q}}}{\sqrt{A_{\mathbf{q}}^2 - B_{\mathbf{q}}^2}} \delta(\omega - \epsilon_{\mathbf{q},1}) + S_S^{\text{GSFM}}(\mathbf{q} = 0, \omega). \quad (\text{I35})$$

The dynamical spin quadrupole structure factor, as given by Eq. (F16), yields

$$\begin{aligned}S_Q^{\text{FM}}(\mathbf{q}, \omega) &= 2 \frac{A_{\mathbf{q}}}{\sqrt{A_{\mathbf{q}}^2 - B_{\mathbf{q}}^2}} \delta(\omega - \epsilon_{\mathbf{q},1}) + 4\delta(\omega - \epsilon_{\mathbf{q},3}) \\ &\quad + S_Q^{\text{GSFM}}(\mathbf{q} = 0, \omega).\end{aligned}\quad (\text{I36})$$

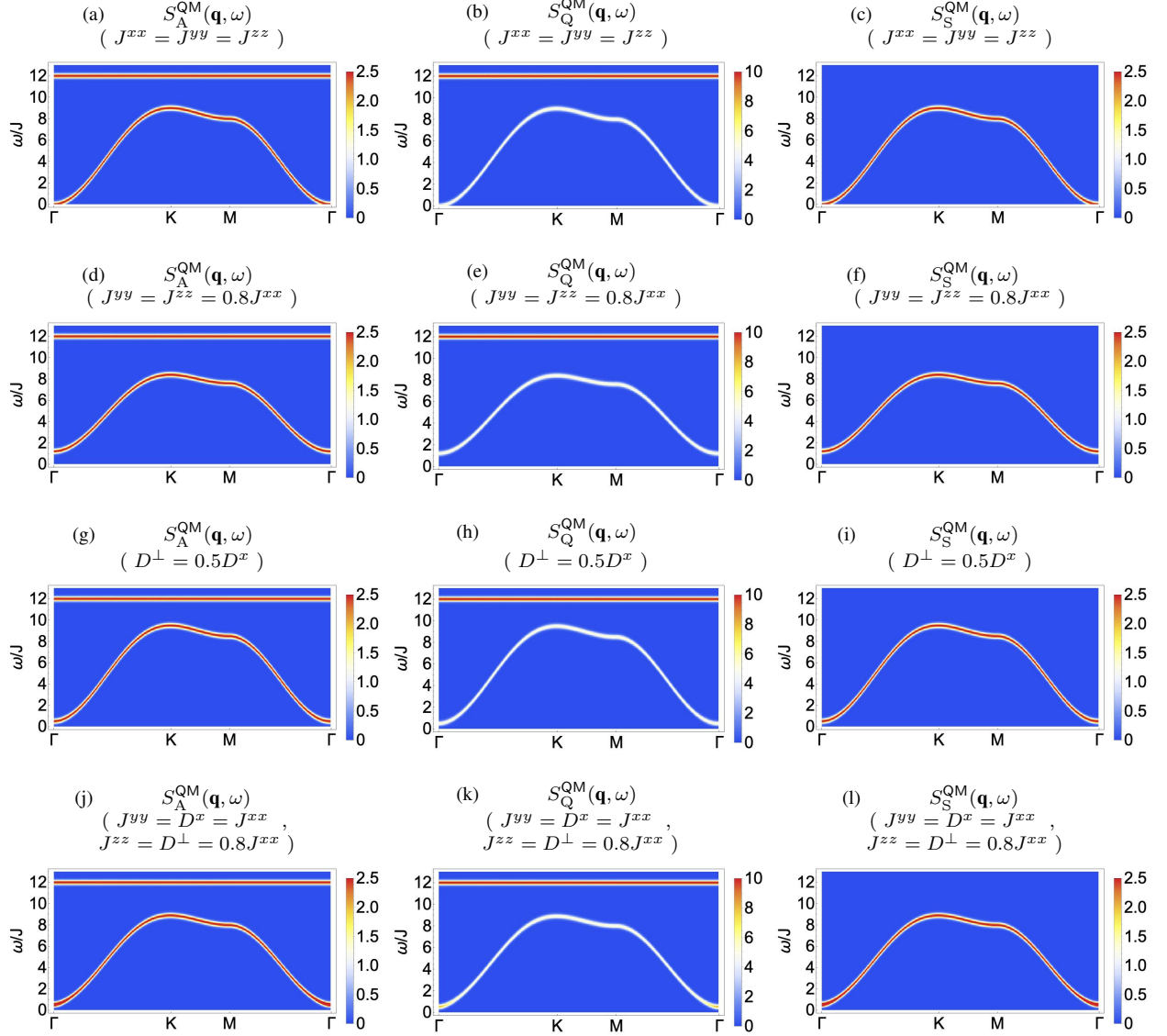


Figure 24. Dynamical structure factors obtained from zero-T quantum calculations for $S_A(\mathbf{q}, \omega)$ (A-matrices consisting of a mixture of dipolar and quadrupolar moments), $S_Q(\mathbf{q}, \omega)$ (quadrupolar moments) and $S_S(\mathbf{q}, \omega)$ (dipolar moments) for the ferromagnetic (FM) phase of the BBQ model on the triangular lattice (Eq. (9)) with J_1 being considered as Heisenberg anisotropic exchange interactions [Eq. (15)] and $J_2 = 0$, and with an additional single ion anisotropic exchange Hamiltonian [Eq. (16)]. (a)–(c) Dynamical structure factors obtained for the isotropic FM state of the Heisenberg Hamiltonian [Eq. (15)] where $J^{xx} = J^{yy} = J^{zz} = -1$ without any single-ion anisotropy [Eq. (16)], $D^\perp = D^x = 0$. (d)–(f) Dynamical structure factors obtained for the easy-plane anisotropic FM state of the Heisenberg Hamiltonian [Eq. (15)] where $J^{yy} = J^{zz} = 0.8J^{xx}$ and $J^{xx} = -1$ without any single-ion anisotropy [Eq. (16)], $D^\perp = D^x = 0$. (g)–(i) Dynamical structure factors obtained for the isotropic FM state of the Heisenberg Hamiltonian [Eq. (15)] where $J^{yy} = J^{zz} = J^{xx} = -1$ with single-ion anisotropy [Eq. (16)], $D^\perp = 0.5D^x$ and $D^x = J^{xx}$. (j)–(l) Dynamical structure factors obtained for the easy-plane anisotropic FM state of the Heisenberg Hamiltonian [Eq. (15)] where $J^{zz} = 0.8J^{xx}$ and $J^{yy} = J^{xx} = -1$ with single-ion anisotropy [Eq. (16)], $D^\perp = 0.8D^x$ and $D^x = J^{xx}$.

The total dynamical factor for the \hat{A} operators defined in Eq. (F21) becomes

$$S_A^{\text{FM}}(\mathbf{q}, \omega) = \frac{A_{\mathbf{q}}}{\sqrt{A_{\mathbf{q}}^2 - B_{\mathbf{q}}^2}} \delta(\omega - \epsilon_{\mathbf{q},1}) + \delta(\omega - \epsilon_{\mathbf{q},3}) + S_A^{\text{GSFM}}(\mathbf{q} = 0, \omega), \quad (\text{I37})$$

where we explicitly summed over the indexes α and β and where the terms of the form $S_O^{\text{GSFM}}(\mathbf{q} = 0, \omega)$ represent the ground state and zero-point energy contribution to the structure factors at $\mathbf{q} = 0$, but are not calculated here, for simplicity reasons. For these 3 results, Eq. (I35), Eq. (I36), and Eq. (I37), we used Eq. (I83), and $\epsilon_{\mathbf{q},1}$, and $\epsilon_{\mathbf{q},3}$ are given in Eq. (I32).

We also check that the sum rule Eq. (66) is indeed satisfied after noticing that the constant terms in Eq. (66) would only contribute for $\mathbf{q} = 0$ and at equal time, and can therefore be neglected. These results are identical to results that one can obtain by performing a conventional multi-bosons expansion.

In Fig. 24, we show results for the dynamical structure factors [Eq. (I35), Eq. (I36), and Eq. (I37)] for the ferromagnetic

state for the anisotropic Heisenberg Hamiltonian with single-ion anisotropy [Eq. (I2)] on the triangular lattice. We first notice that the quadrupolar band $\epsilon_{\mathbf{q},3}$, which corresponds to the $\Delta S = 2$ excitation band associated with the $\beta_{\mathbf{k}}^{\dagger}$ boson, is gapped and non-dispersive. Because it essentially corresponds to the excitation obtained by applying the lowering operator S^+ twice, it is quadrupolar in nature and will only contribute to the quadrupolar structure factor channel. Moreover, such a quadrupolar excitation from a FM ground state has a finite energy cost, and it also doesn't have any neighboring quadrupoles to interact with, so it is therefore localized. The isotropic FM Heisenberg case without single-ion anisotropy is presented in Fig. 24 (a)–(c). As shown in Fig. 24 (d)–(f), we note that the introduction of easy-plane anisotropy with $J^{yy} = J^{zz} \neq J^{xx}$ creates a gap and lifts the dispersion relation according to Eq. (I32) and Eq. (I27). In Fig. 24 (g)–(i), we see that introducing single-ion anisotropy with $D^{\perp} \neq D^{xx}$ also creates a gap and lifts the dispersion relation again according to Eq. (I32) and Eq. (I27). In Fig. 24 (j)–(l), we display the interplay of easy-plane and single-ion anisotropy.

-
- [1] A. Abragam, *The Principles of Nuclear Magnetism* (Oxford University Press, 1961).
 - [2] A. Abragam and B. Bleaney, *Paramagnetic Resonance of Transition Metal Ions* (Oxford University Press, 1970).
 - [3] Patrick Fazekas, *LECTURE NOTES ON ELECTRON CORRELATION AND MAGNETISM* (World Scientific, 1999).
 - [4] Daniel I. Khomskii, *Transition Metal Compounds* (Cambridge University Press, 2014).
 - [5] F.D.M. Haldane, "Continuum dynamics of the 1-D Heisenberg antiferromagnet: Identification with the O(3) nonlinear sigma model," *Physics Letters A* **93**, 464–468 (1983).
 - [6] F. D. M. Haldane, "Nonlinear Field Theory of Large-Spin Heisenberg Antiferromagnets: Semiclassically Quantized Solitons of the One-Dimensional Easy-Axis Néel State," *Phys. Rev. Lett.* **50**, 1153–1156 (1983).
 - [7] Ian Affleck, Tom Kennedy, Elliott H. Lieb, and Hal Tasaki, "Rigorous results on valence-bond ground states in antiferromagnets," *Phys. Rev. Lett.* **59**, 799–802 (1987).
 - [8] Elliott Lieb, Theodore Schultz, and Daniel Mattis, "Two soluble models of an antiferromagnetic chain," *Annals of Physics* **16**, 407–466 (1961).
 - [9] Zheng-Cheng Gu and Xiao-Gang Wen, "Tensor-entanglement-filtering renormalization approach and symmetry-protected topological order," *Phys. Rev. B* **80**, 155131 (2009).
 - [10] Frank Pollmann, Erez Berg, Ari M. Turner, and Masaki Oshikawa, "Symmetry protection of topological phases in one-dimensional quantum spin systems," *Phys. Rev. B* **85**, 075125 (2012).
 - [11] T. Holstein and H. Primakoff, "Field dependence of the intrinsic domain magnetization of a ferromagnet," *Phys. Rev.* **58**, 1098–1113 (1940).
 - [12] P. W. Anderson, "An approximate quantum theory of the antiferromagnetic ground state," *Phys. Rev.* **86**, 694–701 (1952).
 - [13] V. M. Matveev, "Quantum quadrupolar magnetism and phase transitions in the presence of biquadratic exchange," *JETP* **38**, 813 (1974).
 - [14] N. Papanicolaou, "Unusual phases in quantum spin-1 systems," *Nuclear Physics B* **305**, 367 – 395 (1988).
 - [15] Mustansir Barma, "Phonon-induced phase transition in a classical Heisenberg chain," *Phys. Rev. B* **12**, 2710–2715 (1975).
 - [16] AF Andreev and IA Grishchuk, "Spin Nematics," *JETP* **87**, 467–475 (1984).
 - [17] Kenji Harada and Naoki Kawashima, "Quadrupolar order in isotropic Heisenberg models with biquadratic interaction," *Phys. Rev. B* **65**, 052403 (2002).
 - [18] Hirokazu Tsunetsugu and Mitsuhiro Arikawa, "Spin Nematic Phase in S=1 Triangular Antiferromagnets," *J. Phys. Soc. Jpn* **75**, 083701 (2006).
 - [19] Andreas Läuchli, Frédéric Mila, and Karlo Penc, "Quadrupolar Phases of the $S = 1$ Bilinear-Biquadratic Heisenberg Model on the Triangular Lattice," *Phys. Rev. Lett.* **97**, 087205 (2006).
 - [20] Andrew Smerald and Nic Shannon, "Theory of spin excitations in a quantum spin-nematic state," *Phys. Rev. B* **88**, 184430 (2013).
 - [21] Maksym Serbyn, T. Senthil, and Patrick A. Lee, "Exotic $S = 1$ spin-liquid state with fermionic excitations on the triangular lattice," *Phys. Rev. B* **84**, 180403 (2011).
 - [22] Samuel Bieri, Maksym Serbyn, T. Senthil, and Patrick A. Lee, "Paired chiral spin liquid with a Fermi surface in $S = 1$ model on the triangular lattice," *Phys. Rev. B* **86**, 224409 (2012).
 - [23] Cenke Xu, Fa Wang, Yang Qi, Leon Balents, and Matthew P. A. Fisher, "Spin liquid phases for spin-1 systems on the triangular lattice," *Phys. Rev. Lett.* **108**, 087204 (2012).
 - [24] G. Chen, M. Hermele, and L. Radzihovskiy, "Frustrated Quantum Critical Theory of Putative Spin-Liquid Phenomenology in $6H-B-Ba_3NiSb_2O_9$," *Phys. Rev. Lett.* **109**, 016402 (2012).
 - [25] Kyusung Hwang, Tyler Dodds, Subhro Bhattacharjee, and Yong Baek Kim, "Three-dimensional nematic spin liquid in a stacked triangular lattice $6h$ -b structure," *Phys. Rev. B* **87**, 235103 (2013).
 - [26] Finn Lasse Buessen, Max Hering, Johannes Reuther, and Si-

- mon Trebst, “Quantum spin liquids in frustrated spin-1 diamond antiferromagnets,” *Phys. Rev. Lett.* **120**, 057201 (2018).
- [27] Satoru Nakatsuji, Yusuke Nambu, Hiroshi Tonomura, Osamu Sakai, Seth Jonas, Collin Broholm, Hirokazu Tsunetsugu, Yiming Qiu, and Yoshiteru Maeno, “Spin disorder on a triangular lattice,” *Science* **309**, 1697–1700 (2005).
- [28] Yusuke Nambu, Satoru Nakatsuji, and Yoshiteru Maeno, “Coherent Behavior and Nonmagnetic Impurity Effects of Spin Disordered State in NiGa_2S_4 ,” *Journal of the Physical Society of Japan* **75**, 043711 (2006).
- [29] Subhro Bhattacharjee, Vijay B. Shenoy, and T. Senthil, “Possible ferro-spin nematic order in NiGa_2S_4 ,” *Phys. Rev. B* **74**, 092406 (2006).
- [30] Michael E. Valentine, Tomoya Higo, Yusuke Nambu, Dipanjan Chaudhuri, Jiajia Wen, Collin Broholm, Satoru Nakatsuji, and Natalia Driehko, “Impact of the Lattice on Magnetic Properties and Possible Spin Nematicity in the $S = 1$ Triangular Antiferromagnet NiGa_2S_4 ,” *Phys. Rev. Lett.* **125**, 197201 (2020).
- [31] Yong-Hao Gao, Xu-Ping Yao, Fei-Ye Li, and Gang Chen, “Spin-1 pyrochlore antiferromagnets: Theory, model, and materials’ survey,” *Frontiers of Physics* **15**, 63201 (2020).
- [32] K. W. Plumb, Hitesh J. Changlani, A. Scheie, Shu Zhang, J. W. Krizan, J. A. Rodriguez-Rivera, Yiming Qiu, B. Winn, R. J. Cava, and C. L. Broholm, “Continuum of quantum fluctuations in a three-dimensional $S = 1$ Heisenberg magnet,” *Nature Physics* **15**, 54–59 (2019).
- [33] Shu Zhang, Hitesh J. Changlani, Kemp W. Plumb, Oleg Tchernyshyov, and Roderich Moessner, “Dynamical Structure Factor of the Three-Dimensional Quantum Spin Liquid Candidate $\text{NaCaNi}_2\text{F}_7$,” *Phys. Rev. Lett.* **122**, 167203 (2019).
- [34] J. R. Chamorro, L. Ge, J. Flynn, M. A. Subramanian, M. Mourigal, and T. M. McQueen, “Frustrated spin one on a diamond lattice in NiRh_2O_4 ,” *Phys. Rev. Materials* **2**, 034404 (2018).
- [35] Wojciech Miüller, Mogens Christensen, Arfhan Khan, Neeraj Sharma, René B. Macquart, Maxim Avdeev, Garry J. McIntyre, Ross O. Piltz, and Chris D. Ling, “ $\text{YCa}_3(\text{VO})_3(\text{BO}_3)_4$: A Kagomé Compound Based on Vanadium(III) with a Highly Frustrated Ground State,” *Chemistry of Materials* **23**, 1315–1322 (2011).
- [36] J. G. Cheng, G. Li, L. Balicas, J. S. Zhou, J. B. Goodenough, Cenke Xu, and H. D. Zhou, “High-Pressure Sequence of $\text{Ba}_3\text{NiSb}_2\text{O}_9$ Structural Phases: New $S = 1$ Quantum Spin Liquids Based on Ni^{2+} ,” *Phys. Rev. Lett.* **107**, 197204 (2011).
- [37] J. A. Quilliam, F. Bert, A. Manseau, C. Darie, C. Guillot-Deudon, C. Payen, C. Baines, A. Amato, and P. Mendels, “Gapless quantum spin liquid ground state in the spin-1 antiferromagnet $6\text{HB-Ba}_3\text{NiSb}_2\text{O}_9$,” *Phys. Rev. B* **93**, 214432 (2016).
- [38] B. Fak, S. Bieri, E. Canévet, L. Messio, C. Payen, M. Viaud, C. Guillot-Deudon, C. Darie, J. Ollivier, and P. Mendels, “Evidence for a spinon Fermi surface in the triangular $S = 1$ quantum spin liquid $\text{Ba}_3\text{NiSb}_2\text{O}_9$,” *Phys. Rev. B* **95**, 060402 (2017).
- [39] R. M. Fernandes, A. V. Chubukov, and J. Schmalian, “What drives nematic order in iron-based superconductors?” *Nature Physics* **10**, 97 EP – (2014).
- [40] Cheng Luo, Trinanjan Datta, and Dao-Xin Yao, “Spin and quadrupolar orders in the spin-1 bilinear-biquadratic model for iron-based superconductors,” *Phys. Rev. B* **93**, 235148 (2016).
- [41] Zhentao Wang, Wen-Jun Hu, and Andriy H. Nevidomskyy, “Spin Ferroquadrupolar Order in the Nematic Phase of FeSe ,” *Phys. Rev. Lett.* **116**, 247203 (2016).
- [42] Shou-Shu Gong, W. Zhu, D. N. Sheng, and Kun Yang, “Possible nematic spin liquid in spin-1 antiferromagnetic system on the square lattice: Implications for the nematic paramagnetic state of FeSe ,” *Phys. Rev. B* **95**, 205132 (2017).
- [43] Hsin-Hua Lai, Wen-Jun Hu, Emilian M. Nica, Rong Yu, and Qimiao Si, “Antiferroquadrupolar order and rotational symmetry breaking in a generalized bilinear-biquadratic model on a square lattice,” *Phys. Rev. Lett.* **118**, 176401 (2017).
- [44] Eugene Demler and Fei Zhou, “Spinor bosonic atoms in optical lattices: Symmetry breaking and fractionalization,” *Phys. Rev. Lett.* **88**, 163001 (2002).
- [45] Adilet Imambekov, Mikhail Lukin, and Eugene Demler, “Spin-exchange interactions of spin-one bosons in optical lattices: Singlet, nematic, and dimerized phases,” *Phys. Rev. A* **68**, 063602 (2003).
- [46] Dan M. Stamper-Kurn and Masahito Ueda, “Spinor Bose gases: Symmetries, magnetism, and quantum dynamics,” *Rev. Mod. Phys.* **85**, 1191–1244 (2013).
- [47] Laurent de Forges de Parny, Hongyu Yang, and Frédéric Mila, “Anderson Tower of States and Nematic Order of Spin-1 Bosonic Atoms on a 2D Lattice,” *Phys. Rev. Lett.* **113**, 200402 (2014).
- [48] T. Zibold, V. Corre, C. Frapolli, A. Invernizzi, J. Dalibard, and F. Gerbier, “Spin-nematic order in antiferromagnetic spinor condensates,” *Phys. Rev. A* **93**, 023614 (2016).
- [49] Steven R. White and Ian Affleck, “Spectral function for the $S = 1$ Heisenberg antiferromagnetic chain,” *Phys. Rev. B* **77**, 134437 (2008).
- [50] H. H. Zhao, Cenke Xu, Q. N. Chen, Z. C. Wei, M. P. Qin, G. M. Zhang, and T. Xiang, “Plaquette order and deconfined quantum critical point in the spin-1 bilinear-biquadratic Heisenberg model on the honeycomb lattice,” *Phys. Rev. B* **85**, 134416 (2012).
- [51] Ido Niesen and Philippe Corboz, “A tensor network study of the complete ground state phase diagram of the spin-1 bilinear-biquadratic Heisenberg model on the square lattice,” *SciPost Phys.* **3**, 030 (2017).
- [52] Ribhu K. Kaul, “Spin nematic ground state of the triangular lattice $S = 1$ biquadratic model,” *Phys. Rev. B* **86**, 104411 (2012).
- [53] Annika Völl and Stefan Wessel, “Spin dynamics of the bilinear-biquadratic $S = 1$ Heisenberg model on the triangular lattice: A quantum Monte Carlo study,” *Phys. Rev. B* **91**, 165128 (2015).
- [54] E. M. Stoudenmire, Simon Trebst, and Leon Balents, “Quadrupolar correlations and spin freezing in $S = 1$ triangular lattice antiferromagnets,” *Phys. Rev. B* **79**, 214436 (2009).
- [55] F. Bloch, “Nuclear induction,” *Phys. Rev.* **70**, 460–474 (1946).
- [56] Karlo Penc and Andreas M. Läuchli, “Spin nematic phases in quantum spin systems,” in *Introduction to Frustrated Magnetism: Materials, Experiments, Theory*, edited by Claudine Lacroix, Philippe Mendels, and Frédéric Mila (Springer Berlin Heidelberg, Berlin, Heidelberg, 2011) pp. 331–362.
- [57] Claude Itzykson and Jean B. Zuber, *Quantum field theory / Claude Itzykson and Jean-Bernard Zuber* (McGraw-Hill International Book Co New York, 1980) pp. xi, 515 p. .
- [58] Peter Balla, *The Equation of Motion Method for Spin Systems with Multipolar Hamiltonians*, Master’s thesis, Budapest University of Technology and Economics (2014).
- [59] Kimberly Remund, *Semi-classical Equations of Motion for Quantum Spin Nematics*, Master’s thesis, Ecole Polytechnique Federal Lausanne (2015).
- [60] Hao Zhang and Cristian D. Batista, “Classical spin dynamics based on $\text{SU}(n)$ coherent states,” *Phys. Rev. B* **104**, 104409

- (2021).
- [61] Hiroaki T. Ueda, Yutaka Akagi, and Nic Shannon, “Quantum solitons with emergent interactions in a model of cold atoms on the triangular lattice,” *Phys. Rev. A* **93**, 021606 (2016).
- [62] L. D. Landau and E. M. Lifshitz, *Quantum Mechanics (Non-relativistic Theory)*, 3rd ed. (Butterworth–Heinemann, Oxford, 1977) p. p199.
- [63] A Auerbach, *Interacting Electrons and Quantum Magnetism* (Springer, 1994).
- [64] David P. Landau and Kurt Binder, *A Guide to Monte Carlo Simulations in Statistical Physics*, 4th ed. (Cambridge University Press, 2014).
- [65] R. Moessner and J. T. Chalker, “Properties of a Classical Spin Liquid: The Heisenberg Pyrochlore Antiferromagnet,” *Phys. Rev. Lett.* **80**, 2929–2932 (1998).
- [66] Rico Pohle, Han Yan, and Nic Shannon, “Theory of $\text{Ca}_{10}\text{Cr}_7\text{O}_{28}$ as a bilayer breathing-kagome magnet: Classical thermodynamics and semiclassical dynamics,” *Phys. Rev. B* **104**, 024426 (2021).
- [67] T.L. Gilbert, “A phenomenological theory of damping in ferromagnetic materials,” *IEEE Transactions on Magnetics* **40**, 3443–3449 (2004).
- [68] T. J. Nelson, “A set of harmonic functions for the group $\text{su}(3)$ as specialized matrix elements of a general finite transformation,” *Journal of Mathematical Physics* **8**, 857–863 (1967), <https://doi.org/10.1063/1.1705289>.
- [69] Jin-Quan Chen, Jialun Ping, and Fan Wang, “Lie groups,” in *Group Representation Theory for Physicists*, Chap. 5, pp. 205–280, <https://www.worldscientific.com/doi/pdf/10.1142/0262>.
- [70] Kimberly Remund, Owen Benton, and Nic Shannon, unpublished.
- [71] S. K. Yip, “Dimer state of spin-1 bosons in an optical lattice,” *Phys. Rev. Lett.* **90**, 250402 (2003).
- [72] A. V. Gorshkov, M. Hermele, V. Gurarie, C. Xu, P. S. Julienne, J. Ye, P. Zoller, E. Demler, M. D. Lukin, and A. M. Rey, “Two-orbital $\text{su}(n)$ magnetism with ultracold alkaline-earth atoms,” *Nature Physics* **6**, 289–295 (2010).
- [73] K. Rodríguez, A. Argüelles, A. K. Kolezhuk, L. Santos, and T. Vekua, “Field-induced phase transitions of repulsive spin-1 bosons in optical lattices,” *Phys. Rev. Lett.* **106**, 105302 (2011).
- [74] G. De Chiara, M. Lewenstein, and A. Sanpera, “Bilinear-biquadratic spin-1 chain undergoing quadratic zeeman effect,” *Phys. Rev. B* **84**, 054451 (2011).
- [75] Bela Bauer, Philippe Corboz, Andreas M. Läuchli, Laura Messio, Karlo Penc, Matthias Troyer, and Frédéric Mila, “Three-sublattice order in the $\text{su}(3)$ heisenberg model on the square and triangular lattice,” *Phys. Rev. B* **85**, 125116 (2012).
- [76] Andrew Smerald, Hiroaki T. Ueda, and Nic Shannon, “Theory of inelastic neutron scattering in a field-induced spin-nematic state,” *Phys. Rev. B* **91**, 174402 (2015).
- [77] D. Jaksch, C. Bruder, J. I. Cirac, C. W. Gardiner, and P. Zoller, “Cold bosonic atoms in optical lattices,” *Phys. Rev. Lett.* **81**, 3108–3111 (1998).
- [78] Carsten Honerkamp and Walter Hofstetter, “Ultracold fermions and the $\text{SU}(n)$ hubbard model,” *Phys. Rev. Lett.* **92**, 170403 (2004).
- [79] E. V. Gorelik and N. Blümer, “Mott transitions in ternary flavor mixtures of ultracold fermions on optical lattices,” *Phys. Rev. A* **80**, 051602 (2009).
- [80] C. Kittel, “Model of exchange-inversion magnetization,” *Phys. Rev.* **120**, 335–342 (1960).
- [81] P. Chandra, P. Coleman, and A. I. Larkin, “Ising transition in frustrated heisenberg models,” *Phys. Rev. Lett.* **64**, 88–91 (1990).
- [82] Nicholas Metropolis, Arianna W. Rosenbluth, Marshall N. Rosenbluth, Augusta H. Teller, and Edward Teller, “Equation of state calculations by fast computing machines,” *The Journal of Chemical Physics* **21**, 1087–1092 (1953).
- [83] M. E. J. Newman and G. T. Barkema, *Monte Carlo Methods in Statistical Physics* (Clarendon Press, 1999).
- [84] George Marsaglia, “Choosing a point from the surface of a sphere,” *The Annals of Mathematical Statistics* **43**, 645–646 (1972).
- [85] Y. Amari, private communication.
- [86] Robert H. Swendsen and Jian-Sheng Wang, “Replica Monte Carlo Simulation of Spin-Glasses,” *Phys. Rev. Lett.* **57**, 2607–2609 (1986).
- [87] David J. Earl and Michael W. Deem, “Parallel tempering: Theory, applications, and new perspectives,” *Phys. Chem. Chem. Phys.* **7**, 3910–3916 (2005).
- [88] B. A. Ivanov, R. S. Khymyn, and A. K. Kolezhuk, “Pairing of Solitons in Two-Dimensional $S = 1$ Magnets,” *Phys. Rev. Lett.* **100**, 047203 (2008).
- [89] R. Moessner and J. T. Chalker, “Low-temperature properties of classical geometrically frustrated antiferromagnets,” *Phys. Rev. B* **58**, 12049–12062 (1998).
- [90] P. H. Conlon and J. T. Chalker, “Spin Dynamics in Pyrochlore Heisenberg Antiferromagnets,” *Phys. Rev. Lett.* **102**, 237206 (2009).
- [91] Mathieu Taillefumier, Julien Robert, Christopher L. Henley, Roderich Moessner, and Benjamin Canals, “Semiclassical spin dynamics of the antiferromagnetic Heisenberg model on the kagome lattice,” *Phys. Rev. B* **90**, 064419 (2014).
- [92] A. M. Samarakoon, A. Banerjee, S.-S. Zhang, Y. Kamiya, S. E. Nagler, D. A. Tennant, S.-H. Lee, and C. D. Batista, “Comprehensive study of the dynamics of a classical Kitaev spin liquid,” *Phys. Rev. B* **96**, 134408 (2017).
- [93] Gia-Wei Chern, Kipton Barros, Zhenhao Wang, Hidemaro Suwa, and Cristian D. Batista, “Semiclassical dynamics of spin density waves,” *Phys. Rev. B* **97**, 035120 (2018).
- [94] Mitsuru Akaki, Daichi Yoshizawa, Akira Okutani, Takanori Kida, Judit Romhányi, Karlo Penc, and Masayuki Hagiwara, “Direct observation of spin-quadrupolar excitations in $\text{Sr}_2\text{CoGe}_2\text{O}_7$ by high-field electron spin resonance,” *Phys. Rev. B* **96**, 214406 (2017).
- [95] William H. Press, Saul A. Teukolsky, William T. Vetterling, and Brian P. Flannery, *Numerical Recipes 3rd Edition: The Art of Scientific Computing*, 3rd ed. (Cambridge University Press, New York, NY, USA, 2007).
- [96] Ernst Hairer, Gerhard Wanner, and Syvert P. Nørsett, *Solving Ordinary Differential Equations I – Nonstiff Problems* (Springer Berlin Heidelberg, 1993).
- [97] Rico Pohle, Yutaka Akagi, Kimberly Remund, and Nic Shannon, “Dynamics of ferroquadrupolar order near a topological phase transition,” (in preparation.).
- [98] George B. Arfken and Hans J. Weber, *Mathematical Methods for Physicists – International Edition*, 4th ed. (Academic Press, INC, 1995).
- [99] Ido Niesen and Philippe Corboz, “Ground-state study of the spin-1 bilinear-biquadratic Heisenberg model on the triangular lattice using tensor networks,” *Phys. Rev. B* **97**, 245146 (2018).
- [100] F. P. Onufrieva, “Low-temperature properties of spin systems with tensor order parameters,” *Zh. Eksp. Teor. Fiz.* **89**, 2270 (1985).
- [101] M. E. Zhitomirsky, “Octupolar ordering of classical kagome

- antiferromagnets in two and three dimensions,” *Phys. Rev. B* **78**, 094423 (2008).
- [102] Nic Shannon, Karlo Penc, and Yukitoshi Motome, “Nematic, vector-multipole, and plateau-liquid states in the classical $O(3)$ pyrochlore antiferromagnet with biquadratic interactions in applied magnetic field,” *Phys. Rev. B* **81**, 184409 (2010).
- [103] N. D. Mermin and H. Wagner, “Absence of Ferromagnetism or Antiferromagnetism in One- or Two-Dimensional Isotropic Heisenberg Models,” *Phys. Rev. Lett.* **17**, 1133–1136 (1966).
- [104] Hikaru Kawamura and Atsushi Yamamoto, “Vortex-Induced Topological Transition of the Bilinear–Biquadratic Heisenberg Antiferromagnet on the Triangular Lattice,” *Journal of the Physical Society of Japan* **76**, 073704 (2007).
- [105] Kimberly Remund, Unpublished.
- [106] Rico Pohle, Han Yan, and Nic Shannon, “How many spin liquids are there in $\text{Ca}_{10}\text{Cr}_7\text{O}_{28}$?” (2017), [arXiv:1711.03778](https://arxiv.org/abs/1711.03778) [cond-mat.str-el].
- [107] Allen Scheie, Owen Benton, Mathieu Taillefumier, Ludovic D. C. Jaubert, Gabriele Sala, Niina Jalarvo, Seyed M. Koohpayeh, and Nic Shannon, “Dynamical scaling as a signature of multiple phase competition in $\text{Yb}_2\text{Ti}_2\text{O}_7$,” (2022).
- [108] Owen Benton, unpublished.
- [109] V. G. Bar’yakhtar, V. I. Butrim, A. K. Kolezhuk, and B. A. Ivanov, “Dynamics and relaxation in spin nematics,” *Phys. Rev. B* **87**, 224407 (2013).
- [110] We note that interacting theory predicts a logarithmic correction to this scaling, $c(T) \sim T^2 \ln T$ [109], however published QMC results may not extend to sufficiently low temperatures to distinguish this.
- [111] Jaan Oitmaa, Chris Hamer, and Weihong Zheng, *Series Expansion Methods for Strongly Interacting Lattice Models* (Cambridge University Press, 2006).
- [112] Nic Shannon, (unpublished.).
- [113] B. A. Ivanov and A. K. Kolezhuk, “Effective field theory for the $S = 1$ quantum nematic,” *Phys. Rev. B* **68**, 052401 (2003).
- [114] B. A. Ivanov and R. S. Khymyn, “Soliton dynamics in a spin nematic,” *Journal of Experimental and Theoretical Physics* **104**, 307–318 (2007).
- [115] Tarun Grover and T. Senthil, “Non-abelian spin liquid in a spin-one quantum magnet,” *Phys. Rev. Lett.* **107**, 077203 (2011).
- [116] E. G. Galkina, B. A. Ivanov, O. A. Kosmachev, and Yu. A. Fridman, “Two-dimensional solitons in spin nematic states for magnets with an isotropic exchange interaction,” *Low Temperature Physics* **41**, 382–389 (2015).
- [117] Yutaka Akagi, Yuki Amari, Nobuyuki Sawado, and Yakov Shnir, “Isolated skyrmions in the CP^2 nonlinear sigma model with a Dzyaloshinskii-Moriya type interaction,” *Phys. Rev. D* **103**, 065008 (2021).
- [118] Yutaka Akagi, Yuki Amari, Sven Bjarke Gudnason, Muneto Nitta, and Yakov Shnir, “Fractional Skyrmion molecules in CP^{N-1} model,” *Journal of High Energy Physics* **2021**, 194 (2021).
- [119] Hao Zhang, Zhentao Wang, David Dahlbom, Kipton Barros, and Cristian D. Batista, “ CP^2 Skyrmions and Skyrmion Crystals in Realistic Quantum Magnets,” (2022).
- [120] Yuki Amari, Yutaka Akagi, Sven Bjarke Gudnason, Muneto Nitta, and Yakov Shnir, “ CP^2 Skyrmion Crystals in an $SU(3)$ Magnet with a Generalized Dzyaloshinskii-Moriya Interaction,” (2022).
- [121] David Dahlbom, Hao Zhang, Cole Miles, Xiaojian Bai, Cristian D. Batista, and Kipton Barros, “Geometric integration of classical spin dynamics via a mean-field Schrödinger equation,” (2022).
- [122] Seung-Hwan Do, Hao Zhang, David A. Dahlbom, Travis J. Williams, V. Ovidiu Garlea, Tao Hong, Tae-Hwan Jang, Sang-Wook Cheong, Jae-Hoon Park, Kipton Barros, Cristian D. Batista, and Andrew D. Christianson, “Understanding temperature-dependent $SU(3)$ spin dynamics in the $S = 1$ antiferromagnet $\text{Ba}_2\text{FeSi}_2\text{O}_7$,” (2022).
- [123] Xiaojian Bai, Shang-Shun Zhang, Zhiling Dun, Hao Zhang, Qing Huang, Haidong Zhou, Matthew B. Stone, Alexander I. Kolesnikov, Feng Ye, Cristian D. Batista, and Martin Mourigal, “Hybridized quadrupolar excitations in the spin-anisotropic frustrated magnet FeI_2 ,” *Nature Physics* **17**, 467–472 (2021).
- [124] Mathieu Taillefumier, Owen Benton, Han Yan, L. D. C. Jaubert, and Nic Shannon, “Competing Spin Liquids and Hidden Spin-Nematic Order in Spin Ice with Frustrated Transverse Exchange,” *Phys. Rev. X* **7**, 041057 (2017).